
Investigations into the synthesis of upper-rim functionalised calix[4]arenes and their applications

William H. Gardiner

A thesis submitted in part fulfilment of the requirements for the degree of
Doctor of Philosophy

School of Chemistry, University of East Anglia, Norwich

September 2016

©This copy of the thesis has been supplied on condition that anyone who consults it is understood to recognise that its copyright rests with the author and that use of any information derived there from must be in accordance with current UK Copyright Law. In addition, any quotation or extract must include full attribution.

Declaration

The research described in this thesis is original to the best of my knowledge, except where due reference is made.

William Henry Gardiner

Abstract

In this thesis, the development of three efficient protocols for the generation of upper-rim ABBB, ABAC and ABCD functionalised calix[4]arenes, in addition to a number of novel AAAAAB functionalised calix[6]arenes is described. For the generation of the ABAC type systems, an ionic hydrogenation between the known 1,3-diformyl calix[4]arene and *para*-iodophenyl urea under optimised reaction conditions to favour desymmetrisation through mono-substitution. To generate ABBB type systems, a protocol previously established within the Bew group that exploits the mono-selective Mannich reaction of calix[4]arene, aqueous dimethylamine and formalin is developed. Whilst for the ABCD type systems, previous studies in the Bew group are built upon to show how a mechanochemical, intramolecular, Cannizzaro reaction can function as a highly efficient means of desymmetrising the upper-rim of 1,3-diformyl functionalised calix[4]arenes. It is subsequently demonstrated how this 'suite' of protocols can be applied to the construction of fluorogenic sensors (Chapter 2), redox-active and 1,2,3-triazole linked cavitands (Chapter 3) and non-linear optical materials (Chapter 4); advanced materials which would have been difficult to access efficiently using other means.

Acknowledgements

I would like to thank Dr. Sean Bew and Dr. G. Richard Stephenson for their help, guidance and encouragement over the years. In particular, thanks go to Dr. Sean Bew for giving me the opportunity to work in his laboratory on some interesting projects and for teaching me not to believe everything I read.

This thesis would not have been completed without the help, support, advice, company and friendship of my colleagues and friends in the chemistry department at UEA. In particular, a massive thanks go to my most recent bunch of lab mates: Glyn, Sean, Polly, Deeptee and Luis. They have each in their own way made this experience a lot more enjoyable.

My appreciation is also extended towards UEA and the Interreg projects for funding, as well as the EPSRC mass spectrometry facility in Swansea for obtaining the HRMS analyses.

Thanks to Professor Verbiest and his research group in Leuven for measuring the SHG spectra of the NLO compounds.

Finally, I am very grateful to my mum and family for their love and support.

List of Abbreviations

μ W	Microwave
Å	Ångström
Ac	Acetyl
Ar	Aromatic / aryl
b	Broad
Bn	Benzyl
Boc	<i>tert</i> -Butoxycarbonyl
<i>n</i> -BuLi	<i>normal</i> -Butyl lithium
<i>t</i> -BuLi	<i>tert</i> -Butyl lithium
COSY	Correlation spectroscopy
CuAAC	Copper-catalysed azide-alkyne cycloaddition
d	Doublet
dd	Doublet of doublets
DBU	1,9-Diazabicyclo[5.4.0]undec-7-ene
DC	Direct current
DC _v C	Dynamic covalent chemistry
DCM	Dichloromethane
DFT	Density functional theory
DMF	<i>N,N</i> -Dimethylformamide
DMSO	Dimethyl sulfoxide
DPPA	Diphenylphosphoryl azide
EFISH	Electric field induced second harmonic
Et	Ethyl
FAB-MS	Fast atom bombardment mass spectrometry
FT-IR	Fourier transform infrared
GP1	General Procedure 1
GP2	General Procedure 2
HEPES	4-(2-Hydroxyethyl)-1-piperazineethanesulfonic acid
HPLC	High pressure / performance liquid chromatography

Hz	Hertz
IUPAC	International union of pure and applied chemistry
<i>J</i>	Coupling constant
<i>K_a</i>	Association constant
M	Molar
MALDI-TOF	Matrix assisted laser desorption ionisation time of flight
mCPBA	<i>meta</i> -Chloroperbenzoic acid
Me	Methyl
MEK	Methyl ethyl ketone
MS	Mass spectrometry
MTBE	Methyl <i>tert</i> -butyl ether
NLO	Non-linear optical
NMR	Nuclear magnetic resonance
NOESY	Nuclear Overhauser effect spectroscopy
PBS	Phosphate buffered saline
ppm	Parts per million
Pr	Propyl
RaNi	Raney Nickel
s	Singlet
SHG	Second harmonic generation
t	Triplet
TES	Triethylsilane
TFA	Trifluoroacetic acid
THF	Tetrahydrofuran
TLC	Thin layer chromatography
TMS	Trimethylsilyl
TPP	Triphenylphosphine
TPPO	Triphenylphosphine oxide
UV	Ultraviolet
YAG	Yttrium aluminium garnet

Contents

1.1 History of calix[n]arenes	1
1.2 Nomenclature of calix[n]arenes	2
1.3 Synthesis of calix[4]arenes	3
1.3.2 Synthesis of calix[n]arenes <i>via</i> stepwise and convergent protocols	7
1.3.3 Synthesis of calix[4]arenes using Fisher carbene complexes	9
1.4 The conformations of calix[4]arenes	10
1.5 Functionalisation of calix[4]arenes	13
1.5.2 Selective upper-rim functionalisation of calix[4]arenes	16
1.6 Applications of calix[n]arenes	18
1.6.1 Calix[n]arenes for the separation of metal ions	18
1.6.2 Multicalix[4]arenes for the complexation of metal ions and small molecules	20
1.6.2.1 Multicalix[4]arenes linked directly <i>via para</i> -phenolic carbon atoms	21
1.6.2.2 Multicalix[4]arenes linked <i>via a</i> methylene function	22
1.6.2.3 Multicalix[4]arenes linked <i>via</i> heteroatom containing bridges	24
1.6.3 Calix[n]arenes as metal ion-selective sensors	27
1.6.4 Ion-selective sensors for the precious metals	33
1.6.4.1 Ion-selective sensors for the silver ion	33
1.6.4.2 Ion-selective sensors for Au(I) and Au(III) ions	36
1.6.5 Calix[4]arenes as nonlinear optical materials	42
1.7 Conclusions	43
2.1 Abstract	49

2.2 Methodology	49
2.3 Synthesis of 'core' calix[4]arene scaffold 37	51
2.4 Synthesis of 1,3-diformyl calix[4]arene 139	52
2.5 Synthesis of <i>mono</i> -iodophenylurea calix[4]arene 141 <i>via</i> ionic hydrogenation	55
2.6 Synthesis of ABAC <i>bis</i> -urea calix[4]arene intermediates <i>via</i> a second ionic hydrogenation	57
2.7 Synthesis of ABAC <i>bis</i> -urea calix[4]arene intermediates	58
2.8 Synthesis of dansyl derived fluorophores	68
2.9 Synthesis of 114 <i>via</i> a Suzuki-Miyaura coupling of 137 and 135	70
2.10 Synthesis of sensor 182 <i>via</i> a Sonogashira coupling	72
2.11 Fluorescence studies of sensors 114 and 182	73
2.12 Synthesis of a series of derivatives of sensor 182	77
2.13 Synthesis and fluorescence properties of control compounds 115 and 117	81
2.14 Conclusions and outlook	88
3.1 Abstract	90
3.2 Methodology	90
3.3 Synthesis of monoformyl calix[4]arene 60	92
3.4 Synthesis of upper-rim alkyne functionalised AAAB calix[4]arenes	95
3.5 Synthesis of azide functionalised cone-confined calix[4]arene 129	97
3.6 Synthesis of 1,2,3-triazole-linked cavitands in the calix[4]arene series	97
3.7 Synthesis of 1,2,3-triazole-linked cavitands in the calix[6]arene series	101
3.8 Synthesis of redox active calix[4]arenes	109
3.9 Synthesis of peptidocalix[4]arenes <i>via</i> dynamic covalent chemistry	113
3.10 Synthesis of orthogonally bonded supramolecular assemblies	119
3.11 Conclusions and outlook	129

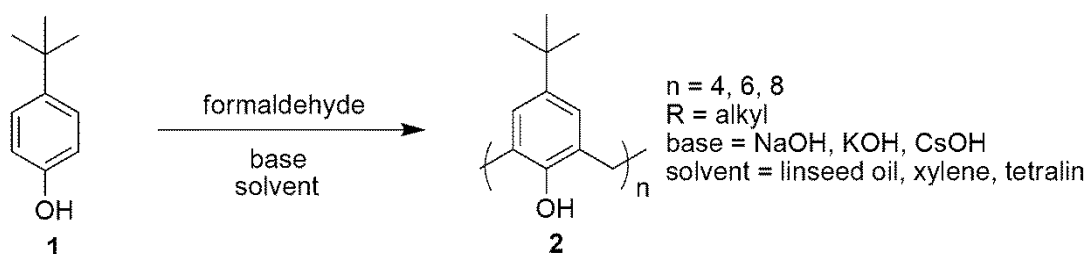
4.1 Abstract	133
4.2 Methodology	133
4.3 Synthesis of <i>bis-iodo-bis-formyl</i> calix[4]arene 258	134
4.4 The reactivity of <i>bis-iodo-bis-formyl</i> calix[4]arene 258 in transition metal mediated couplings	136
4.5 The reactivity of <i>bis-iodo-bis-hydroxymethylene</i> calix[4]arene 276 in transition metal mediated couplings	139
4.5.1 The reactivity of <i>bis-iodo-bis-hydroxymethylene</i> calix[4]arene 276 in Suzuki couplings	140
4.6 Synthesis of ABAB functionalised <i>bis</i> -aldehydes <i>via</i> the oxidation of ABAB functionalised <i>bis</i> -alcohols	142
4.7 The reactivity of <i>bis-iodo-bis-formyl</i> calix[4]arene 258 in Sonogashira couplings	144
4.8 The Cannizzaro reaction of ABAB functionalised <i>bis</i> -aldehyde calix[4]arenes	147
4.9 Synthesis of 206 and 303 <i>via</i> Sonogashira couplings using Cannizzaro derived <i>bis</i> -iodide 259	151
4.10 Variable temperature ¹ H-NMR study of the conformation of Cannizzaro derived calix[4]arene 298	156
4.11 SHG photophysics study of NLOphore calix[4]arenes 260 and 121	164
4.12 Conclusions and outlook	167
General Information	169
Experimental Section	170
References	206

Chapter 1

Introduction

1.1 History of calix[n]arenes

Calix[n]arenes are macrocycles readily available from the base catalysed condensation of *para*-alkyl phenols and aqueous formaldehyde.¹ They were first described in 1944 by Zinke and Zeigler² after a series of experiments inspired by the early work of von Bayer and Baekeland into the chemistry of phenol-formaldehyde resins.³ Bayer reported the reaction of phenol and formaldehyde under hydrochloric acid catalysis to afford a resinous tar, whilst Baekeland was able to find conditions which gave rise to a material with useful properties – one which he named Bakelite, the first production plastic.⁴ In an effort to obtain more tractable products, Zinke and Zeigler decided to study the base catalysed reactions (using alkali metal hydroxides) of alkyl-substituted phenols and formaldehyde. In these experiments *para*-alkyl substituted phenols were found to afford the most tractable products, since the parent phenols may react in both the *ortho* and *para* positions and give rise to cross-linked polymers – Bayer’s so-called ‘resinous tars’. In the sodium hydroxide catalysed reaction of *para*-*tert*-butylphenol with formaldehyde, the Austrian group isolated a crystalline solid with a melting point of 314 °C and a molecular weight of 1725. This molecular weight suggested a cyclic structure comprising of 8 phenolic units, but as this was thought to be unlikely, Zinke and Zeigler instead formulated their products as cyclic tetramers, despite the supposed difficulty in obtaining a ‘satisfactory’ molecular weight (**Scheme 1.1**).²



Scheme 1.1: The base catalysed synthesis of calix[n]arenes

Only later in 1952 was evidence of the cyclic tetramer provided when Ziegler reported further examples of phenols reacting with formaldehyde to give high melting, organic solvent insoluble materials. In this publication⁵, the acetate of the product from *para*-1,1,3,3-tetramethylbutylphenol and formaldehyde was reported to afford needles with the molecular weight of 876, as determined by cryoscopy – a value in excellent agreement with that calculated for the cyclic tetramer. Ziegler was satisfied to take this as proof that all of his products were indeed cyclic tetramers. It was shortly after these results were published that the group of Cornforth – at that time investigating tuberculostatic agents - began a research program into Ziegler’s cyclic tetramers. On repeating the procedure described for *para*-*tert*-butylphenol and formaldehyde, he was surprised to be able to

isolate not one but two products from the reaction. Whilst both materials were crystalline and had elemental analyses consistent with a $(C_{11}H_{14}O)_n$ formula, they had high but non-identical melting points. On the basis of X-ray crystallographic data and molecular models, Conforth concluded that these products were the diastereomers arising from hindered rotation about the methylene bridges, and as such they would be expected to show different chemical and physical properties.⁶ So it was the case then that around the late 1950's the weight of evidence seemed to suggest all of Ziegler's products were indeed cyclic tetramers. Only later in the 1970's did research led by Gutsche at the University of Washington reveal (aided by the advent of NMR spectroscopy) that mixtures produced under Ziegler's conditions were actually composed of *three* major cyclic products; the tetramer, hexamer and octamer. By undertaking a detailed study of the reaction conditions leading to these cyclic oligomers, Gutsche and co-workers were able to identify procedures which allowed reliable access to these 'major calix[n]arenes' ($n = 4, 6, 8$).⁷

1.2 Nomenclature of calix[n]arenes

It was Gutsche that suggested the name 'calix[n]arene' to describe this class of macrocycles.⁸ The prefix 'calix' was chosen to describe the similarity of the shape of the cyclic tetramer in the cone conformation to a Greek vase known as a calix crater, whilst the number in parenthesis indicates the number of phenolic units in the cyclic array. Other, perhaps less appealing, names have been applied to these macrocycles over the years. Ziegler named his cyclic tetramers, 'Mehrkernmethylene-phenol-verbindinge'; Hayers and Hunter favoured, 'cyclic tetrameric novolaks'; whilst Conforth opted for a more systematic name, '1:8:15:22-tetrahydroxy-4:11:18:25-tetra-*m*-benzylenes'.^{2,6,9} Although the calix[n]arene nomenclature was initially considered unacceptable by *Chemical Abstracts* and IUPAC, it eventually attained official status. The numbering of the basic structure of calix[4]arene allows for the naming of derivatives – a numbering system which has been extended for the larger calix[n]arenes (**Figure 1.1**).

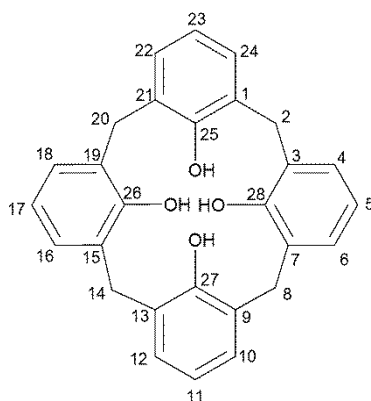


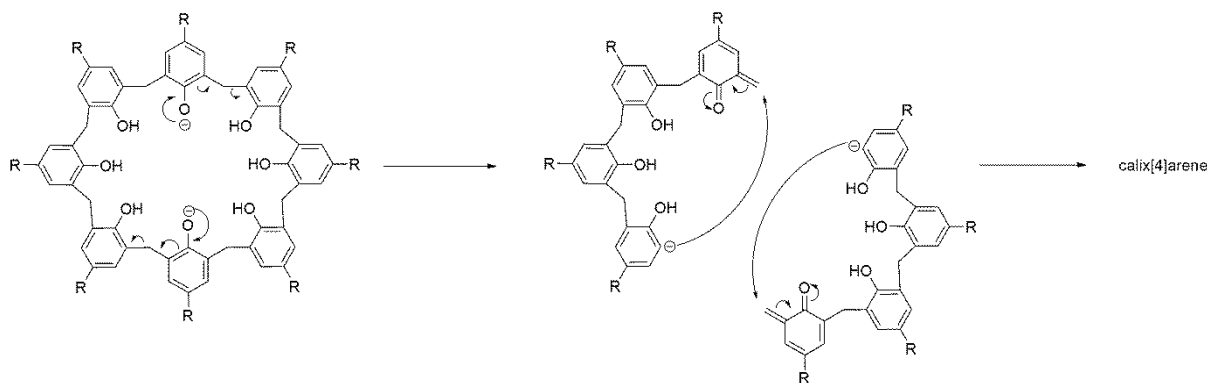
Figure 1.1: The structure and numbering of calix[4]arene

The complex names which arise from the strict application of this nomenclature are usually confined to experimental sections. However, in the case where all of the *para* positions are occupied by a single group, for example, abbreviations are typically applied. So that 5,11,17,23-*tert*-butyl-25,26,27,28-tetra-hydroxycalix[4]arene becomes simply *para-tert*-butylcalix[4]arene (**Scheme 1.1**).

1.3 Synthesis of calix[4]arenes

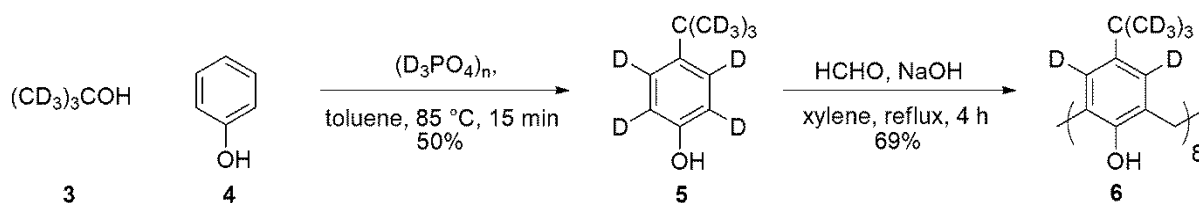
A detailed study of the reaction conditions was undertaken by Gutsche – particularly in regard to the amount and type of base present at each stage – and procedures were established which afforded reproducible access to the major calix[n]arenes (*i.e.* n = 4, 6 and 8). In the synthesis optimised for calix[4]arene, *para-tert*-butylphenol is heated with aqueous formaldehyde and an amount of sodium hydroxide corresponding to 0.045 equivalents with respect to *tert-butyl*-phenol. After heating at 120 °C for 1 to 2 hours, the mixture expands into a viscous mass called ‘the precursor’, which is subsequently heated in refluxing diphenyl ether for 4 hours.¹⁰ An analytical HPLC analysis of this ‘precursor’ reported by Vocanson and co-workers indicated the presence of at least 36 dibenzyl ether- and diphenylmethane-type compounds, in various states of oligomerisation. It is in the second stage of the reaction where linear tetramers are formed, which are believed to be the precursors to the cyclic tetramers. A similar analysis of the protocol developed for calix[8]arene indicated none of the corresponding linear octamers, and in this case the cyclic octamer is thought to be formed by the association of two linear tetramers which condense with the extrusion of water and/or formaldehyde.^{11,12}

There is evidence that some of the components in the ‘precursor’ mixture might be in equilibrium with one another, since the product distributions are found to be more dependent on the reaction conditions than the actual starting materials. In addition, it has been found that both *para-tert*-butylcalix[6] and [8]arene can be converted into *para-tert*-butylcalix[4]arene in high yields (*i.e.* ≥75%) by reacting them under the conditions developed for its synthesis (*i.e.* treatment with 0.01 equivalents of sodium hydroxide in refluxing diphenyl ether). This has been interpreted as forming the product of thermodynamic control (*i.e.* *para-tert*-butylcalix[4]arene) from the products of kinetic control (*i.e.* *para-tert*-butylcalix[6] and [8]arene). The mechanism by which this occurs for *para-tert*-butylcalix[8]arene has been the subject of some debate in the literature. Gutsche and co-workers suggested a mechanism in which the smaller calixarene might arise from a kind of intramolecular ‘molecular mitosis’ (**Scheme 1.2**).^{1,13}



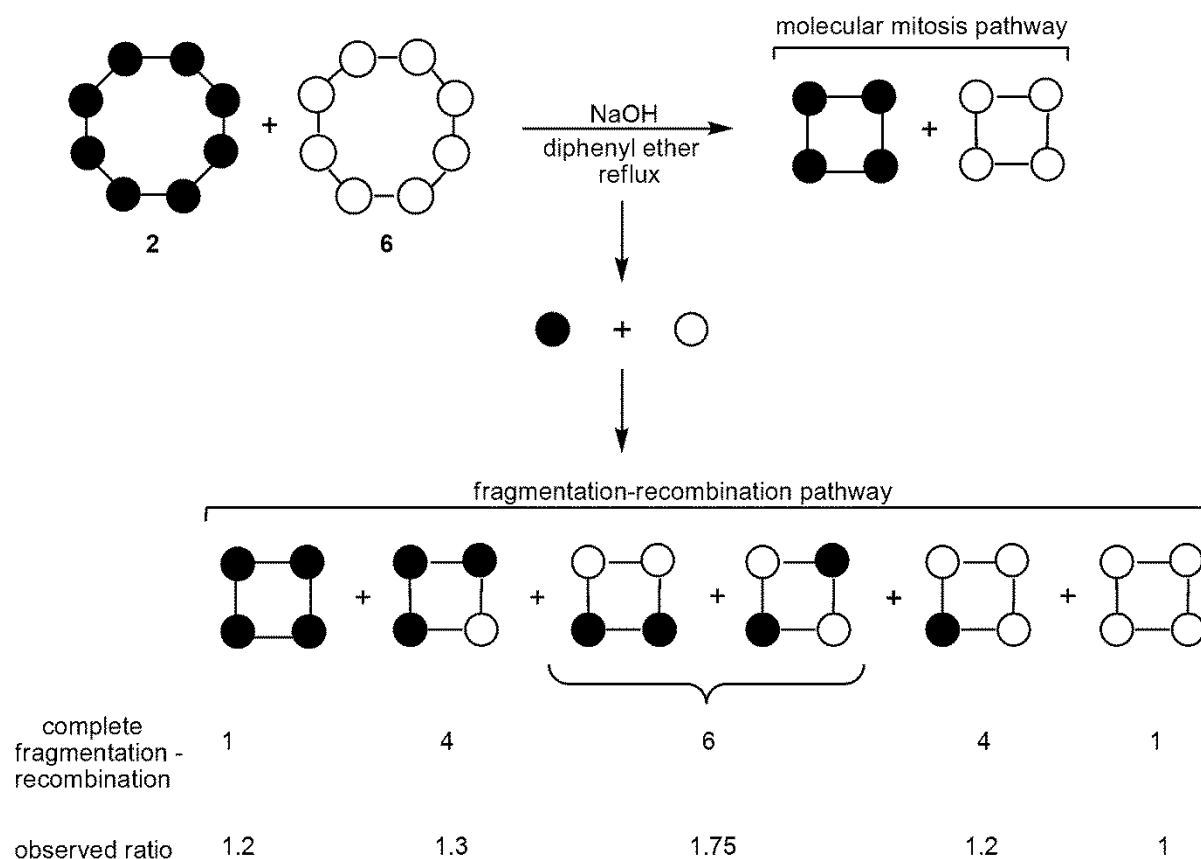
Scheme 1.2: The ‘molecular mitosis’ mechanism suggested by Gutsche to account for the formation of *para*-alkyl-calix[4]arenes from the corresponding *para*-alkyl-calix[8]arenes¹

In an effort to test this hypothesis, Gutsche designed a deuterium labelling study in which a 1:1 mixture of fully deuterated and fully protonated *para*-*tert*-butylcalix[8]arenes would be converted into a mixture of protonated and deuterated *para*-*tert*-butylcalix[4]arenes. The synthesis of the required fully deuterated *para*-*tert*-butylcalix[8]arene was achieved by first reacting d_9 -*tert*-butyl alcohol **3** with phenol **4** in deuterated polyphosphoric acid, followed by cyclisation to the corresponding calix[8]arene **5** under the standard literature conditions affording **6** in 69% yield (**Scheme 1.3**).



Scheme 1.3: The synthesis of deuterated *para*-*tert*-butylcalix[8]arene **6**¹³

With deuterated *para*-*tert*-butylcalix[8]arene **6** in hand, a 1:1 mixture with the protonated analogue was converted to *para*-*tert*-butylcalix[4]arene as a mixture of labelled and unlabelled materials. If the reversion reaction were to occur strictly by the ‘molecular mitosis’ pathway, a 1:1 mixture of deuterated and protonated calix[4]arenes would be expected. If however a fragmentation-recombination pathway were operational, a mixture of calix[4]arenes with both deuterated and protonated residues would result. Analysis of the product distribution by fast atom bombardment mass spectrometry (FAB-MS) indicated the presence of mixed calix[4]arenes, but not in the ratio expected for a complete fragmentation-recombination pathway (**Scheme 1.4**).



Scheme 1.4: The product distribution observed in Gutsche's deuterium cross-over study¹³

These results were interpreted by Gutsche to suggest that fragmentation-recombination is a major pathway in the formation of the smaller calix[4]arene, with the 'molecular mitosis' pathway playing a lesser role than initially supposed. It has been suggested that if one calix[8]arene undergoes 'molecular mitosis' for every three which undergo fragmentation-recombination, the expected ratio of products would be 1.0 : 1.1 : 1.64 : 1.1 : 1.0 – a distribution in reasonable agreement with the observed ratio. However it is also possible that a) the fragmentation-recombination might occur after the 'molecular mitosis' pathway has produced the fully protonated and deuterated calix[4]arenes and b) presumably this distribution could be explained without the need for 'molecular mitosis' if 2+2 or 3+1 cyclisations are considered. Thus, the exact course of events remains unclear.

In the synthesis optimised for *para-tert*-butylcalix[6]arene, a 10-fold increase in the amount of base is required compared to the reaction optimised for *para-tert*-butylcalix[4]arene. In addition it is found that potassium and rubidium hydroxides (atomic radii 2.35 and 2.5 Å respectively) afford higher yields of the cyclic hexamer – a result which suggests a template effect might be operational in its synthesis.¹⁴ The pathway for the formation of *para-tert*-butylcalix[6]arene is considered to be

less well understood than that for *para-tert*-butylcalix[4] or [8]-arenes, and a number of possibilities have been suggested. These have included the direct cyclisation of a linear hexamer; the cyclisation of a pair of hydrogen bonded linear trimers; and a fragmentation-recombination process starting with the cyclic octamer.

Syntheses optimised for the so-called ‘minor calix[n]arenes’ (*i.e.* $n = 5$ and 7) have also been developed, although the products are only available in low yields (*i.e.* 11-20%) after demanding and involved syntheses. The formation of these odd-numbered calix[n]arenes in lower yields has been attributed to the weaker intramolecular hydrogen bonding present between their phenolic units as compared with the major calix[n]arenes.^{15,16} For many years these three major and two minor calix[n]arenes were thought to be the only members of their family, until later studies by Gutsche and co-workers into the acid-catalysed synthesis of calix[n]arenes extended the series from $n = 9$ (the cyclic nonamer) all the way up to $n = 20$ (the cyclic eicosomer).¹⁷ By heating *tert*-butylphenol with *s*-trioxane and *para*-toluenesulfonic acid in chloroform, they were able to generate a mixture of calix[n]arenes (from $n = 4$ to $n = 20$) with a product distribution that was found to be dependent on the concentration of the reaction mixture (**Table 1.1**).

rxn. conc. %w/v	The percentage of <i>para-tert</i> -butylcalix[4 to 20]arenes in the final reaction mixture													
	[4]	[5]	[6]	[7]	[8]	[9]	[10]	[11]	[12]	[13]	[14]	[15]	[16]	[17-20]
1	13.9	8.8	19.3	21.1	19.9	8.6	3.7	1.7	1.1	0.0	0.0	0.0	0.0	0.0
5	5.1	3.7	14.3	23.6	26.2	12.8	5.0	2.9	1.3	1.3	1.1	0.3	0.2	0.0
10	2.5	1.8	10.2	25.0	23.4	13.8	7.0	4.8	3.4	2.8	2.2	1.0	0.5	0.8
20	1.5	1.2	7.5	25.2	22.5	13.6	7.8	5.8	4.3	3.4	2.8	1.8	1.1	1.0
30	1.2	1.0	6.5	23.9	22.2	13.1	7.2	5.7	4.3	3.6	3.3	2.4	1.9	2.7
40	0.9	0.7	4.9	23.7	21.8	12.5	6.9	5.7	4.9	4.1	4.2	2.5	1.9	4.5
50	0.8	0.7	4.3	22.3	19.9	11.8	6.9	6.3	5.1	4.9	4.7	3.7	2.9	5.1
60	0.7	0.6	3.9	21.9	19.3	11.8	7.1	6.1	5.1	4.8	4.3	3.4	2.2	8.1
75	0.6	0.5	3.6	19.9	17.6	11.0	6.8	5.9	5.1	5.1	5.0	3.7	2.8	11.5

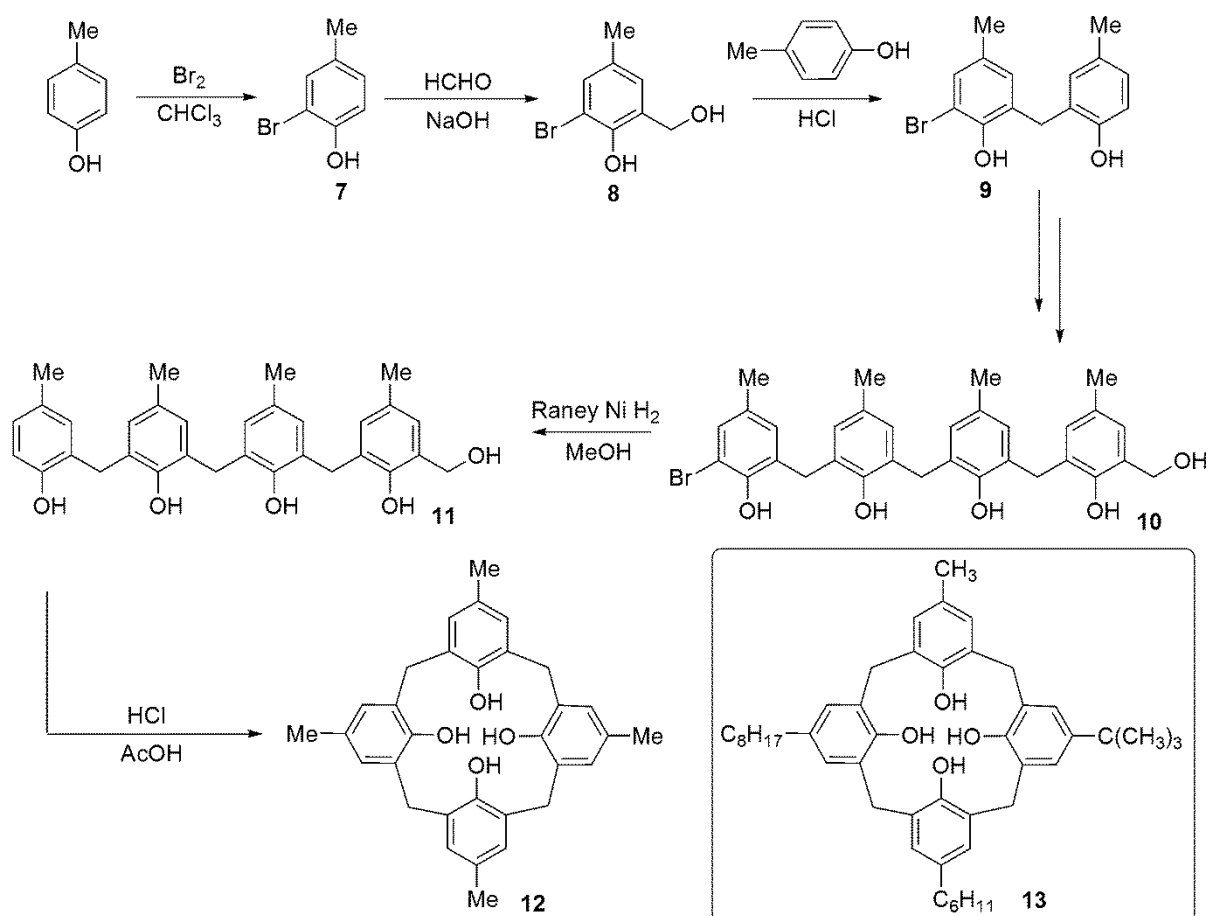
Table 1.1: The composition of calix[n]arenes formed at varying reaction concentrations as measured by w/v of *para-tert*-butylphenol in chloroform – obtained from peak area of one HPLC chromatogram of final reaction mixture (E. Merck C18 Lichrosphere column, 25 mm, 3.9 mm I.D., eluent A = MeCN-AcOH 99:1 v/v, eluent B = CH₂Cl₂-MTBE-AcOH 12:9:0.2 – Column eluted with 65:35 A-B v/v, flow rate: 2 mL min⁻¹)¹⁷

Although there have been no reports detailing the synthesis of a single calix[n]arene where $n \geq 9$, a Lewis acid-catalysed synthesis of *para-tert*-butylcalix[n]arenes developed in the Bew group allows for the isolation of *para-tert*-butylcalix[9]arene by preparative HPLC in high purity (*i.e.* $\geq 95\%$) and modest yield (*i.e.* 30%). Bew and co-workers found that reacting a dichloromethane solution of *para-tert*-butylphenol with *s*-trioxane (1.1 equivalents) and tin (IV)chloride (1 equivalent) at room

temperature for 15 hours afforded a mixture comprised of *para-tert*-butylcalix[8]arene (55%) and *para-tert*-butylcalix[9]arene (30%) along with small amounts (*i.e.* 15%) of linear oligomers and lower calix[*n*]arenes (*i.e.* *n* = 4-7). This protocol represents an improvement over Gutsche's original preparation, and it is hoped that such straightforward access should allow studies to be initiated into this calixarene.¹⁸

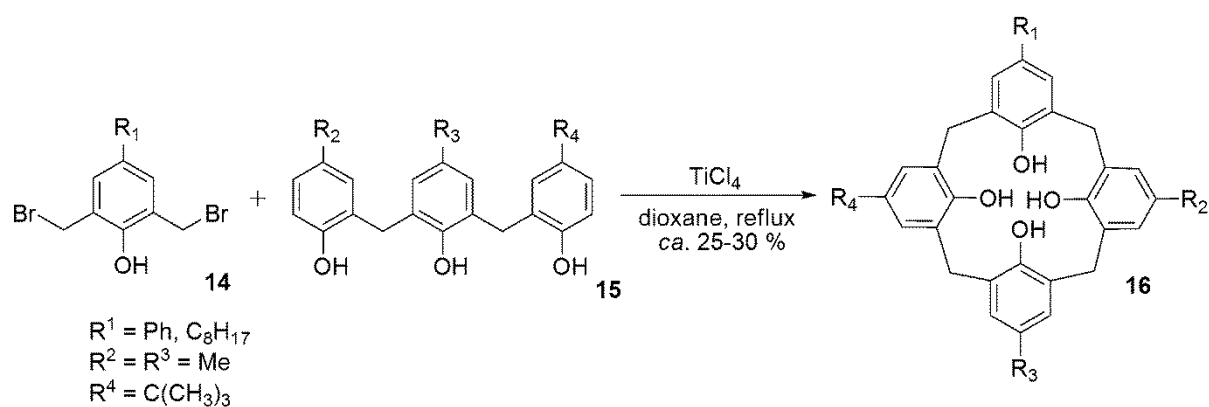
1.3.2 Synthesis of calix[*n*]arenes *via* stepwise and convergent protocols

Whilst the base catalysed syntheses of calix[*n*]arenes have proven to be the most efficacious, alternative protocols have been developed. These include the stepwise syntheses first described by Hayes and Hunter in the 1950's,⁹ and the convergent linking of fragments described by Böhmer in 1987.¹⁹ The stepwise synthesis involves the sequential addition of hydroxymethylene functions and aryl moieties to *para*-cresol blocked at one of its *ortho* positions by a bromine atom. After repeating this process a sufficient number of times, the bromine is removed by hydrogenolysis, and the resulting linear tetramer cyclised under high dilution in acidic conditions (*i.e.* using HCl and AcOH) to afford the cyclic tetramer **12** in an overall 17% yield from *para*-cresol (**Scheme 1.5**).



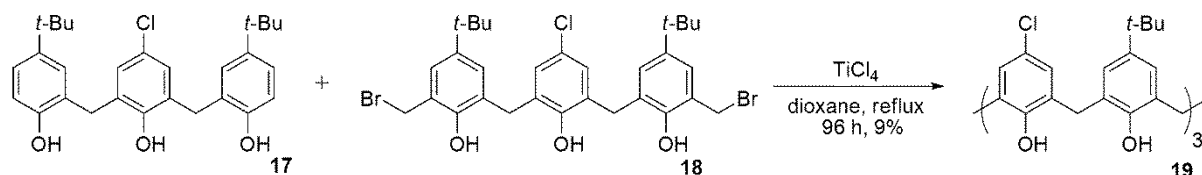
Scheme 1.5: The stepwise synthesis of calix[4]arenes first developed by Hayes and Hunter⁹

The advantage of such a procedure is the flexibility it affords, since differently substituted phenols may be employed at each stage of the oligomerisation process, leading to tetra-substituted calix[4]arenes not easily prepared by other means. In 1987, Volker Böhmer and co-workers were able to demonstrate this by their racemic synthesis of a series of inherently calix[4]arenes appended at the upper-rim with 4 different groups. The tetra-substituted calix[4]arene **13** for example was afforded in a 14% yield from the corresponding linear tetramer. However, the inefficient, time consuming and tedious nature of these syntheses coupled with the low yields inspired Böhmer to investigate a convergent protocol involving the condensation of linear fragments.²⁰ The reaction of a linear trimer **15** and a 2,6-*bis*-halomethylphenol **14** in the presence of titanium tetrachloride in a so-called 3 + 1 convergent synthesis is representative (**Scheme 1.6**).



Scheme 1.6: A 3 + 1 convergent synthesis of calix[4]arene **16** developed by Böhmer et al²⁰

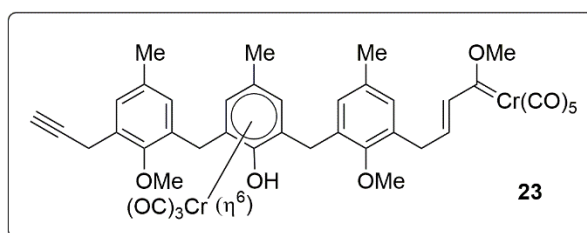
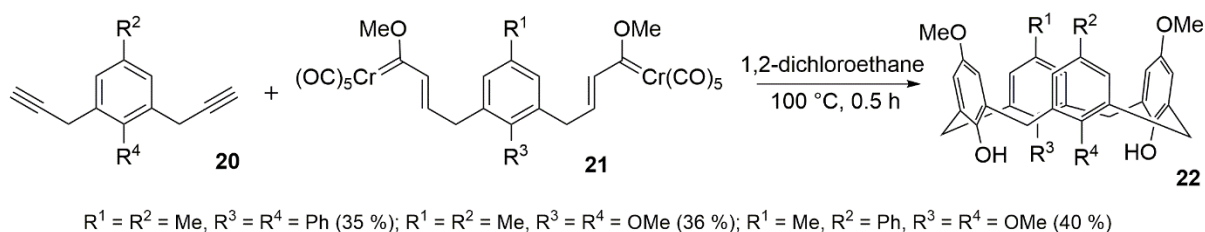
Böhmer reported that yields of cyclic tetramer were optimised when the cyclisation was carried out in dioxane at reflux with titanium tetrachloride as the promoter and possible template molecule (since high dilution was not required). This protocol retains much of the flexibility of the Hayes and Hunter procedure, whilst allowing for the racemic preparation of asymmetrically-substituted (\pm)-calix[4]arenes in much improved yields (*i.e.* up to 30%). The extension of this fragment based approach to calix[5], [6] and [8]arenes has also been reported.²¹⁻²³ In one such example, the 3 + 3 procedure reported by de Mendoza was found to afford the corresponding hexamer alternately functionalised with electron-withdrawing substituents in a 9% yield (**Scheme 1.7**).²¹



Scheme 1.7: A 3 + 3 convergent synthesis of calix[6]arene **19** reported by de Mendoza²¹

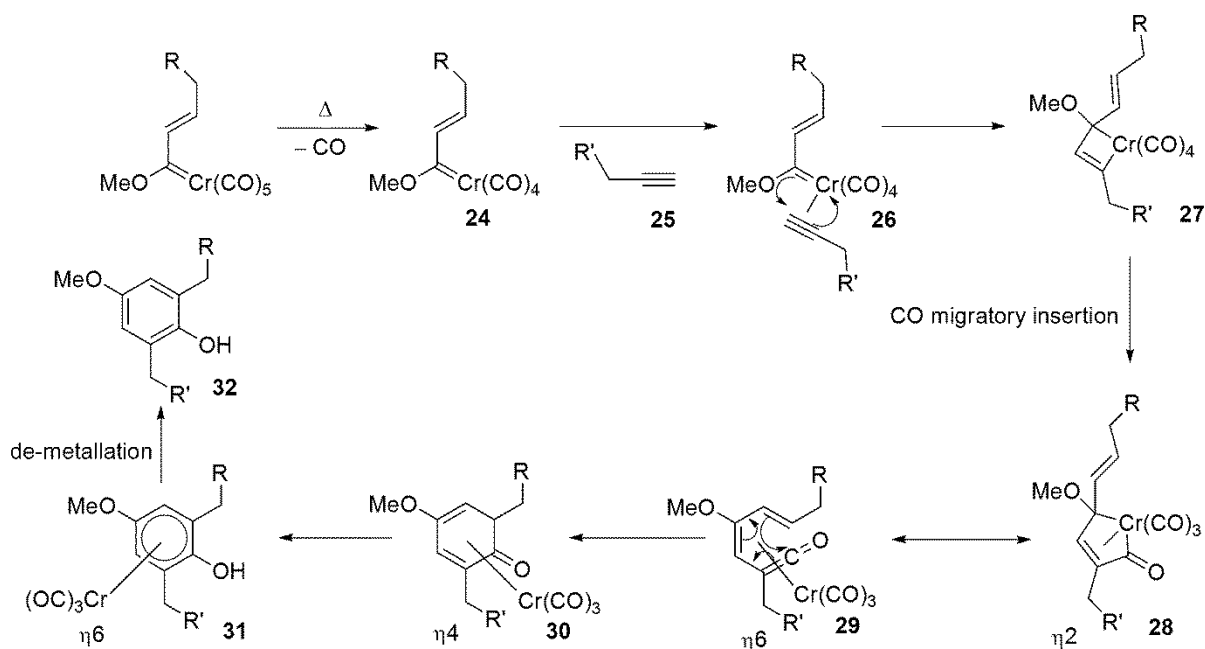
1.3.3 Synthesis of calix[4]arenes using Fisher carbene complexes

More recently, Wulff and co-workers have extended the scope of the convergent methodology to include the synthesis of calix[4]arenes *via* the triple annulation of Fisher carbene complexes with appropriate alkynes.²⁴ In what could be characterised as a 3 + 1 approach, *bis*-propargylbenzene **20** reacts with the carbene complex **21** in a process which forms two of the phenol rings of the calixarene in addition to the 16-membered ring of the macrocycle **22**. Since the reaction is thought to proceed *via* the intermediate carbene complex **23**, the concentration regime (*ca.* 2.5 mM) is critical to the success of the reaction. At 25 mM, the isolated yield of cyclic tetramer falls from 36 to 16% due to the formation of linear oligomers (**Scheme 1.8**).



Scheme 1.8: Wulff's synthesis of calix[4]arenes via the benzannulation reaction of Fisher Carbene complexes²⁴

The details of the mechanism by which the phenolic moieties are formed has been the subject of much study, and good evidence for the transient intermediates has now been established.²⁵ The reaction is thought to begin with the initial rate-limiting dissociation of CO; this allows for the coordination of the alkyne **25** to the chromium carbonyl complex **24**, and the subsequent formation of a transient metallocyclobutene intermediate **26**. It is at this stage that the regioselectivity is determined – usually by steric factors – and consistent with many organometallic insertions and additions, it is the least hindered end of the alkyne which couples to the carbene carbon.²⁶ Subsequent migratory insertion forms the η² metallocyclopentenone species **27**, which may also be described as the η⁶ vinyl ketene **29**. Such complexes are thought to rearrange thermally to afford η⁴ cyclic ketones **30**, which readily undergo tautomerisation to the corresponding η⁶ phenols **31**. The de-metallation of these arene-chromium complexes is generally facile, with weak donor solvents such as acetone sufficient to promote the process (**Scheme 1.9**).



Scheme 1.9: The general mechanism for the benzannulation reaction involving Fischer carbene complexes²⁶

One notable difficulty with this reaction is its atom efficiency with regard to the Cr(0) by-products – there is currently no mild protocol available to regenerate the Fischer carbene starting materials, and therefore no catalytic process.²⁷

1.4 The conformations of calix[4]arenes

In solution at room temperature, calix[4]arenes bearing free hydroxyl functions are conformationally mobile and may exist in four favoured conformations. These were first described by Cornforth in the 1950's, as a means of explaining the two products isolated from the reaction of *para-tert*-butylphenol and formaldehyde under Ziegler's conditions. It was not until the 1970's that variable temperature ¹H-NMR studies revealed the barrier to inversion was not as great as had been initially supposed on the basis of molecular models, which suggested that therefore Cornforth's original analysis must have been incorrect. *Para-tert*-butylcalix[4]arene was found to undergo conformational inversion at *ca.* 150 s⁻¹ at 60 °C in CDCl₃ ($\Delta G^\ddagger = 15.7$ Kcal mol⁻¹) as calculated from the coalescence temperature of the two doublets which arise from the methylene protons.^{28,29} These conformations, designated by Cornforth are based on the number of aryl groups projecting upwards (u) or downwards (d) relative to the mean plane defined by the methylene functions, were later named by Gutsche as 'cone' (u,u,u,u), 'partial cone' (u,u,u,d), '1,2-alternate' (u,u,d,d) and '1,3-alternate' (u,d,u,d) (**Figure 1.2**).

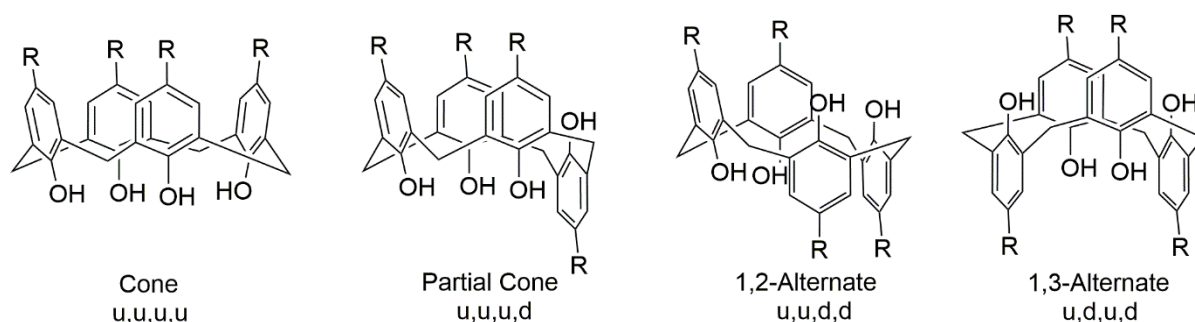


Figure 1.2: The conformations of calix[4]arenes¹

Of these four possible conformations, it is the ‘cone’ which is favoured in solution due to the strong intramolecular hydrogen bonding present between the hydroxyl functions on the lower-rim.³⁰ Interconversion between the cone (u,u,u,u) **33** and its mirror image inverted cone conformer (d,d,d,d) **34** is possible, although slow at room temperature, and is presumed to occur *via* an ‘oxygen-through-the-annulus’ type pathway. It has been suggested that this process might occur *via* a concerted pathway (thereby maintaining the circular hydrogen bonding),³¹ but computational studies have indicated that a so-called ‘broken chain pathway’ is more likely to be operative (**Figure 1.3**).³²



Figure 1.3: The interconversion between the cone and inverted cone conformers¹

Upon heating *para-tert-butylcalix[4]arene* to $\geq 60\text{ }^{\circ}\text{C}$ in CDCl_3 , the pair of doublets ($J = 13\text{ Hz}$) arising from the non-equivalent geminal methylene protons (*i.e.* H_a and H_b) coalesce into a sharp singlet as a result of fast exchange between the two cone conformers (**Figure 1.3**). Although this interconversion is slow at room temperature, it is important to be able to lock the conformation of a given calix[4]arene for a given application. This can be readily achieved by etherification or esterification at the lower-rim with a carbon chain three or more units in length. The resulting derivatives are conformationally stable – even at elevated temperatures – since such a chain cannot pass through the annulus.³³ The exact conformation(s) produced in a given alkylation reaction are found to be dependent on the groups which are appended. For example, the allyl ether of *tetrahydroxycalix[4]arene* is locked in the partial cone conformation whilst the propyl ether is locked in the cone conformation.³⁴

Whilst X-ray crystallography gives the most conclusive means for characterising the conformation of an alkylated calix[4]arene, it is ^1H - and ^{13}C -NMR spectra that provide a simpler and more accessible alternative. An inspection of the ^1H -NMR spectra of the most commonly encountered conformations reveals characteristic splitting patterns for the methylene protons. In the cone conformation, a cone calix[4]arene with C_{4v} symmetry will give rise to a pair of doublets for its methylene bridge protons with a $\Delta\delta$ value (the difference in chemical shift between high and low field doublets) of *ca.* 0.9 ± 0.2 ppm. In contrast, a $\Delta\delta$ value of 0 is observed for a calix[4]arene in the 1,3-alternate conformation with D_{2d} symmetry, and the pair of doublets is replaced by a sharp singlet. In the partial cone and 1,2-alternate conformations the splitting patterns become more complex, but are still characteristic.

In a similar way, de Mendoza and co-workers have shown that the ^{13}C -NMR resonance for the methylene bridges also provide useful information about the conformations of calix[4]arenes.³⁵ When the phenolic groups on either side of the methylene bridges are *syn* (e.g. in the cone conformation) the ^{13}C -NMR resonance occurs at *ca.* δ 31, whilst when they are *anti* (e.g. in the 1,3-alternate conformation) the resonance occurs at *ca.* δ 37 ppm. This observation provides a highly useful means of characterising substituted calix[4]arenes which give rise to similar ^1H -NMR signals for the methylene bridges in both cone and 1,3-alternate conformations. These spectral characteristics are summarised below (**Table 1.2**).

Conformation	Multiplicity of Ar-CH₂-Ar in ^1H-NMR	Chemical shift of Ar-CH₂-Ar in ^{13}C-NMR
Cone	One pair of doublets	Ca. 31 ppm for syn-orientation
Partial cone	Two pairs of doublets (1:1 ratio) or one pair of doublets and one singlet (1:1 ratio)	Ca. 31 ppm for syn-orientation Ca. 37 ppm for anti-orientation
1,2-Alternate	One pair of doublets and one singlet (1:1 ratio)	Ca. 31 ppm for syn-orientation Ca. 37 ppm for anti-orientation
1,3-Alternate	One singlet	Ca. 37 ppm for anti-orientation

Table 1.2: Characteristic ^1H -NMR and ^{13}C -NMR data for the methylene bridges of calix[4]arenes in all four possible conformations³⁵

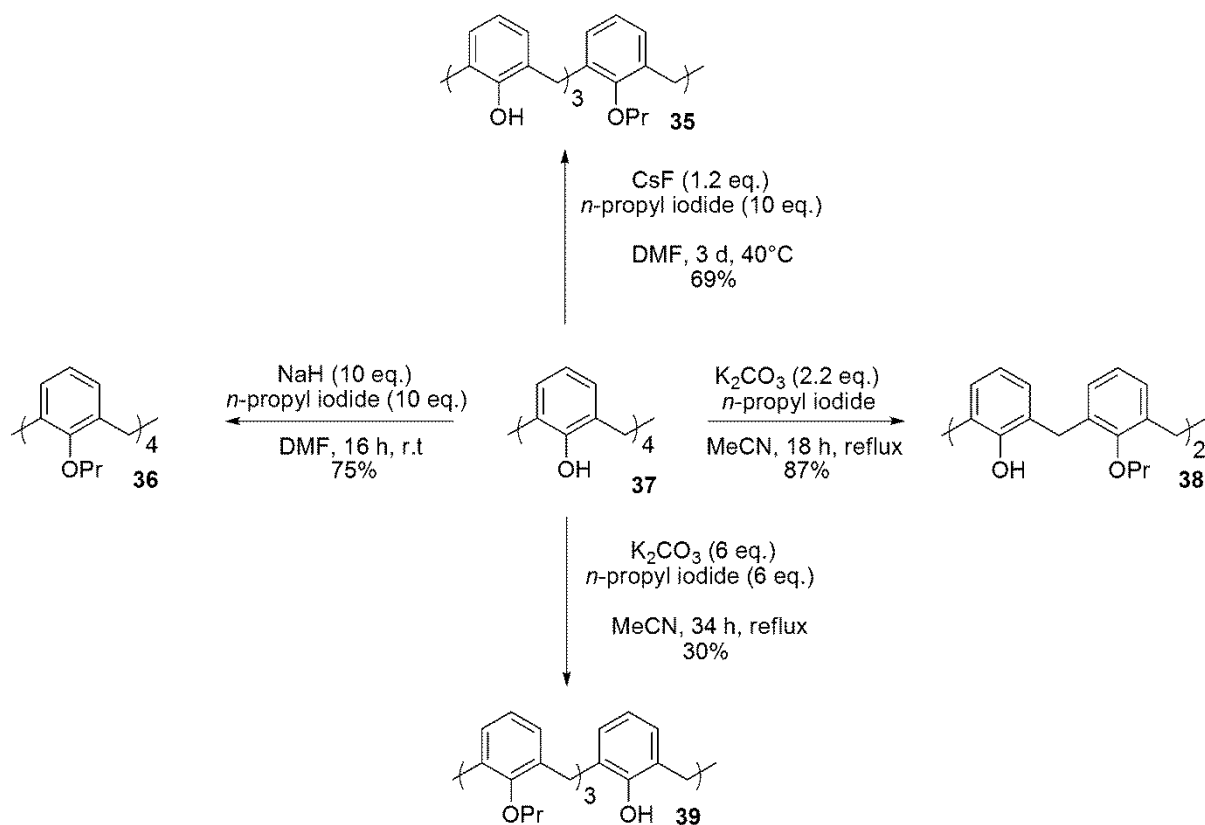
It is noteworthy that the ^{13}C -NMR chemical shifts of a wide range of derivatives were found to be strongly independent of either the *para* substituent or the phenolic protecting group. The solvent

employed for the analysis also had little effect, suggesting that these differences are more strongly steric than electronic in origin.

On moving to the larger calix[n]arenes, the number of possible conformations quickly increases. Whilst calix[4] and [5]arenes both have only four true up/down conformers, calix[6]arene has eight and calix[8]arene has sixteen. A variable temperature $^1\text{H-NMR}$ study of the conformational characteristics of a series of ethers and esters of calix[6] and [8]arenes revealed these compounds to be much more flexible than the corresponding calix[4]arene derivatives.²⁹ This is due to the larger annuli present in these systems, which allow relatively low barriers to conformational inversion at room temperature. If the ether groups are large enough however, conformational freezing can be observed. In the $^{19}\text{F-NMR}$ of the hexakis(trifluoroacetate) of *para-tert*-butylcalix[6]arene for example, the broad singlet arising from the trifluoroacetate groups at 20 °C is resolved into eight sharp lines at -40 °C. A comparison with the hexakis(trifluoroacetate) of *para-tert*-octylcalix[6]arene indicated that, for this system, inversion in the *tert*-butyl case was taking place *via* a 'para substituent through the annulus' pathway, since the barrier to inversion was measured to be 4.4 Kcal mol⁻¹ higher.

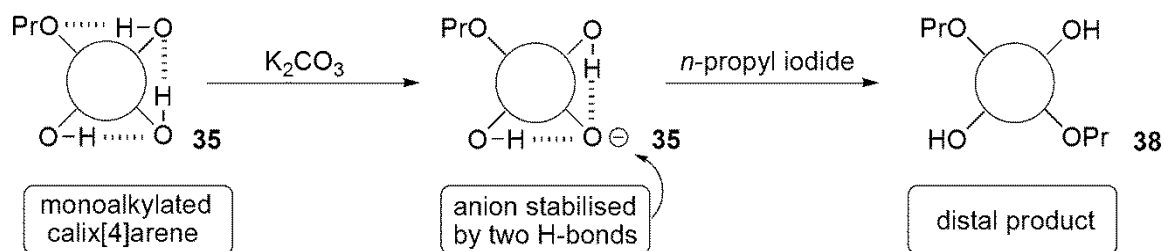
1.5 Functionalisation of calix[4]arenes

The calix[4]arene that is derived from *para-tert*-butylphenol is already functionalised with four hydroxyl groups at its lower-rim, and as a consequence the esters were some of the first derivatives to be prepared.³⁴ In the reactions with acid halides and sodium hydride, it is generally found that acylation goes to completion if the acid halide is used in excess. Similarly, in the reactions with acid halides and AlCl_3 or acid anhydrides and H_2SO_4 , tetra-functionalised products are the norm. Exceptions have been reported however, and in the reaction of *para-tert*-butylcalix[4]arene, sodium hydride and excess benzoyl chloride, only the A,C-diester is formed.³⁶ These findings have been exploited as a means of inducing selective functionalisation at the upper-rim, since the phenolic moieties are more reactive towards electrophiles than their corresponding esters.³⁷ Studies into the etherification of calix[4]arenes initially focused on the identification of methods for their partial substitution. Employing bases weaker than sodium hydride and/or limiting the amount of alkylating reagent has allowed for the preparation of a series of mono-, di-, tri- and tetra-substituted ethers at the lower-rim. Tetraalkylation is usually affected by the use of sodium hydride and an excess of alkylating reagent – see for example **36** in *Scheme 1.10*.³⁸



Scheme 1.10: Procedures for the selective O-propylation of calix[4]arene³⁴

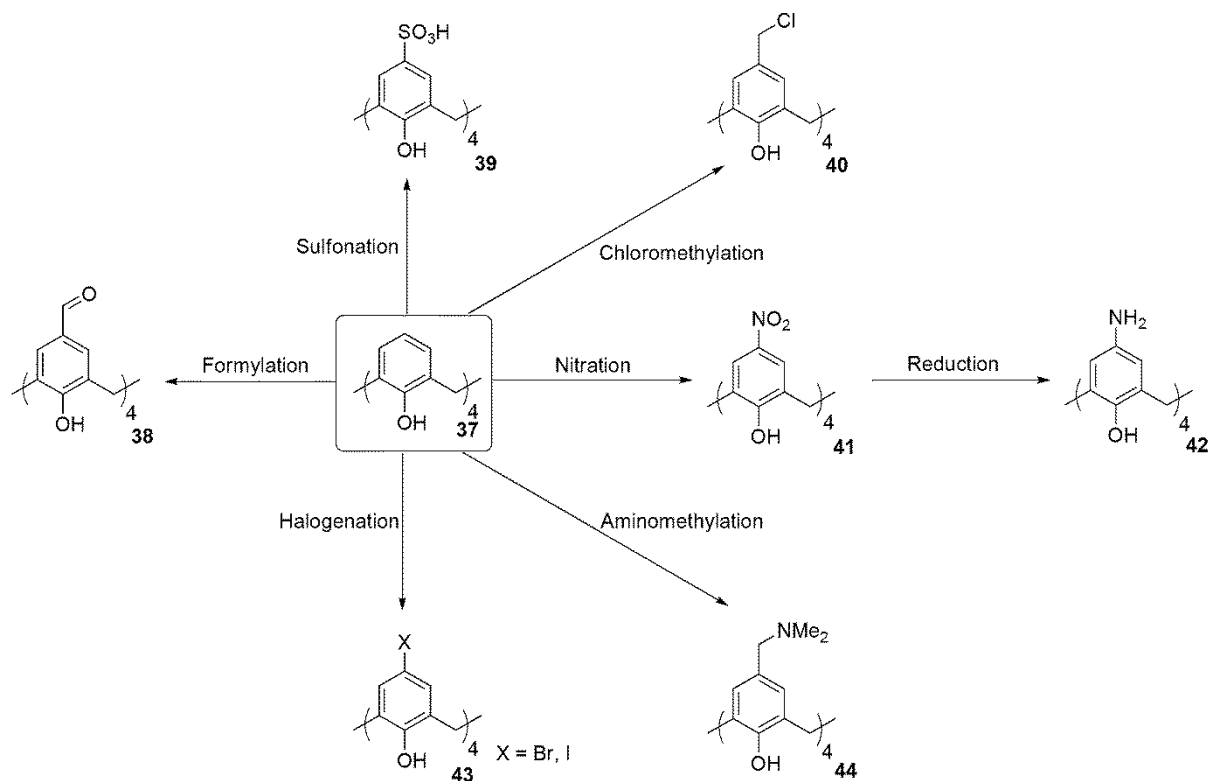
Di-ethers of the form **38** may be either be proximal (*i.e.* A,B) or distal (*i.e.* A,C as in **38**). The distal ethers are formed preferentially under most conditions, and thus their synthesis is generally more readily achieved than the corresponding proximal products. The A,C-selectivity observed in the O-propylation utilising 2.2 equivalents of potassium carbonate as the base has been explained on the basis of the mechanism.³⁹ Thus, following mono-O-alkylation of calix[4]arene **35**, deprotonation of the hydroxyl group directly opposite the alkyl ether affords a mono-anion stabilised by two hydrogen bonds. This interaction holds the calix[4]arene in the cone conformation and directs the second electrophile (**Scheme 1.11**).



Scheme 1.11: Rienhoudt's rationalisation for the observed A,C-selectivity³⁹

If more than two equivalents of potassium carbonate are used, further deprotonation is possible and mixtures of alkylated products are obtained.

A wide range of procedures for the functionalisation of the aryl upper-rim of calix[4]arenes have been reported. Upper-rim functionalisation of the calix[4]arene derived from *para-tert*-butylphenol has been achieved by a two-step *isop*-substitution for example, in a procedure which allows for its nitration using a mixture of HNO₃/AcOH in high yield **41** (*i.e.* 88%).^{40,41} More generally however, the *tert*-butyl substituent is first removed *via* a Lewis acid catalysed transalkylation in the presence of phenol as a *tert*-butyl acceptor molecule. The free *para*-positions are then accessible for functionalisation by electrophilic aromatic substitution, and a wide array of functional groups have been introduced (*i.e.* I, Br, NO₂, SO₃H, SO₂Cl, CHO, COAr, CH₂Cl, CH₂NMe₂).^{1,42} With these groups in place subsequent derivatisation is possible, and this allows for the construction of intricately functionalised calix[4]arenes (**Scheme 1.12**).

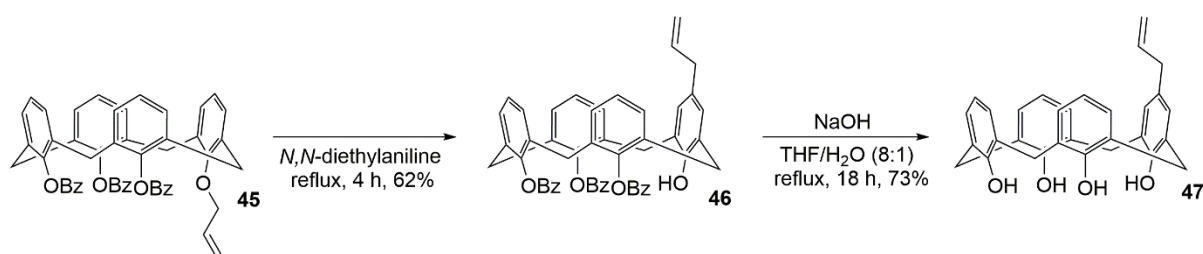


Scheme 1.12: General methods for the upper-rim functionalisation of calix[4]arene **37**^{42,43}

The introduction of a halide (*i.e.* I or Br) at the upper-rim allows for further derivatisation *via* transition metal coupling reactions (*i.e.* Suzuki, Sonogashira, Ullmann or Heck), whilst the introduction of amine or carboxylic acid functionalities has allowed peptide couplings to be performed.^{44–46}

1.5.2 Selective upper-rim functionalisation of calix[4]arenes

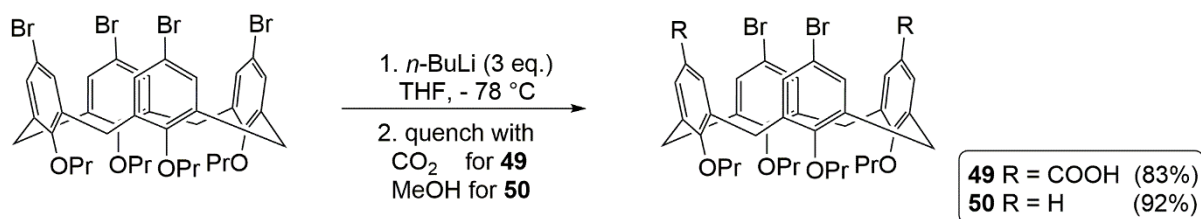
The selective functionalisation of the calix[4]arene motif has been a key theme within the field for many years, since such highly functionalised structures have the potential to act as enzyme mimics, optical sensors, complexing agents and HPLC stationary phases (to name but a few examples, see section 1.5).^{47,48} One of the first examples of such a synthetic method was reported by Gutsche, and took advantage of the result that when *tetra*-hydroxy-calix[4]arene is treated with excess benzoyl chloride in pyridine, only the tribenzoate is obtained. Reacting the resulting calix[4]arene with allyl bromide, a subsequent Claisen rearrangement and hydrolysis afforded *mono*-allylcalix[4]arene **47** – and after further manipulations, a series of monofunctionalised calix[4]arenes were obtained (**Scheme 1.13**).⁴⁹



Scheme 1.13: Gutsche's synthesis of *mono*-allylcalix[4]arene **47** via the Claisen rearrangement of allyl ether **46** and basic hydrolysis⁴⁹

The main disadvantage with this route is the relatively high temperature employed for the Claisen rearrangement (*i.e.* > 200 °C). More general (and far milder) protocols have been developed which take advantage of the increased reactivity of phenols over their corresponding ethers and esters towards electrophilic aromatic substitution. Since methods for the selective partial functionalisation of the lower-rim have been found, the subsequent partial functionalisation at the upper-rim has proven to be straightforward in many cases.^{39,42} For example, the bromination of 25,27-di-hydroxy-26,28-di-*n*-propoxycalix[4]arene with elemental bromine in dichloromethane affords an excellent yield of the corresponding 5,17-dibromo substituted product **49** (*i.e.* 95%).⁵⁰

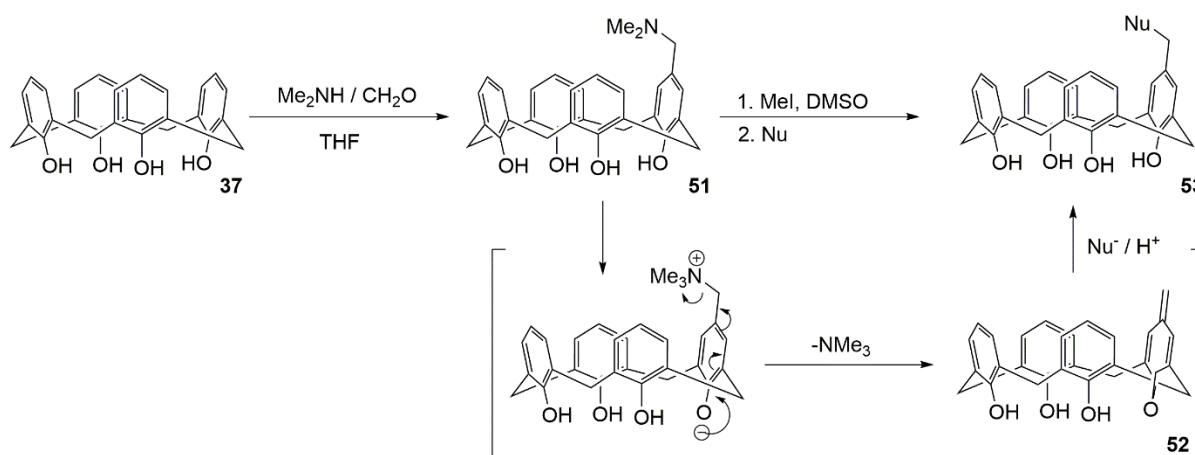
In a complementary approach, Larsen and co-workers have described a chemoselective bromine to lithium exchange on 5,11,17,23-tetrabromo-25,26,27,28-tetrapropoxy-calix[4]arene **48**, with *n*-butyllithium in tetrahydrofuran. Employing an excess of *n*-butyllithium (*i.e.* 3 *eq.*), it was found that the 5,17-dilithiated species was formed selectively, since subsequent reactions with carbon dioxide or methanol produced high yields of the corresponding substitution products (*i.e.* **49** and **50** in 83 and 92% respectively). *Tetra*-substituted products however, were only observed when excess *t*-butyllithium was employed for the Br-Li exchange (**Scheme 1.14**).⁵¹



Scheme 1.14: The selective bromine to lithium exchange reported by Larsen⁵¹

This method provides a convenient means of generating *tetra*-substituted calix[4]arenes with AABB substitution at the upper-rim.

The direct preparation of calix[4]arenes substituted with one, two or three groups at the upper-rim without first preparing the required esters such as **45** or ethers has been met with more difficulty, and as a result there are only a handful of procedures which can afford, selectively, calix[4]arenes by this route. Be that as it may, an important example of this type of protocol for the synthesis of *mono*-functionalised calix[4]arenes was reported by Gutsche *et al.*, and involves the aminomethylation of calix[4]arene **37** with formaldehyde (2 eq.) and dimethylamine (2.2 eq.) in tetrahydrofuran at room temperature for 3 hours. Under these conditions, only the monoamine is obtained since this product is highly insoluble in the reaction medium and precipitates from solution before further reaction can occur. This fortuitous result allowed for the preparation of a series of derivatives *via* treatment with methyl iodide in dimethyl sulfoxide to form the quaternary ammonium salt, and subsequent reaction with a range of nucleophiles (*i.e.* NaCN, NaOPh, NaOEt) presumed to occur *via* a quinonemethide intermediate **52** (**Scheme 1.15**).⁵²



Scheme 1.15: Gutsche's quinonemethide route to *mono*-functionalised non-configurationally confined calix[4]arenes⁵²

Recent work in the Bew group has extended the usefulness of this approach by identifying conditions which allow for the high yielding O-propylation (*i.e.* 69%) of the monoamine **51**, thereby locking it in the cone conformation.⁵³ Subsequent functional group manipulations allowed for the

preparation of a series of synthetically useful derivatives. These results are discussed in greater detail in Chapter 3.

1.6 Applications of calix[n]arenes

Much of the interest in calix[n]arene chemistry has been generated by the prospect of utilising these macrocycles for practical applications.¹ Indeed, some of the first investigations into their chemistry were motivated by the desire to obtain a better understanding of the process which formed Bakelite, the first production plastic.^{2,4} Whilst the parent *para-tert*-butylcalix[n]arenes have found limited application, the great variation in structure made possible by functionalisation of the upper and/or lower-rims has allowed the design and synthesis of a wide range of complexing agents, HPLC stationary phases, optical and fluorescent sensors, negative resists for electron beam lithography, and ion-sensitive electrodes.^{46,54–57} Many of these applications take advantage of the ability of the calix[n]arenes to bind small molecules or metal ions within their cavities, whilst those which do not tend to use the calix[n]arenes as ‘scaffolds’ on which to place reactive or useful functionalities in specific orientations.

1.6.1 Calix[n]arenes for the separation of metal ions

One of the earliest patents describing an application of *para-tert*-butylcalix[8]arene was issued in 1984, and was concerned with its use in the recovery of caesium from nuclear waste – and in particular the radioactive isotope ¹³⁷Cs, which has a half life of 30 years.^{58,59} Such selective recovery of ¹³⁷Cs (and ⁹⁰Sr – half life of 27.7 years) from the long-lived radionuclides would remove around 90% of the heat produced by these high activity wastes, and facilitate their disposal. Since the lanthanides and actinide elements are chemically very similar, their separation *via* conventional liquid-liquid extraction or chromatography is found to be very challenging – and as a result, much research effort and funding has been directed towards identifying ion-selective complexing agents.⁶⁰ Early investigations were directed towards the use of cobalt dicarbollide – a boron cluster species featuring a trivalent pi-bonded cobalt ion. However, as the cation exchanging ability of this compound was found to strongly decrease with increasing acidity or sodium ion concentration, its application in the nuclear industry has been limited.⁶¹ More recent efforts in this area have focused on calix[4]arene-crown complexes exemplified by **55** – in part because of the ability to ‘fine tune’ their structures and also for the relative ease with which they can be attached to solid supports. For example, Ungaro and co-workers have described the efficient chromatographic separation of potassium and caesium ions *via* the immobilisation of calix[4]arene-crown **56** onto silica gel (**Figure 1.4**).⁵⁸

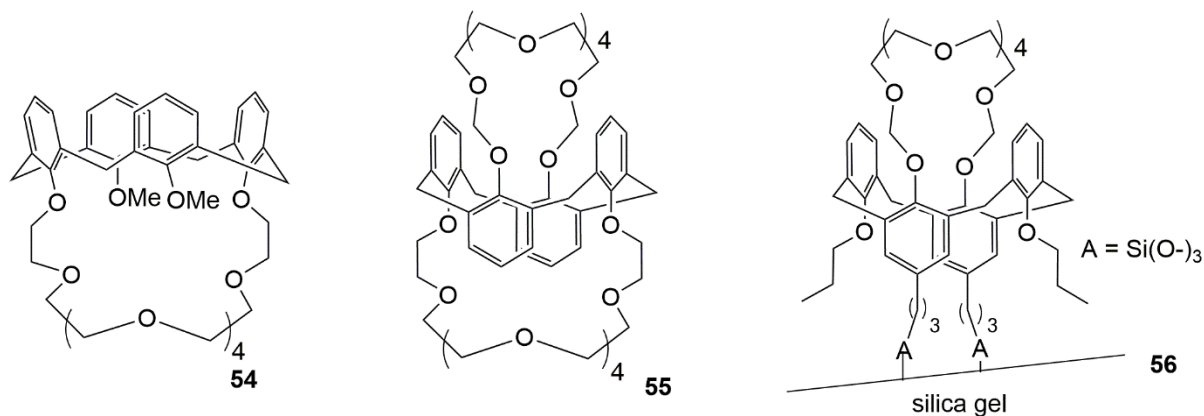


Figure 1.4: Calix[4]arene-crown ethers used for the selective complexation of caesium⁵⁸

After some optimisation, the Italian group were able to observe a selectivity factor of $\alpha_{K^+/Cs^+} = 3.29$ for the separation of potassium and caesium ions (eluent MeOH, 5 μm particle size, 15 x 0.4 cm I.D., flow rate 0.4 mL min⁻¹, r.t., $t_0 = 2.6$ min., conductivity detector). This result is significant since the separation of the relatively small amounts of radioactive caesium from the potassium and sodium ions is a necessary step in many nuclear waste management schemes.⁶²

Ion-selective chelators based on calix[n]arenes have also been developed for the separation of other nuclides.⁶³ Arnaud-Neu and co-workers found that the ability of calix[6]arene amides such as **57** to differentiate between Sr²⁺ and Na⁺ was influenced significantly by the size of calix[n]arene as well as the functionalisation at the lower-rim. In the extraction of metal picrate salts from water into dichloromethane, the *para*-dealkylated hexaamide **57** was able to extract 45% of the Sr²⁺ ions, whilst by comparison only 4.8% of the Na⁺ ions were complexed (**Figure 1.5**).

R = CH₂CONEt₂

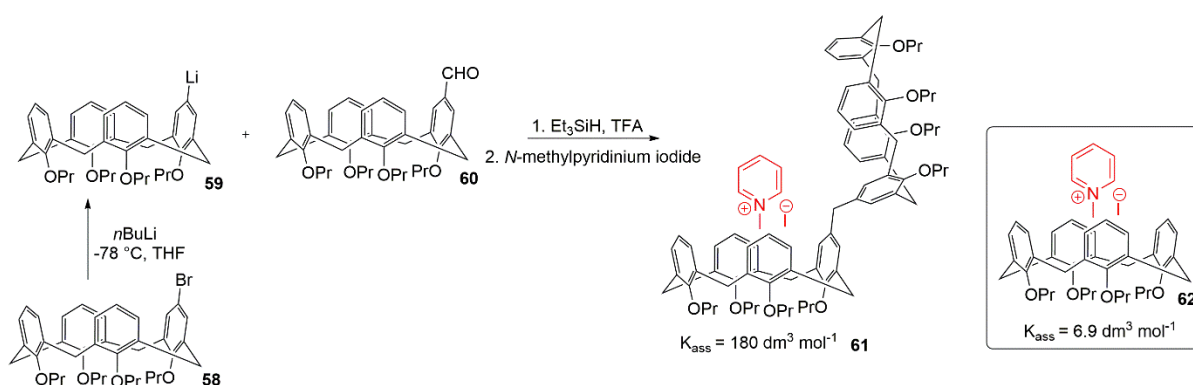
Percentage extraction (%E) of alkali and alkali earth picrates from water into dichloromethane solution using the calix[6]arene amide 57									
Li ⁺	Na ⁺	K ⁺	Rb ⁺	Cs ⁺	Mg ²⁺	Ca ²⁺	Sr ²⁺	Ba ²⁺	
%E=	5.2	4.8	7.5	17.2	45.4	2.6	25.7	45.0	58.0

Figure 1.5: Arnaud-Neu's extraction of metal picrates from water into dichloromethane⁶³

This result represented an improvement in terms of selectivity over dicyclohexyl-18-crown-6 (at the time considered as one of the best selective Sr²⁺ extractants) which has an extraction selectivity (*i.e.* %E(Sr²⁺)/%E(Na⁺)) equal to 9 under these conditions, compared with $S = 10$ for the calix[6]arene amide **57**.

1.6.2 Multicalix[4]arenes for the complexation of metal ions and small molecules

Whilst a large number of research programs have been directed towards the development of calix[4]arenes for the separation of cations and anions, it is interesting to note that most of these studies have focused on the monocalix[n]arenes (*i.e.* those comprised of only one calix[n]arene unit), whilst compounds which feature several linked units are relatively few in number.⁶⁴ This is interesting since multicalixarenes of this type might be expected to show synergistic effects which result from having several proximate cavities, and therefore in this way the receptor properties of an individual component calix[n]arene might be amplified. Indeed, the design and synthesis of dimeric calix[4]arene receptors which do display these synergistic properties has been presented in the literature by a number of research groups.⁶⁴ One early example of such a receptor was described by Shinkai and co-workers, who reported that *bis*-calix[4]arene **61** binds the *N*-methylpyridinium cation with an association constant of about $180 \text{ dm}^3 \text{ mol}^{-1}$ – a value in large excess of that measured for the monomeric **62**, which binds the same guest with the much lower association constant of about $6.9 \text{ dm}^3 \text{ mol}^{-1}$ (Scheme 1.16).⁶⁵



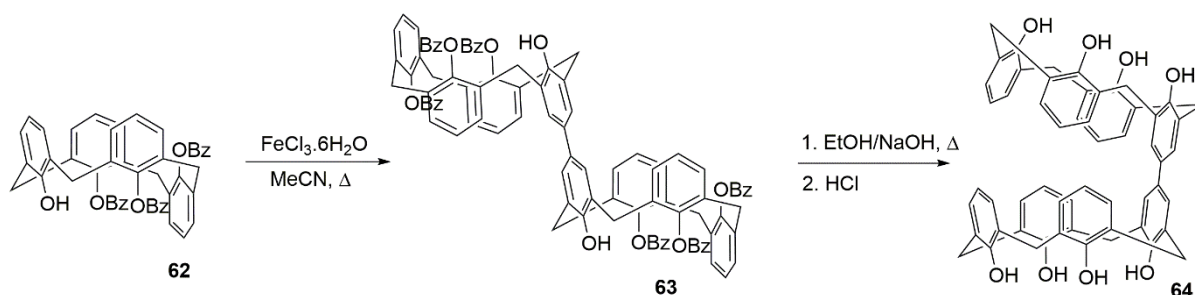
Scheme 1.16: Shinkai's synthesis of the dimeric calix[4]arene **61**⁶⁵

The synthesis of **61** was achieved *via* the addition of lithiated **59** (obtained *via* lithium-halogen exchange of **58**) to the formyl group of **60**, followed by a triethylsilane-trifluoroacetic acid mediated reduction of the resulting secondary alcohol. This two-step process resulted in the formation of a methylene bridge linking the upper-rim of both calix[4]arene units (although the yield was not reported).

With the earliest examples of such multicalix[4]arenes exemplified by **61** typically showing improvements in binding affinity for their guests over their monomeric analogues, a number of research groups initiated projects directed at their synthesis for evaluation as complexing agents. Since a particular focus has been placed on the variation of the length, type and geometry of the bridge employed to link the calix[4]arene units, the following section is structured accordingly.

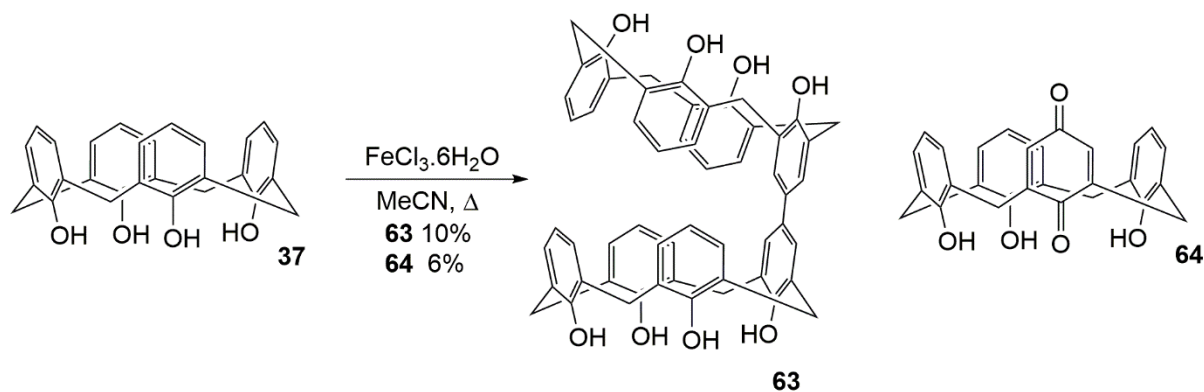
1.6.2.1 Multicalix[4]arenes linked directly *via para*-phenolic carbon atoms

The first synthesis of a so-called 'bridgeless' (*i.e.* directly coupled aryl-to-aryl) calix[4]arene dimer was reported by Neri and co-workers in 1998.⁶⁶ Motivated by the possibility of producing compounds which might have application in the purification of fullerenes, the Italian group were able to synthesise **64** in a 55% overall yield *via* the oxidative coupling of the readily available tribenzoate **62** followed by basic hydrolysis (**Scheme 1.17**).



Scheme 1.17: Neri's synthesis of the 'bridgeless' bis-calix[4]arene *via* oxidative coupling of **62**⁶⁶

By contrast, attempts at the direct oxidative coupling of *tetra*-hydroxycalix[4]arene **37** under the same conditions only led to the formation of **65** in a 10% isolated yield, with calix[4]monoquinone **66** and polymeric coupling/oxidation products comprising the remaining mass balance (**Scheme 1.18**).

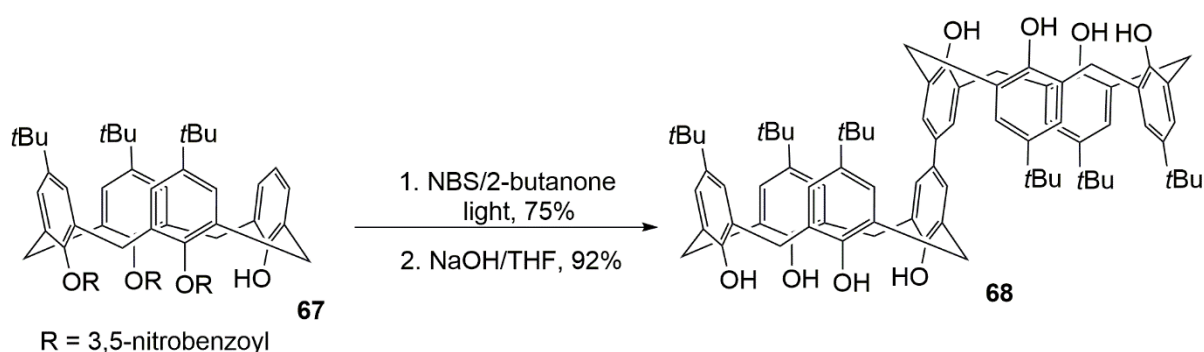


Scheme 1.18: Neri's synthesis of **65** *via* the direct coupling of tetra-hydrocalix[4]arene **37**⁶⁶

Investigations into the derivatisation of **65** were also undertaken by Neri *et al*, and they found that O-alkylation with a range of electrophiles (*i.e.* *n*-propyl iodide, 2-bromoethyl ether and *para*-*tert*-butylbenzyl bromide) afforded good yields (*i.e.* 55 to 60%) of the corresponding cone-cone bis-calix[4]arenes when sodium hydride was used as the base in anhydrous *N,N*-dimethylformamide.⁶⁷

In an extension of this work, de Mendoza and co-workers were able to synthesise the related 'bridgeless' calix[4]arene dimer **68** *via* a presumed radical pathway. Treatment of the *tris*-*O*-3,5-dinitrobenzoyl calix[4]arene **67** with *N*-bromosuccinimide in 2-butanone, under ambient light,

afforded the intermediate bis-calix[4]arene in a 75% isolated yield. A subsequent basic hydrolysis afforded the dimeric receptor **68** in a 92% yield (**Scheme 1.19**).⁶⁸

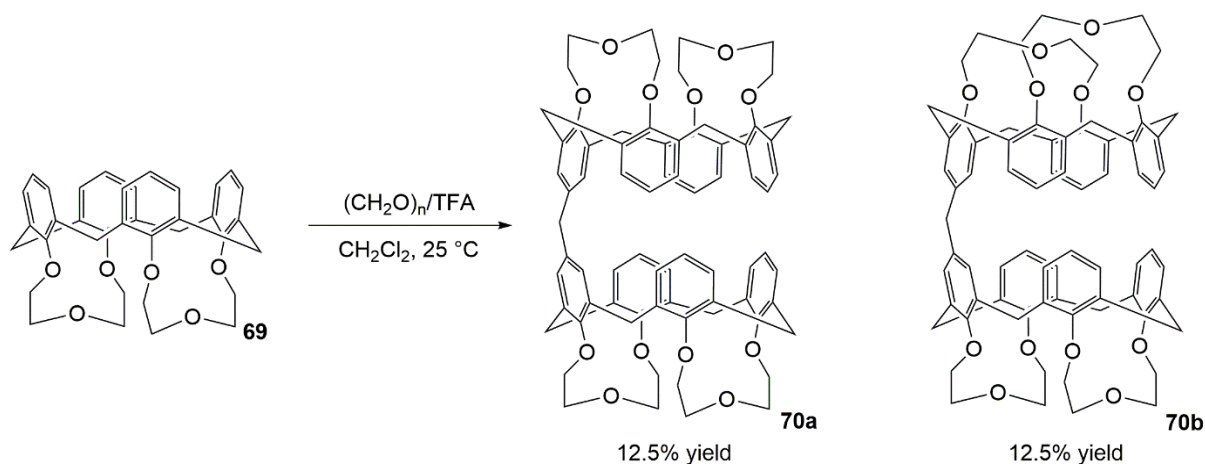


Scheme 1.19: de Mendoza's synthesis of a 'bridgeless' multicalix[4]arene via a supposed radial coupling⁶⁸

In addition to this much improved synthesis, the Spanish group were able to demonstrate that **68** functioned as a receptor for both C₆₀ and C₇₀ fullerenes. Job plot analyses of UV-vis titration data obtained in toluene solution indicated that both fullerenes formed stable host/guest 1:1 and 2:1 complexes with **68**, depending on the concentration. At submillimolar concentrations (*i.e.* 0.14 mM) both complexes coexist, whilst at higher concentrations (*i.e.* 1.4 mM) a 1:2 stoichiometry was found to be representative of the predominant species.

1.6.2.2 Multicalix[4]arenes linked via a methylene function

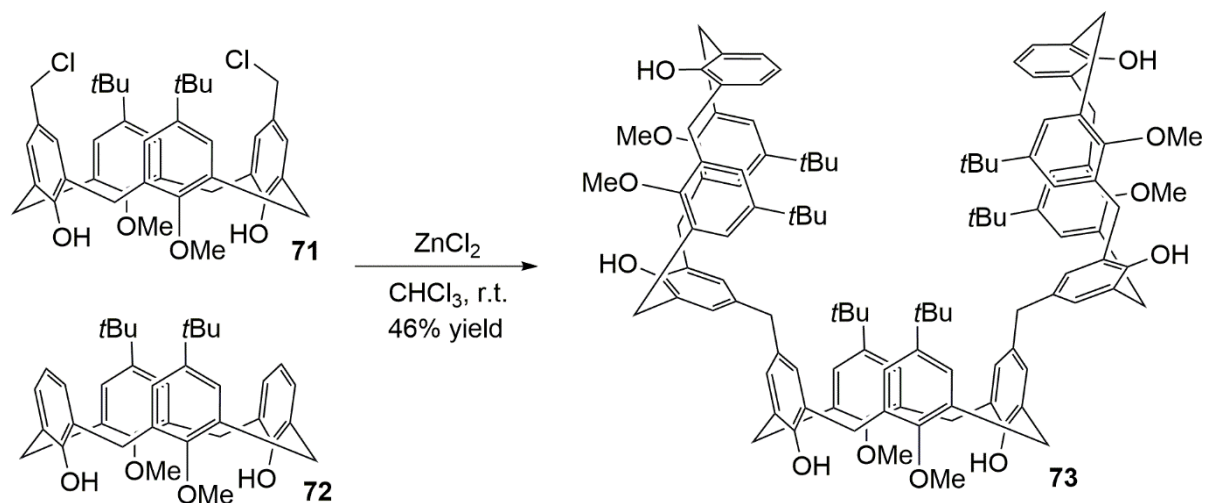
The synthesis of multicalix[4]arenes with more flexible 'linkages' (*i.e.* compared to Neri and de Mendoza's 'bridgeless' analogues) has also been an active area of research. By variation of the type, length and geometry of the bridge between the two calix[4]arenes, it has been proposed that cavitands with unique binding properties might be generated.⁶⁹ Inspired by this possibility, in 2000 Arduini and co-workers reported the synthesis of the methylene linked multicalix[4]arene **70** via the reaction of **69** with *para*-formaldehyde in dichloromethane at room temperature under acidic (*i.e.* TFA) conditions. This process led to the formation of a pair of inseparable diastereomeric multicalix[4]arene dimers **70a** and **70b** in a combined 25% isolated yield (**Scheme 1.20**).⁶⁹



Scheme 1.20: Arduini's synthesis of the methylene bridge linked multicalix[4]arene dimers **70a** and **70b**⁶⁹

Studies into the binding properties of **70** (employed as a diastereomeric mixture) were undertaken using ¹H-NMR titrations for a range of guests chosen on the basis of their shape, size and charge distribution. Tetramethyl- and tetraethylammonium iodides were selected as examples of spherical cations with symmetric charge distribution, whereas *N*-methylpyridinium, *N*-methyl-2-picolinium and *N*-methyl-4-picolinium iodides were chosen as being representative of 'flat cations' with an asymmetric charge distribution. In these experiments, it was found that **70** forms a 1:1 host/guest complex with *N*-methylpyridinium iodide with an association constant of about 10,000 M⁻¹ (-Δ*G* of *ca.* 23 kJ/mol) which compares favourably to the value recorded for the reference compound **69** of about 400 M⁻¹ (-Δ*G* of *ca.* 15 kJ mol⁻¹) thus illustrating a strong cooperative effect.

With dimeric capsules of the form **70** linked by methylene bridges having already received some attention, in 2002 Zheng and co-workers looked towards the synthesis of a number of other higher order multicalix[4]arenes which might be considered to fit within this series.⁷⁰ Inspired in part by the efforts of Reinhoudt and co-workers – who were able to demonstrate the ability of a mixed calix[4]arene-resorcin[4]arene trimer to form a 1:1 host/guest complex with the steroid prednisolone 21-acetate⁷¹ – the Chinese group developed a range of larger calix[4]arene assemblies linked together by methylene bridges. In this way, Zheng's research group aimed to contribute to the emerging trend of designing cavitands able to complex larger molecules such as steroids, sugars and alkaloids. Attempting to repeat Reinhoudt's synthesis of the bis(chloromethyl)-di-*tert*-butylcalix[4]arene **71** under modified conditions (varying the chloromethylating agent, Lewis acid and reaction temperature) led, surprisingly, to the formation of a small quantity (*i.e.* 4%) of the linear trimer **73**, amongst higher linear and cyclic oligomers (not shown). Optimising their synthetic protocol for **73** allowed for its synthesis from **72** and the chloromethylated precursor **71** in a 46% isolated yield (**Scheme 1.21**).

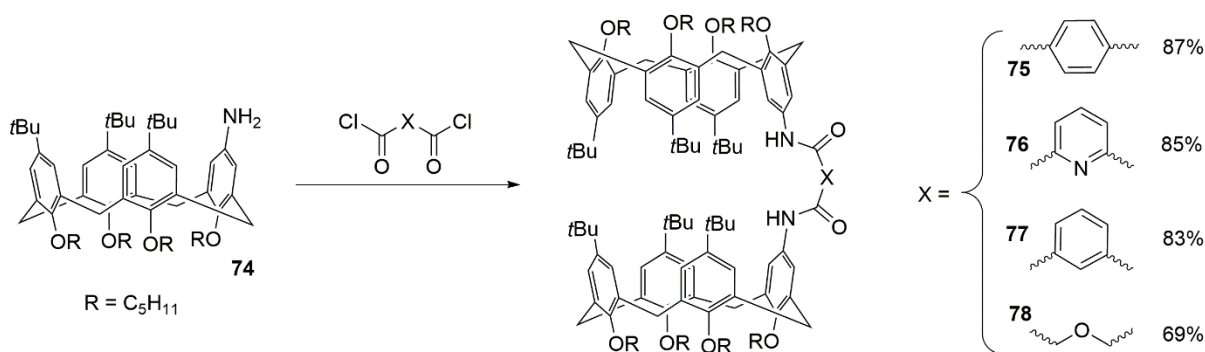


Scheme 1.21: Zheng's optimised conditions for the synthesis of the calix[4]arene trimer **73**⁷⁰

Unfortunately Zheng and co-workers have not, to the best of my knowledge, published any results to date which describe the ability of **73** or its related analogues to complex small molecules.

1.6.2.3 Multicalix[4]arenes linked *via* heteroatom containing bridges

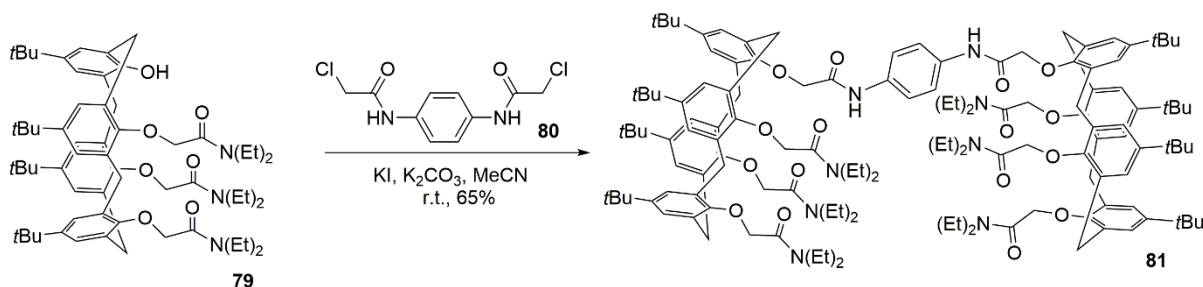
With some of these early studies into upper-rim linked multicalix[4]arenes demonstrating strong cooperative binding effects in the complexation of ions and small molecules, a number of research groups began programs directed at synthesising multicalix[4]arenes with bridges of varying type, length and geometry.⁶⁴ Since low yields and involved purification steps (*e.g.* requiring preparative TLC) characterised many of the early approaches towards these compounds, an additional focus has been the identification of high yielding, operationally simple protocols. So it was that Mogck and co-workers developed the synthesis of a series of amide linked *bis*-calixarenes **75** to **78** by the reaction of monoamine **74** with a range of *di*-acid chlorides (**Scheme 1.22**).⁷²



Scheme 1.22: Mogck's facile synthesis of amide linked cavitanes **75** to **78**⁷²

These reactions all proceeded readily at room temperature, and the corresponding amide linked *bis*-calix[4]arenes could be isolated in high yields (*i.e.* 69 to 87%) and purity by precipitation with cold methanol.

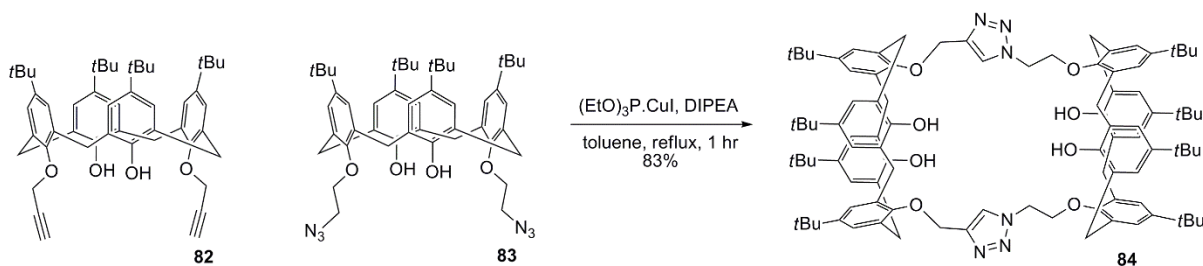
This diamine/acid chloride coupling protocol has also been applied successfully to the lower-rim by Reinhoudt and co-workers in their preparation of *bis*-calix[4]arene ligands for dinuclear lanthanide ion complexation.⁷³ Reacting the *tris*-amide **79** with 0.5 eqⁿ of the spacer **80** afforded a 64% isolated yield of the *bis*-calix[4]arene ligand **81** (**Scheme 1.23**).



Scheme 1.23: Reinhoudt's synthesis of the lower-rim linked hexa-amide **81** for lanthanide ion complexation⁷³

The ability of **81** to form a mixed heterodinuclear complex with Eu^{3+} and Nd^{3+} was studied by photoluminescence spectroscopy, and it was found that in this system the Nd^{3+} ion acts as an energy acceptor for the Eu^{3+} ion with an efficiency of greater than 50%.

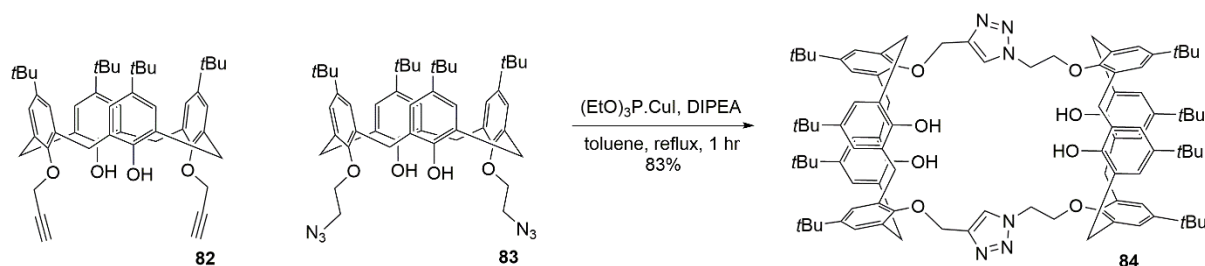
Heterocycle-linked cavitands have also received some attention, and as part of their studies into 1,3-dipolar addition as a tool for the synthesis of a range of multivalent structures, Santoyo-González and co-workers reported the synthesis of the double-bridged *bis*-calix[4]arene **84** as a mixture of all three possible regioisomers (the ratio was unspecified) in a 90% overall yield (**Scheme 1.24**).⁷⁴



Scheme 1.24: Santoyo-González's synthesis of the double-bridged *bis*-calix[4]arene **84**⁷⁴

Although the reaction proceeded slowly (reportedly requiring five days at reflux) the dimeric **84** was clearly formed with high selectivity over competing linear oligomeric, or higher cyclic, compounds – presumably as a result of a faster *intramolecular* 1,3-dipolar addition in the second stage of the reaction. The Spanish group were later to reinvestigate this 1,3-dipolar reaction for the construction of further calix[4]arene-based cavitands by employing the 1,4-regioselective copper(I) catalysed variant first described by Sharpless and co-workers in 2002.⁷⁵ Interestingly, repeating the same reaction which had initially afforded the cavitant **84** as a mixture of regioisomers now afforded,

under copper(I) catalysis, an 83% yield of **84** as a single regioisomer after heating at reflux for 1 hour. This selectivity has been explained on the basis of the mechanism, but the details of this are still being debated in the literature and a number of different proposals have been made (**Scheme 1.25**).^{76,77}



Scheme 1.25: Santoyo-González's modified synthesis of **84** under copper(I) catalysis⁷⁶

This application of the CuAAC reaction clearly demonstrates its potential in the synthesis of calix[4]arene based cavitands, although it is rather unfortunate that no complexation studies were reported involving **84** since the incorporation of triazole rings in the structure presumably makes the cavity an attractive one for host-guest studies. Indeed, triazoles are well known for their ability to participate in a range of supramolecular interactions (*e.g.* hydrogen and halogen bonding) and a number of systems have been developed to take advantage of these properties.⁷⁸ For example, a recent report by Flood and co-workers demonstrated the ability of co-polymers of methyl methacrylate and aryl-triazole based anion receptors to bind the chloride anion through the formation of triazole-based $\text{CH}\cdots\text{Cl}^-$ hydrogen bonds **85** (**Figure 1.6**).⁷⁹

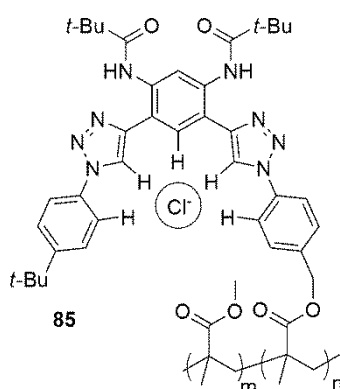


Figure 1.6: Chloride binding through the formation of triazole based $\text{CH}\cdots\text{Cl}^-$ hydrogen bonds⁷⁹

1.6.3 Calix[n]arenes as metal ion-selective sensors

The incorporation of fluorophores and chromophores onto calix[n]arenes optimised for the binding of small molecules and cations has allowed for the development of optical sensors.⁸⁰ In a chromophoric system, the complexation of a guest ion results in a measureable bathochromic or hypsochromic shift of the absorption. An early example of such a system was reported by Shinkai and co-workers, and involved the complexation of Na⁺ ions by the calix[4]arene-crown **86** appended with a *para*-nitrophenylazo chromophore. This sensor displayed a high selectivity for sodium over potassium ions, with a Na⁺/K⁺ selectivity of >1260 – a value which makes it ideal for optical sensing applications. Interestingly, it was observed that solutions of **86** stored in soda-glass vials rapidly turn deep green, indicating the presence of its Na⁺ complex (Figure 1.7).⁸¹

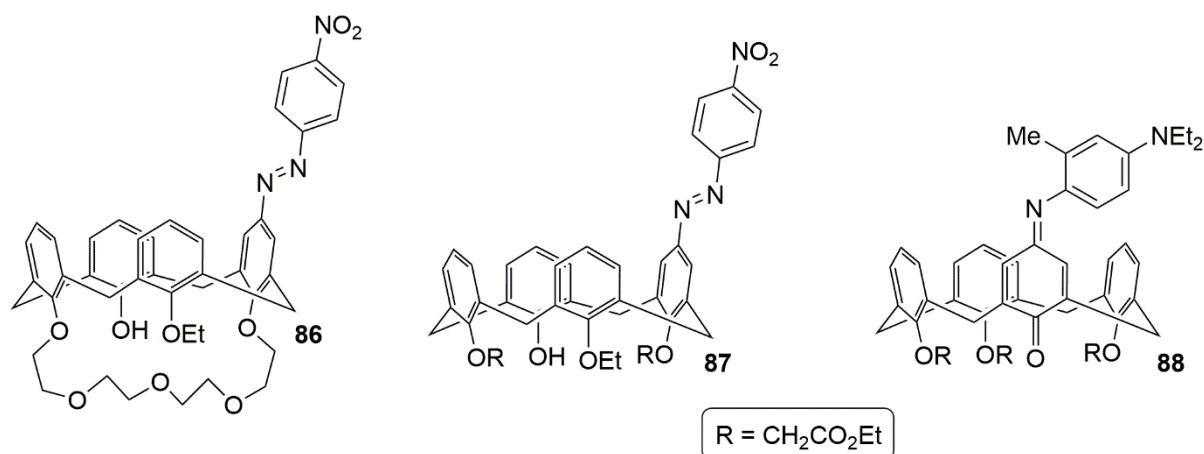


Figure 1.7: Some early examples of calix[4]arene derived chromogenic sensors⁸¹

Without the crown ether appended at the lower-rim, the corresponding calix[4]arene derivative **87** – also reported by Shinkai and co-workers – forms a 1:1 complex with Li⁺ as indicated by UV absorption studies.⁸² Later investigations by Kubo and co-workers into their novel indoaniline derived calix[4]arenes **88**, demonstrated that the structure appended with CH₂CO₂Et chains at the lower-rim displays a large bathochromic shift (*ca.* 110 nm) and concomitant increase in absorption intensity on complexation with Ca²⁺ ions. In contrast, the addition of NaSCN, KSCN or Mg(ClO₄)₂ to a solution of **88** resulted in only minor bathochromic shifts (*i.e.* 12 to 40 nm) suggesting the sensor is specific for Ca²⁺ ions.⁸³

Whilst these chromophoric systems have met with some success, the incorporation of a fluorescent moiety has the advantage of greatly increasing the sensitivity which is available. In these types of sensors, the complexation of a guest ion is either measured by an increase or decrease in the fluorescence intensity, a change in the emission wavelength, or a change in the monomer/excimer emission ratio.⁸⁴ The most common design for a fluorescent sensor involves linking a fluorescent

moiety to a coordinating functional group *via* a spacer. Upon coordination of a metal ion, a number of different mechanisms may lead to the concomitant enhancement or quenching of fluorescence. These are summarised below with reference to the simplified Jablonski diagram (**Figure 1.8**).

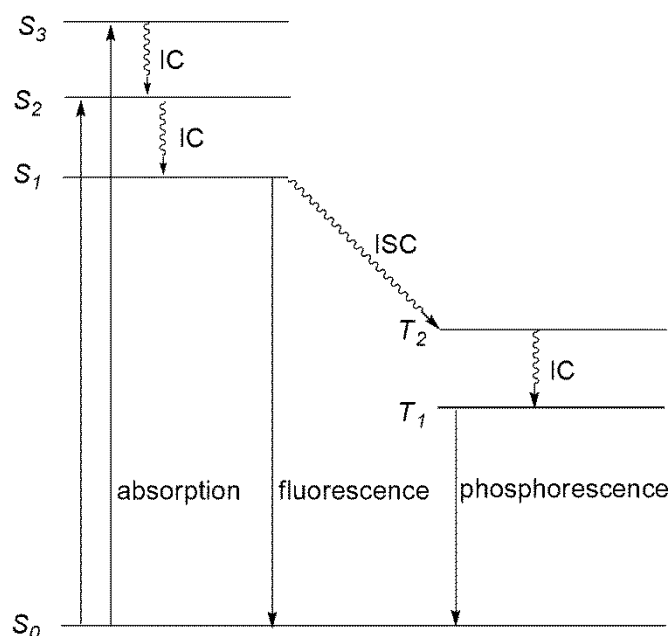
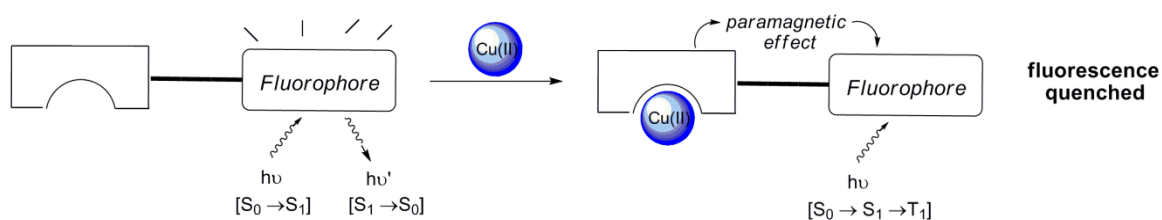
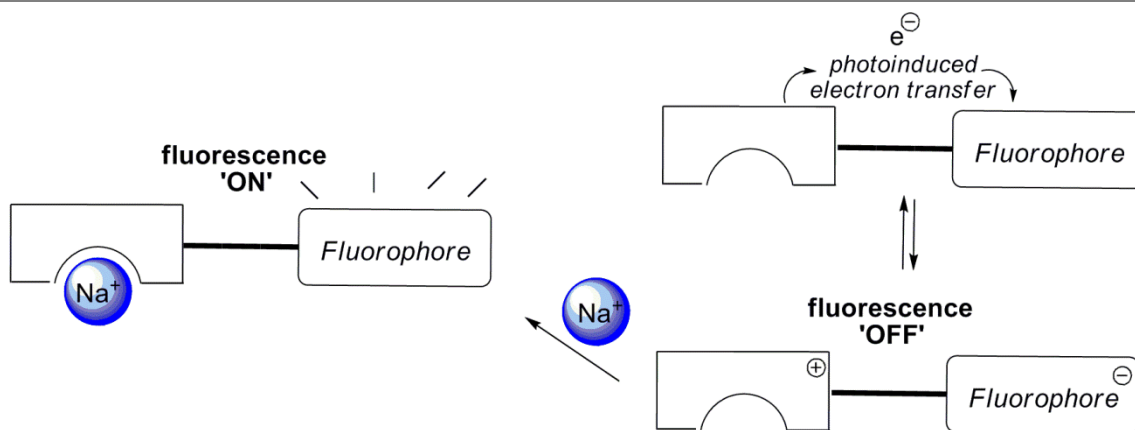


Figure 1.8: Jablonski diagram highlighting the key electronic transitions involved in fluorescence and phosphorescence. IC = internal conversion, ISC = intersystem crossing.

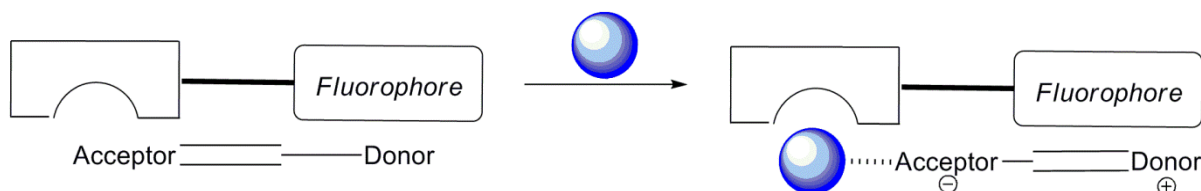
- **Paramagnetic fluorescence quenching** – the complexation of a paramagnetic metal ion (*i.e.* Cu(II), Fe(III), Co(II), *etc.*) in close proximity to a fluorophore tends to increase the rate formally forbidden processes like intersystem crossing (ISC). This has the result of promoting phosphorescence (*i.e.* from T_1) and quenching fluorescence (*i.e.* from S_1).



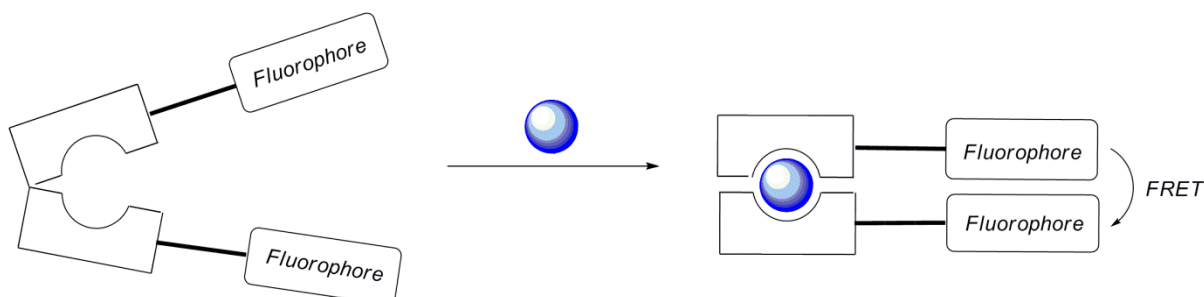
- **Photoinduced electron transfer** – in a PET process, charge separation is brought about by an internal photoinduced redox reaction between a donor (or acceptor) molecule and the fluorophore. In the S_1 excited state, the electronic structure is significantly different to the ground state and the fluorescence is typically quenched. Upon complexation of a metal ion such as Na^+ , the energy of the lone pairs involved in the redox process is reduced and the fluorescence is restored.



- *Photoinduced charge transfer* – in this process, charge separation occurs between donor and acceptor moieties linked *via* a conjugated π -system. The complexation of a metal ion can result in either the enhancement or quenching of fluorescence depending on the particular fluorophore, metal ion or coordination mode which is employed.

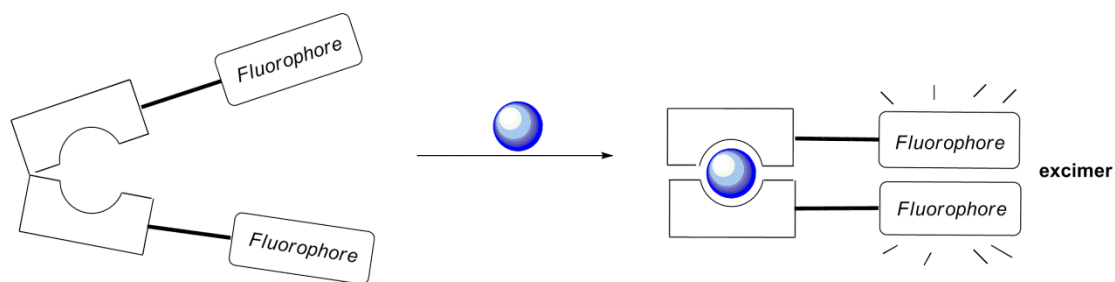


- *Fluorescence resonance energy transfer* – the FRET mechanism involves the non-radiative transfer of energy when a fluorophore in the excited S_1 state relaxes to S_0 and simultaneously excites an acceptor fluorophore. In the absence of other processes, subsequent relaxation of the acceptor is accompanied by the emission of a photon. The FRET mechanism is highly distance dependent (the efficiency falls with the inverse sixth power of intermolecular separation) and operates only over short distances (*i.e.* 10 to 100 Å). If the coordination of a metal ion alters the intermolecular separation between donor and acceptor fluorophores, this can be detected in the emission spectra.

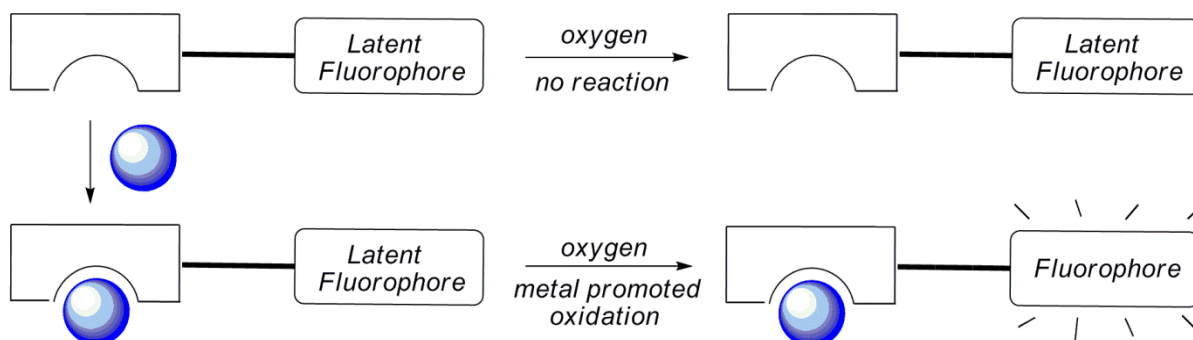


- *Formation of excimers* – the formation of an excimer (excited dimer) occurs when the interaction between the ground and excited states are of a given fluorophore are sufficiently strong. The emission of such species is always found at a lower energy than the corresponding monomers, and the ratio between free monomer and excimer can be observed. The presence of metal ions typically affects the formation of these excimers, and the resulting changes in the emission spectra can be used as a quantitative measure of their concentration. Fluorescent sensors which operate in this way

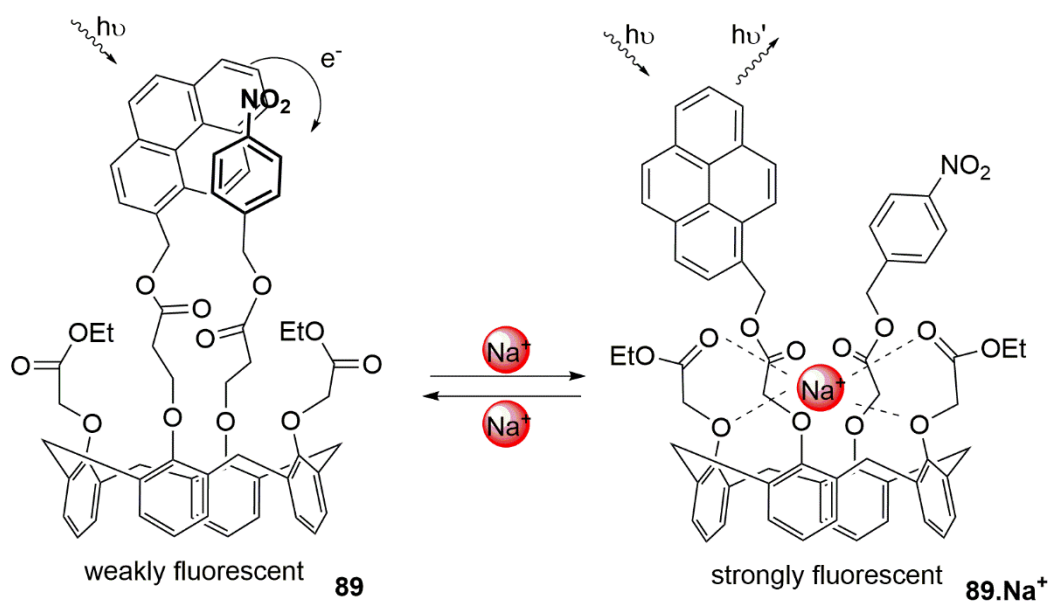
are generally termed 'ratiometric' because the relative intensities of emissions between the monomer and dimer can be measured.



• *Reaction based sensors* – in these systems, the formation of a fluorescent molecule is promoted by the presence of a metal ion. These reaction based sensors are generally irreversible, but are particularly useful for the OFF-ON detection of metal ions which typically quench fluorescence (*i.e.* Cu^{2+}). Sensors which operate in this way are generally termed 'chemodosimeters'.



One early example of an ion-selective calix[n]arene sensor thought to operate *via* a PET process was reported by Shinkai and co-workers in 1992.⁸⁵ They found that calix[4]arene **89** appended with a pyrene fluorophore and a *para*-nitrophenol moiety (acting as a fluorescence quencher) displayed an increase in fluorescence intensity of around 7 times on complexation of the Na^+ ion (**Scheme 1.26**).



Scheme 1.26: Shinkai's fluorescent sensor **89** for the detection of Na⁺ ions thought to operate via a PET mechanism⁸⁵

On the basis of ¹H-NMR studies, the enhancement in fluorescence intensity was suggested to arise from a conformational change upon complexation resulting in the increased separation of the pyrene fluorophore and *para*-nitrophenol quencher. With this greater separation, the PET process is less efficient, and therefore the fluorescence intensity is increased. The selectivity of the sensor towards a range of group 1 alkali metal ions was also studied, and it was found that Na⁺ (using NaSCN) was bound most strongly with an association constant of $K_{ass}/\text{mol dm}^{-3} = 4.3$. In contrast, values of 1.2 for LiSCN, 2.2 for CsSCN and 2.9 for KSCN were measured.

Fluorescent sensors capable of greater selectivity between metal ions have also been developed. Dabestani and co-workers based at the Oak Ridge National Laboratory synthesised the caesium selective probe **90**, as part of a research program directed towards the sensing, recovery and treatment of the nuclide ¹³⁷Cs.⁸⁶ It was found that **90** with its 1,3-alternate *di*-deoxygenated calix[4]arene-crown displayed a high selectivity for Cs⁺ over Rb⁺, K⁺, Na⁺ and Li⁺ ions (**Figure 1.9**).

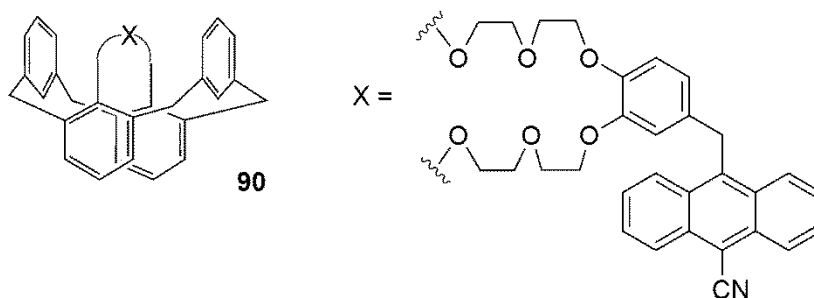


Figure 1.9: Dabestani's fluorescent sensor which displays a high selectivity for caesium ions⁸⁶

On studying the emission behaviour of **90** in MeOH/CHCl₃ (1:1, v/v) at 0.2 μM, the American group observed a 20-fold increase in the fluorescence intensity upon Cs⁺ ion coordination – a concentration at which no other group 1 alkali metal ion gave a significant response. At 20 μM, the fluorescence response was observed to be enhanced 54 times relative to that of free ligand upon complexation with Cs⁺. These results represent the greatest fluorescence response to Cs⁺ binding yet reported.

The design of fluorogenic calix[n]arene based probes which bind heavy metal ions such as Hg²⁺, Pb²⁺ and Cd²⁺ is also a highly active area of research.⁸⁷ The presence of these ions in the environment at elevated levels can have serious consequences for human health, and consequently, strict limits have been placed on the concentrations permitted in for example drinking water by the World Health Organisation.⁸⁸ The maximum allowed concentration for Hg²⁺ is 2 μg/L, whilst for Cd²⁺ it is 5 μg/L and for Pb²⁺ the level is set at 15 μg/L. As a result, methods for the sensitive and selective detection of these metals have been the focus of many research programs.⁸⁹ Whilst sophisticated analytical methods such as atomic absorption and emission spectroscopies, electrochemistry and cold vapour atomic fluorescence spectroscopy are available for the detection of metal ions, fluorescent sensors have the potential to offer a simpler and more cost effective alternative. Of the many possible chelating moieties available (*i.e.* crown ethers, cryptands, sulfides), functionalised calix[4]arenes have received much attention because of their ability to bind metal ions, in addition to the ease with which fluorophores or additional ligands can be attached.

One of the first calix[4]arene-based sensors for the selective recognition of Hg²⁺ was reported by Bartsch and co-workers in 1999.⁹⁰ The sensor **91** displayed a remarkable selectivity for Hg²⁺, with the quenching efficiency unaffected even in the presence of a 100-fold excess of a range of other metals (*i.e.* Ag⁺, Tl⁺, Cd²⁺, Co²⁺, Cu²⁺, Pd²⁺) (**Figure 1.10**).

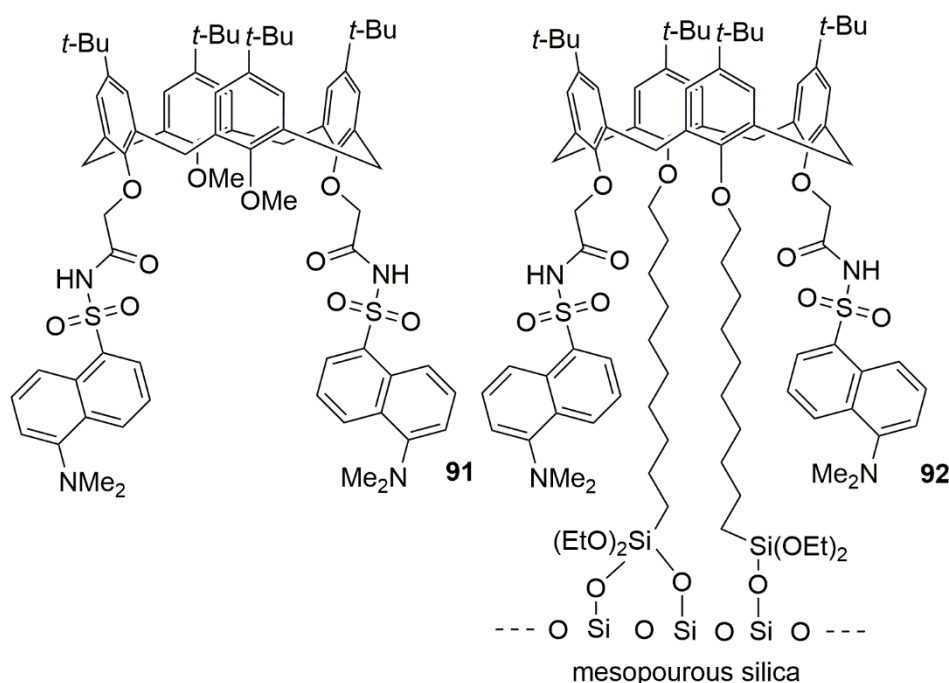


Figure 1.10: Bartsch's and Leray's dansyl appended calix[4]arenes for the selective detection of Hg²⁺ ions⁹⁰

Upon Hg^{2+} extraction into chloroform using **91** from dilute solutions of the metal in nitric acid (pH = 2.5), the fluorescence intensity was observed to decrease accordingly with enhanced Hg^{2+} extraction. In this case, quenching of the dansyl fluorophore was proposed to occur *via* electron transfer of the excited moiety to the proximate mercury ion. Under the conditions of their experiments, a detection limit of 5 μM for Hg^{2+} was achieved. Although later investigations by Leray and co-workers demonstrated that a greater sensitivity (*i.e.* down to 0.3 μM) was available if **91** was employed in aqueous solutions of acetonitrile ($\text{MeCN-H}_2\text{O}$, 6:4 v/v).⁹¹ Studies to examine the effect of introducing competing metal ions into the nitric acid solutions (in a 100-fold excess) indicated the sensing ability of **1** remained unaffected in their presence, with only a $\pm 3\%$ deviation observed in emission intensity for all of the metals tested. Modifying the design by immobilisation onto mesoporous silica has allowed **92** to be used for the reversible detection of Hg^{2+} ions in water.⁹² The somewhat lower sensitivity (*i.e.* 0.33 μM) and lower stability of the resulting Hg^{2+} complex as compared to **91** was attributed to a loss of ligand flexibility and hindered access to the cavity.

1.6.4 Ion-selective sensors for the precious metals

Interest in developing sensors for the precious metals (*i.e.* gold, silver and platinum) has grown out of their widespread use and importance in a range of industrial processes and products.⁹³ In particular, the pollution of the environment from their accidental or improper release is a concern as many of these metal ions are potentially hazardous to human health. An excessive intake of silver ions can, for example, lead to the build-up of insoluble silver precipitates in the skin which cause it to appear blue (a condition called argyria).⁹⁴ Soluble salts of gold such as gold(III) chloride are known to cause damage to the liver, kidneys and nervous system,⁹⁵ whilst some platinum salts can cause damage to DNA, resulting in autoimmune disorders and cause hearing problems.⁹⁶ Efficient and sensitive methods for the detection of these metals in environmental and biological matrices are therefore of high importance. As discussed previously, the traditional analytical methods for the detection of these ions (*e.g.* atomic emission spectroscopy) might be surpassed in terms of sensitivity and at reduced cost if fluorescent sensors can be employed.

1.6.4.1 Ion-selective sensors for the silver ion

A large number of small molecule non-calix[4]arene based fluorescent probes capable of sensing Ag^+ ions have been developed in recent years.⁹³ For example, Shamsipur and co-workers reported that their sensor – comprised of a sulfur-containing macrocycle appended to a dansyl fluorophore **93** – forms a 1:1 complex upon binding with Ag^+ ions in acetonitrile solution, and shows a concomitant decrease in fluorescence intensity (**Figure 1.11**).⁹⁷

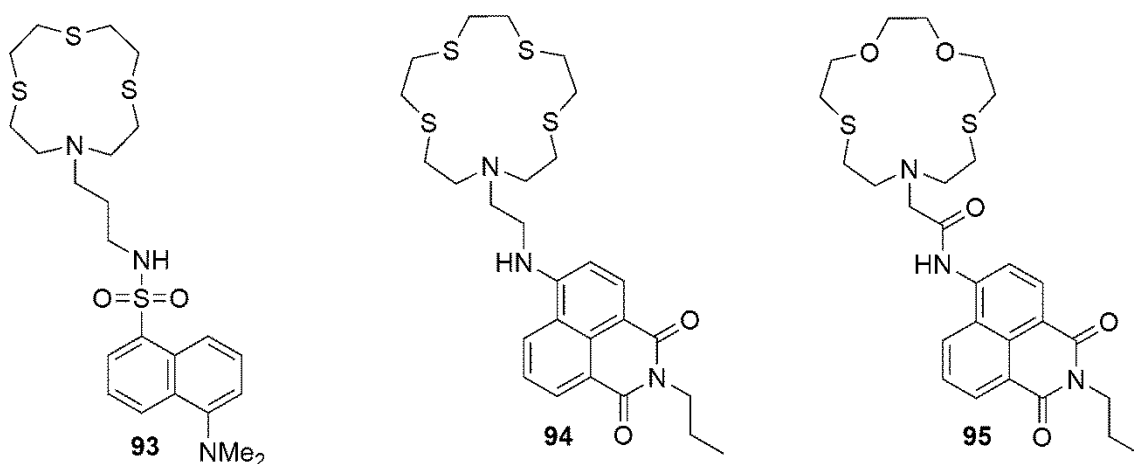
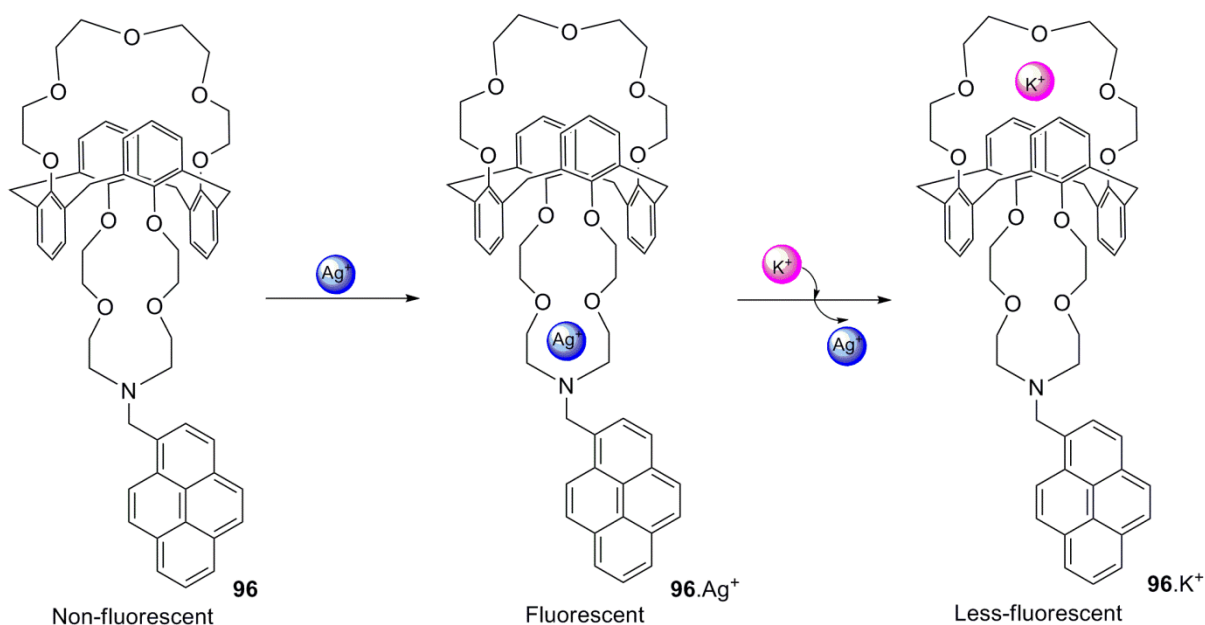


Figure 1.11: Fluorescent probes optimised for the detection of Ag^{+97}

In addition, appreciable selectivity for the Ag^+ ion over Cu^{2+} , Tl^+ and Cd^{2+} was observed along with short response times (*i.e.* ≤ 40 s). A similar design **94** which incorporates the naphthalimide fluorophore was reported by Qian and co-workers in 2010.⁹⁸ Interestingly, this probe exhibited dual sensing behaviours for Ag^+ and Hg^{2+} . Upon addition of Hg^{2+} to a solution of **94** in ethanol-water (20:80 v/v) a 5-fold increase in fluorescence intensity was observed, whilst the subsequent addition of silver(I) resulted in a quenching of the fluorescence emission. In an extension of this work, Yoon and co-workers designed probe **95** which detected silver(I) ions in MeCN-water (1:1 v/v) solutions.⁹⁹ A 14-fold enhancement in fluorescence emission was observed upon the addition of Ag^+ ions (the Ag^+ source was not reported), and an appreciable association constant between **95** and Ag^+ was measured (*i.e.* $K_a = 1.64 \times 10^{-5} \text{ M}^{-1}$).

Calix[4]arene derived sensors for silver(I) by contrast are relatively few in number, although a three examples have been reported to date.⁹³ In 2002, Yoon and co-workers reported the ability of the calix[4]arene-crown derivative **96** to detect silver(I) *via* a chelation-enhanced fluorescence effect (CHEF). Upon binding of silver(I) ions, the inhibition of the inherent PET process resulted in a 50-fold enhanced fluorescence. This fluorescence could be quenched by subsequent addition of K^+ , which was thought to promote the decomplexation of silver(I) in a process the authors termed ‘molecular taekwondo’ (**Scheme 1.27**).¹⁰⁰



Scheme 1.27: Yoon's silver(I) sensor which operates via a chelation-enhanced fluorescence effect¹⁰⁰

The 1:1 stoichiometry of the silver(I) complex **96.Ag⁺** was confirmed both *via* a Job plot of the titrations with AgClO₄, and by means of high resolution mass spectrometric analysis. In the FAB-MS, only the molecular ion at *m/z* 1061.1 for **96.Ag⁺** could be observed and no higher (*i.e.* 1:2 or 2:1 **96.Ag⁺**) complexes were detected.

Appending two 1,3-di[*bis*(2-picolyl)]amide moieties to the lower-rim of *para-tert*-butylcalix[4]arene allowed Rao and co-workers to detect silver(I) ions at a concentration as low as 450 ppb. The sensor **97** was determined to have formed a 1:1 complex with Ag⁺, with an association constant, *K_a*, of about 11,110 ± 200 M⁻¹ from Job plot titrations. The control molecules **98**, **99** and **100** showed no fluorescence response to the silver(I) ion, indicating that the preorganised structure provided by the calix[4]arene scaffold coupled with the 1,3-di[*bis*(2-picolyl)]amide moieties are essential for its action as a fluorescent probe (**Figure 1.12**).¹⁰¹

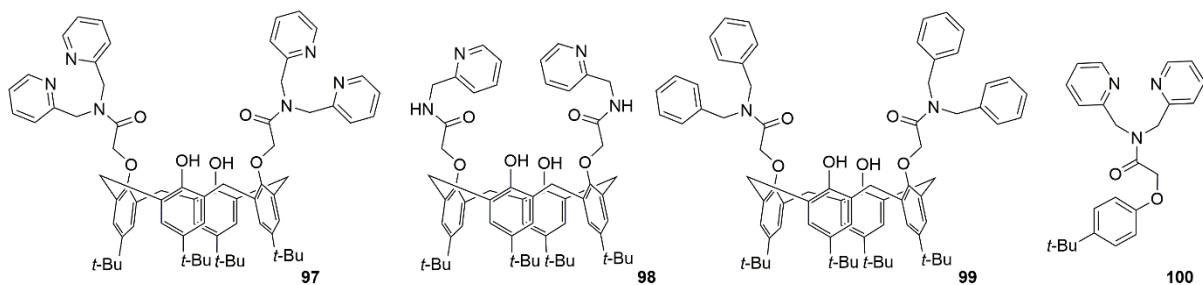
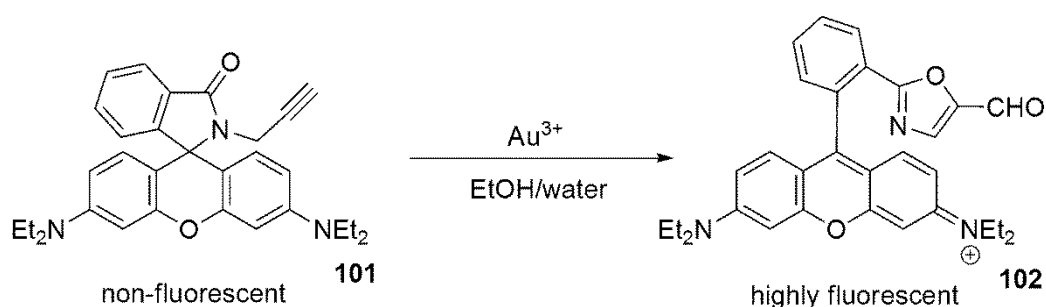


Figure 1.12: Rao's fluorescent probe **97** for silver(I) and the control molecules **98**, **99** and **100**¹⁰¹

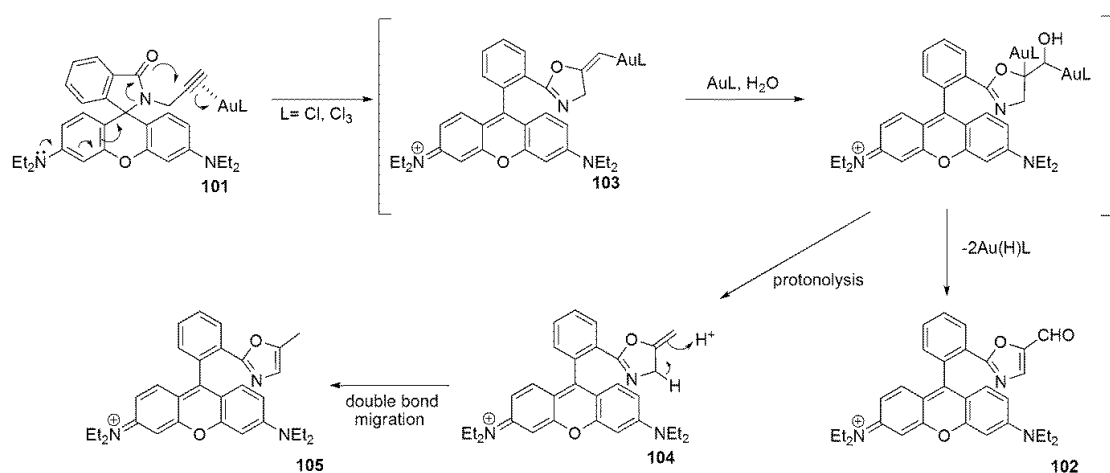
1.6.4.2 Ion-selective sensors for Au(I) and Au(III) ions

Whilst many ion-selective sensors have been reported for silver(I), only relatively few probes have been developed for the Au(I) and Au(III) ions to date.⁹³ This is perhaps surprising given the surge of interest in using gold catalysis for the construction of complex organic molecules in both academia and industry, and of course its high cost.¹⁰² Most designs for gold-selective fluorogenic sensors make use of the strong alkynophilicity of Au(I) and Au(III) ions to activate carbon-carbon triple bonds towards nucleophilic attack. In a typical probe, this activation will lead – after the addition of a nucleophilic component – to a new molecule with a greater fluorescence emission. For example, Yoon and co-workers reported the Au(III) selective rhodamine derived chemodosimeter **101** which displayed a 100-fold enhancement in fluorescence emission upon reaction with gold(III)chloride in EtOH-HEPES buffer (pH 7.4, 0.01 M) (**Scheme 1.28**).¹⁰³



Scheme 1.28: Yoon's rhodamine derived probe for the detection of Au(III) ions¹⁰³

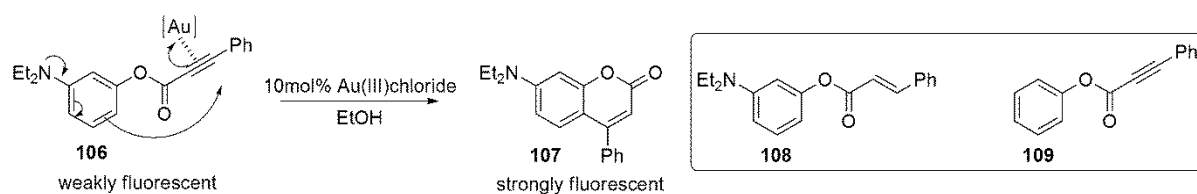
Probe **101**, reported in 2009, represented the first example of an ion-specific fluorogenic sensor for the Au(III) ion. Using the data collected from fluorescence titrations of Au(III) with **101** (1 μM) in EtOH-water (1:1, v/v), a detection limit of 63 ppb was estimated. The proposed reaction mechanism leading to the formyloxazole compound **102** is thought to involve the Au(III) catalysed hydration of the vinyl gold species **103** and a subsequent 'double elimination' (**Scheme 1.29**).¹⁰⁴



Scheme 1.29: The mechanism proposed by Egorova and co-workers for the reaction of **101** with Au(III)¹⁰⁴

When the reaction was conducted in anhydrous acetonitrile the hydration of the vinyl gold intermediate **103** was inhibited, and the methyloxazole **105** was formed as the major product – presumably *via* double bond migration of the less stable exomethylene compound **104**.

In further efforts directed towards the development of a sensor for Au(III), Yoon and co-workers also reported the rationally designed OFF-ON chemodosimeter **106**.¹⁰⁵ Upon treatment with gold(III)chloride in ethanol solution at 30 μ M concentration, the weakly fluorescent aryl alkyne **106** undergoes an efficient intramolecular cyclisation to afford the strongly fluorescent coumarin derivative **107** (**Scheme 1.30**).



Scheme 1.30: Yoon's rational design for an OFF-ON chemodosimeter selective for Au(III)¹⁰⁵

The control compounds **108** and **109** failed to react under these conditions, indicating the importance of both the alkyne and diethylamino moieties in the hydroarylation process. Surprisingly perhaps, the probe **107** failed to react with the Au(I) ion – no reaction was observed even after the addition of 10 equivalents of PPh₃AuCl. This presumably arises from a weaker interaction between the Au(I) ion and the alkyne component, compared with the more highly charged Au(III) ion.¹⁰⁵

In 2015, Chinapang and co-workers reported fluorescent probe **110** for the detection of both Au(I) and Au(III) ions which is thought to operate *via* a chelation-enhanced fluorescence effect.¹⁰⁶ Their design consisted of a fluorescent 1,8-naphthalimide moiety linked to a ferrocene quencher *via* an alkyne as a signal transducer. As anticipated, both compounds prepared for this study possessed low quantum efficiencies compared to the parent 1,8-naphthalimide fluorophore due to an intramolecular PET effect (**Figure 1.13**).

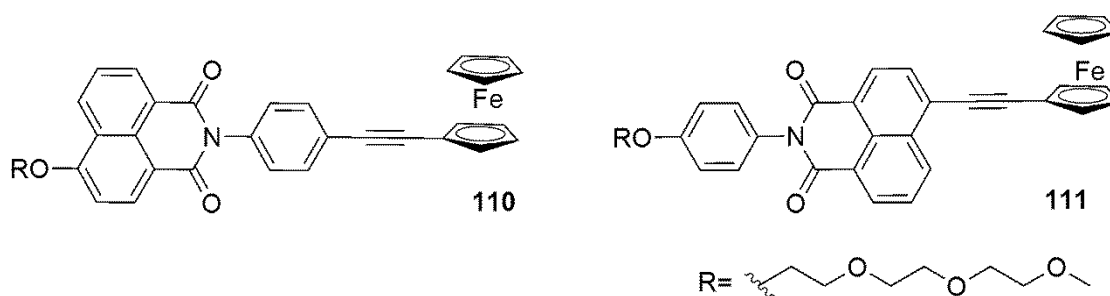


Figure 1.13: Chinapang's design for a Au(I)-Au(III) sensor based on the CHEF effect¹⁰⁶

Upon treating compound **110** with Au(I) or Au(III) ions in MeCN-PBS buffer (pH = 8) (1:1 v/v) fluorescence enhancements of 3 and 9 folds were observed, respectively. In contrast, no significant effect was found for compound **111**. Density functional theory calculations (B3LYP/LANL2DZ) and ^{13}C -NMR studies of the probe indicated the gold ions (Au(I) and Au(III)) were likely to be coordinated to the carbon-carbon triple bond in **110** resulting in decreased charge transfer between donor and acceptor moieties, and enhanced emission. After some optimisation of the analytical procedure, the Thai group was able to achieve Au(III) detection down to a concentration of 95 ppb.

Although many ion sensors using calix[4]arenes have been described, no examples of *upper-rim* functionalised calix[4]arene based sensors for the Au(III) ion have been reported. Even now, at the close of the project, only one example of a *lower-rim* functionalised calix[4]arene based sensor for the Au(III) ion has been reported.¹⁰⁷ Ocak and co-workers described the synthesis and fluorescence properties of the 2-hydroxynaphthalide appended Schiff base **112** which was reported to function as a highly selective probe for the Au(III) ion over a range of mono-, di- and trivalent cations (*e.g.* Ag^+ , Tl^+ , Cd^{2+} , Co^{2+} , Cu^{2+} , Pd^{2+} , Sb^{3+} , V^{3+}) (**Figure 1.14**).

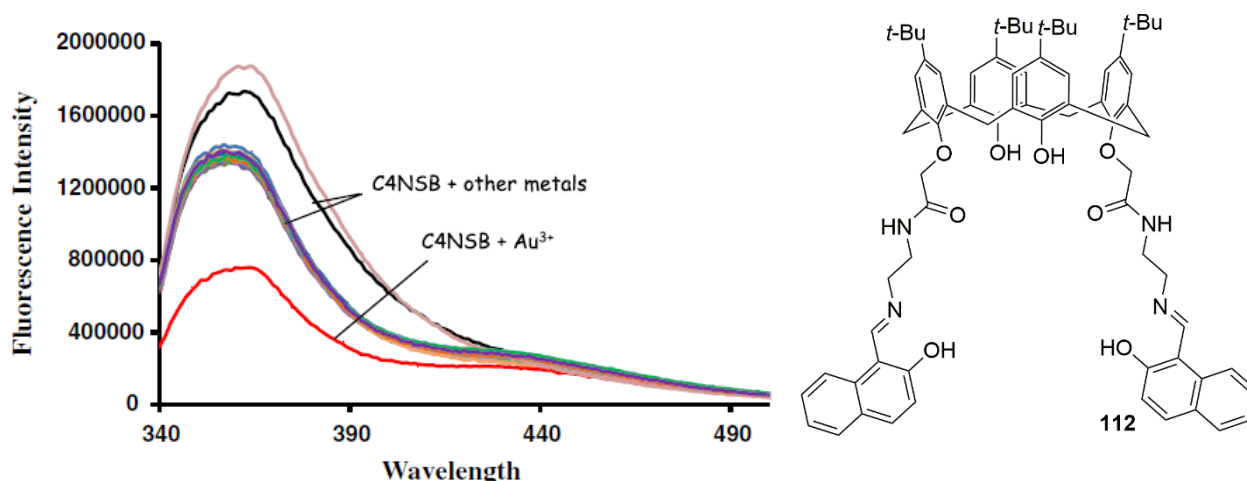


Figure 1.14: Ocak's design for a calix[4]arene based Au(III) selective sensor **112** and fluorescence spectra in the presence of a range of metal ions (reproduced from [107])¹⁰⁷

Upon treating **112** (13 μM) with Au(III) ions (10 equivalents) in EtOH-water (1:1 v/v) solution the Turkish group reported a 59-fold decrease in fluorescence emission, whilst in contrast 'the fluorescence response of receptor **112** did not produce any significant distinctions upon interaction with different metals'. However, using the same definition of 'fold decrease' as the authors and supposing the top-most curve represents the fluorescence response of the free receptor **112**, a *ca.* 30-fold decrease can also be calculated for the closely spaced set of curves representing the majority of the 'other metals' – thereby making the claim of 'no significant distinctions' seem erroneous.

Notwithstanding this claim about selectivity, a subsequent Job plot analysis indicated a 1:1 stoichiometry for the **112**.Au³⁺ complex which led the authors to propose a binding mode whereby both imine functions are involved in coordination to a single metal ion. Further analysis to establish whether the arrangement of ligands provided by the calix[4]arene scaffold was required for the action of the probe (*e.g.* by studying an analogue such as **113**) was not performed (**Figure 1.15**).

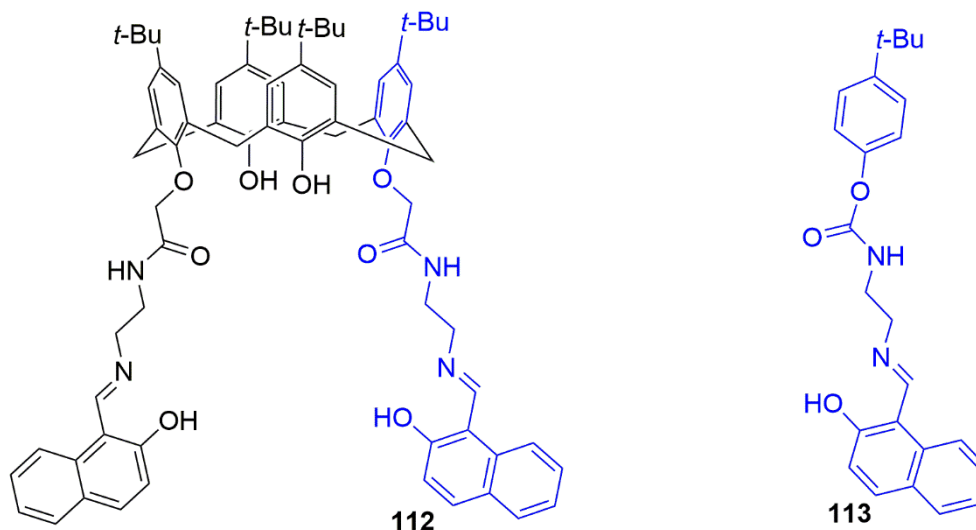


Figure 1.15: An analogue **113** of calix[4]arene based **112** which might be used to ascertain the importance of the calix[4]arene scaffold to its function as a probe for Au(III) ions

In addition, it is unfortunate that no ¹H-NMR titrations of probe **112** with Au(III) were performed since these may have provided valuable insight into the nature of the **112**.Au³⁺ complex.

Considering the small number of probes available for the detection of the synthetically important Au(III) ion (indeed in 2008 there were no examples) coupled with the well established use of calix[4]arenes as scaffolds on which to build fluorescent sensors, in 2008 Bew and co-workers initiated a study into the use of intricately functionalised calix[4]arenes of the form **114** for the selective detection of Au(III) over a range of competing metal ions (*i.e.* Cd²⁺, Ag⁺, Pd²⁺, Hg²⁺, Pt²⁺, Li⁺, Na⁺) (**Figure 1.16**).¹⁰⁸

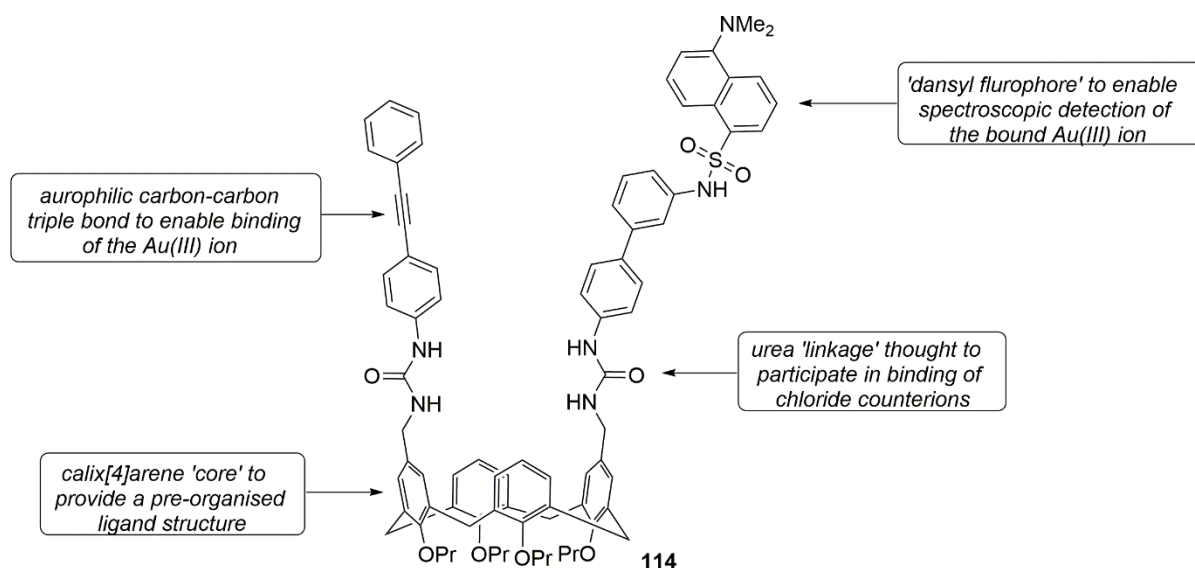


Figure 1.16: Bew's first generation design for a calix[4]arene based sensor selective for the Au(III) ion¹⁰⁸

This first generation design incorporates the aurophilic alkyne functional group linked to the upper rim of a calix[4]arene scaffold *via* a urea moiety. On the opposing side of the macrocyclic ring is appended the 5-(dimethylamino)naphthalene-1-sulfonyl or 'dansyl' fluorophore *via* a second urea linkage with biaryl spacer. This fluorophore was incorporated into the design to allow for the spectroscopic detection of the Au(III) ion upon binding of the metal to the alkyne. Preliminary fluorescence studies indicated that a 95% reduction in emission intensity could be observed upon the sequential addition of sodium tetrachloroaurate (1 to 5 equivalents) to a solution of **114** in methanol ($5 \mu\text{M}$, $\lambda_{\text{ex}} = 288 \text{ nm}$, $\lambda_{\text{max}} = 522 \text{ nm}$) (**Figure 1.17**).

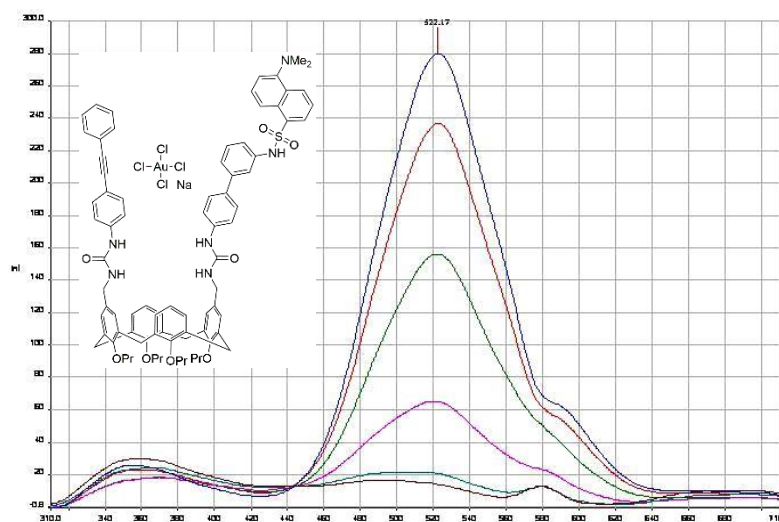


Figure 1.17: The reduction in fluorescence intensity observed on the addition of 1-5 eqⁿ of Au(III) to **114** ($R = \text{Pr}$) ($5 \mu\text{M}$ in methanol, $\lambda_{\text{ex}} = 288 \text{ nm}$, $\lambda_{\text{max}} = 522 \text{ nm}$)¹⁰⁸

The addition of a range of other metal ions (*i.e.* Cd^{2+} , Ag^+ , Pd^{2+} , Hg^{2+} , Pt^{2+} , Li^+ , Na^+) to methanolic solutions of **114** resulted in only minor spectral changes – even after the addition of up to 30 equivalents. In further efforts to establish the importance of the calix[4]arene core and the alkyne functionality for the operation of the sensor, several control compounds (*i.e.* **115**, **116** and **117**) were synthesised (**Figure 1.18**).

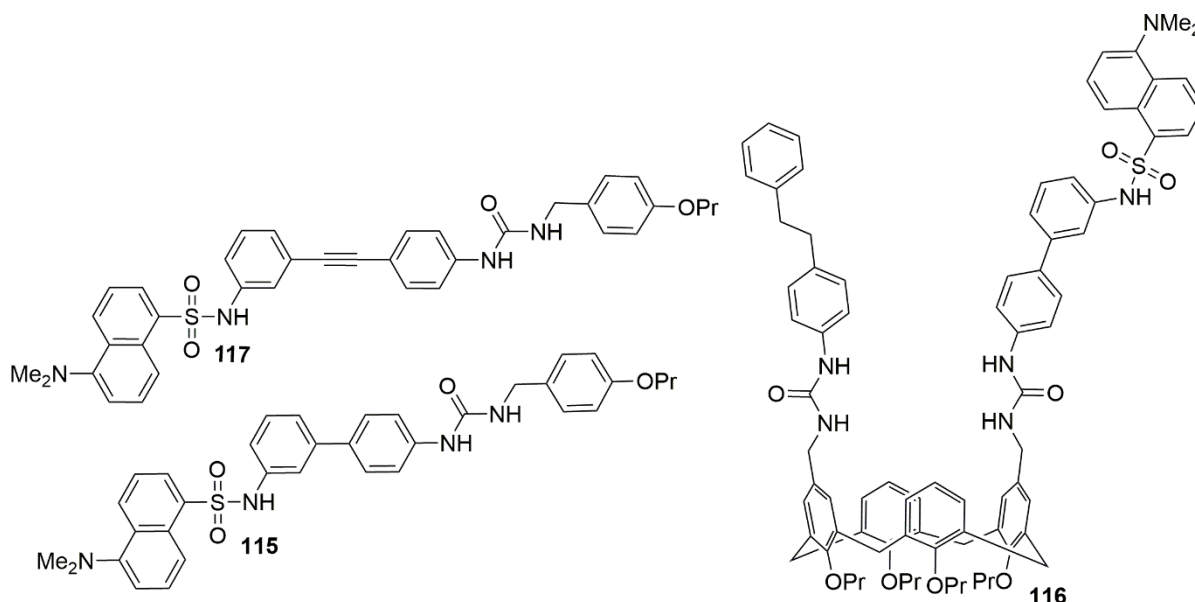


Figure 1.18: Control compounds synthesised as part of Bew's preliminary investigations into the development of an ion-selective probe for Au(III) ¹⁰⁸

Compound **115** lacks the carbon-carbon triple bond and compound **117** lacks the calix[4]arene core, whilst compound **116** is missing both of these features. A fluorescence study indicated only minor spectral changes for this set of compounds even after the addition of up to 30 equivalents of sodium tetrachloroaurate, thereby strongly suggesting the importance of both of these structural elements (*data shown for 116 - Figure 1.19*).

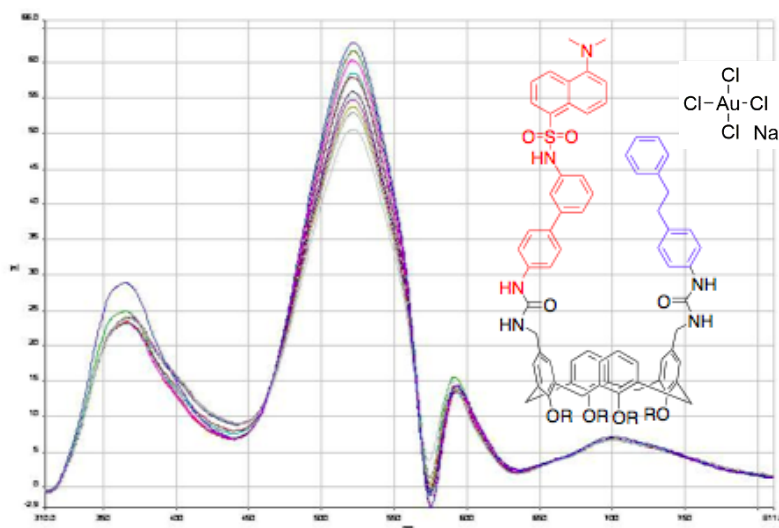


Figure 1.19: The minor spectral changes observed on addition of 1-30 eqⁿ of Au(III) to compound **116** ($R = \text{Pr}$) ($5 \mu\text{M}$, $\lambda_{\text{ex}} = 288 \text{ nm}$, $\lambda_{\text{max}} = 525 \text{ nm}$)¹⁰⁸

On the basis of these preliminary studies, Bew and co-workers hypothesised that the fluorescence quenching observed for **114** arises from Au(III) coordination to the alkyne moiety and a subsequent charge transfer process from the excited state of the dansyl fluorophore to the proximal Au(III) ion.

1.6.5 Calix[4]arenes as nonlinear optical materials

Calix[4]arenes have also been exploited in the production of nonlinear optical materials.^{46,109–113}

These are materials in which the dielectric polarisation, P , responds in a nonlinear fashion to the intensity of light which travels through it. This has several consequences, many of which make these materials eminently useful; i) the refractive index of a nonlinear optical material varies with light intensity, ii) the frequency of light can be altered as it travels through a nonlinear optical material and iii) photons can interact whilst inside a nonlinear optical material, allowing 'light to control light'.

In such materials, the structural element responsible for the nonlinear optical properties (generally referred to as the 'NLOphore') is typically comprised of one or more donor (D) and acceptor (A) moieties connected *via* a conjugated π -system.¹¹⁴ The earliest examples of such systems based on calix[4]arenes were pioneered by Reinhoudt and co-workers in 1992, and exploited their conformational malleability to produce a series of *tetra*-nitrated analogues (*i.e.* **118**, **119** and **120**) bearing D- π -A dipoles locked in a variety of different orientations (**Figure 1.20**).¹⁰⁹

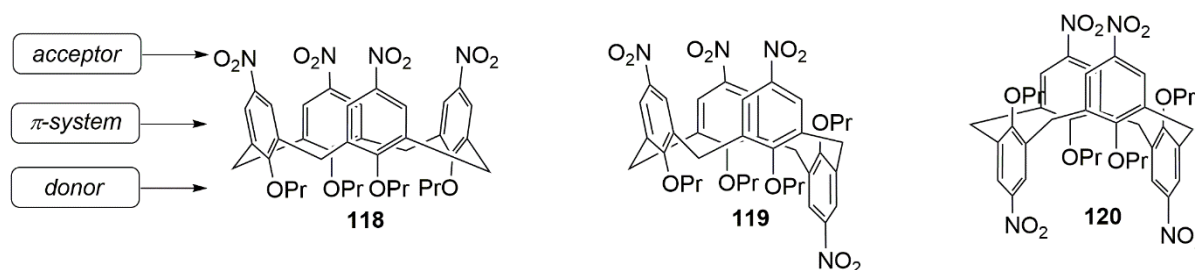


Figure 1.20: Tetra-nitrated calix[4]arenes synthesised as part of Reinhoudt's study into NLOphores¹⁰⁹

In an effort to determine the influence of these orientations on the second-order nonlinear polarizability, or first hyperpolarizability, β , the Dutch group employed the technique of electric field induced second harmonic generation (EFISH).¹¹⁵ It was found that compounds **118** and **119** both exhibit β_2 values of about 30×10^{-30} esu, whilst the centrosymmetric **120**, as anticipated, does not display any frequency-doubling of 1064 nm laser light (Nd:YAG laser) since it has no net dipole moment.

In a later publication,¹¹⁰ the same research group studied the macroscopic NLO properties of oriented thin-films of **118** prepared by spin-casting and subsequent poling using a strong DC electric field. By employing **118** in a so-called 'doped' polymer film of poly(methylmethacrylate), materials

with promising second-order optical properties and high stabilities could be formed containing as much as 65 weight% **118**.

More recently, Hennrich and co-workers have described the synthesis and optical properties of a series of alkynyl functionalised D- π -A calix[4]arenes exemplified by **121** (Figure 1.21).⁴⁶

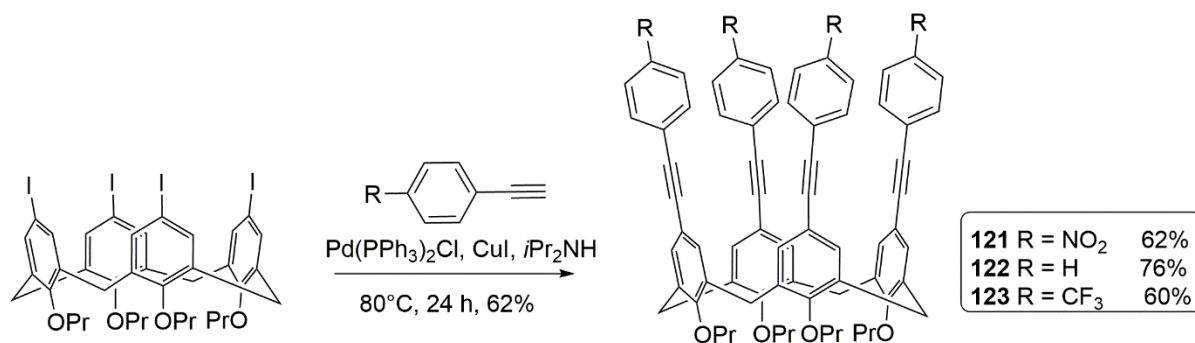


Figure 1.21: Hennrich's first generation design for alkynyl functionalised D- π -A calix[4]arenes⁴⁶

These NLOphores were readily synthesised *via* Sonogashira couplings, and were demonstrated to display enhanced second-order nonlinearities compared to Reinhoudt's tetra-nitrated calix[4]arenes **118** and **119**. More interestingly, the Spanish group were able to derive values for the opening angle of the calix[4]arene cavity from the measured values of the hyperpolarizability, β . Thus in doing so, the technique of hyper-Rayleigh Scattering (HRS) (employed to measure β) was demonstrated to be a powerful analytical tool for the structural determination of such D- π -A calix[4]arenes in solution.

1.7 Conclusions

In this introductory review covering the synthesis, functionalisation and selected applications of the calix[4]arenes it has been seen how their unique structural features have been exploited by a large number of industrial and academic researchers for the production of complexing agents (Sections 1.5.1 and 1.5.2), optical and fluorescent sensors (Sections 1.5.3 and 1.5.4) and non-linear optical materials (Section 1.5.5). With such a diverse array of publications covering these research areas, it is clear that much has already been achieved. However, within these sub-fields, it has also been demonstrated that a number of important challenges still remain. For example, there are still relatively few examples of: a) calix[4]arene based ion-selective sensors for the detection of the precious metals (in particular Au(I) and Au(III)), b) protocols for the rapid and operationally simple construction of multicalix[4]arene based cavitands, and c) NLOphores based on calix[4]arene scaffolds.

It is proposed that these challenges could be addressed, at least in part, by advances in synthetic methodology. Indeed, from my reading of the literature, I suggest that the lack of suitable or

efficient protocols for the synthesis of intricately functionalised calix[n]arenes (*e.g.* in particular those with ABAC and ABCD substitution patterns at the upper-rim) has been a limiting factor in the development of many such applied systems. To present just one example, Shinkai's fluorescent sensor **89** discussed in section 1.6.3 was only accessed in a *ca.* 11% yield after a lengthy synthesis involving 6 linear steps from commercially available starting materials. Given that syntheses of this type are common in many preparative schemes throughout calix[4]arene chemistry, new developments in the application of modern synthetic methods such as 'click' chemistry and transition metal mediated coupling reactions are clearly required.

1.8 Aims of the project

This PhD project had three distinct aims which are all linked by the theme of advancing synthetic methods for the selective upper-rim functionalisation of calix[4]arenes. The first of these aims was directed at the development of protocols for the synthesis of ABAC functionalised calix[4]arenes, and in particular those which would enable us to build upon preliminary results obtained by Bew and co-workers that concerned the synthesis of a calix[4]arene based sensor (*i.e.* **114**) for the rapid and highly sensitive detection of the Au(III) ion (review section 1.5.4.2) (**Figure 1.22**).¹⁰⁸

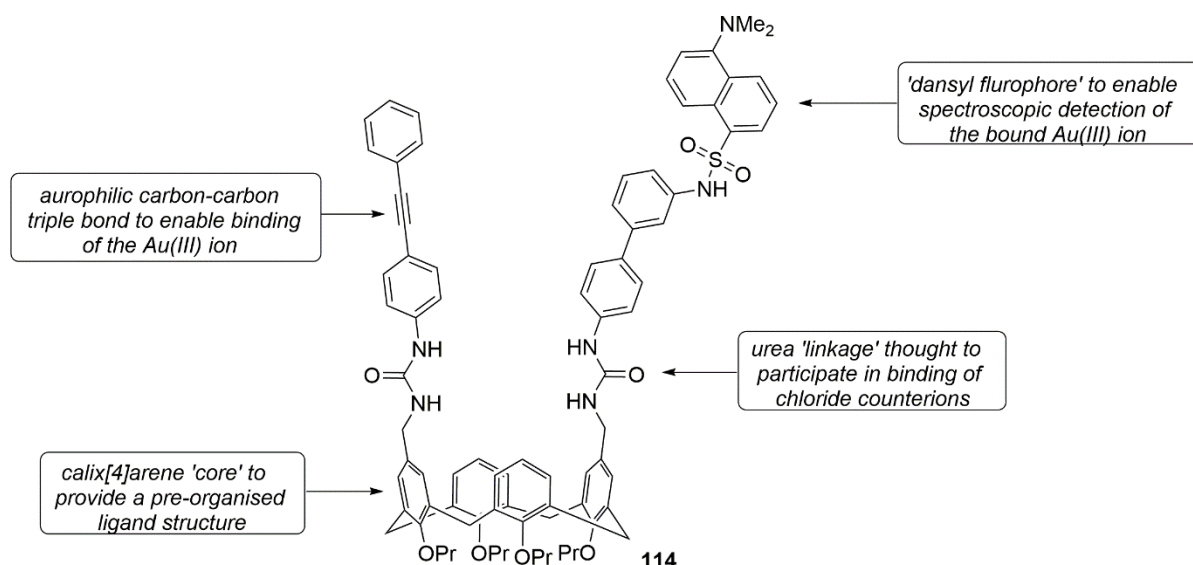


Figure 1.22: Bew's first generation design for a calix[4]arene based sensor for the Au(III) ion¹⁰⁸

With preliminary findings indicating that **114** could act as a highly sensitive sensor for the Au(III) ion over a range of other metal ions (*i.e.* Cd²⁺, Ag⁺, Pd²⁺, Hg²⁺, Pt²⁺, Li⁺, Na⁺), it was proposed that a detailed study of the structure and function of **114** would allow for the development of a series of highly specific and highly sensitive 'second generation' Au(III) sensors. Specifically, I was interested in generating derivatives of **114** such as **124** and **125** which carry electron rich and electron poor aryl groups respectively to assess what effect, if any, this might have on the sensitivity and/or selectivity

of these probes by modifying the electronic environment of the alkyne functional group (**Figure 1.23**).

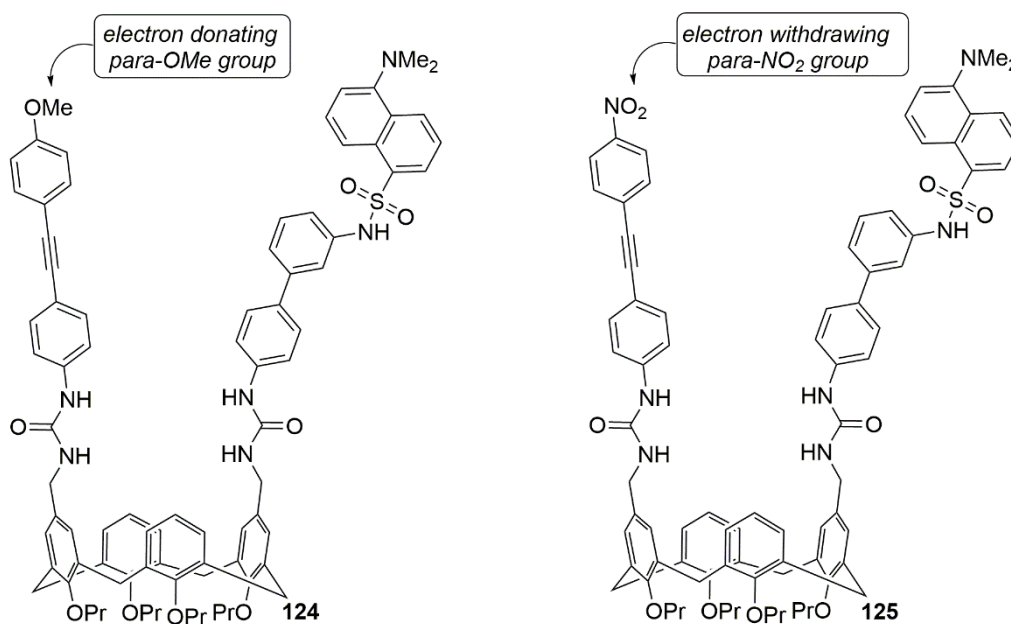


Figure 1.23: Proposed 'second generation' derivatives of calix[4]arene based sensor **114**

I was also interested in the possibility of introducing a second carbon-carbon triple bond into the structure of these probes in an effort to see if this would enhance sensitivity by providing an additional metal binding site. With this aim in mind, the synthesis of a further set of derivatives based on **114** which contained this additional structural feature was proposed (**Figure 1.24**).

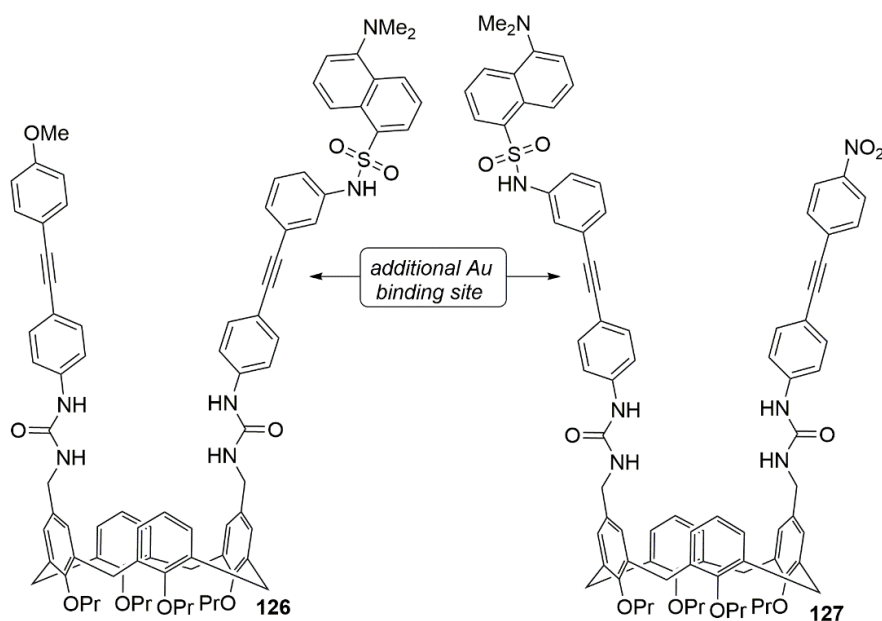
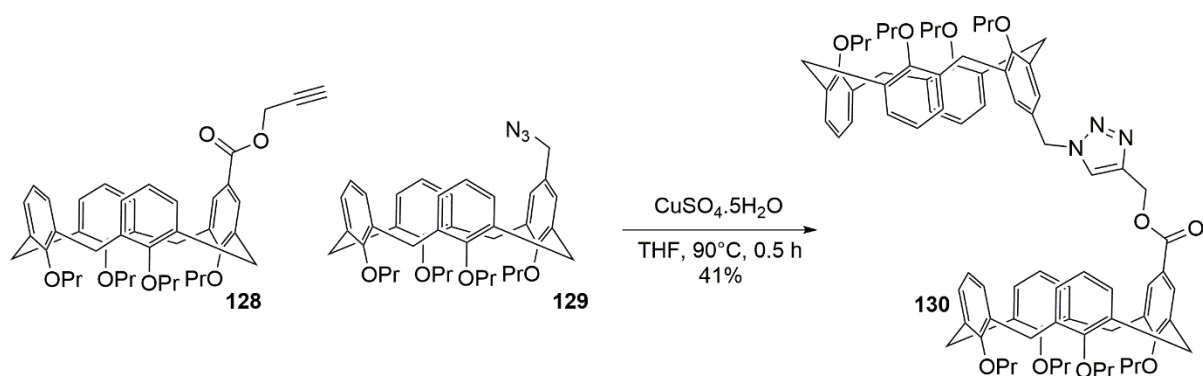


Figure 1.24: Proposed 'second generation' derivatives of calix[4]arene based sensor **114** which feature an additional metal binding site

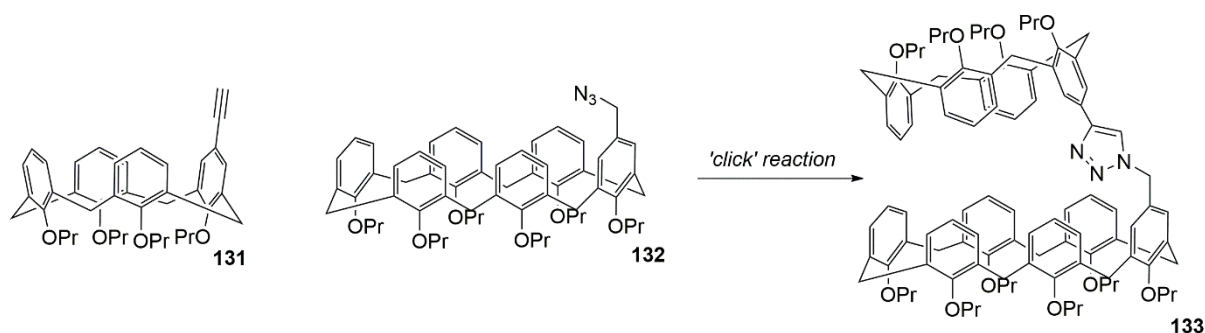
It was envisioned that these structure-function studies would ultimately allow us to chemically ‘tune’ the upper-rim substituents in such a way to optimise this sensor for the detection of Au(III) ions.

The second aim of this project was to optimise synthetic protocols for the synthesis of AAAB functionalised calix[4]arenes for their use in the development of a novel series of 1,2,3-triazole linked calix[n]arene based cavitands as complexing agents. In particular, I was interested in building upon preliminary results obtained within the Bew and Stephenson laboratories which indicated that the copper-catalysed azide-alkyne cycloaddition (CuAAC) reaction would provide an operationally simple means for their rapid assembly (**Scheme 1.31**).⁵³



Scheme 1.31: Bew and Stephenson’s synthesis of 1,2,3-triazole linked multicalex[4]arene **130**⁵³

I was envisioned that extending these studies into the preparation of a series of novel mono-functionalised calix[4] and [6]arenes such as **131** and **132** would allow for the construction of a second generation family of upper-rim 1,2,3-triazole linked cavitands such as **133** (**Scheme 1.32**).



Scheme 1.32: Proposed mono-functionalised calix[4] and [6]arenes which should allow access to a new family of 1,2,3-triazole linked cavitands exemplified by **133**

In accordance with literature reports detailing the synthesis and properties of multicalex[4]arenes (**Section 1.6.2 and references therein**), it was proposed that by varying the structure of the connecting heterocycle bridge and the size of the calix[n]arene macrocycle, a series of cavitands with unique binding properties towards guests such as anions, cations and small neutral molecules could be generated.

The third aim and final aim of this project was to advance synthetic protocols for the preparation of ABAC and ABCD functionalised calix[4]arenes that would, in turn, enable us to readily generate the first examples of calix[4]arene derived nonlinear optical materials which incorporate a 'molecular switch' of some sort within their structures (**Figure 1.25**).

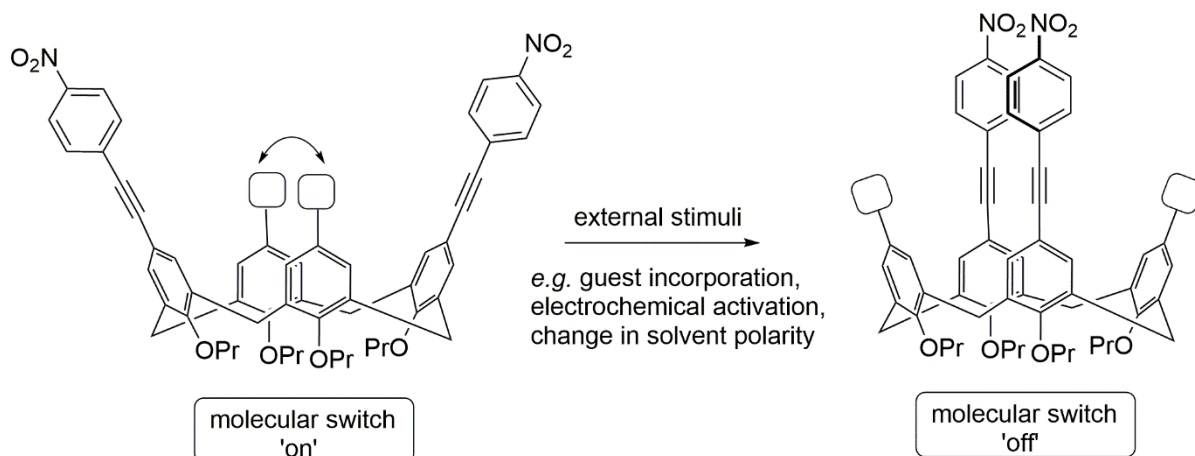


Figure 1.25: The proposed general design for switchable NLOphores

In this way, it was proposed that these second generation NLOphores could respond (*i.e.* by way of a conformational change between the two pinched-cone conformers) to external stimuli (*e.g.* changes in solvent polarity, inclusion of a guest, or electrochemical activation). Crucially, it was anticipated that in accordance with previous literature studies (**Section 1.6.5 and references therein**) any conformational change so induced would result in the direct modulation of NLO-properties by changing the angle between the two D- π -A moieties.

Chapter 2: Results and Discussion

Studies Towards the Development of a Fluorogenic
Sensor Optimised for the Gold(III) ion

2.1 Abstract

A series of urea functionalised calix[4]arenes featuring ABAC substitution at the upper-rim have been designed and synthesised as part of the conclusion to a project which was originally directed towards their application as fluorogenic sensors for the detection of Au(III) ions. In this chapter, a novel protocol for the operationally simple synthesis of such ABAC-functionalised calix[4]arenes *via* the application of ‘ionic hydrogenation’ and transition-metal mediated coupling methodologies is presented. Their intended use as fluorogenic probes for the detection of the Au(III) ion was investigated *via* fluorescence spectroscopy, and is critically discussed with reference to preliminary results obtained within the Bew group.

2.2 Methodology

With such a highly functionalised set of molecular targets required (*e.g.* **124** and **125**) I decided it would be best to initiate this project by considering the synthetic pathways that had been described previously both within the Bew research group, and the literature, applying the ones that appeared most suited to my synthetic targets. This review indicated that several fundamentally different reaction protocols were available. The original synthesis of **114** (Section 1.5.4.2) was achieved *via* the sequential Sonogashira and Suzuki-Miyaura couplings of pre-assembled building blocks **134** and **135** onto the readily generated *bis*-iodourea calix[4]arene **136** (Figure 2.1).¹¹⁶

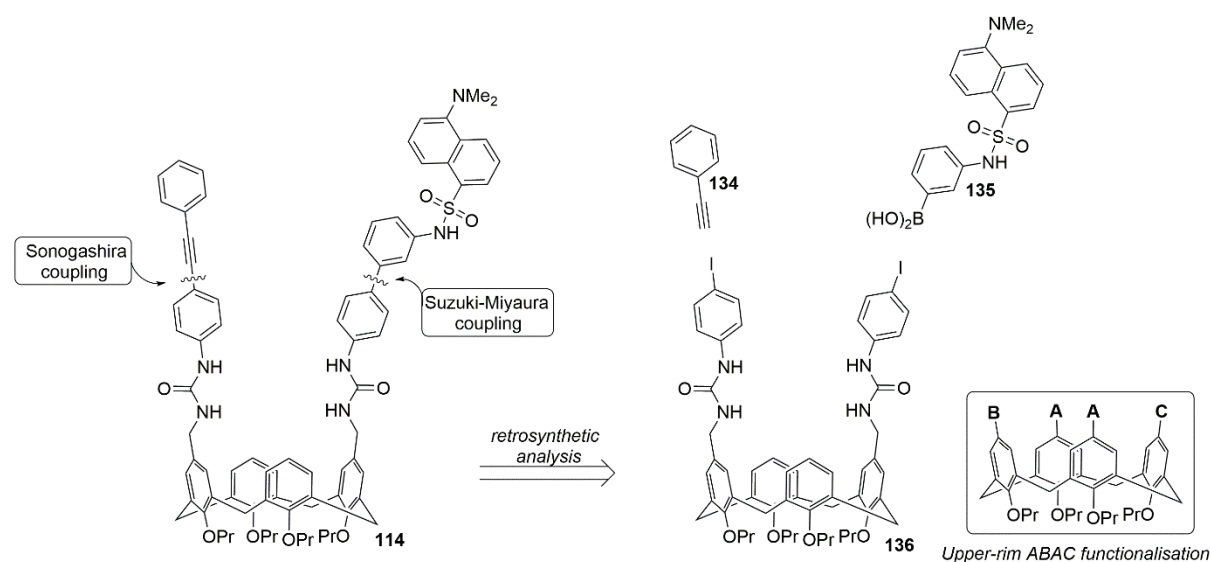
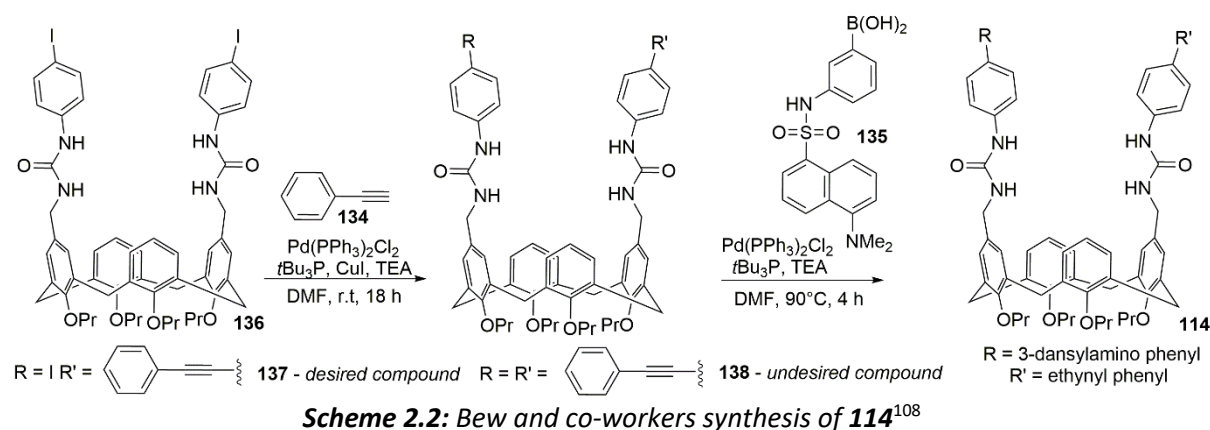


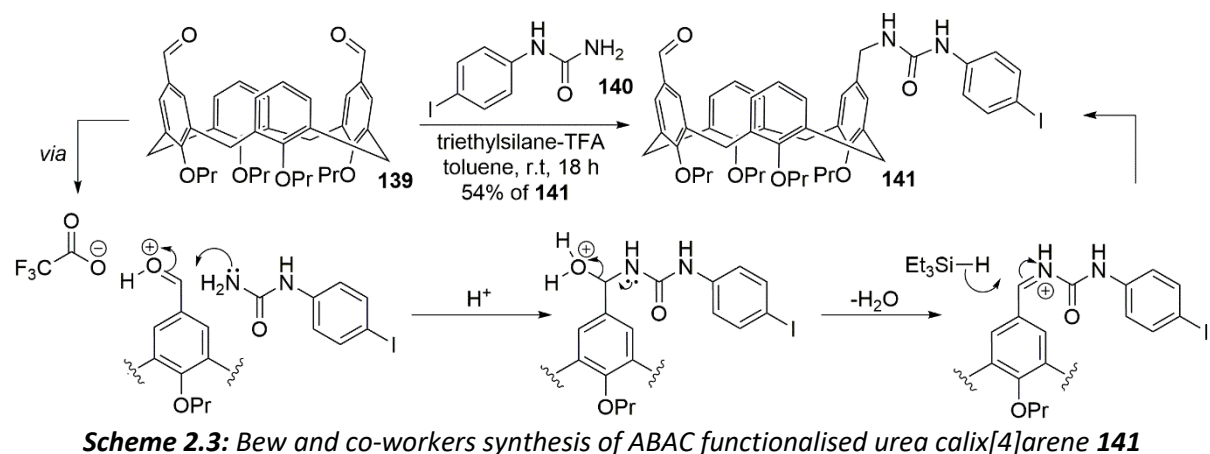
Figure 2.1: Bew and co-workers retrosynthesis of Au(III) specific sensor **114**¹⁰⁸

In this synthesis, the ABAC substitution pattern was established early on by a Sonogashira coupling employing *bis*-iodourea calix[4]arene **136** and 1.1 equivalents of phenyl acetylene **134**. Unfortunately, despite exhaustive efforts, separation of the desired *mono*-substituted product **137** from both the remaining starting material **136** and the *bis*-1,3-substituted product **138** by column

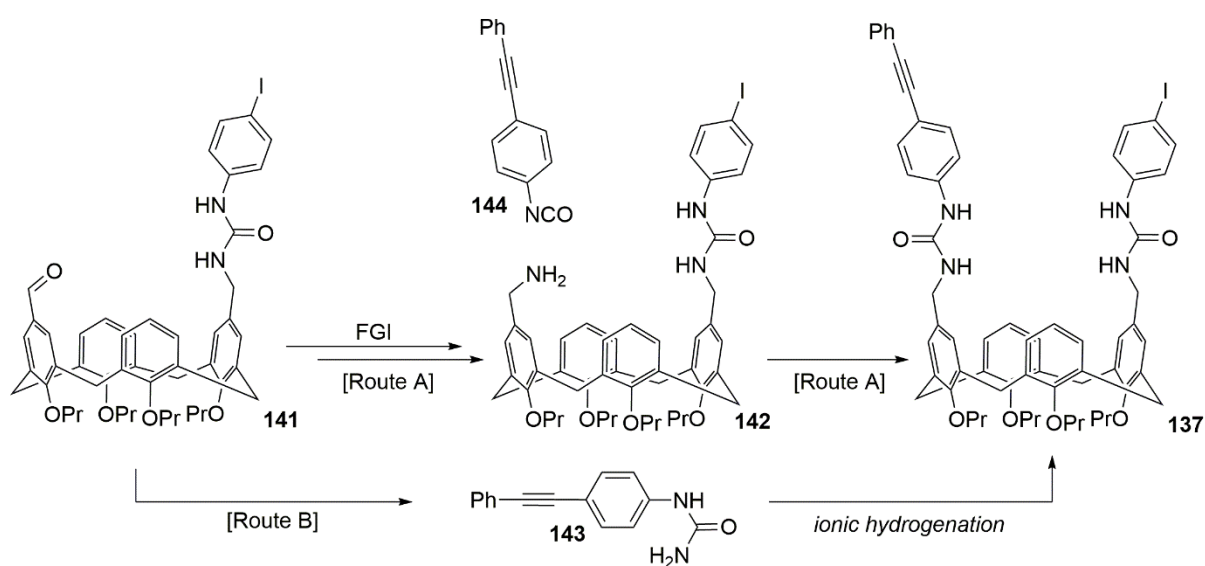
chromatography could not be achieved. Thus in order to complete the synthesis, this impure mixture was employed directly in the Suzuki-Miyaura coupling with dansyl boronic acid **13**. The hope was that by taking it through to the fully functionalised compound it would be easier to purify. From the resulting complex mixture (*i.e.* containing **135**, **136**, **137**, **138** and **114**) the desired **114** was, eventually, isolated – but only *via* extensive flash column chromatography. Furthermore, it was isolated in poor yield (*i.e.* 24% from **136**) and moderate purity ($^1\text{H-NMR}$ and mass spectrometric data indicated some contamination by, at the least, *bis*-substituted **138**) (**Scheme 2.2**).



On account of these difficulties, I was keen to attempt a new route and as such devised a retrosynthesis of **114** in which the upper-rim ABAC substitution pattern would be established much earlier in the synthesis and by an operationally simple means. A review of the literature indicated that Bew and co-workers have achieved the introduction of a structurally similar ABAC substitution *via* an ionic hydrogenation protocol wherein 1,3-diformyl calix[4]arene **139** is reacted with 1.2 equivalents of aryl urea **140** under reducing conditions (*i.e.* triethylsilane-TFA) to afford, in moderate yield (*i.e.* 54%) but high purity, the mono-substituted **141** after chromatographic separation from the corresponding *bis*-substituted **136** and unreacted starting materials **139** and **140** (**Scheme 2.3**).¹¹⁶



It was anticipated that by employing **141** as the key starting material in this synthesis, the difficulties encountered with chromatographic separation in the original preparation of **114** would be obviated, since in this one step, the ABAC substitution pattern is neatly established. With compound **141** identified, a number of alternative strategies to complete this new synthetic plan were devised. It was proposed that a more advanced intermediate **137** could be obtained *via* a second ionic hydrogenation with a suitably functionalised urea (*i.e.* **143**) providing that the carbon-carbon triple bond of **143** was resistant to reduction under these conditions. Alternatively, it was anticipated that functional group interconversion (FGI) of the formyl group in **141** to the benzylamine in **142** might allow the second urea group to be fashioned *via* the reaction with a suitably functionalised isocyanate (*i.e.* **144**) (Scheme 2.4).



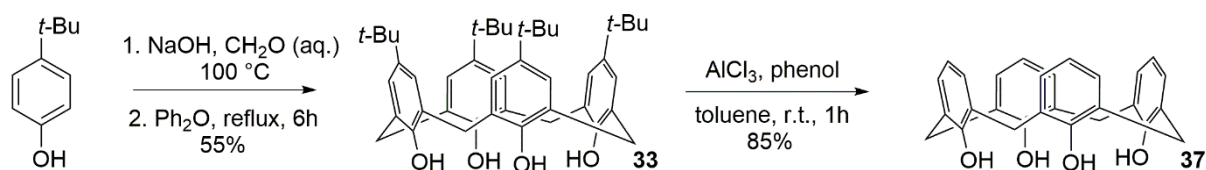
Scheme 2.4: Proposed synthetic routes A and B towards an 'advanced intermediate' **137**

Since the use of aryl isocyanates for the generation of the urea functionality is well established within the calix[*n*]arene field, it was felt that the application of this amine-isocyanate reaction to this system was quite reasonable.^{37,48,117,118} With analytically pure samples of **137** in hand, it was anticipated that further elaboration in the same mode as previously described (*i.e.* Suzuki-Miyaura coupling with the dansyl boronic acid **135**) would allow for the generation of sensor **114** in high purity. If either route A or B were successful, it was presumed that extension to include a series of derivatives for use in my structure-function studies would be trivial.

2.3 Synthesis of 'core' calix[4]arene scaffold **37**

At the outset of this project a reliable, scalable and high yielding protocol for the synthesis of calix[4]arene **37** was required, as this material is the key starting point for the synthesis of all the highly functionalised calix[4]arene derivatives (**114**, **124**, **125**). Thus following a literature procedure

originally developed by Gutsche and co-workers, *tert*-butylphenol and formaldehyde were condensed under basic conditions (*i.e.* sodium hydroxide) on a 500 g scale to afford *para-tert*-butylcalix[4]arene **33** in a 55% yield after recrystallisation from toluene. The formation of **33** was confirmed by comparison of its ¹H-NMR spectrum in CDCl₃ to the literature values. Broad resonances observed at 4.2 and 3.5 ppm were attributed to the methylene bridges and a broad singlet at 10.3 ppm to the phenolic protons indicative of the cone conformation enforced by the strong hydrogen bonding of all phenolic OH's at the lower-rim. The subsequent removal of the *tert*-butyl groups was affected by treatment of **33** with phenol and aluminium chloride in a retro Friedel-Crafts reaction; this afforded an 85% yield of 'core' calix[4]arene **37** (**Scheme 2.5**).

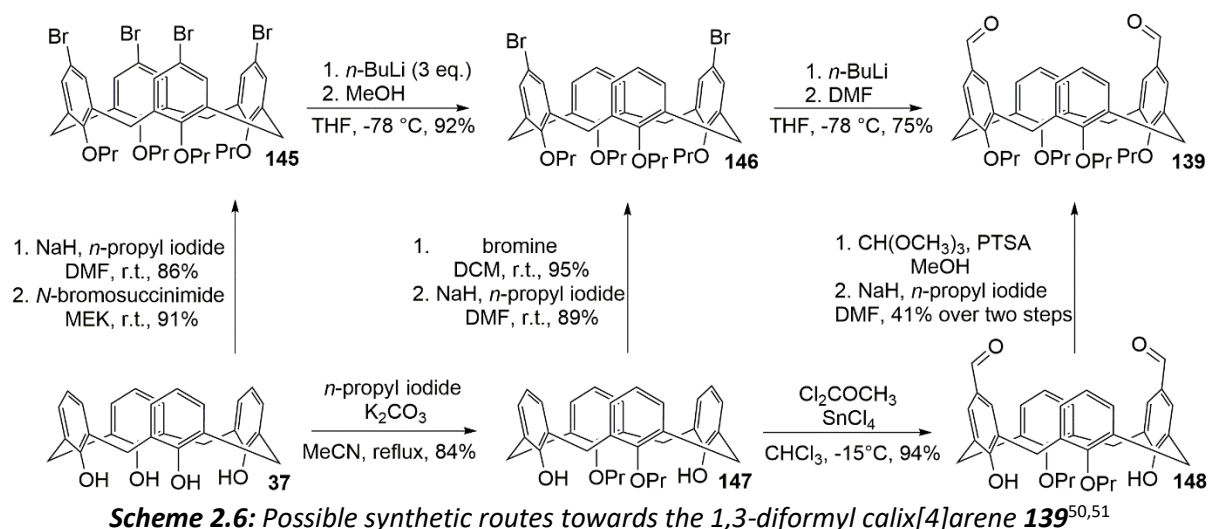


Scheme 2.5: The reaction sequence affording 'core' calix[4]arene **37** via the de-*tert*-butylation of **33**⁷

The function of phenol in this de-*tert*-butylation reaction is to act as a scavenger for the *tert*-butyl group, without which the reaction could not proceed to completion. Inspection of the ¹H-NMR spectrum of **37** revealed two sets of aromatic signals – a singlet at 7.0 ppm and a doublet at 6.7 ppm – confirming the loss of the *para*-substituted *tert*-butyl group. In addition, the remaining signals (*i.e.* s 10.2, s 7.0, d 6.7, brs 4.2, brs 3.5 ppm) and ¹³C-NMR spectrum both correlated well with those originally reported by Gutsche for the same compound.⁷

2.4 Synthesis of 1,3-diformyl calix[4]arene **139**

Satisfied that I could readily prepare the 'core' calix[4]arene **37** on a large scale (*i.e.* 30 g), I looked towards the synthesis of the known 1,3-diformyl calix[4]arene **139**. This would be the key starting material for the generation of the required *mono*-iodophenylurea calix[4]arene **141**. A literature review, and previous studies within the Bew group, indicated a number of possible synthetic routes towards **139** (**Scheme 2.6**).



Larsen and co-workers reported the synthesis of **139** via a four-step sequence from calix[4]arene **37**.⁵¹ The *tetra*-o-propylation of calix[4]arene **37** was achieved in an 86% yield by reaction with sodium hydride and *n*-propyl iodide in *N,N*-dimethylformamide. Exhaustive bromination of the free *para* positions was undertaken using an excess of *N*-bromosuccinimide in methyl ethyl ketone, whilst a selective 1,3-debromination was affected by treatment with *n*-butyllithium in tetrahydrofuran affording the corresponding di-lithiated species, which was subsequently quenched with methanol to afford a 92% yield of **146**. Finally, treatment of **146** with *n*-butyllithium in tetrahydrofuran followed by reaction with *N,N*-dimethylformamide and hydrolysis (H₂O) afforded a 75% yield of **139** after recrystallisation from *n*-hexane. In a slightly modified approach, Stanstny and co-workers described the preparation of **139** via the bromination of 1,3-dipropoxy calix[4]arene **147** using bromine in dichloromethane. A subsequent high yielding o-propylation (*i.e.* 89%) afforded precursor **146** which was transformed into **139** via the same halogen-lithium exchange reaction described by Larsen.⁵⁰

In an alternative preparation, Ungaro and co-workers have described a route employing the Gross formylation of 1,3-dipropoxy calix[4]arene **147** using 1,1-dichloromethyl methyl ether and tin(IV)chloride in chloroform. The resulting diformyl calix[4]arene **148** is then protected as its corresponding *bis*-dimethyl acetal, before o-propylation with sodium hydride and *n*-propyl iodide in *N,N*-dimethylformamide. The function of the acetal protecting group is to promote the formation of the cone confined calix[4]arene, since direct o-propylation of **148** is reported to afford significant quantities of the partial cone conformer. Indeed, even with the acetal protecting group in place, small quantities of the partial cone conformer (*c.a.* 15%) must be removed via flash column chromatography.¹¹⁹

Keen to avoid any chromatography in the preparation of **139**, and based on previous investigations within the group, I opted to follow the route described by Stanstny and co-workers. Thus following their procedure, calix[4]arene **37** was transformed into 1,3-dipropoxy calix[4]arene **147** by reaction with *n*-propyl iodide and potassium carbonate in refluxing acetonitrile overnight. A straightforward trituration with methanol was sufficient to afford **147** in an excellent yield (*i.e.* 87%) and purity ($\geq 95\%$ by $^1\text{H-NMR}$).

Initial attempts at the bromination of **147** following the literature protocol only returned moderate yields (*i.e.* 50%) of desired product **146a**. As the halogenated product **146a** is highly insoluble in the reaction medium, and is simply collected by suction filtration, I was puzzled as to why the high yield (*i.e.* 95%) reported by Stanstny could not be reproduced. Reasoning that the reaction had not gone to completion, the reaction time was extended from 1 hour (as described in the literature) to 3 hours – this minor adjustment then allowed **146a** to be isolated in a comparable 90% yield. A subsequent high-yielding *o*-propylation (*i.e.* 92%) of the two remaining phenolic units proceeded without incident to afford the precursor to **139**. With this material in hand, I was in a position to attempt the formylation reaction under the conditions reported by Larsen and co-workers. Performing the reaction on a 10 g scale I was delighted to be able to obtain **139** in a 65% yield after recrystallisation from *n*-hexane. The $^1\text{H-NMR}$ spectrum was in accordance with literature reports, and displayed a singlet at 9.47 ppm arising from the two equivalent formyl protons (**Figure 2.2**).

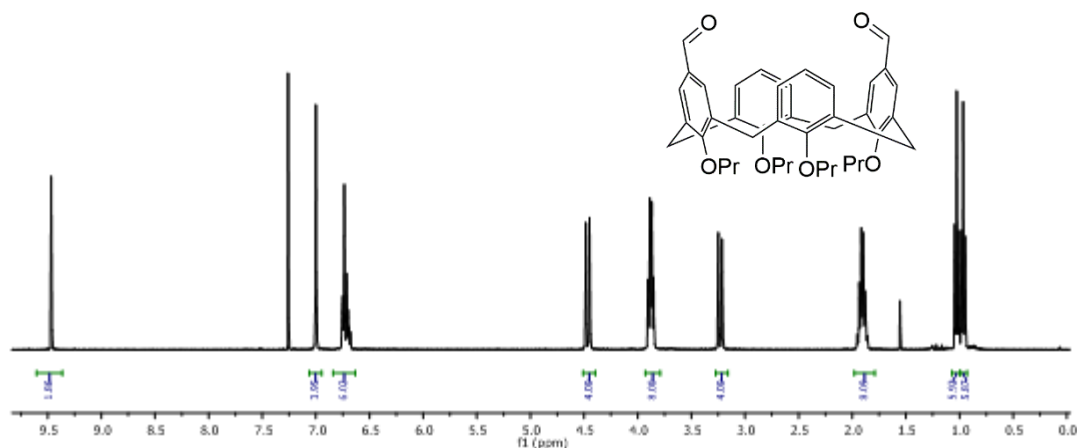
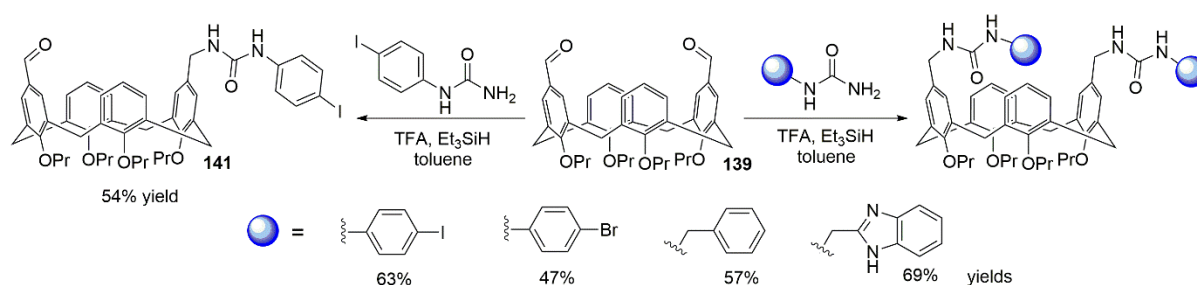


Figure 2.2: The $^1\text{H-NMR}$ spectrum of diformyl calix[4]arene **139** (500 MHz, CDCl_3)

In addition, a mass ion was observed at 649.2 in the MALDI spectrum which corresponds to $[\text{M}+\text{H}]^+$ further confirming the identity of this sample of **139**.

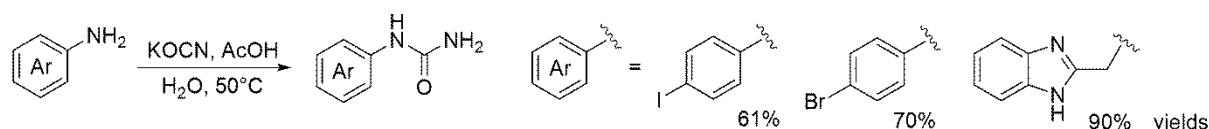
2.5 Synthesis of *mono*-iodophenylurea calix[4]arene **141** via ionic hydrogenation

Satisfied that I now had access to multi-gram quantities of **139** with which to continue these investigations, I looked towards the preparation of the required *mono*-iodophenylurea calix[4]arene **141** – the synthesis of which has been previously reported by the Bew group. By employing the conditions first developed by Dube and Scholte for the reductive *N*-alkylation of carbamates and ureas, Bew and co-workers found that **139** can be efficiently transformed into a wide array of highly functionalised upper-rim urea (and carbamate) derived calix[4]arenes, and importantly for this application, the *mono*-substituted **141** could also be isolated in a 54% yield (**Scheme 2.7**).^{116,120}



Scheme 2.7: Bew's synthesis of urea functionalised calix[4]arenes by reaction of aryl ureas with **139** under reducing conditions¹¹⁶

Since previous routes towards aryl urea functionalised calix[4]arenes have involved the use of aryl isocyanates which are, in general, lachrymatory and moisture sensitive, this route represents an improvement in terms of safety and convenience.³⁷ Additionally, the syntheses of the required aryl ureas could be performed under mild conditions (*i.e.* at 50 °C) by reaction of the corresponding aniline with potassium cyanate in aqueous acetic acid (**Scheme 2.8**).

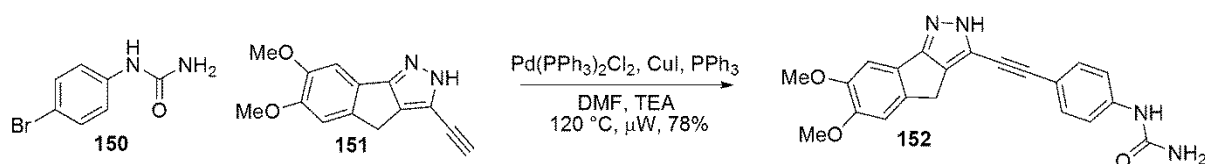


Scheme 2.8: The preparation of aryl ureas from their corresponding anilines by reaction with KOCN¹¹⁶

Confident that the ionic hydrogenation route would be satisfactory for the preparation of large quantities of the required *mono*-iodophenylurea calix[4]arene **141**, I set about preparing *para*-iodophenyl urea **149** by reaction of *p*-iodoaniline and potassium cyanate. Recrystallisation of the impure product from boiling methanol afforded a 68% yield of analytically pure **149**. Characterisation of this material by ¹H-NMR spectroscopy in d₆-DMSO allowed both sets of NH protons to be clearly observed (*i.e.* NH at 8.61 ppm and NH₂ at 5.89 ppm). Cautious about the long-term photochemical stability of the carbon-iodine bond in **149**, I opted to store this reagent in the dark.

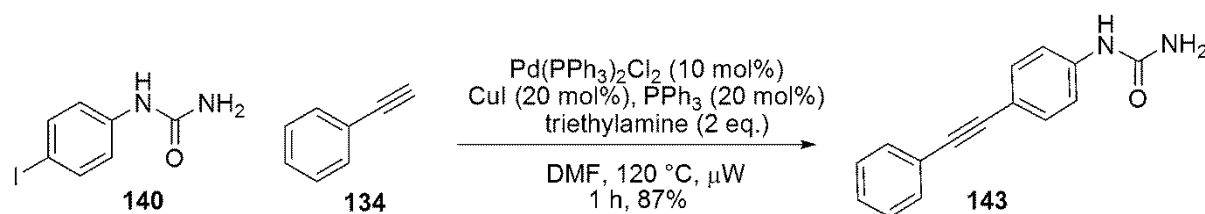
2.6 Synthesis of ABAC *bis*-urea calix[4]arene intermediates *via* a second ionic hydrogenation

Anticipating that the target aryl urea **143** might be accessed *via* the Sonogashira coupling between *para*-iodophenyl urea **149** and phenylacetylene **134**, I conducted a literature search in order to identify a suitable set of coupling conditions. Although no examples of Sonogashira couplings involving **149** were identified, Tao and co-workers have reported the synthesis of the kinase inhibitor **152** *via* the coupling of *p*-bromophenyl urea **150** with the tricyclic pyrazole **151** under palladium catalysis (Scheme 2.9).¹²¹



Scheme 2.9: Tao and co-workers' application of the Sonogashira reaction to *p*-bromophenyl urea¹²¹

By employing Pd(PPh₃)₂Cl₂ as their palladium[0] source and copper(I)iodide as the co-catalyst, the American group obtained a 78% yield of the kinase inhibitor **152** after 4 hours reaction time at 120 °C in *N,N*-dimethylformamide. Encouraged by this result, and anticipating that aryl iodide **140** was likely to be more reactive than the aryl bromide **150** in any such analogous process, it was decided to employ these conditions for a test reaction. Thus I performed the reaction on a 1 mmol scale, and was delighted to observe complete consumption of **140** by TLC analysis after only 1 hour at 120 °C under microwave irradiation (Scheme 2.10).

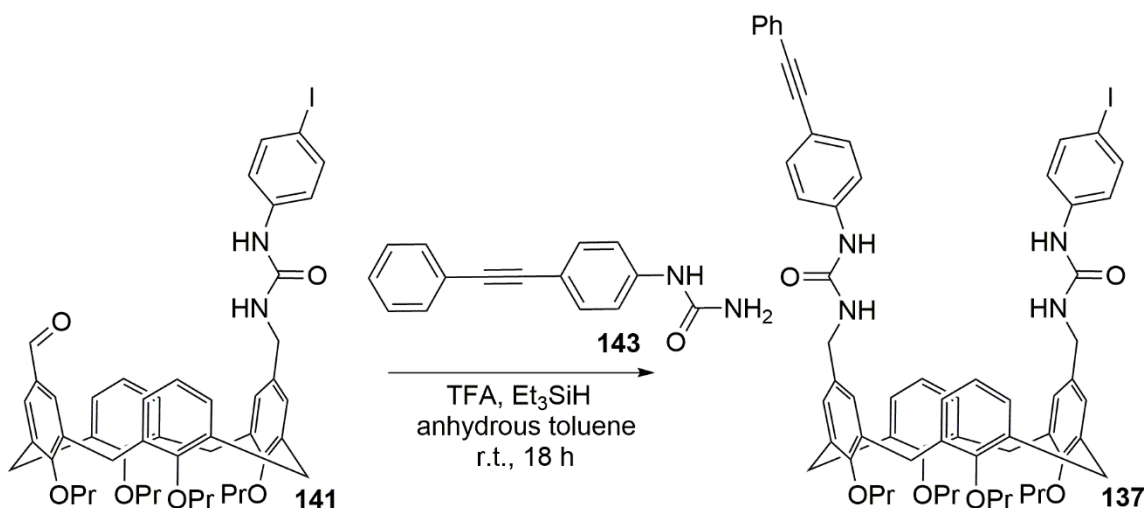


Scheme 2.10: Synthesis of aryl urea **143** *via* a Sonogashira coupling

On account of the low solubility of the product **143** in a range of organic solvents, trituration with diethyl ether proved a convenient way to obtain analytically pure **143** in an 87% yield – its formation being confirmed by a full physicochemical analysis. In the ¹³C-NMR spectrum (d₆-DMSO) for example, the urea carbonyl was observed at 155.7 ppm, whilst the alkynyl carbons were observed at 89.9 and 87.9 ppm. Furthermore, a mass ion was observed at 259.23 which corresponds to [M+Na]⁺ in the MALDI spectrum, thus providing additional evidence for the identity of **143**.

With samples of both the *mono*-iodophenylurea calix[4]arene **141** and the newly synthesised urea **143** in hand, I was now in a position to attempt the synthesis of 'advanced intermediate' **137** *via* the

ionic hydrogenation outlined earlier. For a first attempt, it was thought reasonable to follow the published procedure closely with regards to the number of equivalents of aryl urea, triethylsilane (TES) and trifluoroacetic acid (TFA) that were employed. Thus I opted to perform a test reaction using an excess of aryl urea **143** (*i.e.* 2 equivalents) and 6 equivalents of both TES and TFA in anhydrous toluene on a 0.1 mmol scale (**Scheme 2.11**).



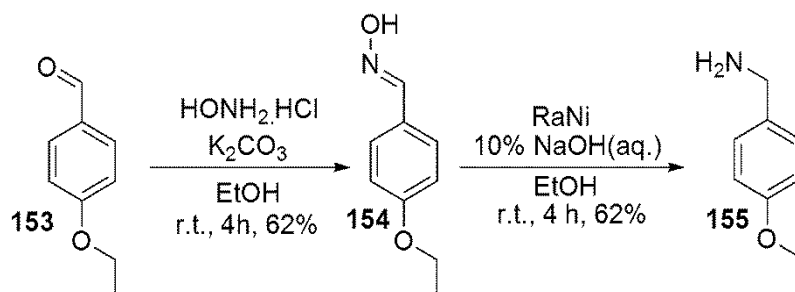
Scheme 2.11: Test ionic hydrogenation reaction

After stirring the reaction mixture at room temperature for 18 hours, TLC analysis indicated that all of the starting material **141** had been consumed. Analysis of the impure material by ¹H-NMR spectroscopy indicated that a complex mixture of products had been formed – possibly *via* the partial and/or full reduction of the alkyne, as has been reported in analogous (non-calixarene) systems by Zdanovich and co-workers¹²² – all attempts at isolating a pure sample of **137** from this mixture failed. Attempts at reducing the molar equivalents of TFA and TES (*i.e.* to 1.2 eq.) and stopping the reaction immediately after **141** had been consumed, or reducing the temperature (*i.e.* to -10 °C) all led to the formation of complex mixtures. Suspecting therefore that it might be best to incorporate the alkyne later in this synthesis, it was decided to continue these investigations *via* route A (**Scheme 2.4**).

2.7 Synthesis of ABAC *bis*-urea calix[4]arene intermediates *via* the aminomethyl functionalised **142**

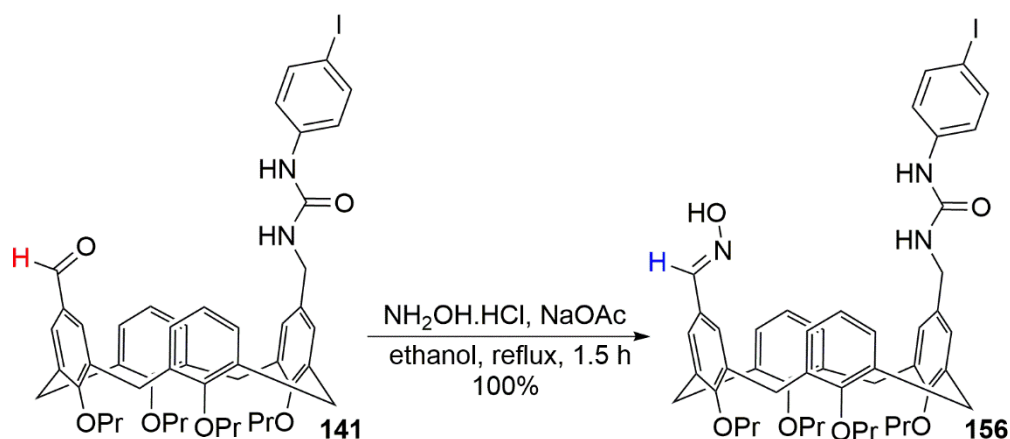
After the somewhat disappointing result encountered with the first attempt at the synthesis of **137**, I was keen to explore other options for its formation from ABAC functionalised **141**. Returning to the proposed retrosyntheses (**Scheme 2.4**), I began to reconsider the possibility that transforming the formyl group in **141** to the aminomethyl group in **142** might allow for the second urea function to be introduced *via* the reaction with an appropriately functionalised isocyanate (*i.e.* **144**). A review of the literature indicated a number of methodologies which might be suitable for this transformation

(i.e. CHO to CH₂NH₂). For example, Medda and co-workers have reported the transformation of a series of aryl aldehydes to their corresponding amines *via* a two step process involving the reduction of intermediate oximes (i.e. **154**) with Raney nickel in ethanol (**Scheme 2.12**).¹²³



Scheme 2.12: Medda's two-step conversion of aryl aldehyde **153** into aryl benzylamine **155**¹²³

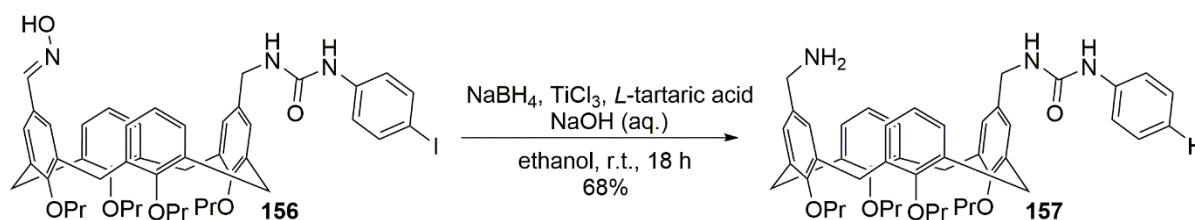
The reduction of aryl oximes to amines has also been achieved *via* reaction with lithium aluminium hydride,¹²⁴ zinc in hydrochloric acid,¹²⁵ hydrogen over palladium,¹²⁶ and the combination of sodium borohydride with nickel(II)chloride.¹²⁷ Whilst I was somewhat concerned about the stability of the carbon-iodine bond in substrate **141** to many of these conditions, since the reagents were at hand, I opted to investigate this reductive pathway for the formation of the aminomethyl functionalised calix[4]arene **142**. To synthesise the required oxime calix[4]arene **156**, I opted to employ the conditions reported by Sarodnick and co-workers.¹²⁸ I was delighted to observe that treating an ethanolic solution of *mono*-iodophenylurea calix[4]arene **141** with hydroxylamine hydrochloride and sodium acetate resulted in the quantitative formation of the desired oxime **156** after 1.5 hours at reflux (**Scheme 2.13**).



Scheme 2.13: The synthesis of oxime **156** via condensation of **141** with hydroxylamine hydrochloride

The identity of **156** was confirmed by a comprehensive physicochemical analysis; particularly characteristic was the appearance of a new singlet at 7.70 ppm in the ¹H-NMR spectrum arising from

the oxime proton (coloured in blue). Encouraged by this straightforward preparation coupled with the quantitative yield, I was now in a position to explore methods for the reduction of the oxime functional group to its corresponding primary amine **142**. As noted above, it was anticipated that the choice of reduction methodology was likely to be critical since the hydrodehalogenation of aryl iodides, bromides and chlorides is also known to occur readily under reducing conditions.¹²⁹ Thus whilst searching for a mild protocol, I was drawn towards a 1989 report from Miller and co-workers wherein they describe the combination of sodium borohydride and titanium(III) chloride in ethanol as an ideal system for the reduction of alpha-oximino esters.¹³⁰ Applying Miller's conditions directly to this substrate, I was pleased to observe the complete consumption of oxime **156** (TLC analysis) after 18 hours at room temperature (**Scheme 2.14**).

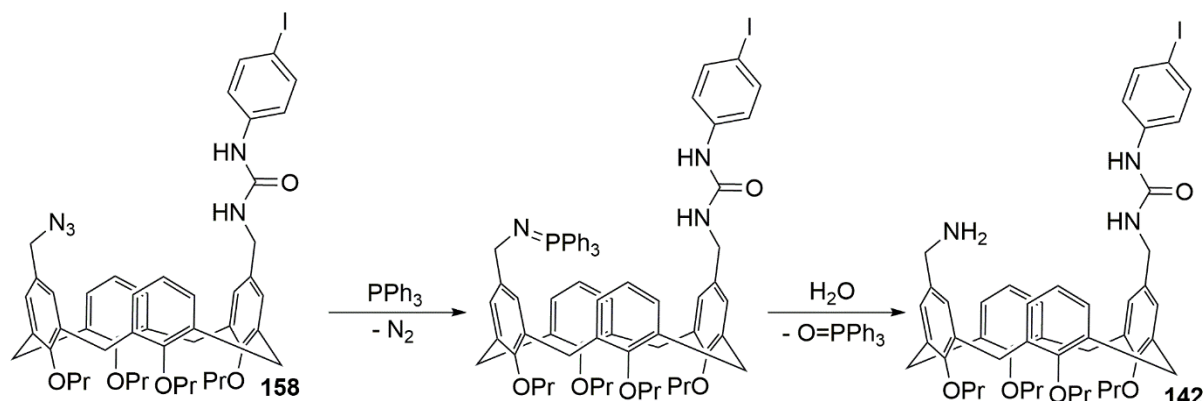


Scheme 2.14: The reduction of oxime **156** to primary amine **157**

Unfortunately, the subsequent analysis of the crude reaction mixture by ¹H- and ¹³C-NMR spectroscopy revealed that, in addition to efficiently reducing the oxime functionality, the combination of sodium borohydride and titanium(III) chloride had also affected the hydrodehalogenation of the carbon-iodine bond. A comprehensive physicochemical analysis of a pure sample obtained after isolation by flash column chromatography confirmed this; particularly characteristic was the multiplet at 7.24 ppm in the ¹H-NMR spectrum arising from the phenyl urea (when a pair of doublets would be expected for **142**) and the missing signal for the carbon atom carrying the iodine atom in the ¹³C-NMR (expected at ca. 85 ppm due to the heavy atom effect).

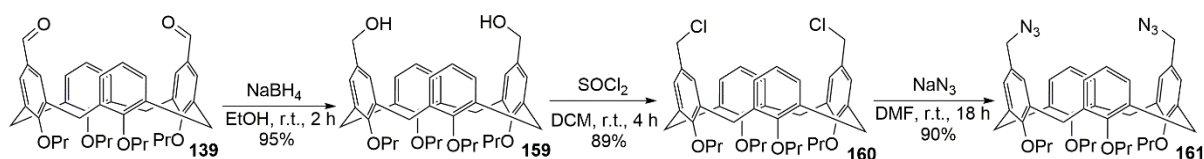
Disappointed by the lack of chemoselectivity, and unable to find an analogous example in the literature to follow (*i.e.* oxime reduction in the presence of an aryl iodide) it was reasoned that simply screening a range of alternative reducing agents might allow the identification of some suitable conditions. Thus I attempted the reduction of oxime **156** using a) lithium aluminium hydride (1.2 eq.) in THF at room temperature, b) magnesium (1.1 eq.) and ammonium formate (2 eq.) in ethanol at room temperature, and c) 10 mol% palladium on carbon and ammonium formate (2 eq.) in ethanol at reflux. Unfortunately, under these alternative conditions I observed either no reaction (Mg/NH₄HCO₂) or complete reduction (LiAlH₄ and Pd/NH₄HCO₂) to afford **157** as in the sodium borohydride/titanium(III) chloride case.

Surmising that I would need to affect this reductive amination process (*i.e.* **141** to **142**) under milder conditions, I returned to the literature to identify a more suitable, milder procedure. This review indicated the possibility of using the azide group as a synthon for the amino group present in **142** since azides are readily reduced to amines using a combination of the Staudinger reaction and hydrolysis. Importantly for this system, since this reduction is typically carried out with the very mild reducing agent triphenylphosphine, there would seem little chance of promoting the additional hydrodehalogenation I had encountered previously (**Scheme 2.15**).



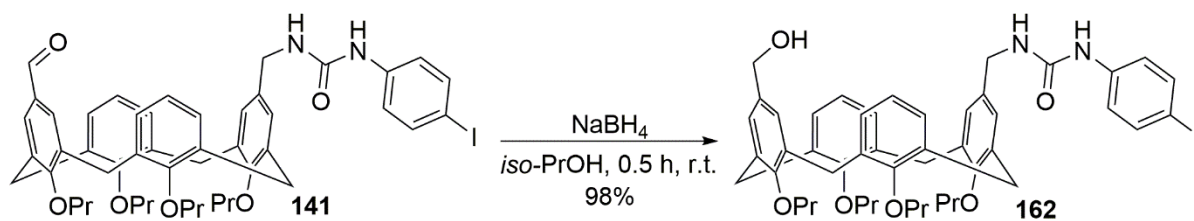
Scheme 2.15: Synthesis of **142** via the proposed Staudinger reduction/hydrolysis reaction of **158**

With the Staudinger reaction in mind for the synthesis of **142**, I first needed to identify a suitable route for the transformation of *mono*-iodophenylurea calix[4]arene **141** to the required *mono*-azidomethyl calix[4]arene **158**. A survey of the literature revealed that the synthesis of the related *bis*-azidomethyl calix[4]arene **161** from the 1,3-diformyl calix[4]arene **139** has been reported by Baldini and co-workers *via* a three-step synthetic sequence. This proceeds *via* borohydride reduction of **139** to afford primary alcohol **159**, subsequent chlorination of **159** with SOCl_2 to afford **160**, and finally $\text{S}_{\text{N}}2$ displacement of **160** with sodium azide to generate **161** (**Scheme 2.16**).¹³¹



Scheme 2.16: Baldini's synthesis of *bis*-azidomethyl calix[4]arene **161**¹³¹

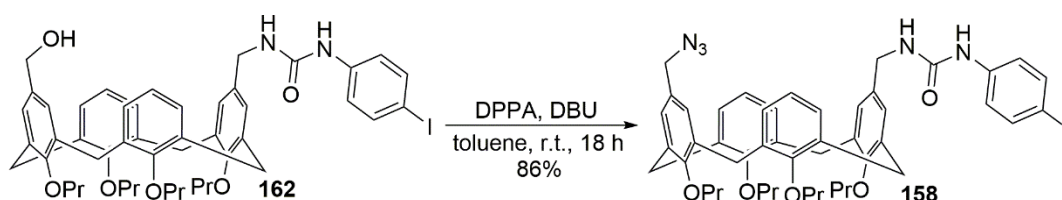
Anticipating that the carbon-iodine bond present in **141** would be inert to this set of transformations, I was keen to apply this methodology to this substrate. Thus I set about attempting to reduce the aldehyde in *mono*-iodophenylurea calix[4]arene **141** to the alcohol in **162** by reaction with sodium borohydride. Reacting **141** with 1.5 equivalents of sodium borohydride in *iso*-propanol (**141** was poorly soluble in ethanol) I was pleased to observe complete conversion into **162** after just 0.5 hours at room temperature in an almost quantitative yield (**Scheme 2.17**).



Scheme 2.17: Synthesis of primary alcohol **162** via reduction of aldehyde **141**

The $^1\text{H-NMR}$ spectrum of **162** in CDCl_3 confirmed that reduction had taken place; thus the disappearance of the formyl resonance at 9.42 ppm and the subsequent appearance of a singlet arising from the methylene group of the $-\text{CH}_2\text{OH}$ at 4.24 ppm was indicative of this transformation having worked. In the $^{13}\text{C-NMR}$ spectrum of **162** the disappearance of the formyl resonance at 193.2 ppm in **141** and the subsequent appearance of a resonance at 64.6 ppm for the methylene carbon further confirmed this structural assignment. Furthermore, the formation of **162** was confirmed by HRMS analysis; a mass ion was observed at 914.3596 which corresponds to $[\text{M} + \text{NH}_4]^+$.

With a protocol for the generation of hydroxymethylene calix[4]arene **162** established, I was now in a position to attempt the next two steps in the proposed synthetic scheme; transformation of the primary alcohol into a leaving group (*i.e.* Cl^-) followed by $\text{S}_{\text{N}}2$ displacement with sodium azide. However since I was both keen to avoid the addition of more steps to the synthesis than absolutely necessary, and aware of the widespread use of diphenylphosphoryl azide (DPPA) to achieve this transformation (*i.e.* $-\text{CH}_2\text{OH}$ to $-\text{CH}_2\text{N}_3$) in one step, I opted to consider its use in this system. A review of the literature indicated that DPPA is typically used in combination with the organic base 1,8-diazabicyclo[5.4.0]undec-7-ene (DBU) in toluene solution, and has been applied successfully to a wide array of chemical systems.^{132–134} I chose therefore to attempt the direct conversion of the hydroxymethylene calix[4]arene **162** into the desired *mono*-azidomethylene calix[4]arene **158** by reaction with excess (*i.e.* 2 eq. each) of DPPA and DBU in anhydrous toluene (**Scheme 2.18**).

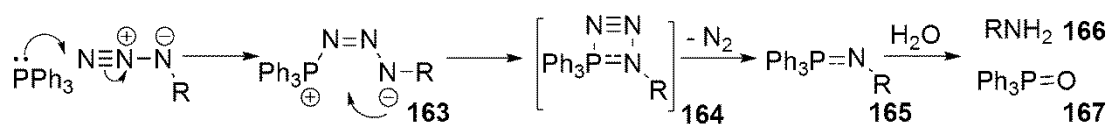


Scheme 2.18: Synthesis of primary azide **158** via reaction of primary alcohol **162** with DPPA and DBU

Following a straightforward purification by flash column chromatography I was delighted with the excellent (*i.e.* 86%) yield of the desired *mono*-azidomethylene calix[4]arene **158**. The presence of the azidomethylene group was confirmed *via* FT-IR spectroscopy, with the azide giving rise to an intense

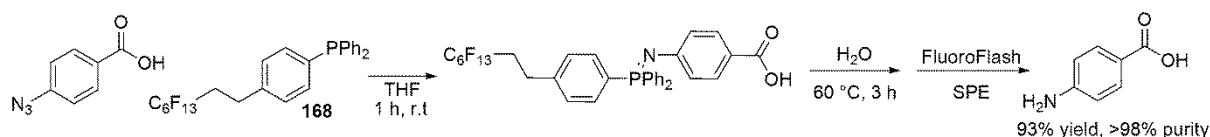
and sharp band at 2096 cm^{-1} . In addition, in the $^1\text{H-NMR}$ spectrum of **158** the methylene CH_2OH resonance present in starting material **162** as a singlet at 4.24 ppm was no longer observed; in its place was a singlet at 4.01 ppm which I have assigned to the methylene CH_2N_3 protons. Further confirmation of the identity of **158** came from HRMS analysis with the expected mass ion observed at 939.3661 for $[\text{M} + \text{NH}_4]^+$.

With access to the novel *mono*-azidomethylene calix[4]arene **158** in an 84% overall yield from **162**, and confident I could now prepare it in multi-gram quantities, I looked towards the reduction of the azide group under Staudinger conditions. This reaction is thought to proceed *via* the nucleophilic addition of triphenylphosphine to the azide functional group, resulting in the formation of an unstable phosphorazide **163**. Subsequent extrusion of nitrogen gas *via* a four-membered ring transition state **164** leads to the formation of an iminophosphorane **165** which is readily hydrolysed affording the corresponding amine **166** and triphenylphosphine oxide **167** (Scheme 2.19).^{135,136}



Scheme 2.19: Proposed mechanism for the Staudinger reduction of azides to iminophosphoranes **165** and their subsequent hydrolysis to afford amines¹³⁵

From an operational point of view, as the reaction produces one equivalent of triphenylphosphine oxide per azide unit reduced – a compound which is typically troublesome to remove *via* flash column chromatography – a number of workers have investigated the use of polymer-bound or fluororous-tethered triphenylphosphines to aid in purification.^{137,138} For example, Lindsley and co-workers have described an interesting application of a fluororous-tethered triphenylphosphine **168** to this reaction.¹³⁷ Their optimised protocol for the reduction of a wide range of functionalised azides involved stirring **168** with an azide for 1 hour at room temperature in THF, followed by the addition of an excess of water and heating to 60 °C for a further 3 hours. After this time, the excess fluororous-tethered triphenylphosphine **168** and triphenylphosphine oxide can be easily removed by fluororous solid-phase extraction, affording the desired amine in excellent yield and purity (Scheme 2.20).



Scheme 2.20: Lindsley's reduction of *para*-azidobenzoic acid using fluoros-tethered triphenylphosphine **168**¹³⁷

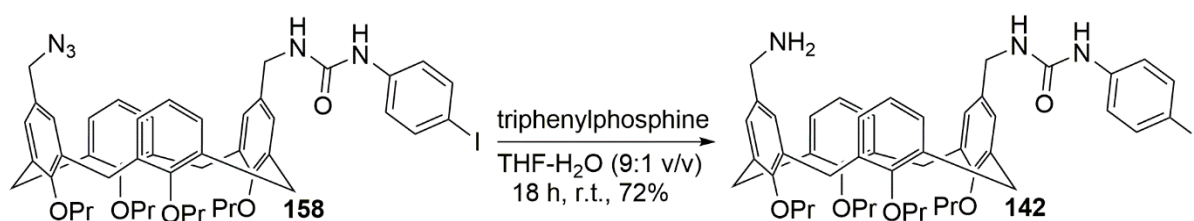
A direct comparison with polystyrene-bound triphenylphosphine revealed that such polymer-bound reagents were far less effective. In the reduction of *para*-azidobenzoic acid with polystyrene bound triphenylphosphine, an increased reaction time of 36 hours (3 hours using **168**) was required to hydrolyse significant quantities of the intermediate surface bound iminophosphorane. Thus the desired aniline was isolated in poor yield (*i.e.* 26%) and modest purity (*i.e.* 85%) after filtration of the reaction mixture to remove the polymer supported reagent. However, the authors made an additional comparison with NovaGel™ supported triphenylphosphine which performed better than the polystyrene bound triphenylphosphine under identical conditions; affording *para*-aminobenzoic acid in 60% yield and 85% purity. This improved yield is presumably due to the structure of NovaGel™ resins, which are comprised of aminomethylated polystyrene partially derivatised with methyl-PEG₂₀₀₀-*para*-nitrophenyl carbamate. This derivatisation is thought to enable particularly efficient swelling in a range of organic solvents (*e.g.* THF, DMF and MeCN) thus allowing for a greater surface area to be exposed compared with conventional polystyrene resins.

With these details in mind, and intrigued by the possibility of applying the fluoros SPE technology to my system, I decided to investigate its feasibility. After some investigation it was a disappointment to find that the extremely high cost of both the required fluoros-tethered triphenylphosphine **168** and fluoros silica gel (*i.e.* £485/50 g from Aldrich) would preclude their use. Since I was however still interested in employing some kind of tethered or polymer supported TPP for the reduction of the *mono*-azidomethylene calix[4]arene **158** (*i.e.* in order to avoid potential problems with the removal of TPPO) it was decided to investigate the use of NovaGel™ supported triphenylphosphine instead. With literature precedence for its use in the Staudinger reduction, I was reasonably confident that this system would, after optimisation, allow the identification of a high yielding synthesis of **142**.

Initiating these investigations into the polymer-supported reduction of the *mono*-azidomethylene calix[4]arene **158**, I decided to undertake a test reaction on a 0.02 mmol scale using an excess (*i.e.* two equivalents) of the NovaGel™ supported triphenylphosphine in wet THF. After agitating the mixture at room temperature for 18 hours, I was pleased to find that FT-IR analysis (through observation of the characteristic azide absorption at *ca.* 2100 cm⁻¹) indicated complete consumption

of **158**. Aware that some of the desired calix[4]arene may still be bound to the surface of the polymer as the iminophosphorane, I opted to warm the reaction to 60 °C for a further 18 hours to ensure complete hydrolysis and liberation of the amine. Removing the NovaGel™ by filtration and the solvent by evaporation, I was disappointed to obtain a complex mixture which ¹H-NMR analysis indicated to be comprised merely of multiple impurities (presumably originating from the TPP resin). All further attempts at hydrolysis of the desired calix[4]arene from the NovaGel™ under more forcing conditions (*i.e.* heating with KOH in THF/water) failed to yield any calix[4]arene derived material, and so it was decided to examine the use of ‘solution phase’ triphenylphosphine instead.

Undertaking a test reaction, *mono*-azidomethylene calix[4]arene **158** was stirred with an excess of triphenylphosphine (*i.e.* two equivalents) in wet THF at room temperature overnight. Gratifyingly, TLC analysis indicated the complete consumption of **158** and the formation of a new ‘spot’ which stained purple with ninhydrin – strongly suggesting the formation of desired primary amine **142**. I was delighted to find that, in direct contrast to my earlier concerns about purification, the desired product **142** could be readily isolated by flash column chromatography in a 72% yield (**Scheme 2.21**).

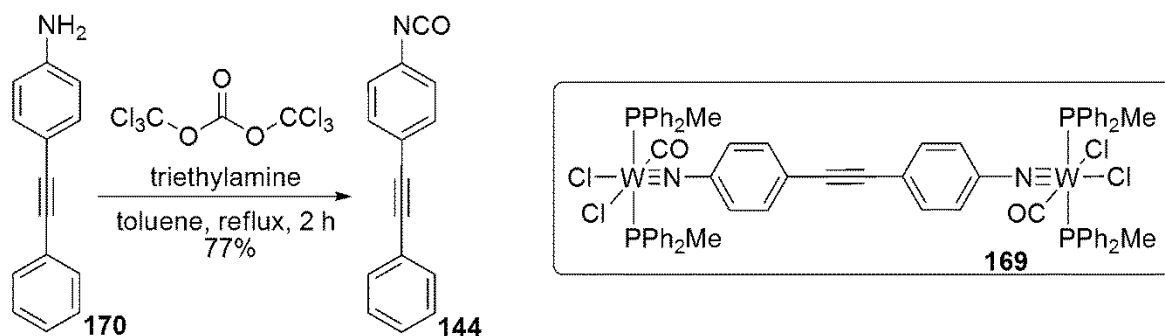


Scheme 2.21: Synthesis of primary amine **142** via the Staudinger reaction of primary azide **158**

The complete reduction of **158** was confirmed by the disappearance of the methylene resonance at 4.01 ppm arising from the CH₂N₃ protons and the formation of a singlet at 3.33 ppm in the ¹H-NMR spectrum of **142** – a signal assigned to the CH₂NH₂ protons. A mass ion was observed at 896.3494 in the HRMS analysis which corresponds to [M+H]⁺, thereby further confirming the formation of **142**.

With an operationally simple protocol for the preparation of pure samples of **142** established, I could start to investigate the reaction with isocyanates for the introduction of the second urea group (**Scheme 2.4**). In the first instance, a method was required for the preparation of the aryl isocyanate **144** with which to react with **142**. A review of the literature indicated the synthesis of aryl isocyanates is typically achieved by the reaction of either phosgene, or a phosgene equivalent like triphosgene, with an amine under anhydrous conditions.¹³⁹ A direct search for compound **144** revealed that Hogarth and co-workers reported its synthesis during their explorations into the electrochemistry of ditungsten complexes exemplified by **169**.¹⁴⁰ The English group reacted 4'-amino

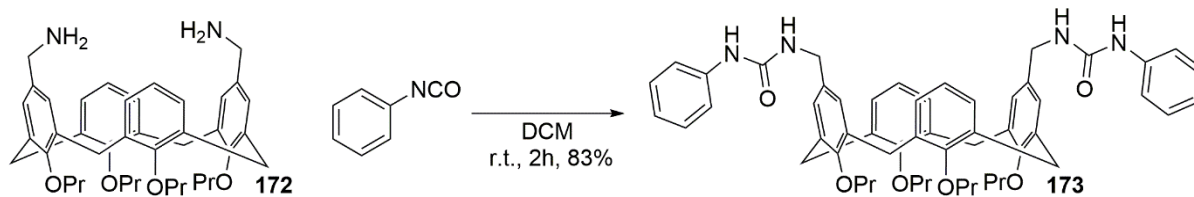
diphenylacetylene **170** with triethylamine and triphosgene in anhydrous toluene to afford, after purification *via* sublimation, a 77% yield of the corresponding aryl isocyanate **144** (Scheme 2.22).



Scheme 2.22: Hogarth's synthesis of **144** developed as part of studies towards electrochemically active ditungsten complexes such as **169**¹⁴⁰

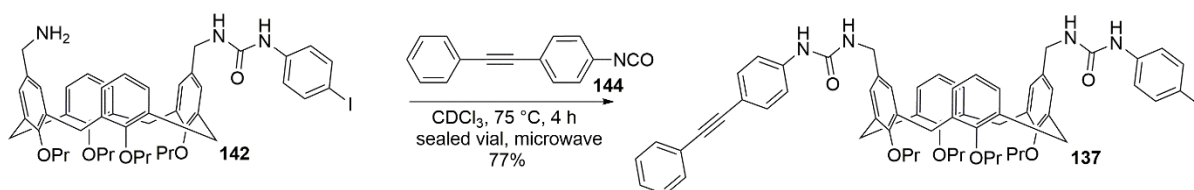
Attracted to the operational simplicity of this procedure, and keen to avoid the use of phosgene gas, I opted to employ the procedure outlined in Scheme 2.22 for the preparation of **144**. Without a commercial sample of 4'-amino diphenylacetylene **170** to hand, I searched the literature to identify a suitable protocol for its preparation. Following the method of Belger and co-workers, I obtained **170** in an 84% yield *via* the Sonogashira coupling (Pd(PPh₃)₄, CuI, Et₃N, THF, reflux, 4 h) of phenylacetylene with *p*-iodoaniline **171**.¹⁴¹ This aniline (*i.e.* **170**) was found to be somewhat sensitive to degradation (presumably *via* an oxidative pathway). For this reason it was quickly transformed into the corresponding isocyanate **144** following the method of Hogarth. I opted to forgo the sublimation step, since the ¹H-NMR spectrum indicated **144** was already of high purity (*ca.* 98%) following a work up by filtration (to remove triethylamine hydrochloride) and evaporation (to remove solvent). The presence of the isocyanate group was confirmed by FT-IR spectroscopy, giving rise to an intense absorption at 2296 cm⁻¹ (this characteristic band generally occurs at about 2200 cm⁻¹).¹⁴²

Pleased that I was able to readily reproduce the synthesis of isocyanate **144**, and with samples of *mono*-aminomethyl calix[4]arene **142** to hand, I was in a position to attempt their coupling. A review of the literature revealed that the reaction of amines and isocyanates to afford ureas has been well studied in a wide variety of systems, and is generally considered to be facile.¹⁴³ For example, the reaction of phenyl isocyanate and benzylamine is essentially complete after stirring for 0.5 hours at room temperature in hexane.¹⁴⁴ In the case of calix[4]arene derived primary amines such as **172**, Casnati and co-workers reported the reaction with phenyl isocyanate (2.2 eqⁿ) at room temperature for 2 hours in dichloromethane was sufficient to afford **173** in an 83% isolated yield after recrystallisation from ethanol (Scheme 2.23).³⁷



Scheme 2.23: Casnati's synthesis of bis-1,3-urea **173** via the coupling of bis-amine **172** and phenyl isocyanate³⁷

Anticipating that the rate of reaction between primary amine **142** and aryl isocyanate **144** would be similar to Casnati's system, but still curious to establish exactly what time frame would be required, I opted to carry out a test reaction in an NMR tube and follow its progress *via* ¹H-NMR spectroscopy. Thus performing the reaction in anhydrous CDCl₃ (0.02 M) at room temperature, and recording ¹H-NMR spectra every hour for 18 hours, I was surprised to find that no reaction had taken place – both components remained unchanged. Somewhat puzzled by this result, I decided to transfer the reaction mixture into a sealed microwave vial and heat it at 75 °C for 4 hours to see if this would promote urea formation. Gratifyingly, I observed complete conversion of **142** into the desired 'advanced intermediate' **137** by ¹H-NMR analysis (**Scheme 2.24**).



Scheme 2.24: Synthesis of 'advanced intermediate' **137** under microwave irradiation

A subsequent purification *via* flash column chromatography afforded a 77% isolated yield of pure **137**. A full physicochemical analysis confirmed the identity of **137**. I was able to identify both the carbon-carbon triple and the carbon-iodine single bonds *via* ¹³C-NMR spectroscopy, with signals observed at 89.6, 88.8 and 85.5 ppm respectively. High resolution mass spectrometric analysis of **137** identified a mass ion at 1132.4455 which corresponds to [M + NH₄]⁺, thereby further confirming the identity of **137**. I was particularly pleased with this result since the isolation of pure samples of **137** *via* the Sonogashira coupling methodology previously developed within the Bew group had not been possible (**Figure 2.4**).¹⁰⁸

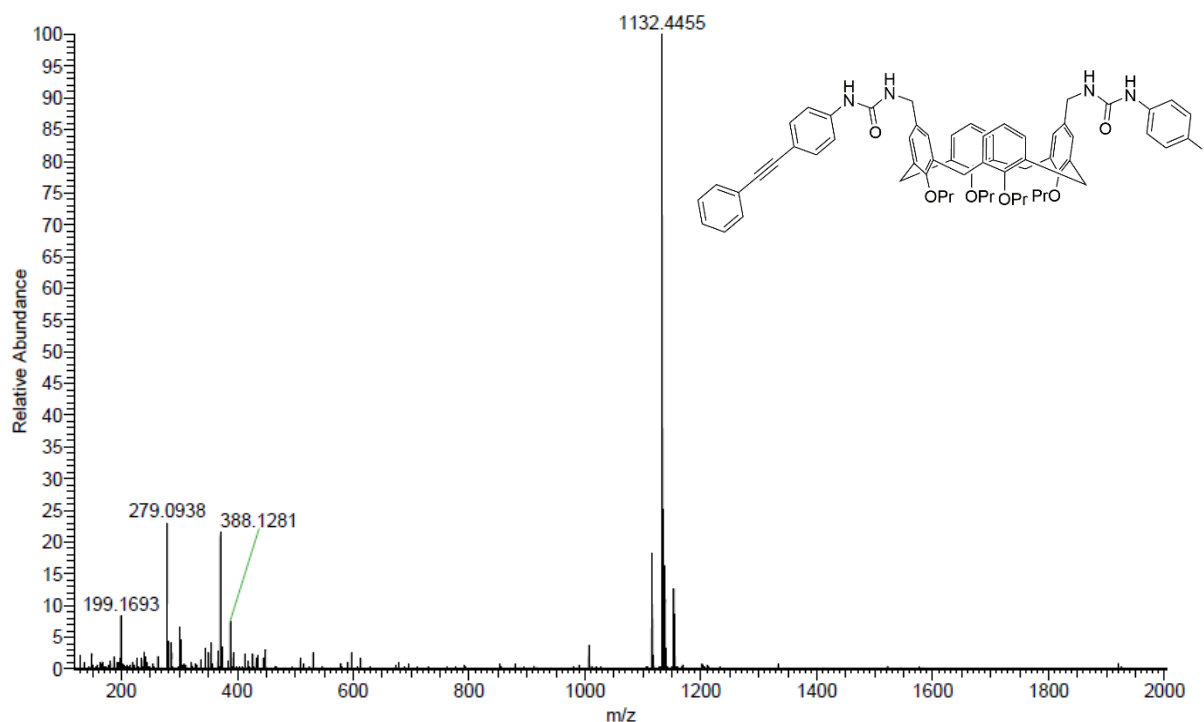
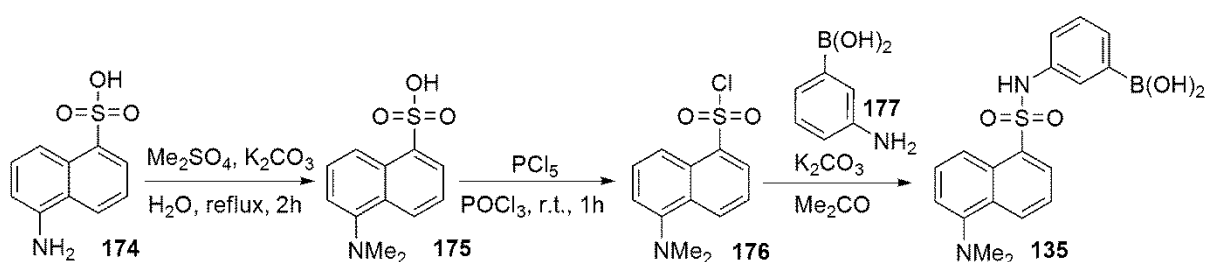


Figure 2.4: High resolution mass spectrum of compound **137** showing $[M + NH_4]^+$ at 1132.4455

2.8 Synthesis of dansyl derived fluorophores

With a protocol established for the generation of pure samples of the ABAC substituted **137**, I turned my attention to the synthesis of the required 3-(dansylamino)-phenylboronic acid **135** which I intended to install as the same fluorophore employed in the original design. Although this compound is commercially available, its high cost (*i.e.* £297/mmol) necessitated a synthesis from cheaper starting materials. A review of the literature indicated that a short sequence of reactions beginning with the significantly more affordable 5-amino-1-naphthalenesulfonic acid **174** (*i.e.* 5p/mmol) was the most suitable option (Scheme 2.25).^{145–147}



Scheme 2.25: Synthesis of 3-(dansylamino)-phenylboronic acid **135**^{145–147}

Following the literature procedure, 5-amino-1-naphthalenesulfonic acid **174** was *N*-dimethylated by treatment with dimethyl sulfate at reflux under aqueous basic conditions; **175** was afforded as a pale purple solid in 90% isolated yield. Subsequently, transformation of the sulfonic acid **175** to the sulfonyl chloride **176** was undertaken using phosphorous pentachloride in phosphorous oxychloride. The desired dansyl chloride **176** was afforded as an orange oil which crystallised on standing in a pleasing 72% yield. The ¹H-NMR spectrum of **176** displayed a singlet at 2.91 ppm integrating to six hydrogen atoms which were assigned to the equivalent *N*-methyl groups. The aromatic signals were assigned on the basis of their chemical shift and splitting patterns. For example, the lowest field doublet (at 8.70 ppm) presumably arises from the proton *para* to the strongly electron-withdrawing sulfonyl chloride (**Figure 2.5**).

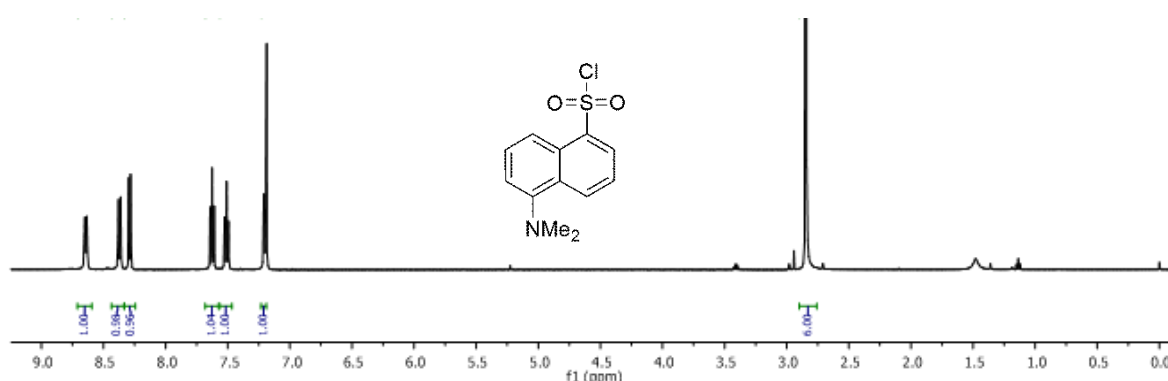
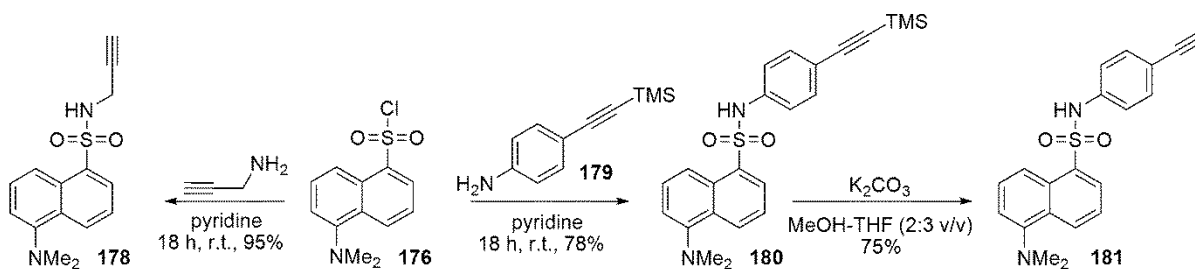


Figure 2.5: The ¹H-NMR spectrum of dansyl chloride **176** (500 MHz, CDCl₃)

Before proceeding onwards, generating sulfonamide **135** *via* reaction with 3-aminophenylboronic acid **177**, I paused to consider how the preparation of a series of alkyne functionalised dansyl sulfonamides might allow access to the set of ‘*bis*-alkyne’ modified sensors proposed at the outset of this project (**Section 1.7**). These were required since one of the aims was to investigate how the incorporation of a second carbon-carbon triple bond within the sensor might affect its sensitivity and/or selectivity. With this in mind, I wanted to synthesise a series of additional dansyl sulfonamides containing a triple bond. A subsequent Sonogashira coupling with ‘advanced intermediate’ **137** might then allow for its incorporation. A literature search revealed that Chui and co-workers have reported the synthesis of two novel alkyne modified dansyl derivatives **178** and **181** as part of their studies directed towards the development of new bio-imaging probes with anti-cancer properties (**Scheme 2.26**)¹⁴⁸

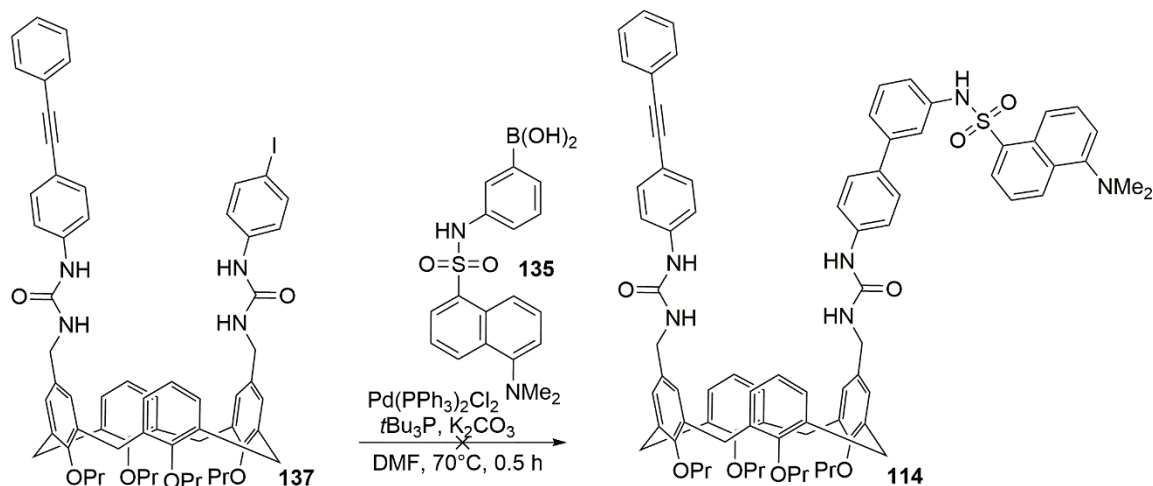


Scheme 2.26: Chui's synthesis of alkyne functionalised dansyl derivatives **178** and **181**¹⁴⁸

Chui's bio-imaging probe **178** was synthesised from dansyl chloride **176** by sulfonamide formation with propargylamine, whilst a two-step procedure (*i.e.* sulfonamide formation; TMS deprotection) was required for **181**. The removal of the TMS protecting group was presumably performed after coupling since *para*-ethynyl aniline decomposes rapidly in air *via* a supposed oxidative pathway.¹⁴⁹ With such apparently simple procedures available for the synthesis of **178** and **181**, I decided to prepare samples of these compounds in addition to the 3-(dansylamino)-phenylboronic acid **135** described earlier. Thus by following the procedures of Chui and Elfeky, compounds **178**, **135** and **181** were prepared in 95%, 82% and 54% yields respectively *via* the reaction of dansyl chloride **176** with the appropriate amine under basic conditions. To confirm the formation of these materials, I compared my ¹H- and ¹³C-NMR spectra to those in the literature. In the case of **178**, the ¹H-NMR spectrum displayed the propargylic CH₂ as a doublet at 3.77 ppm with a coupling constant of *J* = 2.5 Hz. These values compare favourably with those in the literature – thus Rubeinshtein and co-workers also observed a doublet at 3.77 ppm with a coupling constant of *J* = 2.4 Hz.¹⁵⁰

2.9 Synthesis of **114** *via* a Suzuki-Miyaura coupling of **137** and **135**

Now that I had synthesised a key intermediate in the scheme (*i.e.* **137**) along with a small set of alkynyl and boronic acid modified fluorophores, I was in a good position to attempt the final bond forming reactions required to assemble **114**. In the first instance, I wanted to repeat a synthesis that Bew and co-workers had used to generate probe **114** *via* a Suzuki reaction using 'advanced intermediate' **137** and 3-(dansylamino)-phenylboronic acid **135**.¹¹⁶ Additionally, it was important to check that I could reproduce the results obtained in the original fluorescence studies before preparing further, novel derivatives. Thus with pure samples of both reactants to hand, I anticipated the coupling would afford **114**, hopefully with an improved yield and higher purity. Starting off my first attempt at this reaction, I used conditions previously developed within the Bew group since they had been shown to generate some of the desired compound **114** (Scheme 2.27).



Scheme 2.27: Attempted synthesis of **114** via the Suzuki-Miyaura coupling of **137** and **135**

It was disappointing to find therefore that after heating **137** in anhydrous *N,N*-dimethylformamide at 70°C with boronic acid **135** (1.2 equivalents), tri-*tert*-butylphosphine (20 mol%), PdCl₂(PPh₃)₂ (10 mol%) and potassium carbonate (2 equivalents) for 0.5 hours, no conversion into the desired product **114** could be detected using ¹H-NMR by monitoring the disappearance of the pair of doublets at 7.57 and 7.34 ppm (*J* = 7.7 Hz) which I assigned to the phenyl ring carrying the reactive iodine atom. Initially I suspected the problem may lie with one of the reagents; I opted to prepare a fresh sample of PdCl₂(PPh₃)₂ and confirm the purity of the tri-*tert*-butylphosphine additive *via* ³¹P-NMR. Only a trace (*ca.* <5%) of the corresponding tri-*tert*-butylphosphine oxide was revealed by the presence of a minor signal at 59.8 ppm in the ³¹P-NMR spectrum. However, repeating the reaction with these ‘new’ reagents I was still unable to observe any conversion after 0.5 h. Thus I decided to heat the mixture for a further 18 h at 70 °C.

Subsequent analysis by ¹H-NMR spectroscopy indicated a complex mixture of products. However, TLC analysis indicated the presence of a new strongly fluorescent ‘spot’ which I thought might correspond to the desired product **114**. Purification of this mixture *via* flash column chromatography allowed for the isolation of a sample of **114**, but in a disappointing 18% yield. Its formation was confirmed by a comprehensive physicochemical analysis. The ¹H-NMR spectrum of **114** is displayed below and clearly shows a singlet at 2.81 ppm (arising from the dimethylamino group) and doublets at 8.44 (*J* = 8.5 Hz), 8.31 (*J* = 8.4 Hz) and 8.14 (*J* = 7.3 Hz) ppm (arising from the naphthalene ring) which suggested the dansyl fluorophore had been incorporated as anticipated. In the ¹³C-NMR spectrum of **114**, the signal which was observed at 85.5 ppm in **137** was no longer present; thus confirming the loss of the carbon-iodine bond. Furthermore, a mass ion was observed in the HRMS analysis at 1313.6141 which corresponds to [M+H]⁺ for **114** (Figure 2.6).

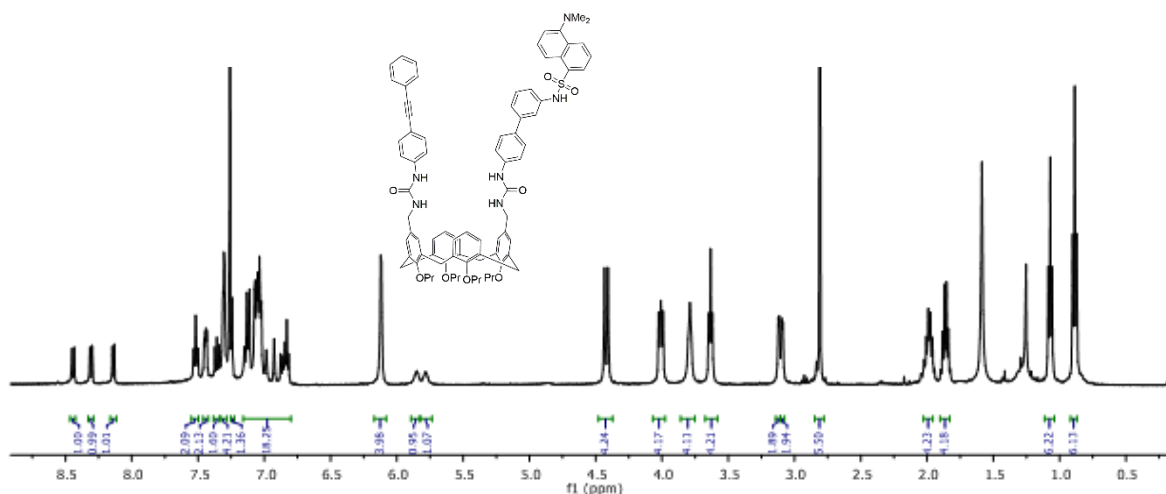


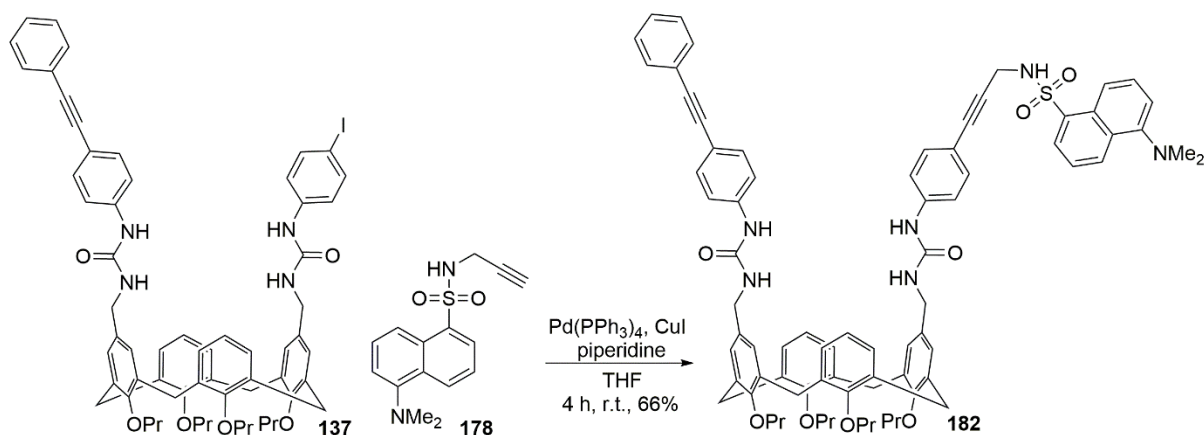
Figure 2.6: The $^1\text{H-NMR}$ spectrum of sensor **114** (500 MHz, CDCl_3)

Whilst I was pleased to have been able to access a sample of sensor **114**, it was felt that the low conversion and resulting low yield (*i.e.* 18%) were unacceptable – particularly at this stage of the synthesis. Thus I made several attempts to optimise this reaction by screening a series of palladium(0) pre-catalysts, ligands and inorganic bases but was unable to identify any systems which would result in a high conversion to **114**.

Unsure of whether the low reactivity was arising from the aryl iodide **137** (*via* slow oxidative addition) or the boronic acid **135** (*via* slow transmetalation) I decided that from a time efficiency point of view it would be better to initiate the studies into the Sonogashira coupling of **137** and return at a later date to solve these Suzuki couplings.

2.10 Synthesis of sensor **182** *via* a Sonogashira coupling

After the somewhat disappointing results with the Suzuki-Miyaura coupling, I was keen to investigate conditions for the Sonogashira coupling of **137** with the alkyne modified **178** and **181**. I opted to initiate these investigations with propargylamide **178**, simply because I had more of this material to use. Searching the literature, I endeavoured to find a suitable set of conditions; I was however disappointed that no examples of any Sonogashira couplings employing either **178** or **181** could be identified. I opted instead to employ a standard set of reaction conditions [*i.e.* $\text{Pd}(\text{PPh}_3)_4$ (10 mol%), CuI (20 mol%), piperidine] that have been used widely in the literature (**Scheme 2.28**).¹⁵¹



Scheme 2.28: Synthesis of novel sensor **182** via the Sonogashira coupling of **137** and **178**

I was delighted to find that after only 4 hours TLC analysis indicated complete consumption of starting material **137**. Subsequent work-up and purification by flash column chromatography (silica gel) afforded an unoptimised 66% yield of a yellow solid, which a comprehensive physicochemical analysis confirmed was target compound **182**. The $^1\text{H-NMR}$ spectrum confirmed the presence of the dansyl moiety with a singlet at 2.77 ppm (arising from the dimethylamino group) and doublets at 8.45 ($J = 8.5$ Hz), 8.25 ($J = 7.3$ Hz) and 8.33 ($J = 8.6$ Hz) ppm (arising from the naphthalene ring). In the FT-IR spectrum of **182**, the alkyne absorptions expected at around 2200 cm^{-1} were too weak to be distinguished. However, the $^{13}\text{C-NMR}$ spectrum provided strong evidence for the incorporation of the second carbon-carbon triple bond; four signals were observed at 82.0, 84.6, 88.9 and 89.7 ppm which are indicative of the presence of two distinct triple bonds. Finally, a mass ion was observed at 1275.5988 in the HRMS analysis which corresponds to $[\text{M}+\text{H}]^+$ for **182**.

2.11 Fluorescence studies of sensors **114** and **182**

With a successful route established for the synthesis of **182**, I was keen to begin the fluorescence studies and investigate whether **182** would also act as a sensor for the Au(III) ion as had been anticipated. Firstly however, I wanted to be able to reproduce the preliminary results obtained by Bew and co-workers with the analytically pure sample of Suzuki-Miyaura derived probe **114**.¹⁰⁸ This was to ensure that any impurities present in the original sample (as indicated by $^1\text{H-NMR}$ analysis) had not adversely interfered with the results.

I began by recording the UV absorption spectrum of **114** in methanol ($5\ \mu\text{M}$) to identify the value of λ_{max} that I would employ as the excitation wavelength for the fluorescence measurements. This was determined to be 287 nm – a value in close agreement to that recorded previously in the Bew group (*i.e.* 288 nm).¹⁰⁸ Next I recorded the fluorescence spectrum of **114** in methanol ($5\ \mu\text{M}$) and observed a broad emission band with $\lambda_{\text{em}} = 522$ nm. Since broad emission spectra and values for λ_{em} in this

range (c.a. 460 to 520 nm) are reported to be characteristic for the dansyl group, I was satisfied that this emission band did indeed arise from the fluorophore in **114**.⁸⁷ Unfortunately, since I was using an excitation wavelength of 287 nm I also observed a signal at 574 nm arising from the scattering of 574 nm light generated by second order diffraction at the monochromator. This is an effect well documented in fluorescence spectroscopy and is usually corrected for by the use of high band pass filters, or computer software.¹⁵² Without access to either, I opted to simply employ a longer excitation wavelength (*i.e.* 360 nm) so that this second order signal would appear outside of the spectral window. This is a common technique, and in this case resulted in no change in the emission spectrum, with λ_{em} for **114** still observed at 522 nm.

By recording additional spectra every two minutes for 0.5 hours, I then observed that the emission intensity remained constant over time - this demonstrated the photochemical stability of the dansyl group under these conditions (**Figure 2.7**).

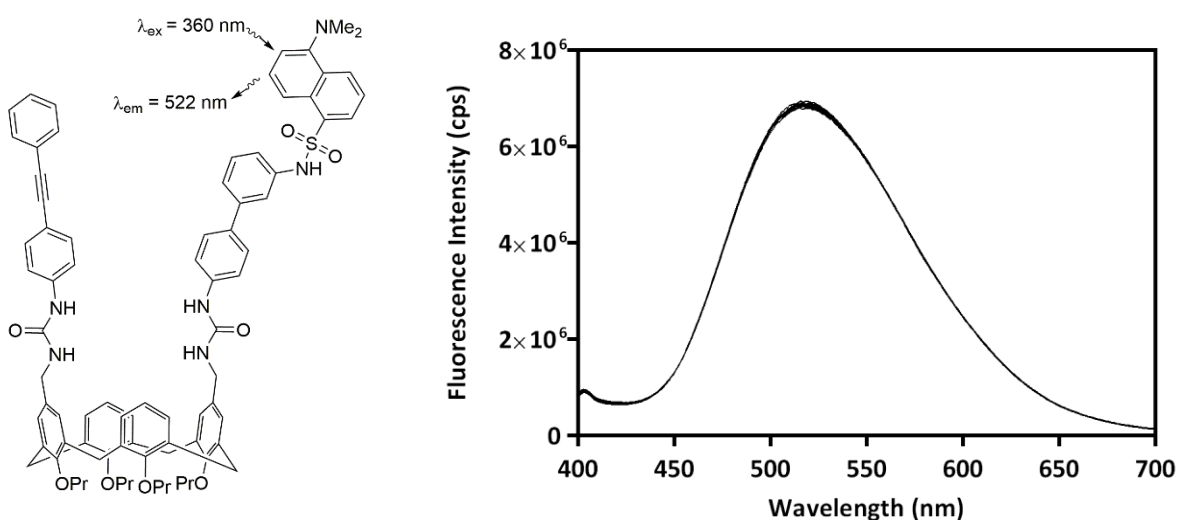


Figure 2.7: Fluorescence spectra of **114** in MeOH ($5 \mu\text{M}$) ($\lambda_{ex} = 360 \text{ nm}$, $\lambda_{em} = 522 \text{ nm}$) recorded every two minutes for 0.5 h displaying high photochemical stability

With this result established, I was keen to investigate the effect of titrating a methanolic solution of sodium tetrachloroaurate into a solution of **114** to investigate whether any fluorescence quenching could be observed. In the first instance, I opted to simply add three equivalents of sodium tetrachloroaurate (1.5 mM in methanol) to see if any quenching effect was observed. By recording spectra every minute for one hour, I was pleased to observe the same fluorescence quenching as had been reported previously (**Figure 2.8**).

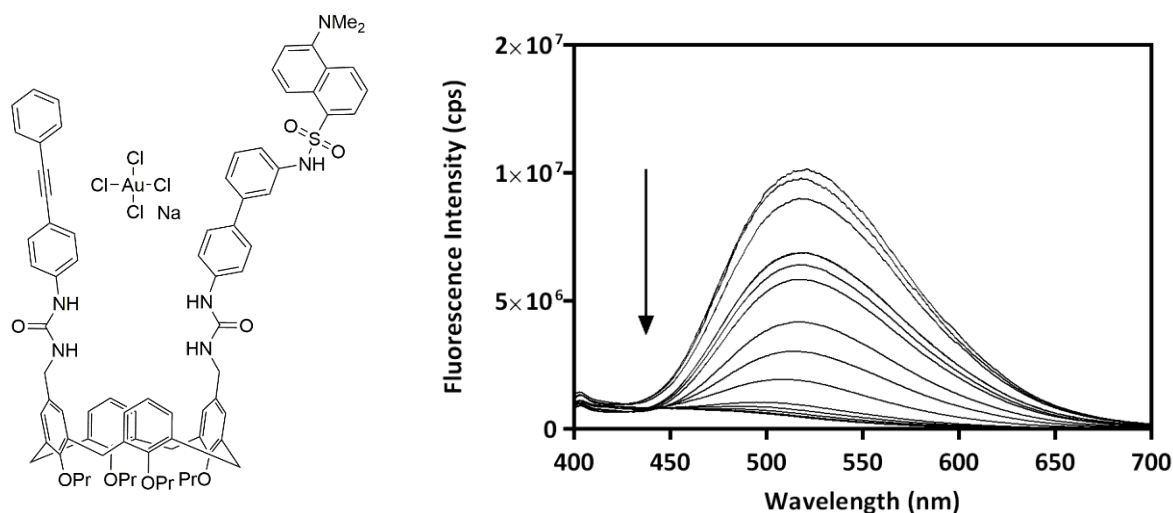


Figure 2.8: Fluorescence spectra of **114** in MeOH ($5 \mu\text{M}$) ($\lambda_{\text{ex}} = 360 \text{ nm}$, $\lambda_{\text{em}} = 522 \text{ nm}$) recorded every four minutes for 1 hour, after the addition of NaAuCl_4 (3 equivalents), displaying a decrease in fluorescence emission. Only spectra recorded every 4 minutes are included for clarity.

Before proceeding onwards to test the fluorescence properties of design **182**, it was important to first confirm the selectivity of Bew's probe **114** for the Au(III) ion, over and above other metal ions. To do this, I decided to study the effect on the fluorescence emission of **114** from the addition of large excesses (*i.e.* 20 equivalents) of Li^+ , Hg^{2+} , Ag^+ , Cd^{2+} and Pt^{2+} metal ions. In the first trial, I was pleased to observe that after the addition of 20 equivalents of lithium perchlorate to a methanolic solution of probe **114**, no significant change in fluorescence intensity resulted (**Figure 2.9**).

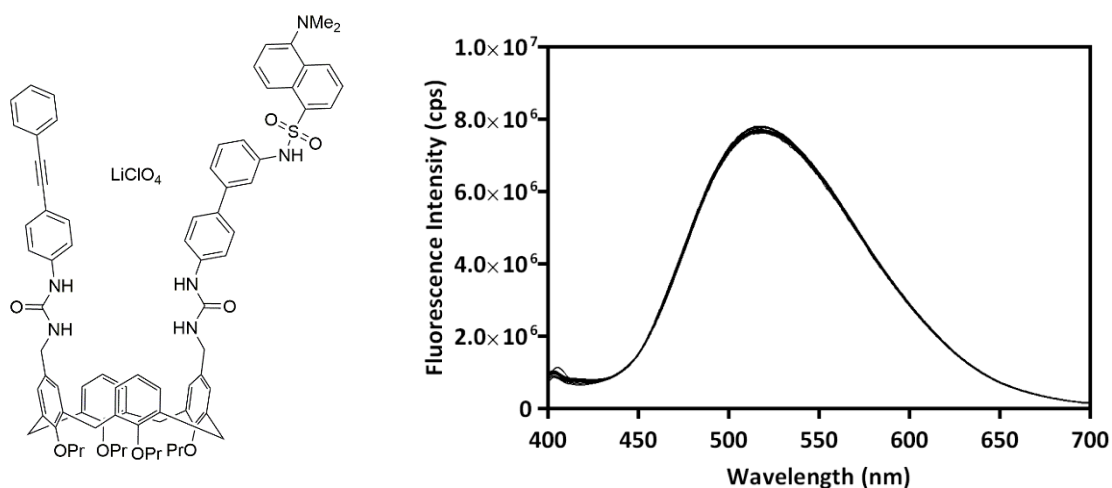


Figure 2.9: Fluorescence spectra of **114** in MeOH ($5 \mu\text{M}$) ($\lambda_{\text{ex}} = 360 \text{ nm}$, $\lambda_{\text{em}} = 522 \text{ nm}$) recorded every four minutes for 1 hour, after the addition of LiClO_4 (20 equivalents), displaying no significant change in fluorescence intensity.

Further experimentation revealed that treating **114** with 20 equivalents of mercuric chloride, silver perchlorate, cadmium carbonate or platinum(II) chloride resulted in no significant quenching or enhancement of the fluorescence response. Thus, these results confirmed the selectivity of **114** as a fluorescent probe for sodium tetrachloroaurate and obviated the possibility that trace impurities in the original sample (as indicated by NMR and MS data) may have interfered with these results.

Pleased with these preliminary fluorescence studies using probe **114**, I was keen to see whether the 'bis-alkyne' **182** might also have the capacity to function as an ion selective probe. I initiated these studies with **182** by recording its UV absorption spectrum and identifying λ_{max} at 288 nm. This is a value similar to that recorded for **114** and is indicative of the presence of the dansyl fluorophore. However, since this wavelength (*i.e.* 288 nm) would lead to a second order signal in the spectral window at 576 nm, I decided to proceed as before and employ a longer excitation wavelength (*i.e.* at 360 nm). To ensure I was justified in doing so, I recorded fluorescence spectra of **182** in methanol (5 μM) at 288 and 350 nm and observed no significant differences in peak shape or λ_{em} (517 nm at both excitation wavelengths) in addition to high photochemical stability.

With this result established, I wanted to test the effect on fluorescence emission of **182** upon titration of Au^{3+} , Li^+ , Hg^{2+} , Ag^+ , Cd^{2+} and Pt^{2+} metal ions. Since my particular interest was the effect of Au^{3+} , I chose to study this ion first. Thus I started by adding three equivalents of sodium tetrachloroaurate (1.5 mM in methanol) to a solution of **182** in methanol and was delighted to observe a *ca.* 96% reduction in the relative fluorescence intensity of **182** after 1 hour at room temperature (**Figure 2.10**).

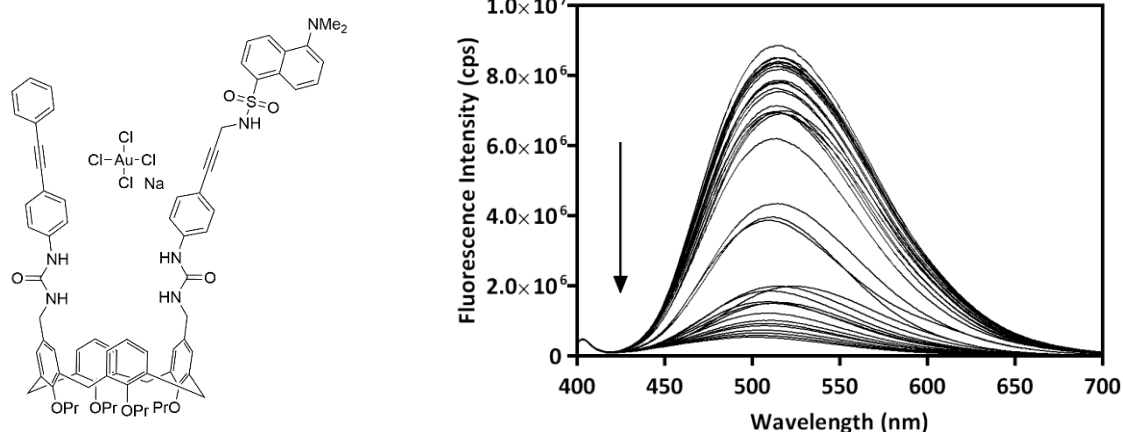


Figure 2.10: Fluorescence spectra of **182** in MeOH (5 μM) ($\lambda_{\text{ex}} = 360 \text{ nm}$, $\lambda_{\text{em}} = 517 \text{ nm}$) recorded every minute for 1 hour, after the addition of NaAuCl_4 (3 equivalents), displaying a decrease in fluorescence emission.

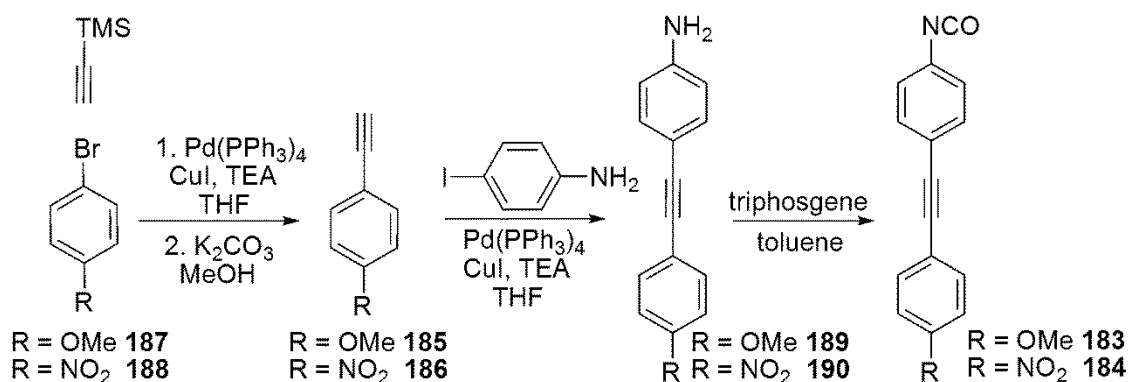
It is noteworthy that no significant difference in kinetic profile was observed between **114** and **182**; both compounds required about 1 hour to reach *ca.* 95% of their original fluorescence emission. However, I anticipated that a more detailed analysis might still uncover some trends within the proposed series of derivatives (*e.g.* **126** and **127**).

Next, I needed to examine the selectivity profile for **182** towards other metal ions, to establish whether it could be employed as a Au(III) selective sensor similar to **114**. Thus, I treated methanolic solutions of **182** with 20 equivalents of lithium perchlorate, mercuric chloride, silver perchlorate, cadmium carbonate or platinum(II) chloride. In each case I observed no significant change in emission intensity – a result which suggests that **182** does indeed show a high selectivity towards the Au(III) ion.

2.12 Synthesis of a series of derivatives of sensor **182**

At this stage of my investigations I was delighted to have demonstrated that modified design **182** functioned as an ion selective sensor for Au(III), in addition to establishing an operationally simple route for its synthesis. However, as I still had limited evidence as to the exact nature of the Au(III).**182** interaction, I wanted to investigate further. As preliminary studies within the Bew group (**Section 1.5.4.2**) indicated that an analogue of **114** lacking the carbon-carbon triple bond (*i.e.* **116**) did not show any fluorescence quenching upon treatment with sodium tetrachloroaurate in methanol (up to 20 equivalents), I wanted to examine the effect of varying the steric and/or electron nature of the alkyne group in **182**. In this way, I hoped to obtain some supporting evidence for coordination of the Au(III) ion to the alkyne group (evidenced indirectly through changes in rate of fluorescence quenching), if this were indeed operative in this system.

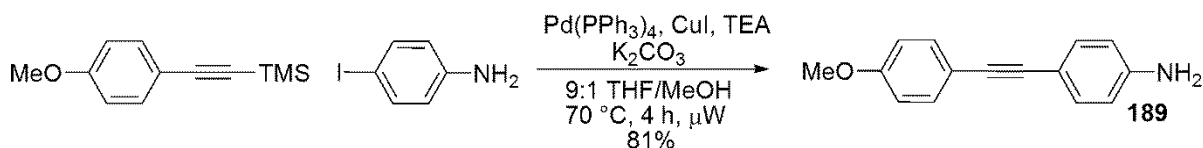
To proceed with the generation of these derivatives (*e.g.* **126** and **127**) I required a robust method for the synthesis of derivatives of isocyanate **144**. A literature search revealed that neither **183** or **184** had been reported previously, but from earlier studies I anticipated that **183** and **184** could be synthesised *via* an analogous route to that used for **144** (*i.e.* Sonogashira coupling of *para*-iodoaniline with phenylacetylene, then treatment with triphosgene). Thus I needed access to the aryl acetylenes **185** and **186** which a literature search indicated could be readily generated from the corresponding aryl bromides **187** and **188** *via* Sonogashira coupling with trimethylsilylacetylene and subsequent deprotection (**Scheme 2.29**).



Scheme 2.29: The proposed route towards isocyanate derivatives **126** and **127**

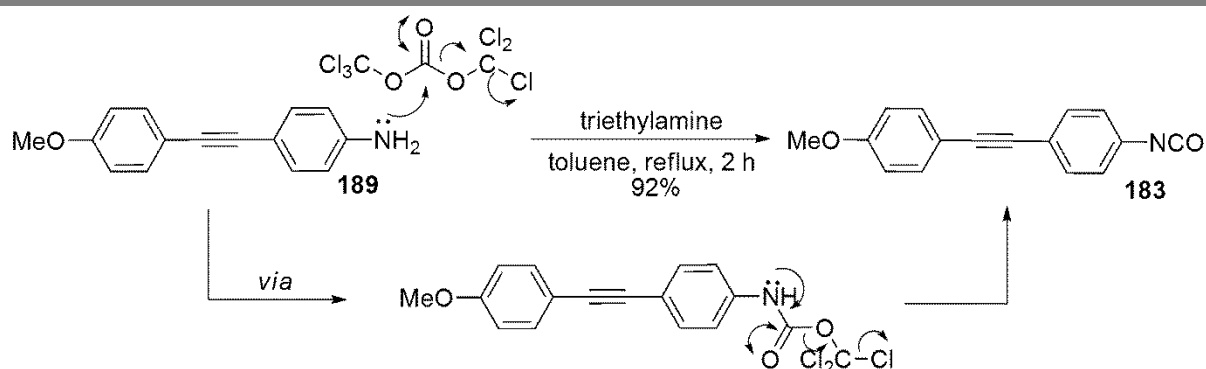
Initiating the synthesis of **183** from commercially available 4-bromoanisole **187** I performed its Sonogashira coupling with TMS acetylene (2 eqⁿ) in a sealed microwave vial (90 °C, 4 hours). After purification *via* flash column chromatography, TMS-protected **185** was afforded in an 82% yield. Subsequently, **185** was generated in 92% yield following deprotection by treatment with a large excess of K₂CO₃ in methanol. A subsequent Sonogashira coupling with *para*-iodoaniline afforded the aniline **189** in a modest (*i.e.* 52%) yield after purification *via* flash column chromatography. In this case, the remaining mass balance comprised homocoupled **185**, unreacted *para*-iodoaniline and a complex mixture of decomposition products which could not be identified by ¹H-NMR.

Suspecting that the low reactivity of *para*-iodoaniline coupled with the high reactivity of **185** towards decomposition were contributing to the modest yield, I was curious to investigate whether employing TMS-protected **185** directly in combination with K₂CO₃ and methanol in the Sonogashira coupling might improve the yield by promoting the 'slow release' of **185**. Gratifyingly, conducting the reaction under these modified conditions afforded a significantly improved yield (*i.e.* 81%) of the desired aniline **189** as a yellow solid (**Scheme 2.30**).



Scheme 2.30: Employing a 'slow release' strategy to afford an improved yield of aniline **189**

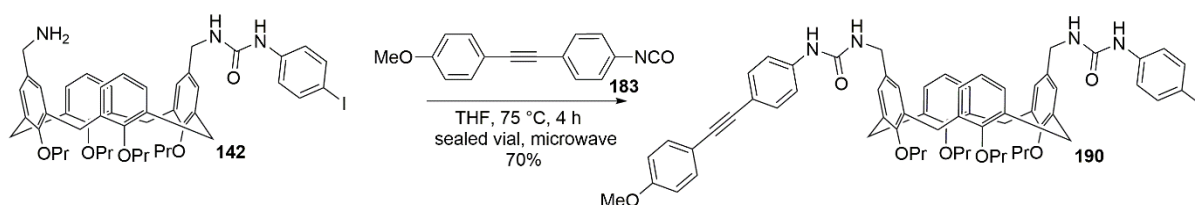
With **189** in hand, I needed to quickly transform it to the corresponding isocyanate **183** since it rapidly decomposed in air over the course of a day, turning black. Thus a toluene solution of freshly prepared **189** was treated with triphosgene (0.4 equivalents) at reflux for two hours affording a 92% yield of desired isocyanate **183** after work up by filtration (to remove triethylamine hydrochloride) and concentration in *vacuo* (to remove solvent). The FT-IR analysis of **183** confirmed the transformation had taken place as expected; a strong absorption was observed at 2284 cm⁻¹, which is characteristic of the isocyanate functional group (**Scheme 2.31**).



Scheme 2.31: Synthesis of isocyanate **183** via treatment of **189** with triphosgene

Interestingly, **183** was found to be more suited to long term storage than **189**. Samples of **183** stored under air in a sealed vial were found to contain >95% of the original isocyanate by $^1\text{H-NMR}$ after one month at room temperature. In contrast, samples of **189** stored in the same way merely contained a complex mixture of products. Pleased with the facile synthesis of **183** *via* this route (**Scheme 2.29**), I opted to generate the corresponding *para*-nitro functionalised **184** by the same means. Thus I prepared TMS-protected **186** *via* a Sonogashira coupling of **188** and TMS acetylene in 79% yield. Employing this compound directly in a subsequent Sonogashira coupling with *para*-iodoaniline under these modified conditions (*i.e.* with *in situ* deprotection) afforded a 68% yield of **190**. This compound was then quickly transformed into the corresponding isocyanate **184** in an 87% yield by treatment with triphosgene and TEA in refluxing toluene.

With isocyanates **183** and **184** in hand, I was ready to investigate their reactions with *mono*-aminomethyl calix[4]arene **142** under the conditions established previously. Starting with *para*-methoxy substituted **183** (as there was more available) I performed its reaction with **142** under microwave irradiation in dry tetrahydrofuran. After heating the mixture at 75 °C for 4 hours, subsequent TLC analysis indicated a clean 'spot to spot' transformation. Simply removing the solvent *in vacuo* followed by trituration with ether to remove excess **183** afforded analytically pure **190** in a 70% yield (**Scheme 2.32**).

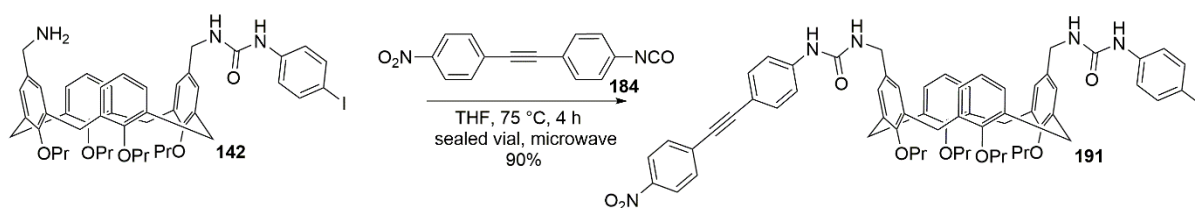


Scheme 2.32: Synthesis of intermediate **190** via reaction of amine **142** and isocyanate **183**

A comprehensive physicochemical analysis confirmed this structural assignment. In the $^1\text{H-NMR}$ spectrum of **183** the -OMe group was observed as a singlet at 3.83 ppm, with the rest of the spectrum appearing broadly similar to that of **137**. The presence of the carbon-carbon triple bond

was confirmed by resonances at 87.5 and 85.1 ppm in the ^{13}C -NMR, whilst the carbon-iodine bond (required for the subsequent Sonogashira coupling) was still intact as evidenced by a signal at 84.2 ppm. Furthermore, a mass ion was observed at 1162.4559 which corresponds to $[\text{M}+\text{NH}_4]^+$ for **137**.

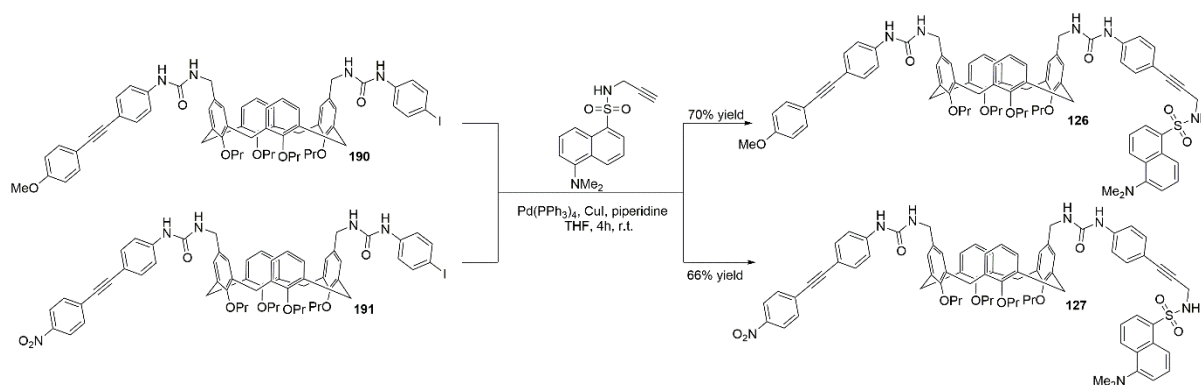
Confident now in the preparation of compounds such as **190**, I next synthesised *para*-nitro analogue **191** via the reaction of freshly prepared isocyanate **184** with *mono*-aminomethyl calix[4]arene **142** under the 'standard' microwave conditions. After four hours at 75 °C, TLC analysis indicated complete consumption of **142**. Purification via trituration with ether afforded a pleasing yield (*i.e.* 90%) of analytically pure **191** (Scheme 2.33).



Scheme 2.33: Synthesis of intermediate **191** via reaction of amine **142** and isocyanate **184**

A comprehensive physicochemical analysis confirmed this structural assignment. In the ^1H -NMR spectrum of **191** a pair of doublets were observed at 8.21 ($J = 8.9$ Hz) and 7.66 ($J = 8.9$ Hz) arising from the *para*-nitro substituted benzene ring, with the rest of the spectrum appearing broadly similar to both **190** and **137**. Similar to compounds **190** and **137** the presence of the carbon-carbon triple and carbon-iodine bonds were confirmed by the characteristic resonances at 87.1, 85.5 and 83.9 ppm respectively. Furthermore, a mass ion was observed at 1177.4302 in the HRMS analysis which corresponds to $[\text{M}+\text{NH}_4]^+$ for **191**.

The final step in the synthetic plan was to couple **190** and **191** with propargylamide **178** under Sonogashira conditions to access the required 'bis-alkyne' sensors **126** and **127**. Following on from the successful generation of sensor **182** by these means, I opted to employ identical reaction conditions to provide the best chance of obtaining **126** and **127** in high yields. Thus I performed both Sonogashira coupling reactions in parallel, and was delighted to find that in both cases the starting materials (*i.e.* **190** and **191**) had been consumed after four hours at room temperature (TLC analysis). Subsequent purifications via flash column chromatography afforded **126** and **127** in 70% and 66% yields respectively (Scheme 2.34).



Scheme 2.34: Synthesis of 'bis-alkyne' sensors **126** and **127** via Sonogashira couplings

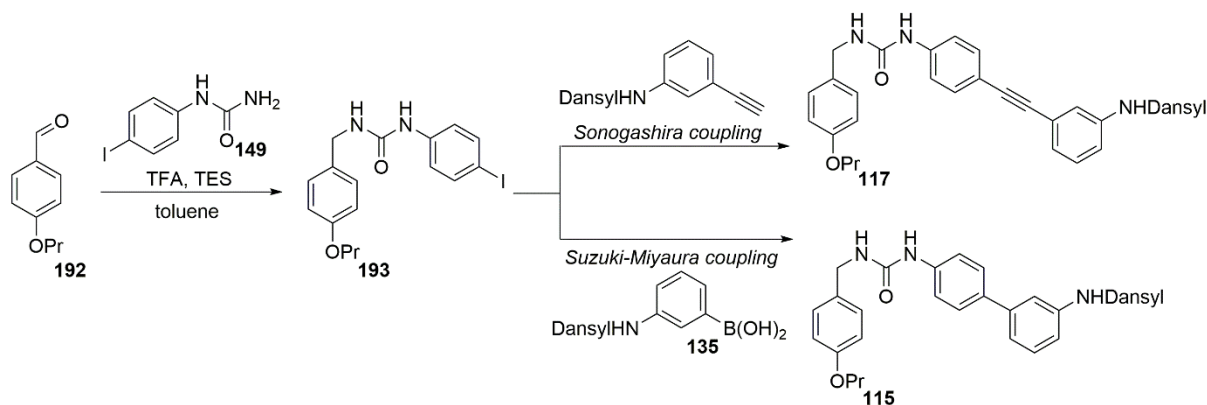
The formation of **126** and **127** were confirmed by comprehensive physicochemical analyses. In the case of **126** the introduction of the dansyl fluorophore was confirmed by doublets at 8.45 ($J = 8.5$ Hz), 8.25 ($J = 7.3$ Hz) and 8.22 ($J = 8.6$ Hz) in the $^1\text{H-NMR}$ spectrum. The $^{13}\text{C-NMR}$ spectrum of **126** displayed signals at 88.9, 88.3, 84.7 and 82.0 ppm indicative of the presence of two distinct carbon-carbon triple bonds. Furthermore, a mass ion was observed at 1305.6093 in the HRMS which corresponds to $[\text{M}+\text{H}]^+$ for **126**. The $^1\text{H-NMR}$ data for **127** was broadly similar to that of **126** – doublets at 8.48 ($J = 8.6$ Hz), 8.32 ($J = 8.6$ Hz) and 8.16 ($J = 7.2$ Hz) confirmed the introduction of the dansyl fluorophore. In the $^{13}\text{C-NMR}$ spectrum of **127**, a strong downfield shift of the *para*-nitrophenyl substituted alkyne carbons was observed in comparison to *para*-methoxy substituted **126**; these signals appeared at 95.4 and 89.7 ppm, thereby illustrating the strongly electron withdrawing nature of the *para*-nitro functional group.

2.13 Synthesis and fluorescence properties of control compounds **115** and **117**

Having demonstrated the amenability of this synthetic route for the generation of derivatives **126** and **127**, I was keen to examine their fluorescence properties. However, before proceeding with these studies, I felt it was important to re-examine the series of 'control compounds' **115**, **116** and **117** which previous studies within the Bew group had indicated *did not* show any fluorescence quenching upon treatment with sodium tetrachloroaurate (up to 30 equivalents) in methanol (Section 1.5.4.2). This was important since I was recording these spectra on a more modern fluorescence spectrometer and required a self-consistent set of data for publication.

Without pure samples of 'control compounds' **115**, **116** or **117** to hand, I required a suitable route for their synthesis. Since no experimental detail was available for **115** and **117**, I opted to start by developing a route from *para*-propoxybenzaldehyde **192** using the same ionic hydrogenation/transition metal mediated chemistry I had experience of using in the calix[4]arene series. Thus I anticipated that an ionic hydrogenation using *para*-propoxybenzaldehyde **192** and

para-iodophenylurea **149** would afford common intermediate **193**, which could be subsequently derivatised using either Suzuki-Miyaura or Sonogashira couplings to afford control compounds **115** and **117** (Scheme 2.35).



Scheme 2.35: Proposed route to **115** and **117** from *para*-propoxybenzaldehyde **192**

Initiating this route, *para*-propoxybenzaldehyde **192** was reacted with an excess (*i.e.* 1.5 eqⁿ) of *para*-iodophenylurea **149** under reducing conditions (TFA-triethylsilane) in toluene to afford an 81% yield of common intermediate **193** after purification *via* flash column chromatography. The ¹³C-NMR of **193** confirmed that the carbon-iodine bond was, as anticipated, inert to this transformation with a resonance observed at 83.56 ppm confirming its presence (Figure 2.11).

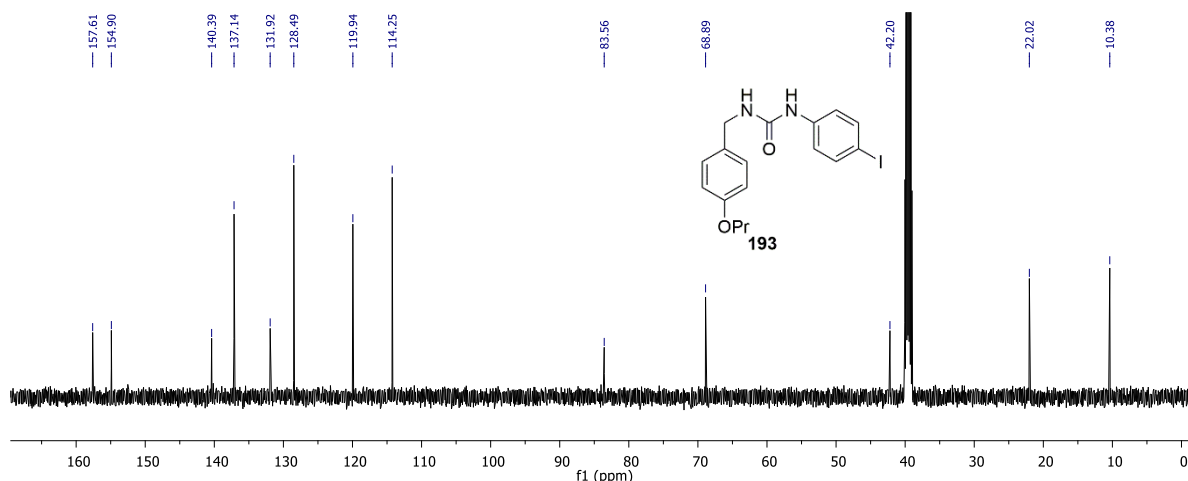
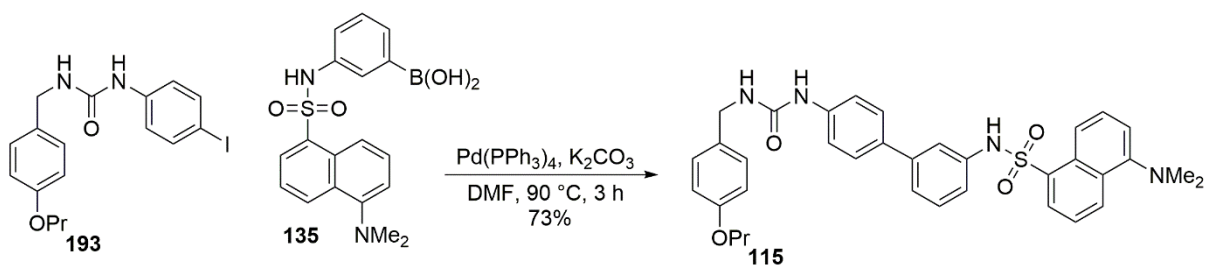


Figure 2.11: ¹³C-NMR spectrum of common intermediate **193** (124 MHz, d⁶-DMSO)

Confident in the ionic hydrogenation for the synthesis of intermediate **193** in high yield and purity (>95% by ¹H-NMR), I was ready to generate control compounds **115** and **117** *via* transition metal mediated couplings. Since I had immediate access to the required 3-(dansylamino)-phenylboronic acid **135** from the earlier studies (Section 2.8) I opted to attempt the Suzuki-Miyaura of **193** and **135** first. Thus a DMF solution of **193** and **135** was heated at 90 °C for three hours under palladium(0) catalysis employing potassium carbonate as the inorganic base (Scheme 2.36).



Scheme 2.36: Synthesis of Suzuki-Miyaura derived control compound **115**

Monitoring this reaction by TLC analysis, I observed complete consumption of iodide **193** after three hours at 90 °C and the concomitant formation of a new strongly fluorescent component. Isolation of this material *via* flash column chromatography and a comprehensive physicochemical analysis revealed this to be the desired coupled product **115**, obtained in a 73% yield. The ¹H-NMR spectrum of **115** displayed doublets at 8.40 (*J* = 8.4 Hz), 8.36 (*J* = 8.4 Hz) and 8.13 (*J* = 7.4 Hz) ppm arising from the naphthalene ring, thus confirming the introduction of the dansyl fluorophore.

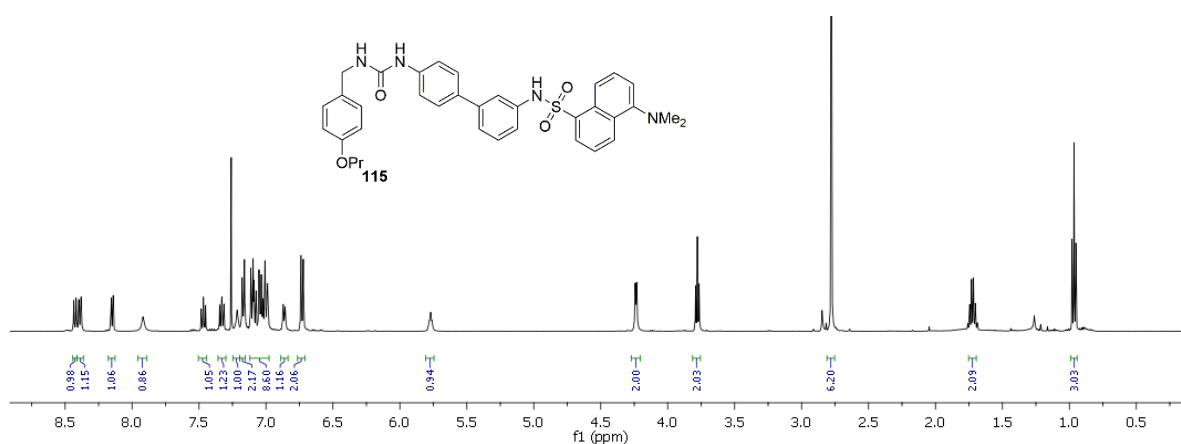


Figure 2.12: ¹H-NMR spectrum of control compound **115** (500 MHz, CDCl₃)

Interestingly, the 73% yield is significantly higher than obtained in the analogous coupling with the calix[4]arene-based ‘advanced intermediate’ **137** (*i.e.* 18% yield, **Section 2.9**) suggesting that the calix[4]arene core dramatically modulates the reactivity of that system. Notwithstanding, I was pleased to have accessed one of the key control compounds needed to prove that the selectivity observed towards Au(III) ions was unique to calix[4]arene based compounds such as **114**.

As I had already initiated the fluorescence studies with sensor **114** and was confident performing the fluorescence titration experiments, I opted to test the control compound **115** before proceeding onwards with the synthesis of **117**. It was anticipated that, in line with previous fluorescence studies performed in the Bew group, compound **115** would not show any significant change in fluorescence emission when treated with methanolic solutions of lithium chloride, mercuric chloride, silver perchlorate, cadmium carbonate, platinum(II) chloride or, most crucially, sodium tetrachloroaurate.

Thus I started by recording the UV absorption spectrum of **115** in methanol (5 μM) and observed $\lambda_{\text{max}} = 284 \text{ nm}$. Since it was anticipated that using this as the excitation wavelength would give rise to a second order band in the fluorescence spectrum of **115**, I decided to proceed as before and confirm that the use of a longer excitation wavelength (*i.e.* 360 nm) did not affect the peak shape or maximum. This was indeed found to be the case; a broad peak was observed with $\lambda_{\text{max}} = 525 \text{ nm}$ for both excitation wavelengths. Next I wanted to assess the photochemical stability of **115** in methanol (5 μM) over time, and did this by recording fluorescence spectra every two minutes for 0.5 hours (Figure 2.13).

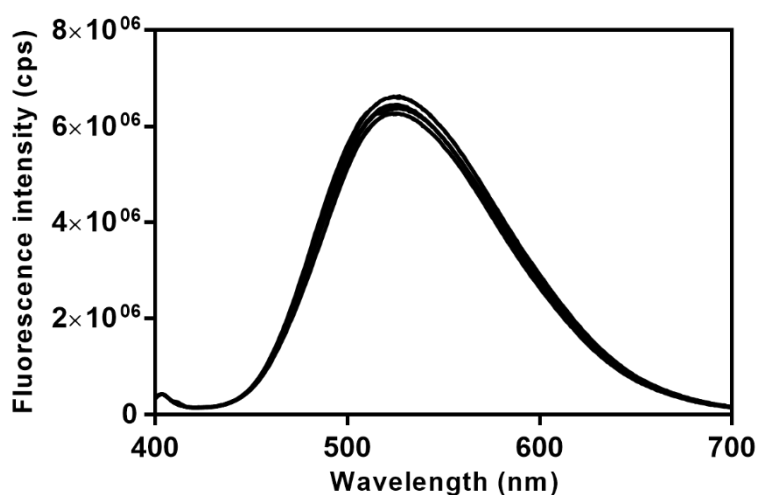


Figure 2.13: Fluorescence spectra of **115** in MeOH (5 μM) ($\lambda_{\text{ex}} = 360 \text{ nm}$, $\lambda_{\text{em}} = 525 \text{ nm}$) recorded every two minutes for 0.5 h displaying high photochemical stability

I was pleased to observe that no significant quenching occurred over this timescale, as indicated by the high degree of overlap between successive measurements. Thus I was confident that no additional processes (*e.g.* photochemical bleaching or quenching by molecular oxygen) were operating on the timescale of these experiments, and was able to begin studying the effect of different metal ions on the fluorescence emission of **115**. As compound **115** had been previously shown to undergo no change in emission upon titration of a methanolic solution of sodium tetrachloroaurate (up to 30 equivalents) I opted to start by repeating this key experiment.

It was therefore extremely disappointing to find that this key experiment with control compound **115** could not be reproduced. Instead of observing no change in fluorescence intensity upon the addition of 30 equivalents of sodium tetrachloroaurate to **115** as previously reported, I observed a 95% reduction in fluorescence intensity after 40 minutes (Figure 2.14).

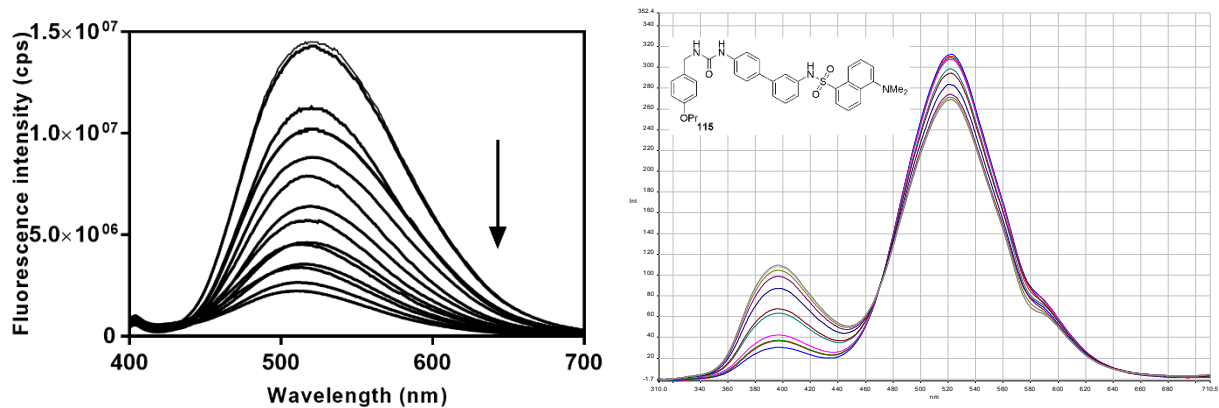


Figure 2.14: Left; Fluorescence spectra of **115** in MeOH (5 μ M) (λ_{ex} = 360 nm, λ_{em} = 525 nm) recorded every four minutes for 1 hour, after the addition of NaAuCl₄ (30 equivalents), displaying a decrease in fluorescence emission. Only spectra recorded every 4 minutes are included for clarity. Right; Original data obtained previously under identical experimental conditions.

Thus these results with **115** clearly indicated that neither the calix[4]arene 'core' nor a carbon-carbon triple bond were required to observe a quenching effect with sodium tetrachloroaurate in methanol. Indeed, this finding cast doubt on the accuracy of the preliminary fluorescence studies with control compounds **116** and **117** too (Section 1.5.4.2). Frustrated by this, I wanted to understand exactly how the quenching effect was operating in these systems (*i.e.* **114** and **115**) and undertook a comprehensive search of the literature to find some answers.

Talanova and co-workers have reviewed the application of dansyl-containing calix[4]arenes for the sensing of 'hazardous' metal ions up to 2010.⁸⁷ In this review, a number of co-ordination modes and quenching mechanisms are discussed between heavy metal ions (particularly Hg²⁺, Cd²⁺ and Tl⁺) and substituted dansyl fluorophores. In the case of HN-dansyl substituted systems (*e.g.* **194**) it is thought that a PET mechanism is the most prevalent; coordinated redox-active transition metals accept electron density from the excited state of the dansyl fluorophore resulting in quenching. In terms of coordination modes, it is thought that the proton-ionisable nature of the HN-dansyl group may provide a site for metal ion complexation (Figure 2.15).

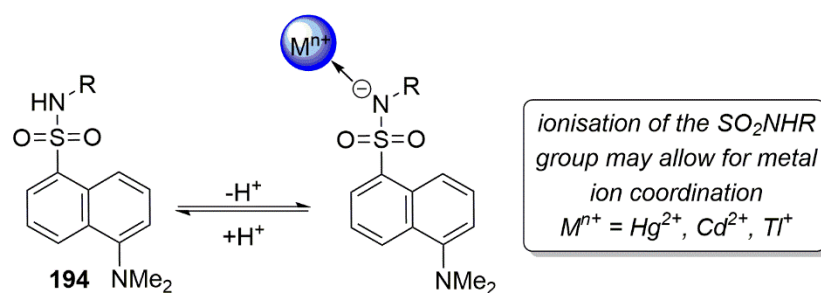


Figure 2.15: Coordination of metal ions (Hg²⁺, Cd²⁺ and Tl⁺) to ionised **194**

Whitesides and co-workers have studied the effect of pH on polyethylene bound dansyl groups such as **195** and observed that in acidic media (pH < 2) the fluorescence emission of **195** is reduced to ca. 98% of its original value at pH > 5. This quenching effect was attributed to protonation of the -NMe₂ group in acidic media (**Figure 2.16**).¹⁵³

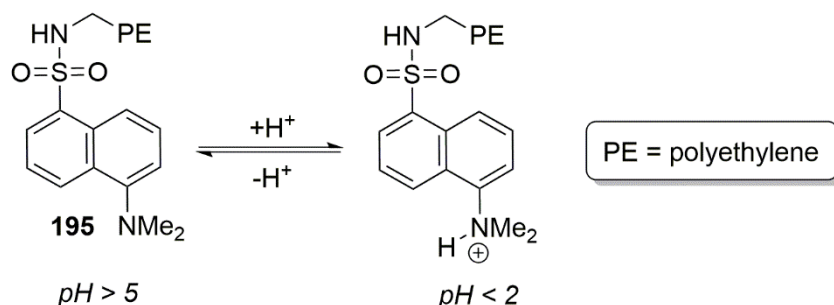


Figure 2.16: Mechanism for fluorescence quenching of polyethylene bound **195** in acidic media

Presumably, this effect could also occur with Lewis acidic species. Thus I began to suspect that the selectivity observed with sensor **114** for sodium tetrachloroaurate over a range of other metal salts could be explained by two possible mechanisms; a) coordination of Au(III) to the ionised sulfonamide or b) coordination of Au(III) to the -NMe₂ group (**Figure 2.17**).

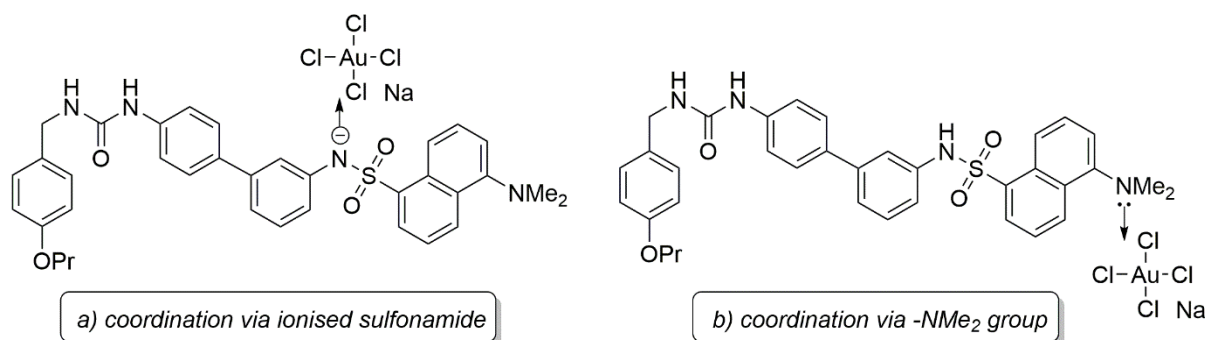
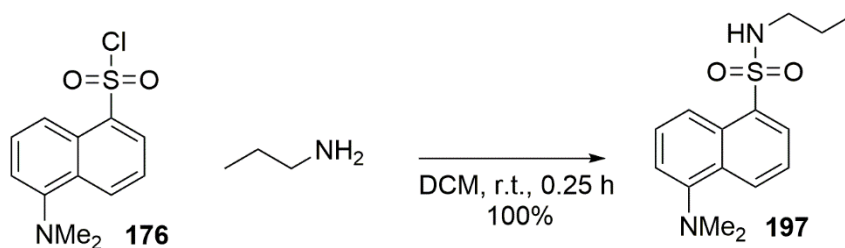


Figure 2.17: Proposed coordination modes resulting in fluorescence quenching for **114**

These coordination modes suggested that even simple alkyl sulfonamide derivatives of dansyl chloride **176** such as **196** would display fluorescence quenching when treated with sodium tetrachloroaurate in methanol. I therefore planned the synthesis of *n*-propylamine derived sulfonamide **197** to test this hypothesis. Reaction of dansyl chloride **176** with an excess of *n*-propylamine (acting as reagent and organic base) in DCM at room temperature for 15 minutes afforded a quantitative yield of **197** after aqueous workup (**Scheme 2.37**).



Scheme 2.37: Synthesis of sulfonamide **197** via reaction of **176** and *n*-propylamine in DCM

The $^1\text{H-NMR}$ spectrum of **197** in CDCl_3 correlated well with data reported by Luis and co-workers for the same compound.¹⁵⁴ The introduction of the propyl chain was confirmed by signals at 0.71 (t, $J = 7.4$ Hz, 3H), 1.25 (m, 2H) and 2.82 (t, $J = 7.5$ Hz, 2H) ppm, whilst the presence of the sulfonamide -NH proton was confirmed by the presence of a triplet at 5.42 ppm ($J = 6.1$ Hz).

With simplified dansyl derivative **197** in hand (*i.e.* compared to the structurally complex **114**) I was able to repeat the fluorescence experiments exactly to test this hypothesis. To proceed, I recorded the UV spectrum of **197** and observed $\lambda_{\text{max}} = 282$ nm. Since (as with the previous studies) this wavelength resulted in a second order diffraction peak in the fluorescence spectrum, I recorded the fluorescence spectrum of **197** using excitation wavelengths of both 282 and 360 nm. I observed no significant changes in peak shape or lambda max (524 nm) between these spectra (excepting the second order peak) and therefore opted to use 360 nm as the excitation wavelength.

Next I recorded a series of fluorescence spectra of **197** (5 μM in methanol) over time (every two minutes for 0.5 hours) and observed high photochemical stability, as indicated the high degree of overlap between successive curves. With this result established, I added three equivalents of sodium tetrachloroaurate in methanol to **197** and recorded fluorescence spectra every two minutes for a further hour. Over much the same time period as for calix[4]arene **114**, calix[4]arene **182** and control compound **115** I observed a 95% reduction in fluorescence intensity after *ca.* 45 minutes at room temperature (**Figure 2.18**).

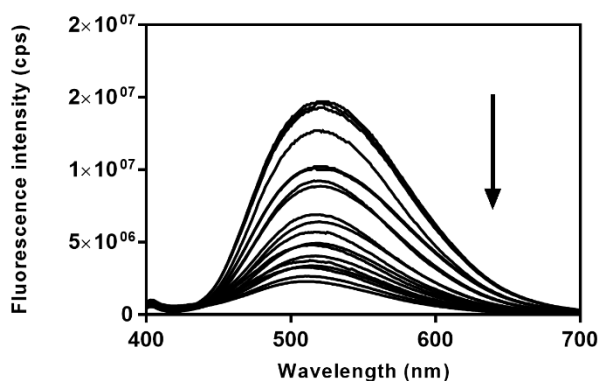


Figure 2.18: Fluorescence spectra of **115** in MeOH (5 μM) ($\lambda_{\text{ex}} = 360$ nm, $\lambda_{\text{em}} = 524$ nm) recorded every four minutes for 1 hour, after the addition of NaAuCl_4 (3 equivalents), displaying a decrease in fluorescence emission.

This result clearly indicates that the mechanism leading to fluorescence quenching in **114**, **115**, **182** and **197** does not require alkyne, calix[4]arene or urea modification of the dansyl fluorophore to operate. Thus the mechanism in each of these cases is likely one of the two possibilities outlined in **Scheme 2.14**, and not as had been indicated by preliminary studies carried out within the Bew group (*i.e.* Au³⁺ coordination to the carbon-carbon triple bond of, for example, **114**).

2.14 Conclusions and outlook

In this project I developed a novel synthesis of urea functionalised calix[4]arenes (*e.g.* **114**, **126**, **127** and **182**) featuring ABAC substitution at the upper-rim. The multi-step synthetic route developed furnished these intricately functionalised calix[4]arenes in high yields and, most significantly, excellent purities. The ionic hydrogenation which generated the required upper-rim ABAC substitution (**Scheme 2.7**) was key to this synthetic strategy, as previous attempts at introducing ABAC substitution *via* a Sonogashira coupling only afforded products of mediocre purity. Attempts at extending the range of derivatives available for fluorescence studies were successful, resulting in the synthesis of three novel 'bis-alkyne' calix[4]arenes (*i.e.* **126**, **127** and **182**). Unfortunately, the use of these compounds as ion-selective sensors for Au(III) was shown to be largely unnecessary – a thorough re-evaluation of preliminary fluorescence studies indicated a simpler quenching mechanism was operative and the original data for compounds **115**, **116** and **117** (**Section 1.5.4.2**) was unreliable.

Chapter 3: Results and Discussion

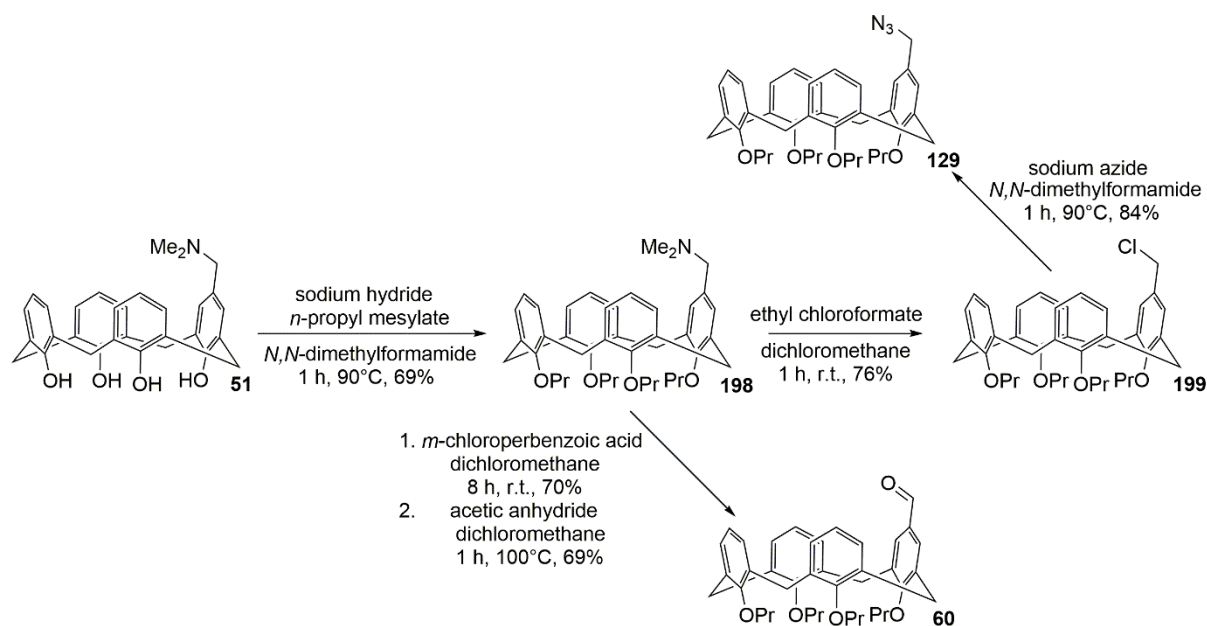
1,2,3-Triazole Linked Cavitands and
Peptidocalix[4]arenes *via* Dynamic Covalent Chemistry

3.1 Abstract

A series of novel upper-rim 1,2,3-triazole linked calix[4] and -[6]arenes has been designed and synthesised *via* the optimisation of a protocol originally developed by Bew and Stephenson for the generation of 'mono-armed' (*i.e.* AAAB and AAAAAB substituted) calix[4] and [6]arenes respectively. The first synthesis of a homodimeric redox-active S–S–linked cavitand has been achieved using this methodology. I also show how, through the application of dynamic covalent chemistry (DC_vC), upper-rim (S)-cysteine and glutathione functionalised calix[4]arenes can be readily accessed. Finally, I show how the application of both CuAAC and redox chemistries towards the same calixarene scaffold can be used to access a new set of structurally unusual, redox-active, multicalixarenes.

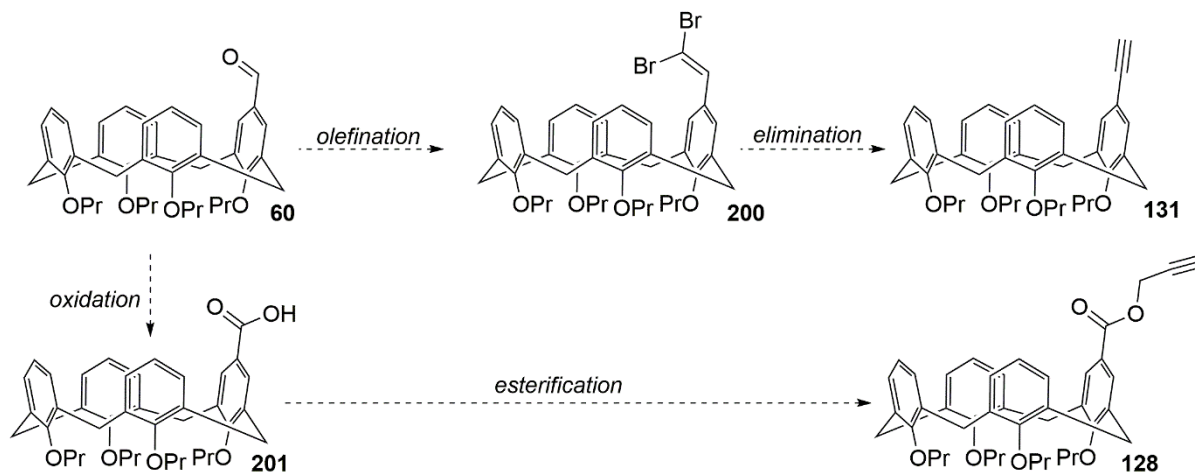
3.2 Methodology

For the preparation of the AAAB and AAAAAB functionalised calix[4] and [6]arenes that I would require for the construction of this novel series of heterocycle linked cavitands (**133 Scheme 1.24**) I reviewed a previous project carried out within the Bew group.⁵³ An exhaustive lower-rim O-propylation of the known⁵² dimethylaminomethyl calix[4]arene **51** using sodium hydride and *n*-propylmesylate in DMF was demonstrated by Bew and co-workers to result in the chemoselective synthesis of the cone-confined derivative **198** in a high (*i.e.* 69%) yield. With this result established, a series of functional group interconversions were then demonstrated to provide rapid access to a range of AAAB functionalised derivatives (*i.e.* **60**, **129** and **199**) (**Scheme 3.1**).



Scheme 3.1: Bew and Stephenson's syntheses of AAAB functionalised calix[4]arenes⁵³

Preliminary findings from the Bew and Stephenson research groups also indicated the possibility of extending the calix[4] O-propylation approach to the calix[6]arene series.¹⁵⁵ Thus, by combining and extending these two studies, I undertook the synthesis of a series of alkyne and azide functionalised calix[4] and [6]arenes such that a new family of triazole linked cavitands could be generated. In the first instance the synthesis of alkyne modified calix[4]arenes **128** and **131** was attempted *via* well known, ‘reliable’, chemistry that started from mono-formyl calix[4]arene **60** which I already had available (**Scheme 3.2**).



Scheme 3.2: Proposed syntheses of mono-alkyne functionalised calix[4]arenes **128** and **131** starting from mono-formyl calix[4]arene **60**

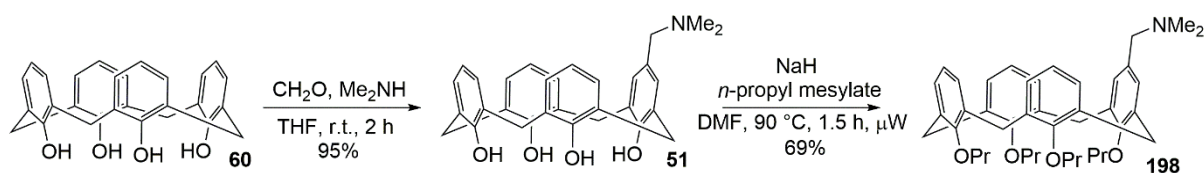
For the first approach, it was anticipated the Corey-Fuchs reaction of mono-formyl calix[4]arene **60** would furnish mono-ethynyl calix[4]arene **131** *via* a base promoted elimination of the intermediate 1,1-dibromovinyl calix[4]arene **200**. The Corey-Fuchs reaction has been successfully applied to a wide variety of systems, and importantly for this application, the four-fold variant leading to the *tetra*-ethynyl modified cone calix[4]arene has been reported by Dyker and co-workers, thereby illustrating the feasibility of my approach to **131**.¹⁵⁶ I also anticipated that propargyl ester **128** would make an ideal ‘building block’ for the click studies, and that it should be readily accessible *via* the oxidation of mono-formyl calix[4]arene **60** to the corresponding carboxylic acid **201**, followed by esterification using propargyl bromide or propargyl alcohol affording **128**.

In order to develop the synthesis of the ‘mismatched’ calix[4]arene-calix[6]arene ([4]-[6]) dimers discussed earlier, I anticipated undertaking a simple reinvestigation of procedures developed previously within the Bew group should allow access, in the first instance, to pure samples of previously unknown mono-azido calix[6]arene **132**.¹⁵⁵ With this important building block in hand, I envisaged a simple CuAAC reaction between **132** and one of the proposed alkyne modified

calix[4]arenes (*i.e.* **128** or **131**) would likely afford the first examples of ‘mismatched’ heterocycle linked ‘[4]-[6]’ dimers.

3.3 Synthesis of monoformyl calix[4]arene **60**

To initiate this aspect of the project, I first required access to multi-gram quantities of mono-formyl calix[4]arene **60** since this was going to be the starting material for both the desired alkynyl calix[4]arenes (**128** and **131**). Its synthesis has been achieved previously within the Bew group *via* a protocol which begins with the chemoselective O-propylation of the known Mannich derived dimethylamino calix[4]arene **51** using *n*-propyl mesylate in *N,N*-dimethylformamide (**Scheme 3.3**).^{52,53}



Scheme 3.3: Synthesis of core intermediate cone-confined tetra-*n*-propyl calix[4]arene **198**.^{52,53}

In the first stage of this process, originally reported by Gutsche and co-workers in 1994, a Mannich reaction of calix[4]arene **37** with excess formaldehyde and dimethylamine in THF leads to a near quantitative (*i.e.* 95%) yield of mono-substituted dimethylamino calix[4]arene **51**.⁵² The selectivity for mono-substitution observed under these conditions is thought to result from the poor solubility of product **51** in the reaction medium, and thus, as the aminomethylation proceeds, the product **51** precipitates out of solution limiting its ability to undergo further reactions.

In the second stage of this process, recently developed within the Bew group, a chemoselective O-propylation of **51** using *n*-propyl mesylate in *N,N*-dimethylformamide leads to a high and reproducible (*i.e.* 69%) yield of cone-confined **198**. The high yield observed under these conditions is attributed to coordination of the nitrogen lone pair to the carbonyl group of an included molecule of *N,N*-dimethylformamide, thereby acting as a ‘supramolecular protecting group’. This helps to prevent the formation of the unwanted *N*-quaternised species. I sought evidence for this unusual process and was delighted to find that support for this proposal comes from X-ray crystal structures reported by Takemura, Dunitz and Rodgers.^{157–159} Takemura *et al.* reported that tertiary amine modified calix[4]arenes such as **202** readily form inclusion complexes with *N,N*-dimethylformamide, whilst Dunitz and Rodgers have provided examples of close contact (*i.e.* 1.49 to 2.91 Å) nucleophilic interactions between the tertiary amines of **203** and **204** and their neighbouring carbonyl groups (**Figure 3.1**).

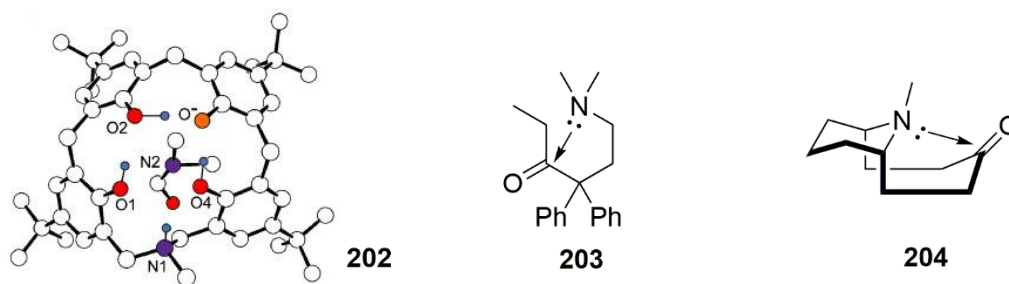


Figure 3.1: Takemura's crystal structure of homoazacalix[4]arene-DMF complex **202** in addition to Dunitz **203** and Rogers **204** examples of close contact $N\cdots C=O$ nucleophilic interactions^{157–159}

A combination of these two effects (*i.e.* complexation within the calix[4]arene cavity and $N\cdots C=O$ interactions) may then be operative in this case. To establish the importance of the solvent, the reaction was also carried out in DMSO and THF, and in these cases only poor yields of **198** could be obtained.⁵³

Finally, it was demonstrated that **198** could be transformed in a short reaction sequence to the monoformyl calix[4]arene **60** *via* oxidation to the corresponding *N*-oxide **205** (not shown), followed by treatment with acetic anhydride that allowed a Polonovski reaction to be undertaken (**Scheme 3.1**).

Satisfied that this route would provide the most efficient means for the generation of multi-gram quantities of **60**, I chose to begin these investigations following the protocol outlined by Gutsche and co-workers for the synthesis of the Mannich derived **51**. I opted to perform the reaction of calix[4]arene **37** with dimethylamine and formaldehyde in THF on a 30 g scale, and was pleased to be able to isolate the desired product **51** in a comparable 94% yield after two hours at room temperature. The formation of **51** was confirmed by comparison of its ¹H-NMR spectrum in CDCl₃ to the values reported in the literature. The $N(CH_3)_2$ protons were, for example, observed as a singlet at 2.21 ppm (literature 2.19 ppm).⁵² With this material in hand, I was in a position to attempt the propylation reaction (*i.e.* **51** to **198**) under the conditions developed within the Bew group. Undertaking this reaction on a 0.5 g scale (I was limited by the size of the microwave vials) in freshly distilled *N,N*-dimethylformamide, I was able to isolate **198** in a comparable 70 % yield after purification by column chromatography on silica gel. The ¹H-NMR spectrum of **198** was in accordance with previous reports, displaying a singlet at 2.08 ppm for the $N(CH_3)_2$ protons and multiplets at 3.84, 1.94 and 1.00 ppm arising from the non-equivalent propyl chains (**Figure 3.2**).

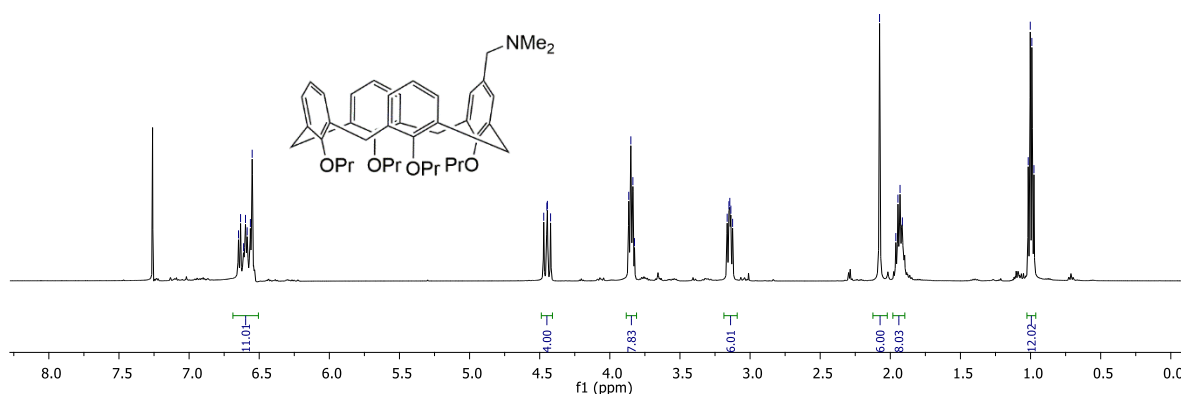
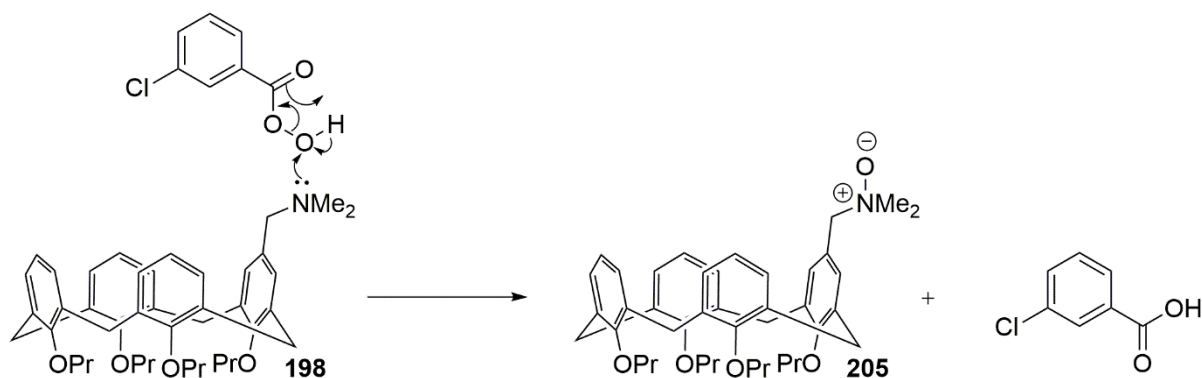


Figure 3.2: $^1\text{H-NMR}$ spectrum of cone-confined dimethylamino calix[4]arene **198** (500 MHz, CDCl_3)

Motivated by the operational simplicity of this procedure, I looked towards generating the corresponding *N*-oxide **205** as this is a key intermediate for the Polonovski reaction that leads to the desired mono-formyl calix[4]arene **60**. Whilst the oxidation of tertiary amines to *N*-oxides has been achieved by a variety of methods (*e.g.* *m*-chloroperbenzoic acid in DCM,¹⁶⁰ hydrogen peroxide in MeCN,¹⁶¹ and Oxone™ in EtOH-H₂O¹⁶²) I was confident that the procedure already optimised within the Bew group would be the most suitable. Thus I opted to perform the oxidation of **198** into **205** using an excess of mCPBA (*i.e.* two equivalents) in chloroform. I was pleased to obtain a 70% yield of **205** after purification by flash column chromatography on silica gel. A plausible mechanism for this process is illustrated below (**Scheme 3.4**).

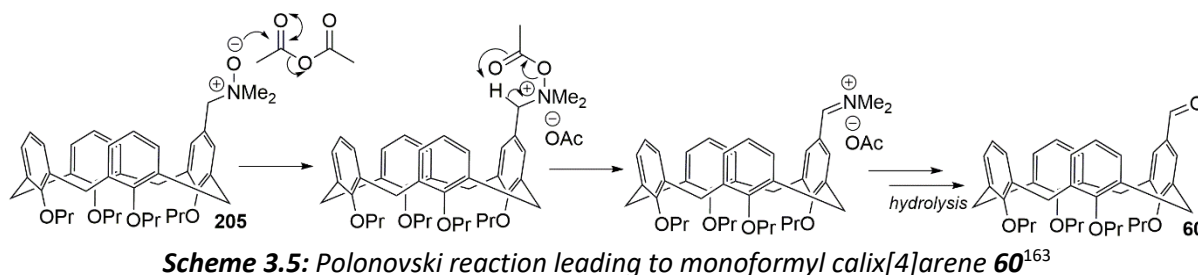


Scheme 3.4: Proposed mechanism for the mCPBA mediated oxidation of **198** into **205**

To confirm the formation of the *N*-oxide **205**, I compared the $^1\text{H-NMR}$ spectrum of this material to that obtained previously in the Bew group and observed a high correlation. Particularly characteristic was the signal arising from the $\text{N}(\text{CH}_3)_2$ protons – in the starting material this was observed at 2.08 ppm, whilst in the oxidised product it appears downfield at 2.26 ppm.

The final step in this synthesis is the treatment of *N*-oxide **205** with acetic anhydride in DCM at 80 °C (sealed vial under microwave irradiation) for 1 hour. These conditions presumably result in acylation of the N-O function at oxygen, followed by alpha elimination and subsequent hydrolysis (upon work-

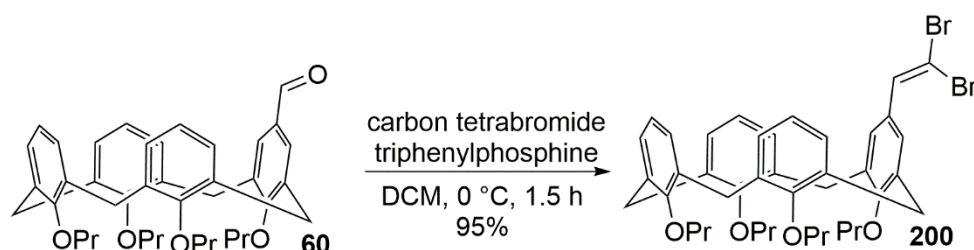
up) to afford the corresponding mono-formyl calix[4]arene **60**, in a reaction named after the inventors; Max and Michel Polonovski (**Scheme 3.5**).¹⁶³



Undertaking this reaction on a 1 mmol scale, I was pleased to isolate **60** in a 69% yield after purification by flash column chromatography on silica gel. The ¹H- and ¹³C-NMR spectra of **60** were in accordance with those reported previously for this compound. For example, the formyl proton afforded a singlet at 9.56 ppm (lit. 9.56 ppm) in the ¹H-NMR spectrum and the formyl carbon afforded a resonance at 191.9 ppm (lit. 191.8 ppm) in the ¹³C-NMR spectrum.¹⁶⁴ By repeating this sequence of reactions on a larger scale (*i.e.* starting with 15 mmol of calix[4]arene **198**), I was able to readily obtain multigram quantities of the desired starting material **60** in a comparable 72% yield with which to develop a route towards alkyne modified **128** and **131**.

3.4 Synthesis of upper-rim alkyne functionalised AAAB calix[4]arenes

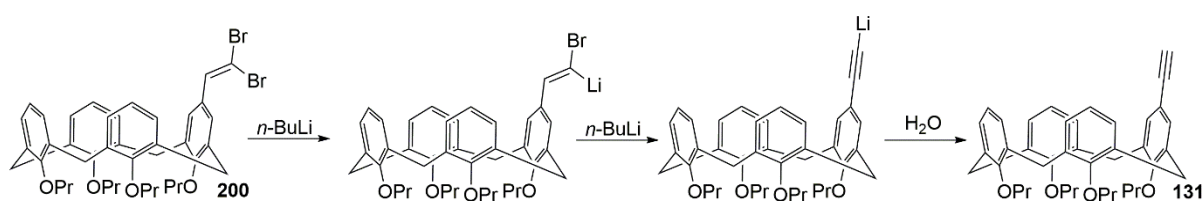
With mono-formyl calix[4]arene **60** in hand, I was in a position to investigate the synthesis of the alkyne modified calix[4]arenes **128** and **131** proposed at the outset (**Section 3.2**). I chose to begin these studies with ethynyl calix[4]arene **131**, since there was some literature precedent for its synthesis provided by Dyker and co-workers who successfully prepared the four-fold ‘tetra-alkyne’ variant *via* a Corey-Fuchs reaction.¹⁵⁶ Motivated by this report, I attempted the synthesis of the required 1,1-dibromovinyl calix[4]arene **200** by treating **60** with an excess (*i.e.* three equivalents) of carbon tetrabromide and triphenylphosphine in DCM at 0 °C (**Scheme 3.6**).



Monitoring the reaction by TLC analysis, I was pleased to observe complete consumption of the starting material **60** with concomitant formation of a new apolar component after 1.5 hours at 0 °C.

A subsequent filtration of the reaction mixture through a short plug of silica, with DCM as the eluent, proved to be sufficient purification to afford an analytically pure sample of **200** in an excellent 95% yield. The formation of **200** was confirmed by a comprehensive physicochemical analysis. In the $^1\text{H-NMR}$ spectrum of **200**, the signal arising from the formyl proton in **60** had disappeared and was replaced by a singlet at 7.05 ppm, which was assigned to the vinylic proton. A subsequent HRMS analysis provided further evidence for the formation of **200**; a mass ion was observed at 777.1982 which corresponds to $[\text{M}+\text{Na}]^+$.

Pleased with the high yield obtained using this procedure, I focused my attention towards the synthesis of terminal ethynyl calix[4]arene **131** *via* treatment of **200** with *n*-butyl lithium in THF. These conditions were expected to result in the formation of a carbon-carbon triple bond *via* a reaction mechanism which is thought to involve lithium-halogen exchange of the 1,1-dibromovinyl species **200**, dehydrohalogenation and subsequent hydrolysis upon work-up (**Scheme 3.7**).¹⁶⁵



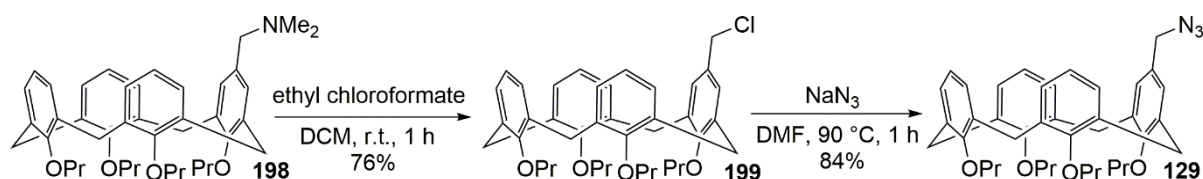
Scheme 3.7: Proposed mechanistic pathway for the conversion of the dibromovinyl calix[4]arene **200** into ethynyl calix[4]arene **131**¹⁶⁵

Opting to perform this reaction under a typical set of conditions, I treated a THF solution of **200** with an excess of *n*-butyl lithium (10 equivalents) at $-78\text{ }^\circ\text{C}$. I was pleased to find that TLC analysis of the reaction mixture after one hour indicated that all of the starting material **200** had been consumed. A subsequent aqueous work-up and purification by flash column chromatography afforded a 54% yield of 1,1-dibromovinyl calix[4]arene **131**. The formation of **131** was confirmed by a comprehensive physicochemical analysis. In the $^1\text{H-NMR}$ spectrum of **131**, the acetylenic proton gave rise to a singlet at 2.86 ppm, whilst in the $^{13}\text{C-NMR}$ the carbon-carbon triple bond was evidenced by signals at 84.8 and 82.3 ppm. Finally, in the HRMS analysis of **131**, a mass ion was observed at 617.3627 which corresponds to $[\text{M}+\text{H}]^+$.

Satisfied that I had established an efficient route towards alkyne functionalised **131**, I was keen to explore its reactivity in the CuAAC reaction. As such, it was decided to return to the synthesis of the proposed propargyl ester **128** (**Section 3.2**) at a later time, and refocus efforts towards the generation of the second building block; mono-azido calix[4]arene **129**.

3.5 Synthesis of azide functionalised cone-confined calix[4]arene **129**

To progress the aim of generating heterocycle-linked cavitands, I needed to access mono-azido calix[4]arene **129**. Fortunately, its synthesis had already been achieved (in the Bew group) *via* a two-step protocol which begins with cone-confined *N,N*-dimethylamino calix[4]arene **198**. Treatment of **198** with ethyl chloroformate in DCM afforded, in high (*i.e.* 76%) yield, chloromethylene calix[4]arene **199**, from which the mono-azido calix[4]arene **129** was obtained in an excellent (*i.e.* 84%) yield by reaction with sodium azide in DMF at 90 °C (**Scheme 3.8**).



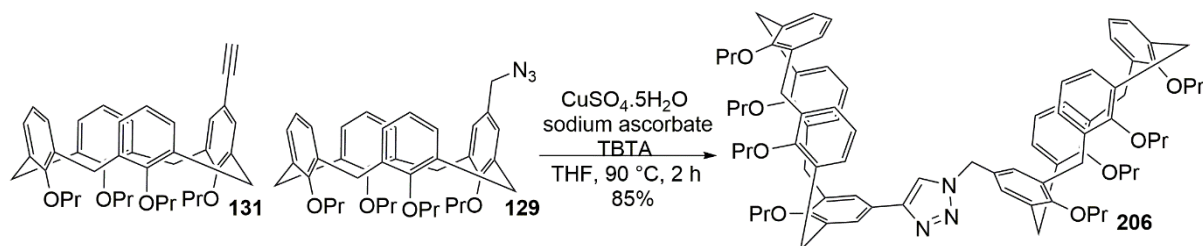
Since the reported overall yield for this transformation (*i.e.* NMe_2 to N_3) was high (*i.e.* 64%) and no flash column chromatography was required, this was a highly convenient route for the synthesis of **129**. Reacting 0.5 mmol of **198** with an excess (*i.e.* 2 eqⁿ) of ethyl chloroformate in DCM, I was pleased to obtain a comparable yield (*i.e.* 74%) of chloromethyl calix[4]arene **199** after one hour reaction time. The ¹H-NMR data were in accordance with that recorded previously in the Bew group, with, for example, a characteristic singlet observed at 4.11 ppm arising from the CH_2Cl protons. Next, to obtain the azide **129** *via* the $\text{S}_{\text{N}}2$ displacement of the chloride on **199**, I treated a DMF solution of **199** with excess of sodium azide at 90 °C for one hour under microwave irradiation. TLC analysis of the reaction mixture indicated complete consumption of **199**, and isolation by aqueous work-up afforded a comparable 89% yield of **129**. To confirm the formation of **129** I compared its ¹H- and ¹³C-NMR spectra to those previously obtained and observed a high correlation. For example, the CH_2Cl peak appearing at 4.11 ppm in the starting material was no longer present; instead a singlet at 3.84 ppm arising from the CH_2N_3 protons was observed. In addition, I recorded the FT-IR spectrum of **129** and observed a strong absorption at 2092 cm^{-1} , characteristic of an azide functional group.

3.6 Synthesis of 1,2,3-triazole-linked cavitands in the calix[4]arene series

With both alkyne (*i.e.* **131**) and azide (*i.e.* **129**) functionalised calix[4]arenes to hand, I was ready to start the investigations into the use of the CuAAC reaction as a means of linking two calix[4]arene units together. A literature search revealed that the combination of copper(II) sulfate, sodium ascorbate and *tris*(benzyltriazolylmethyl)amine has been employed successfully for the catalysis of the CuAAC reaction for a wide variety of different chemical systems, and thus I decided to employ this catalytic system for my reactions.^{166,167} The function of the sodium ascorbate is to reduce the

copper(II) sulfate to an active copper(I) species, which is itself 'protected' from disproportionation to copper(0) and copper(II) as well as re-oxidation to copper(II) by air, through complexation with the ligand tris(benzyltriazolylmethyl)amine.¹⁶⁸

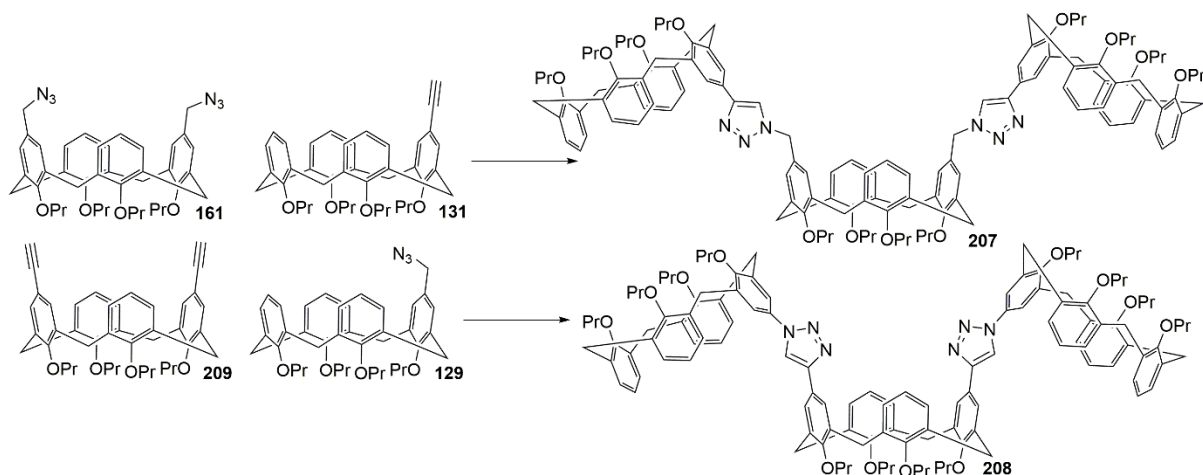
Selecting THF as the solvent for convenience, I decided to attempt a test reaction between ethynyl calix[4]arene **131** and a slight molar excess of monoazido calix[4]arene **129** (*i.e.* 1.1 equivalents) using microwave irradiation at 90 °C (**Scheme 3.9**).



Scheme 3.9: Synthesis of 1,2,3-triazole-linked bis-calix[4]arene cavitand **206**

Monitoring the reaction by TLC analysis, I was pleased to observe the complete consumption of **131** after two hours' reaction time with the concomitant formation of a new, more polar, component. Isolation and purification of this material by column chromatography on silica gel afforded an excellent yield (*i.e.* 85%) of the 1,2,3-triazole-linked *bis*-calix[4]arene cavitand **206**. The formation of **206** (as a single [1,4]-regioisomer) was confirmed by a comprehensive physicochemical analysis. In the ¹H-NMR spectrum for example, the 1,2,3-triazole proton was observed as a singlet at 7.14 ppm, whilst the singlet for the benzylic CH₂ observed at 3.84 ppm in the monoazido calix[4]arene **129** starting material was no longer present and was replaced by a singlet further downfield at 5.03 ppm in the product. Furthermore, in the HRMS analysis of **206**, a mass ion was observed at 1263.7348 which corresponds to [M+H]⁺.

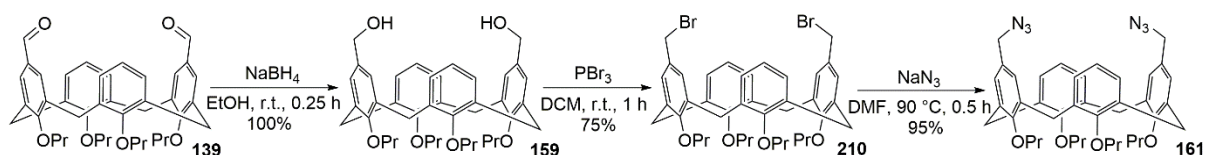
Delighted to have demonstrated the suitability and operational simplicity of the CuAAC reaction for the construction of cavitand **206**, I wanted to further expand its 'operational capacity' and see whether the reaction would be amenable to the synthesis of larger cavitands (*i.e.* those containing three or more calix[4]arene units) or would the steric requirements of such systems be too great to allow an efficient synthesis. To investigate this question, I envisioned the synthesis of the triple calix[4]arenes **207** and **208** *via* the CuAAC reaction of *bis*-functionalised calix[4]arenes **161** and **209** with either mono-azido calix[4]arene **129** or mono-ethynyl calix[4]arene **131** (**Scheme 3.10**).



Scheme 3.10: Proposed synthetic route to [4]-[6]-[4] trimers **207** and **208**

A literature search indicated that the 1,3-*bis*-azide calix[4]arene **161** was readily available *via* a three-step sequence starting from the 1,3-*bis*-formyl calix[4]arene **139** (Section 2.4) which involves borohydride reduction to the 1,3-*bis*-alcohol **159**, bromination with phosphorous tribromide to afford **210**, and finally displacement with sodium azide to furnish **161**.¹⁶⁷ In contrast, the required 1,3-*bis*-ethynyl calix[4]arene **209** was not known, but given the success employing the Corey-Fuchs reaction for the generation of the mono-ethynyl calix[4]arene **131**, I anticipated that the two-fold variant **209** could be accessed similarly.

Since the 1,3-*bis*-azide calix[4]arene **161** was a known compound, I opted to begin these studies by first preparing a sample of this material. Undertaking the reduction of 1,3-*bis*-formyl calix[4]arene **139** with sodium borohydride in ethanol afforded a quantitative yield of the 1,3-*bis*-hydroxymethylene calix[4]arene **159** after 15 minutes at room temperature. Bromination of **159** using phosphorous tribromide in DCM afforded **210** in a 75% yield, whilst the subsequent S_N2 reaction with sodium azide in DMF afforded the desired 1,3-*bis*-azide **161** in 95% yield (Scheme 3.11).



Scheme 3.11: Synthesis of 1,3-*bis*-azide calix[4]arene **161**¹⁶⁷

The formation of **161** was confirmed by ¹H- and ¹³C-NMR spectroscopy; the data were in accordance with those previously reported for this compound. For example, the methylene protons of the N₃CH₂ group were observed as a singlet at 3.95 ppm (lit. 3.94 ppm), whilst the pair of doublets at 4.45 (*J* = 13.4 Hz) and 3.15 (*J* = 13.4 Hz) ppm confirmed the calix[4]arene was 1,3-di-substituted and locked in

the *cone* conformation.¹⁶⁷ In addition, FT-IR analysis (thin film) of **161** displayed a strong absorption at 2098 cm⁻¹ typical for the azide functional group.

Next I wanted to address the synthesis of the 1,3-*bis*-ethynyl calix[4]arene **209** which I suspected could be accessed by the Corey-Fuchs reaction. Starting with 0.6 mmol of the 1,3-*bis*-formyl calix[4]arene **139**, I was pleased that the corresponding 1,3-*bis*-dibromovinyl calix[4]arene **211** could be obtained in an excellent (*i.e.* 96%) yield by reaction with triphenylphosphine and carbon tetrabromide in DCM for 1.5 h. Treating a THF solution of this material at – 78 °C with an excess of *n*-BuLi (*i.e.* 10 equivalents) afforded a modest but reproducible yield (*i.e.* 51%) of the desired and previously unknown 1,3-*bis*-ethynyl calix[4]arene **209** after purification by flash column chromatography on silica gel. The formation of **209** was confirmed by a comprehensive physicochemical analysis. For example, the acetylenic protons gave rise to a singlet at 2.96 ppm in the ¹H-NMR spectrum, whilst the pair of doublets observed at 4.41 (*J* = 13.4 Hz) and 3.13 (*J* = 13.4 Hz) ppm confirmed the calix[4]arene was 1,3-di-substituted and locked in the *cone* conformation. Furthermore, in the HRMS analysis of **206**, a mass ion was observed at 641.3637 which corresponds to [M+H]⁺.

With these azide and alkyne materials to hand, I was ready to investigate the CuAAC reaction as a means of generating the first examples of 1,2,3-triazole-linked triple calix[4]arenes. Since the conditions I had employed for the synthesis of *bis*-calix[4]arene cavitand **206** had been successful, I decided to use the same reagent and solvent combination for the preparation of **207** and **208**. Opting to begin with 1,3-*bis*-azido calix[4]arene **161**, the CuAAC reaction was performed with an excess of the mono-ethynyl calix[4]arene **131** (*i.e.* three equivalents) and I was delighted to find that two hours reaction time at 90 °C was all that was sufficient to promote the complete consumption of **161**. TLC analysis indicated only unreacted **131** and a single new component I presumed to be ‘triple’ calix[4]arene **207**. Subsequent purification by flash column chromatography on silica gel and a comprehensive physicochemical analysis revealed that **207** had been obtained in a 69% yield. Clearly, the progress of the reaction was not impeded to any great extent by the steric requirements imposed by having three calix[4]arene units closely coupled and proceeded at a similar reaction rate to that observed for *bis*-calix[4]arene cavitand **206** (Scheme 3.9). The ¹H-NMR spectrum of **207** displayed a singlet at 7.32 ppm arising from the two equivalent triazole protons, whilst the benzylic protons were observed as a singlet at 5.21 ppm (Figure 3.3). Furthermore, in the HRMS analysis of **207** a mass ion was observed at 1937.1079 which corresponds to [M+H]⁺ thus further confirming the structural assignment.

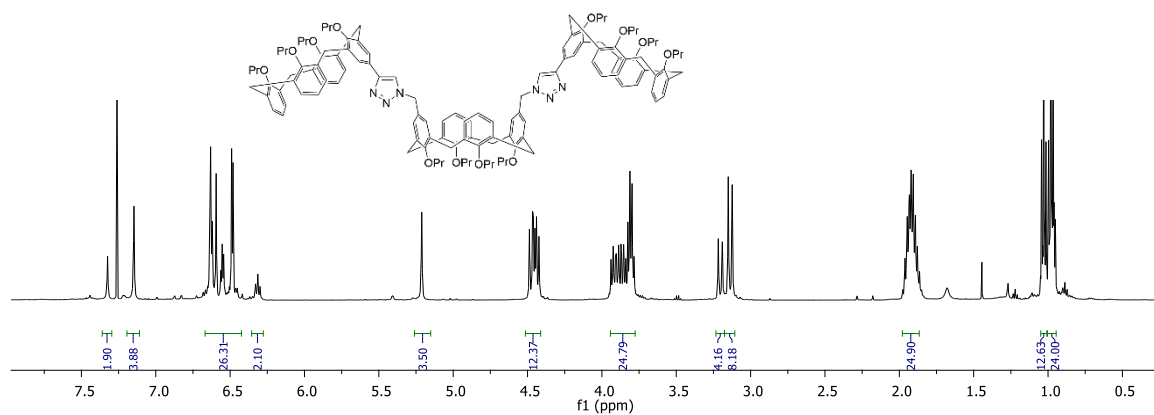
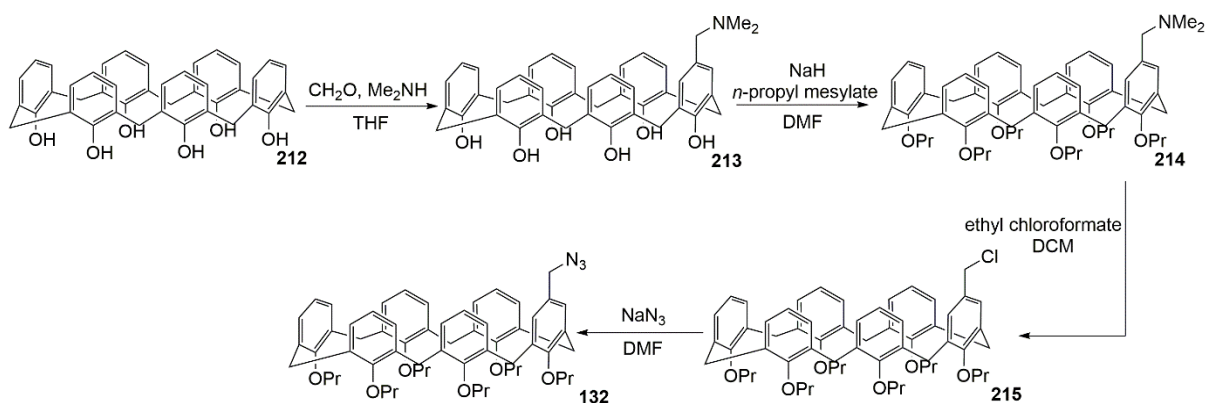


Figure 3.3: The $^1\text{H-NMR}$ spectrum of triple calix[4]arene **207** (500 MHz, CDCl_3)

Pleased with the high yield (*i.e.* 69%) and relatively short reaction time (*i.e.* 2 hours) required for the synthesis of **207**, I wanted to see whether this result could be reproduced in the analogous *bis*-ethynyl **209**/mono-azido **129** system affording **208** (Scheme 3.10). Additionally, since one of the principle motivations of this project was to develop an operationally simple route to cavitands with favourable host-guest properties, I was curious to be able to study the effect of altering the position of the triazole rings on the ability of these materials to complex guests. For this reason, I decided to undertake the CuAAC reaction of the *bis*-ethynyl calix[4]arene **209** with an excess (*i.e.* three equivalents) of mono-azido calix[4]arene **129**. I was pleased to isolate an excellent (*i.e.* 75%) yield of the ‘triple’ calix[4]arene **208** after a comparable two hours reaction time at 90 °C under microwave irradiation. A comprehensive physicochemical analysis confirmed the identity of **208**, with, for example, the triazole protons giving rise to a singlet at 7.22 ppm and the benzylic protons appearing as a singlet at 5.06 ppm.

3.7 Synthesis of 1,2,3-triazole-linked cavitands in the calix[6]arene series

In the introduction to this aspect of the PhD project, I described the desire to extend the versatility of the CuAAC protocol to the synthesis of unusual cavitands composed of different sized macrocycles based on calix[4] and calix[6]arene units. To achieve this aim, I needed to reinvestigate some preliminary findings from the Bew group which indicated the possibility of generating the analogous series of mono-functionalised derivatives (*e.g.* **215** and **132**) *via* the same protocol used for calix[4]arene (Scheme 3.12).¹⁵⁵



Scheme 3.12: The synthesis of mono-functionalised calix[6]arenes developed in the Bew group¹⁵⁵

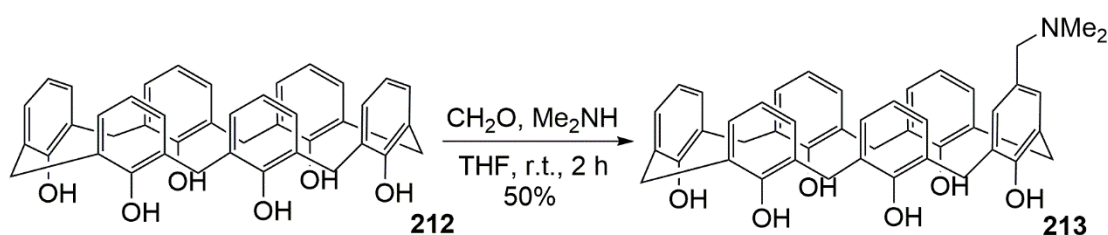
Since only minimal characterisation data had been obtained previously, it was important to re-evaluate this route before employing these materials (*e.g.* **132**) in the synthesis of the desired cavitands (*e.g.* **133**). To initiate this, I first required an efficient and high yielding protocol for the preparation of multi-gram quantities of core starting material calix[6]arene **212**. A search of the literature search indicated a two-step protocol beginning with the synthesis of *para-tert*-butylcalix[6]arene **216** as first described by Gutsche and co-workers, would be the most suitable.¹⁴ Thus, following this literature procedure, *para-tert*-butylphenol and formaldehyde were reacted under basic conditions (potassium hydroxide in refluxing xylenes) to afford an 81% yield of *para-tert*-butylcalix[6]arene **216** after recrystallisation of the impure material from 1:1 acetone-chloroform. The formation of **216** was confirmed by ¹H- and ¹³C-NMR analysis. For example, in the ¹H-NMR spectrum of **216** a broad singlet was observed at 3.86 ppm (lit. 3.90 ppm) arising from the methylene bridges, whilst a sharp singlet observed at 10.53 ppm (lit. 10.42 ppm) was assigned to the phenolic protons.

Treatment of a toluene solution of **216** with aluminium chloride and phenol at room temperature for one hour resulted in its *de-tert*-butylation, affording an excellent yield (*i.e.* 85%) of the required starting material **212** after recrystallization of the impure material from chloroform-methanol. The loss of the *tert*-butyl groups was confirmed by the absence of the singlet at 1.26 ppm, in addition to the introduction of a doublet and a triplet at 7.16 ($J = 7.5$ Hz) and 6.83 ($J = 7.5$ Hz) ppm respectively for the aromatic protons in the ¹H-NMR spectrum. This data correlates with the literature values (*i.e.* δ 10.4 (s, 6H), 7.6 (m, 18H), 4.0 (s, 6H) ppm), thus further confirming the identity of this sample of **212**.¹⁶⁹

With access to multi-gram quantities of **212**, I was in a position to initiate its transformation *via* the Mannich reaction into **213**. One important question at this stage that required an answer was whether this reaction (*i.e.* **212** to **213**) proceeded in a chemoselective fashion (analogous to the calix[4]arene case) to afford only **213** as had been suggested before, or whether the products of

higher substitution might also be present. This analysis had been complicated somewhat previously, since the ^1H -NMR spectra of the mono-substituted calix[6]arenes (e.g. **214** and **215**) were very broad, and additionally, no mass spectrometric analyses were obtained.¹⁵⁵ I anticipated however – based on a review of the literature – that a variable temperature ^1H - or ^{13}C -NMR study of these materials should allow for a more complete characterisation by, for example, ‘freezing-out’ a particular conformation on the ^1H -NMR timescale. Indeed, Reinhoudt and co-workers have reported the successful application of variable temperature NMR to resolve the ^1H -spectra of a series of calix[6]arene derivatives.¹⁷⁰

In the first instance, I had to reproduce the Mannich reaction (*i.e.* **212** to **213**) using the conditions described previously in the Bew group. With multi-gram quantities of **212** available, I opted to perform the reaction on an identical scale (*i.e.* 3.5 mmol). I treated a suspension of calix[6]arene **212** in THF (at 0.06 M) with a slight excess of aqueous formaldehyde (1.2 eqⁿ) and aqueous dimethylamine (1.2 eqⁿ) at room temperature for two hours. Upon addition of the dimethylamine I observed the immediate dissolution of **212**, and after *ca.* 0.5 hours a precipitate started to form. Isolation of this material by suction filtration, after a further 1.5 hours’ reaction time afforded, what was presumed to be, pure **213** in a 50% yield (**Scheme 3.13**).

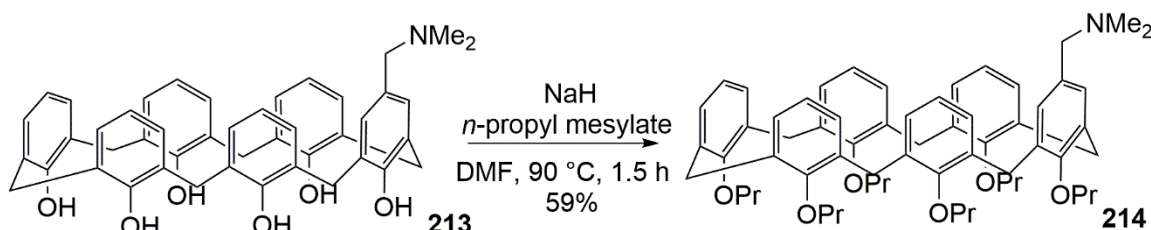


Scheme 3.13: The Mannich reaction of calix[6]arene **212** affording **213**¹⁵⁵

The low yield in this case may have been due to the incomplete consumption of starting material **212** or insufficient time available for the crystallisation of **213**. In any case, since the reaction afforded sufficient material to work with, I decided to return to the optimisation of this protocol at a later date. Unfortunately, and in accordance with previous investigations, the extremely low solubility of **213** in a wide range of organic solvents (e.g. DCM, CHCl_3 , MeOH, DMF and DMSO) prevented me from obtaining an acceptable ^1H - or ^{13}C -NMR spectrum. With no alternative options I therefore decided to proceed with the hexa-O-propylation of **213**, and then fully characterise the resulting hexa-O-propyl ether **214** since this had been reported as significantly more organic soluble than **213**.

Without attempting any purification of **213**, I decided to see if I could reproduce the synthesis of hexa-O-propyl ether **214** by treatment with sodium hydride and *n*-propyl mesylate in anhydrous

DMF. After heating the reaction mixture in a sealed vial at 90 °C for 1.5 hours under microwave irradiation, I was pleased to be able to identify a new, significantly less polar, component by TLC analysis. Purification of this mixture by aqueous extraction (to remove inorganic materials) and a subsequent filtration through silica gel (to remove unreacted **213**) afforded **214** in an unoptimised but reproducible 59% yield (**Scheme 3.14**).



Scheme 3.14: Synthesis of hexa-O-propyl ether **214**¹⁵⁵

Given the significantly improved organic solubility of **214** in a range of solvents, I was able to undertake a comprehensive characterisation by ¹H-NMR, ¹³C-NMR, FT-IR, LRMS, HRMS and melting point analysis. The ambient temperature ¹H-NMR spectrum of **214** in CDCl₃ was very broad, as I had anticipated. Switching to aromatic solvents (*i.e.* d₈-toluene and d₆-benzene) afforded slight improvements in terms of reducing the broadness of the signals; but since no fine structure could be observed even here, I decided to study the effect of varying the temperature on the ¹H-NMR spectrum. Recording the ¹H-NMR spectrum of **214** in d₈-toluene at – 20, 0, 20, 40, 60 and 80 °C I observed slight improvements in resolution. At 60 °C the most well resolved spectrum was obtained, but no fine structure could be confidently assigned. In contrast, the room temperature ¹H-NMR spectrum of **214** in d₆-benzene was the most well resolved, with either heating or cooling the sample adversely affecting the quality of the spectrum (**Figure 3.4**).

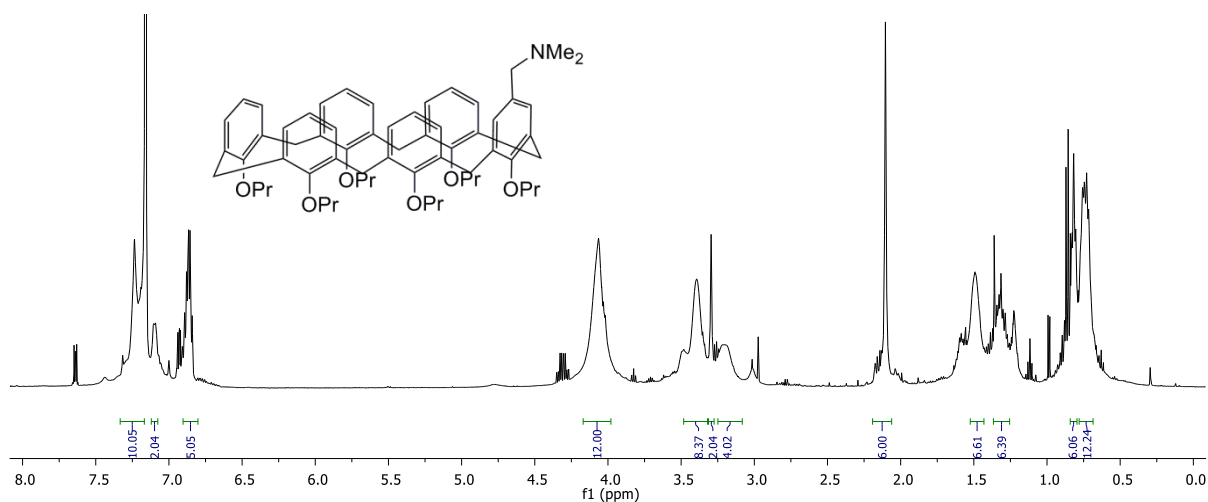


Figure 3.4: The ¹H-NMR spectrum of dimethylamino calix[6]arene **214** (500 MHz, C₆D₆)

The additional minor impurities (for example at *ca.* 7.7 and 4.3 ppm) were present in the NMR solvent, and could not be removed from it by distillation. However, these signals can be readily distinguished from those of **214** by virtue of their 'sharpness' and chemical shifts. In any case, from the integrations and peak positions, I was able to tentatively assign some of the peaks in this spectrum. For example, I assigned the singlet at 3.30 ppm to the benzylic CH_2 protons and the singlet at 2.10 ppm to the $N(CH_3)_2$ protons. These data are, as anticipated, significantly different from those reported previously for this compound in $CDCl_3$, but do seem to confirm that only type of calix[6]arene is present. Turning my attention to the ^{13}C -NMR in d_6 -benzene, resonances were observed at 63.6 and 44.8 ppm which were assigned to the benzylic carbon and the $N(CH_3)_2$ carbons respectively. Still somewhat concerned by the possibility the sample might contain products of higher substitution obscured by the broadness of the 1H -NMR spectrum (*i.e.* carried forward from the Mannich reaction), I analysed **214** by low and high resolution mass spectrometry. Thus I was pleased to only observe significant mass ions arising from **214**, with, for example, a mass ion observed at 946.5978 in the HRMS analysis which corresponds to $[M+H]^+$.

Satisfied this protocol could indeed be applied to the synthesis of a mono-substituted calix[6]arene, I proceeded with the transformation of **214** into the important chloromethyl derivative **215** using the conditions previously developed within the Bew group. Thus I treated a DCM solution of **214** with an excess of ethyl chloroformate (*i.e.* two equivalents) at room temperature for two hours and was pleased to observe the formation of a new, significantly less polar, component by TLC analysis. Purification of this material by filtration through silica gel afforded a modest, but unoptimised, 52% yield of **215**. A full physicochemical analysis of this material (as this had not been obtained previously) confirmed the formation of mono-chloro methylated **215**. In the 1H -NMR spectrum for example, the methylene CH_2Cl protons were observed as a singlet at 4.11 ppm (3.30 ppm in the starting material **214**) whilst in the ^{13}C -NMR the methylene CH_2Cl carbon was observed at 46.5 ppm (63.6 ppm in the starting material **214**). A mass ion was observed at 954.5433 in the HRMS analysis which corresponds to $[M+NH_4]^+$, thus further confirming the formation of **215** (Figure 3.5).

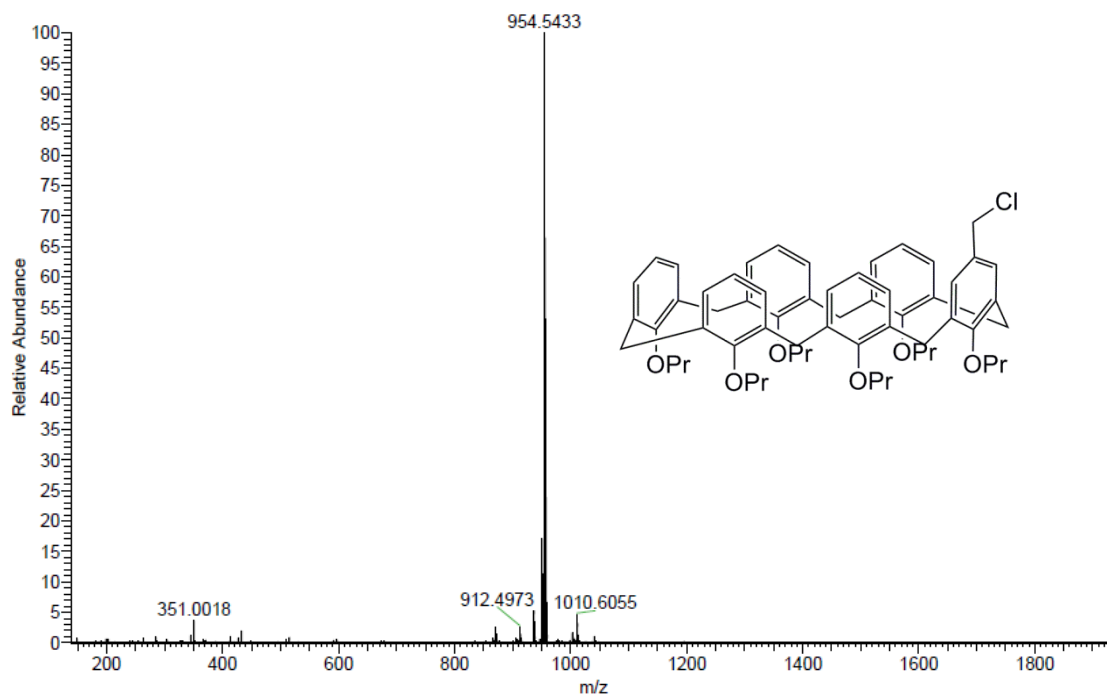
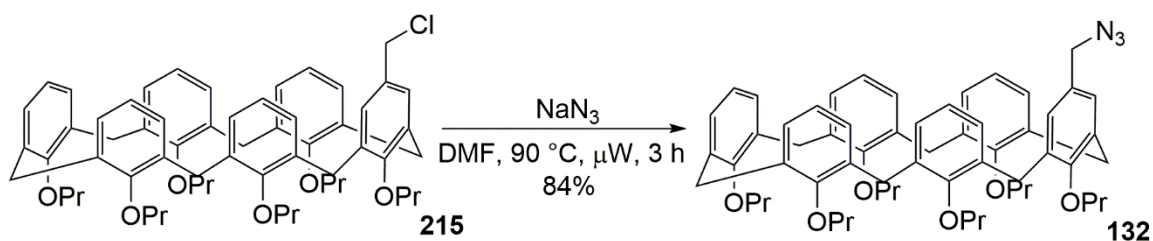


Figure 3.5: The HRMS spectrum of chloromethyl calix[6]arene **215** displaying $[M + NH_4]^+$ at 954.5433

Pleased to have reproduced the synthesis of **215**, albeit in a somewhat modest yield (*i.e.* 52%), I was in a position to attempt the final, important, step in the generation of azidomethyl calix[6]arene **132**. Thus I attempted the synthesis of **132** by heating a DMF solution of **215** with an excess of sodium azide at 90 °C for three hours under microwave irradiation (**Scheme 3.15**).

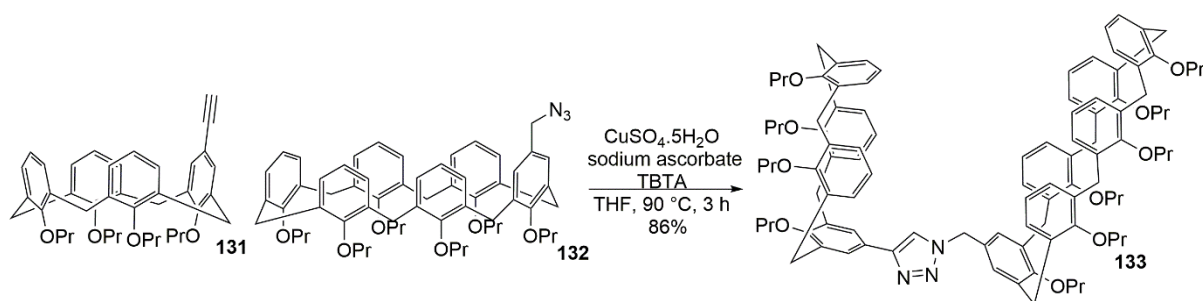


Scheme 3.15: Synthesis of azidomethyl calix[6]arene **132**¹⁵⁵

Analysis of the reaction mixture by TLC after three hours' indicated all of the starting material **215** had been consumed, and a new compound was present. Isolation of this material by liquid-liquid extraction afforded an excellent (*i.e.* 84%) yield of azidomethyl calix[6]arene **132** – the formation of which was established by a comprehensive physicochemical analysis. Although the ¹H-NMR spectrum of **132** was broad, I was confident to assign the singlet observed at 3.85 ppm to the methylene CH₂N₃ protons (4.11 ppm in the starting material **215**) since this resonance integrated to a value of two and was in a similar region to that observed for mono-azido calix[4]arene **129** (3.84 ppm). In the ¹³C-NMR spectrum, this CH₂N₃ function was observed at 54.6 ppm (46.5 ppm in the starting material **215**) strongly suggesting the anticipated S_N2 reaction had occurred. Searching for further confirmation that desired calix[6]arene **132** had indeed been formed, I looked to the FT-IR

spectrum (thin film) and was pleased to observe a strong absorption at 2094 cm^{-1} characteristic of the azide functional group. Additional evidence for the formation of **132** came *via* a HRMS analysis – a mass ion corresponding to $[\text{M}+\text{NH}_4]^+$ was observed at 961.5832.

Having synthesised and fully characterised all of the calix[6]arene derivatives that had been described previously, I was primed to study the reactivity of azidomethyl calix[6]arene **132** in CuAAC chemistry. Since I had only prepared milligram quantities of **132** in the first instance, I elected to initiate studies attempting its CuAAC reaction with a slight excess of the mono-alkyne calix[4]arene **131**, as I anticipated this would be operationally quite simple. Additionally, as the reaction conditions I had employed up to this point had been successful, I opted to use these for the synthesis of **133** (Scheme 3.16).



Scheme 3.16: Synthesis of 1,2,3-triazole-linked ‘double’ cavitand **133**

I was delighted to observe the formation of a new, significantly more polar, component by TLC analysis after one hour’ reaction time. Heating for an additional two hours at 90 °C resulted in the complete consumption of azidomethyl calix[6]arene **132**, and purification of the reaction mixture by flash column chromatography on silica gel allowed for the convenient isolation of the first example of a 1,2,3-triazole-linked [4]-[6] cavitand (*i.e.* **133**) in an excellent 86% yield. The formation of cavitand **133** was confirmed by a full physicochemical analysis, with the ^1H -NMR spectrum in particular displaying interesting features (Figure 3.6).

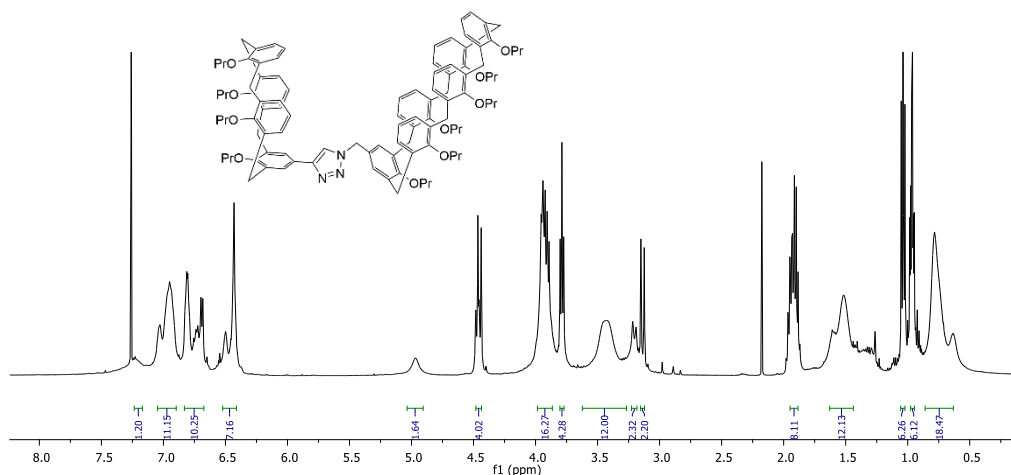
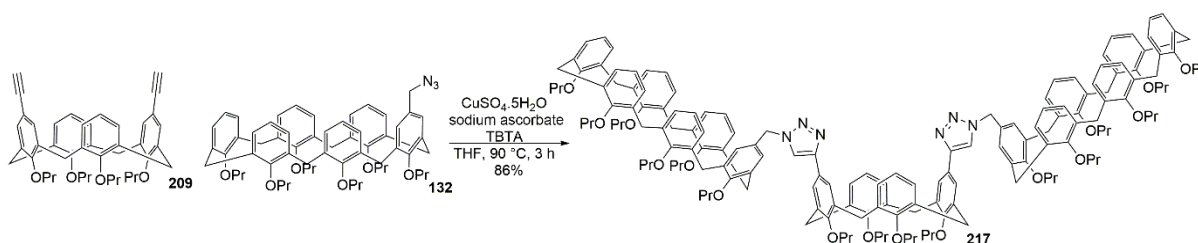


Figure 3.6: ^1H -NMR spectrum of ‘double’ cavitand **133** (500 MHz, CDCl_3)

Focusing in on the pair of doublets arising from the equatorial protons of the calix[4]arene ring (*i.e.* the signals centred at 3.1 ppm), it is evident that one set (*i.e.* at 3.20 ppm) is significantly broader than the other (*i.e.* at 3.14 ppm). A similar observation was made at the axial protons (*i.e.* those centred at 4.4 ppm), except in this case the two signals are overlapped. Presumably these broader doublets arise from the axial and equatorial protons which are proximal to the aryl moiety which carries the triazole, and by extension, the conformationally mobile calix[6]arene unit. This broadening effect is also seen for the triazole proton, which was tentatively assigned to the broad singlet observed at 7.2 ppm.

Pleased to have demonstrated the application of the azidomethyl calix[6]arene **132** for the rapid synthesis of the double [4]-[6] cavitand **133**, the next goal was to see whether it might be possible to extend this positive result to the synthesis of a triple [6]-[4]-[6] cavitand (*i.e.* **217**). Given the success with the triple cavitands **207** and **208**, I anticipated that the reaction of azidomethyl calix[6]arene **132** with *bis*-ethynyl calix[4]arene **209** would proceed readily, but was keen to establish whether any additional reaction time might be required due to the perceived steric requirements of this process. Following the course of the CuAAC reaction by TLC analysis, I was pleased to observe the complete consumption of the *bis*-ethynyl calix[4]arene **209** after a comparable (*i.e.* to **133**) three hours. Isolation of the presumed 1,2,3-triazole-linked 'triple' cavitand by column chromatography on silica gel afforded **217** in an excellent (*i.e.* 85%) yield (**Scheme 3.17**).



Scheme 3.17: Synthesis of the 1,2,3-triazole-linked 'triple' cavitand **217**

The successful formation of **217** was established by a comprehensive physicochemical analysis. In this case, the triazole protons were observed in the $^1\text{H-NMR}$ spectrum as a broad singlet at 7.35 ppm; whilst in contrast to the 'double' cavitand **133**, the axial and equatorial protons of the calix[4]arene unit was not observed to be broadened significantly by the presence of the calix[6]arene units. Searching for further confirmation of the structural assignment, I turned to the HRMS analysis of **217**; gratifyingly, a mass ion was observed at 1561.9144 which corresponds to $[\text{M}+\text{H}]^+$.

3.8 Synthesis of redox active calix[4]arenes

The synthesis of cavitands capable of undergoing predictable conformational changes under the influence of external stimuli is at the forefront of research in supramolecular chemistry.¹⁷¹ For example, in 2012 Diederich and co-workers described the design and synthesis of a so-called redox switchable ‘molecular gripper’ based on the interconversion of the ‘kite’ and ‘vase’ forms of a diquinone-based resorcin[4]arene.¹⁷² Whilst more recently, Perris and co-workers have described the design, synthesis and application of the redox-switchable tetraferrocenyl-resorcin[4]arene **218** as a host for the reversible complexation of *tetra*-alkyl ammonium salts (**Figure 3.7**).¹⁷³

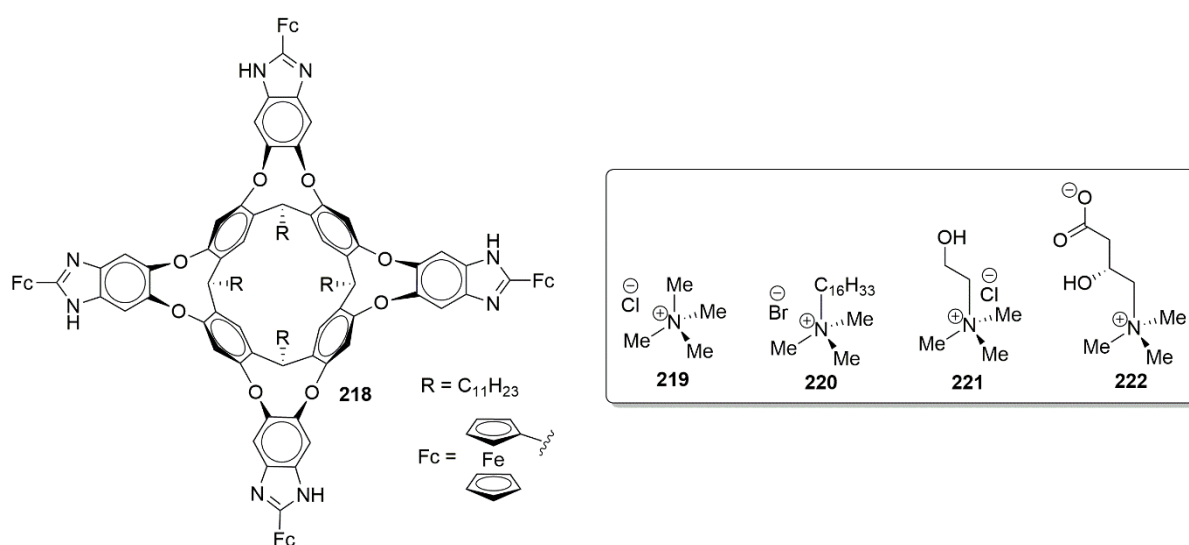
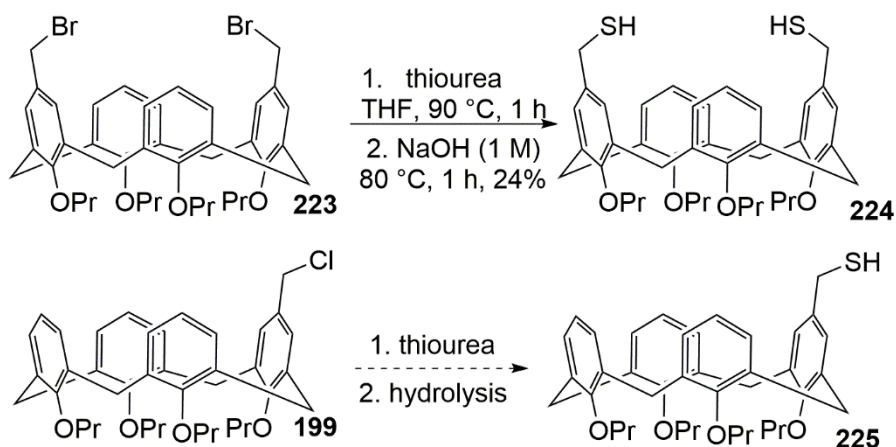


Figure 3.7: Perris’s design for a tetraferrocenyl-resorcin[4]arene based redox-active cavitand **218** and representative *tetra*-alkyl ammonium salt guests **219** to **222**¹⁷³

Studies of **218** using ¹H-NMR, electrochemical and DFT analyses indicated a pseudo-vase conformation enforced by the electrostatic repulsion of the ferrocenium moieties (*i.e.* in the oxidised form) was required for the effective complexation of the *tetra*-alkyl ammonium salt guests **219** to **222**.

With these studies in mind, I was keen to further develop this research in the calix[4]arene series. I considered a modified approach wherein linking two calix[4]arene units *via* a dynamic covalent bond (*e.g.* disulfide, imine or boronic ester) might allow for the reversible generation of a series of cavitands based on **225**. In the first instance I was particularly drawn to the potential of using a disulfide bond; since although they are typically strong (*ca.* 250 kJmol⁻¹) and form easily, they can also be readily broken by the action of a variety of reducing agents (*e.g.* sodium borohydride, dithiothreitol or electrochemically). Searching the literature for methods of introducing the thiol functionality to the upper-rim of calix[4]arenes as well as reviewing some relevant protocols recently developed within the Bew research group, several suitable protocols emerged. Although this

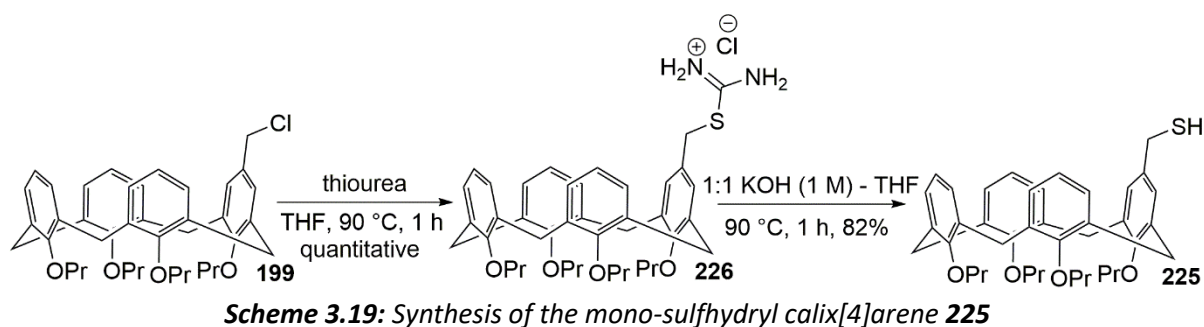
literature review indicated a number of possible methodologies, I decided instead to generate **225** via a protocol the Bew group had used previously for the synthesis of **224** which proceeds by S_N2 displacement of 1,3-bis-bromomethyl calix[4]arene **223** with thiourea and subsequent hydrolysis. Thus I anticipated **225** could be accessed similarly from **199** (Scheme 3.18).⁵³



Scheme 3.18: Synthesis of bis-sulfhydryl calix[4]arene **224** and the proposed synthesis of mono-sulfhydryl calix[4]arene **225**⁵³

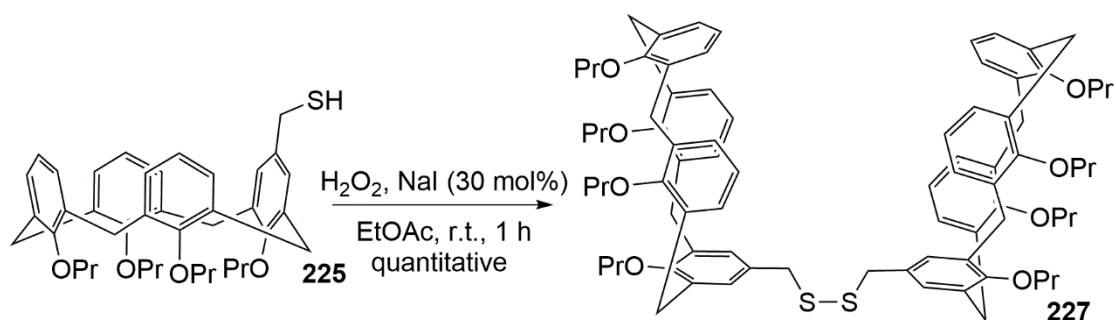
I suspected that the poor yield (*i.e.* 24%) which had been obtained previously for the synthesis of **224** was likely to be as a result of oxidation (*i.e.* to form the intramolecular disulfide or oligomers/polymers), and therefore if the hydrolysis of intermediate thiuronium salt **226** was conducted under strictly anaerobic conditions, a much improved yield should result.

Reacting chloromethylene calix[4]arene **199** with a slight excess of thiourea (*i.e.* 1.1 equivalents) in THF at 90 °C under microwave irradiation for one hour, I observed that (TLC analysis) all of the starting material **199** had been consumed. By simply removing the solvent under reduced pressure, I obtained the impure thiuronium salt **226** in a quantitative yield. The complete conversion of starting material **199** into intermediate **226** was confirmed by ¹H-NMR analysis in d₆-DMSO. Without undertaking any purification at this stage (since this would have only served to remove excess thiourea), I decided to proceed with the hydrolysis of **226**, thus generating mono-sulfhydryl calix[4]arene **225**, under strictly anaerobic conditions. To do this, I thoroughly degassed a 1:1 mixture of THF and aqueous potassium hydroxide (1M) by sparging with nitrogen for five minutes before introducing a sample of thiuronium salt **226**. Heating this mixture at 90 °C for one hour was sufficient to allow, after liquid-liquid extraction and flash column chromatography, the isolation of desired mono-sulfhydryl calix[4]arene **225** in a pleasing 82% yield (Scheme 3.19).



Concerned by the possibility that I may have, in fact, isolated the corresponding disulfide-linked cavitand **227**, a full physicochemical analysis of **225** was undertaken which established that it was the free thiol **225**. Particularly characteristic was the methylenethiol doublet ($J = 7$ Hz) observed in the $^1\text{H-NMR}$ spectrum at 3.35 ppm which arises from coupling to the SH proton. A subsequent HRMS analysis displayed a mass ion at 656.3740 which corresponds to $[\text{M}+\text{NH}_4]^+$, thus providing further evidence for the formation of the monomer **225**.

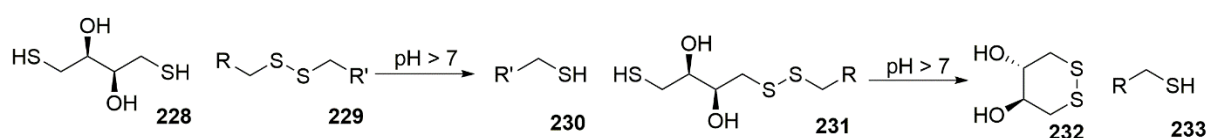
Delighted that I synthesised **225** in a good yield (*i.e.* 82%), I was keen to study its oxidation to the disulfide-linked cavitand **227**. A review of the literature indicated a number of protocols for the oxidation of thiols which might be suitable for use in this system. For example, Kirihara and co-workers have achieved this transformation (*i.e.* thiol to disulfide) for a wide range of substrates in high yields using hydrogen peroxide and a catalytic amount of sodium iodide in ethyl acetate.¹⁷⁴ Attracted to the operational simplicity of this procedure, as well as the short reaction times required (*i.e.* typically ≤ 0.5 hours) I opted to employ these conditions for the oxidation of **225**. Treating an ethyl acetate solution of the mono-sulfhydryl calix[4]arene **225** with one equivalent of hydrogen peroxide and 30 mol% sodium iodide, I isolated a quantitative yield of the corresponding disulfide-linked cavitand **227** after one hour at room temperature (**Scheme 3.20**).



The transformation of **225** into **227** by S-H oxidation was confirmed by a comprehensive physicochemical analysis. As anticipated, the methylene thiol doublet observed at 3.35 ppm in the $^1\text{H-NMR}$ spectrum of the **225** was no longer present, and instead a singlet was observed at 3.43 ppm in the $^1\text{H-NMR}$ spectrum of the product **227** arising from the equivalent methylene protons of the

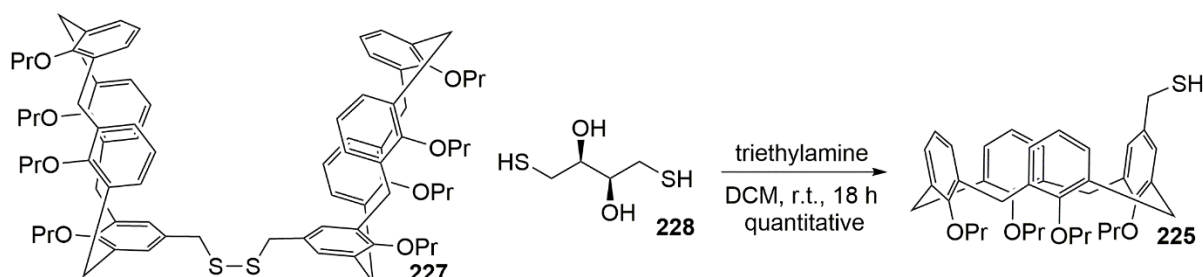
disulfide group. Thus, this doublet-singlet transition represents a convenient spectroscopic marker which I should be able to employ in demonstrating the proposed reversible nature of this cavitand formation.

Next I wanted to examine the possibility of reducing the newly formed cavitand **227** back to its monomeric units (*i.e.* to **225**) and in doing so demonstrate the reversible nature of this cavitand formation. A review of the literature indicated a number of possibilities, but since I was aware of the widespread use of dithiothreitol (Cleland's reagent) in biology to affect the reduction of cysteine-containing proteins, I was keen to consider its application in this system.¹⁷⁵ I first thought it prudent to review the mechanism of this process, to see if it might afford insight into the optimal conditions to employ for the reduction. Hofbauer and co-workers have studied this reduction in detail by Car-Parrinello molecular dynamics simulations, and have confirmed the widely accepted mechanism which proceeds *via* two sequential thiol-disulfide exchange reactions under basic conditions (**Scheme 3.21**).¹⁷⁶



Scheme 3.21: The mechanism for disulfide reduction with dithiothreitol¹⁷⁶

This reaction only proceeds under basic conditions since the thiolate form is required to participate in the thiol-disulfide exchange reaction (*i.e.* **228** and **229** into **230** and **230**), and is driven to completion by the formation of a stable six-membered ring **231** with an internal disulfide bond. A further review of the literature indicated that triethylamine would be an ideal base for this process.¹⁷⁷ Thus I opted to treat a thoroughly degassed dichloromethane solution of disulfide-linked cavitand **227** and dithiothreitol with a slight excess of triethylamine at room temperature. After stirring at room temperature overnight, a ¹H-NMR analysis of the reaction mixture indicated that **227** had been reduced completely to the monomeric **225**. Subsequent purification by column chromatography on silica gel allowed for the isolation of **225** in a quantitative yield (**Scheme 3.22**).



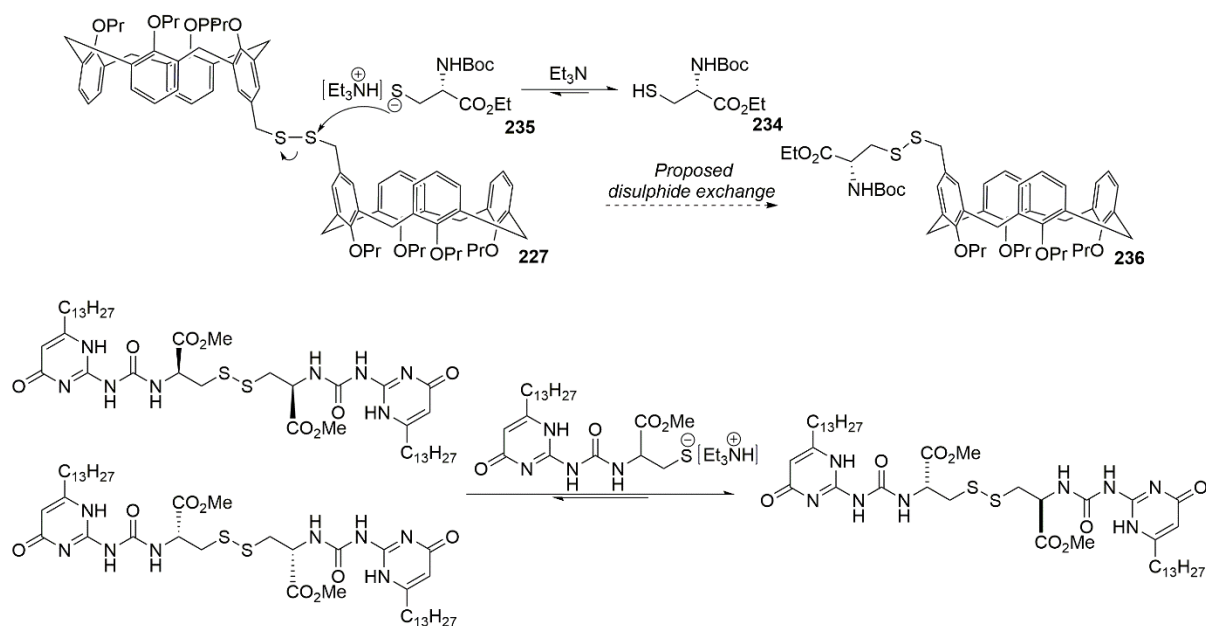
Scheme 3.22: Reduction of disulfide-linked cavitand **227** into monomeric **225** by dithiothreitol

Searching for an alternative reductant that would obviate the need for chromatography, I was also able to demonstrate the use of sodium borohydride in degassed THF. Treating **227** with excess sodium borohydride (*i.e.* 5 eqⁿ) at room temperature for two hours under nitrogen followed by liquid-liquid extraction afforded a quantitative yield of **225**.

3.9 Synthesis of peptidocalix[4]arenes via dynamic covalent chemistry

The application of dynamic covalent chemistry (DC_vC) for the construction of complex molecular architectures is proving to be a powerful methodology which is at the forefront of a number of research programs in synthetic chemistry.^{178,179} In essence, DC_vC is concerned with the use of reversible covalent reactions to assemble molecular components through equilibration to the thermodynamic minimum of a given system.¹⁸⁰ This is in contrast to the majority of 'traditional' synthetic reactions which operate under kinetic control.¹⁸¹ One such dynamic covalent interaction which has found widespread use in DC_vC is the disulfide bond (*i.e.* R-S-S-R) since it can readily undergo disulfide exchange (**Scheme 3.21**) with an appropriate thiolate nucleophile in addition to being a readily accessible functionality.

Aware of the applications of disulfide exchange chemistry for the efficient syntheses of a range of complex materials (*e.g.* macrocycles,¹⁸² capsules¹⁸³ and rotaxanes¹⁸⁴) I became interested by the possibility of employing similar methodology to the thiol/disulfide based calix[4]arenes (*i.e.* **225** and **227**) to generate otherwise inaccessible materials. As a long standing research theme within the supramolecular chemistry community (and in the Bew group) has been concerned with the development of peptide functionalised calix[4]arenes for applications in medicinal chemistry and biology, I opted to focus my initial efforts on the generation of novel peptidocalix[4]arenes through a DC_vC approach.¹ I chose to begin these studies by first proposing a disulfide exchange reaction between the disulfide-linked cavitand **227** and the thiol containing α -amino acid cysteine derivative **234** in the presence of triethylamine. It was anticipated that the use of this weak organic base would promote the formation of small quantities of the nucleophilic cysteine thiolate **235** which might then engage in disulfide exchange with **227** to afford **236**. Indeed, Meijer and co-workers have found triethylamine to act as the ideal base for the promotion of a disulfide exchange process between the stereoisomers of a bifunctional cysteine-based pyrimidinone derivative (**Scheme 3.23**).¹⁸⁵

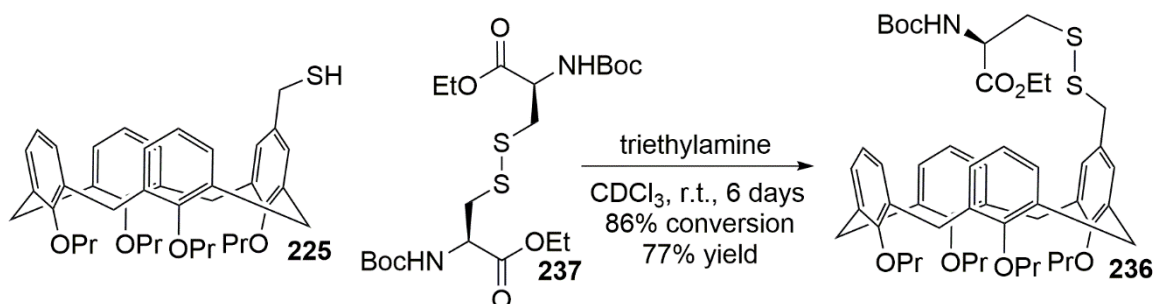


Scheme 3.23: Proposed synthesis of cysteine-calix[4]arene **236** (above) and Meijer's studies of a cysteine-based pyrimidinone (below) which both employ triethylamine promoted disulfide exchange reactions¹⁸⁵

I proposed the use of *N*-Boc ethyl ester of (*S*)-cysteine **234** for this chemistry, primarily in order to increase the organic solubility over the corresponding unprotected amino acid. This compound (*i.e.* **234**) was prepared in one step from commercially available (*S*)-cysteine ethyl ester hydrochloride in a 94% yield *via* treatment with di-*tert*-butyl dicarbonate.¹⁸⁶ With **234** in hand, I was in a position to attempt a test reaction. Selecting degassed CDCl₃ as the reaction solvent (so that I could follow the progress of the reaction by ¹H-NMR spectroscopy) I treated an equimolar solution of disulfide-linked cavitand **227** and (*S*)-cysteine derivative **234** with two equivalents of triethylamine at room temperature. Recording ¹H-NMR spectra every five hours for *ca.* six days, I was surprised to observe that no disulfide exchange had taken place – all of the starting materials remained unchanged. This was particularly puzzling when judged against the number of reports which describe the relative ease of employing cysteine containing compounds for the rapid construction of dynamic combinatorial libraries.¹⁷⁸

Still confident that the desired cysteine modified calix[4]arene **236** could be obtained *via* this type of chemistry, I thought to consider an alternative preparation wherein the proposed disulfide exchange occurs between the mono-sulfhydryl calix[4]arene **225** and the *N*-Boc (*S*)-cystine ethyl ester **237** under basic conditions. The synthesis of the required *N,C*-protected cystine **237** was readily achieved *via* a hydrogen peroxide / sodium iodide mediated oxidation of **234**, and **237** was afforded in a quantitative yield. With **237** in hand, I then attempted a test reaction under the same conditions I had employed previously. Thus I proceeded by combining an equimolar amount of mono-sulfhydryl

calix[4]arene **225** and *N*-Boc (S)-cystine ethyl ester **237** in degassed *d*-chloroform before adding two equivalents of triethylamine (**Scheme 3.24**).



Scheme 3.24: Synthesis of cysteine modified calix[4]arene **236** via disulfide exchange

Monitoring the reaction by $^1\text{H-NMR}$ spectroscopy, I was delighted to observe that approximately 8% of the desired (S)-cysteine modified calix[4]arene **236** had formed after 10 hours reaction time, in conjunction with only 2% of the unwanted cavitant **227**. After a further 40 hours' reaction time the composition of the mixture had changed to 46% of **236** and only 7% of **227**, whilst after 144 hours most of the starting materials had been consumed (< 5% remaining) and so the reaction was stopped. The separation of this mixture by flash column chromatography on silica gel allowed for the isolation of the novel cysteine modified calix[4]arene **236** in a pleasing 77% yield. A full physicochemical analysis of **236** confirmed its formation. For example, in the $^1\text{H-NMR}$ spectrum the *tert*-butyl group was observed as a singlet at 1.45 ppm whilst the benzylic CH_2 gave rise to a singlet at 3.60 ppm (**Figure 3.8**).

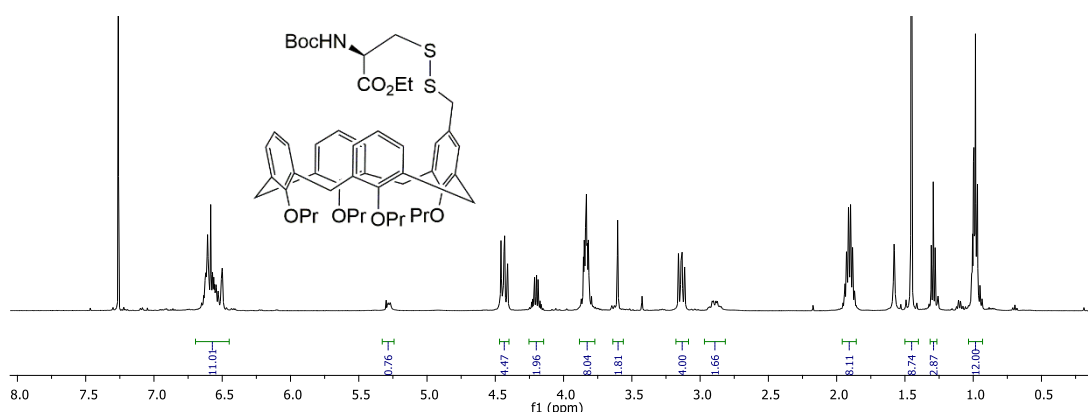
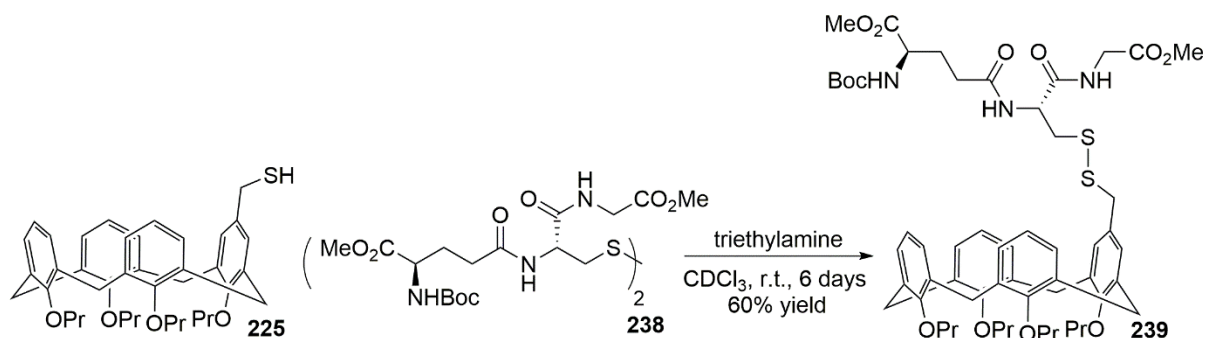


Figure 3.8: The $^1\text{H-NMR}$ spectrum of cysteine modified calix[4]arene **236** (500 MHz, CDCl_3)

Delighted by the relative ease of this synthesis, I wanted to see if it might be possible to employ this protocol for the generation of more complex, peptide functionalised, calix[4]arene. Searching for a suitable thiol containing peptide, thoughts turned to the bioactive tripeptide glutathione, which is known to act as an important antioxidant in a variety of organisms.¹⁸⁷ Similar to the previous work, I anticipated that it would be simpler to work with glutathione in a protected form, so I synthesised

the oxidised glutathione disulfide *N*-Boc methyl ester **238** via the literature procedure in three-steps from commercially available L-glutathione. With this tripeptide in hand, I would then be in a position to attempt the synthesis of peptidocalix[4]arene **239** via disulfide exchange (**Scheme 3.25**).



Scheme 3.25: Synthesis of glutathione modified calix[4]arene **239** via disulfide exchange

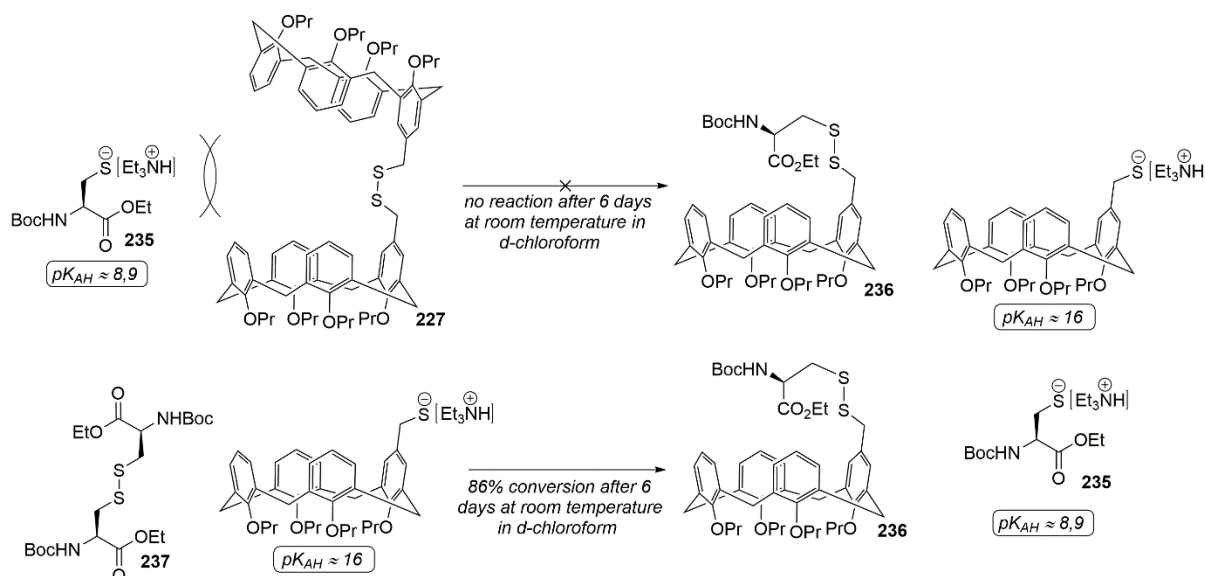
Performing the reaction under the same conditions as described for **236**, I was pleased to be able to isolate a 60% yield of the novel glutathione modified peptidocalix[4]arene **239** after purification by flash column chromatography on silica gel. In a similar way as for the synthesis of **236**, at the end of the reaction (*i.e.* after 144 hours) only a small quantity (*i.e.* 12%) of the undesired cavitand **227** was observed in the ¹H-NMR spectrum of the reaction mixture.

Delighted to have been able to synthesise these novel peptidocalix[4]arenes in high yields via disulfide exchange chemistry, and with further applications in mind, I wanted to be able to rationalise these results from a mechanistic point of view. In particular, I was interested in; a) why no disulfide exchange occurred between cysteine thiolate **235** and the homodimeric cavitand **227**, and b) why the peptidocalix[4]arenes **236** and **239** were formed in preference to the homodimeric cavitand **227**. To answer these questions, I needed to understand the factors which control the rate of thiol-disulfide interchange. A review of the literature revealed that these include; the p*K*_a's of the nucleophilic and leaving group thiols, the nature (*i.e.* size, charge) of any substituents, the solvent employed for the reaction, and the dihedral -C-S-S-C- angle.¹⁸⁸

In the case of the acidity of the thiol components, it has been reported that rate constants for thiol-disulfide interchange tend to be larger for increasing values of p*K*_a for nucleophilic thiols, and for decreasing values of p*K*_a for leaving group thiols. In order to see how this effect might be operating in this system, I needed values for the p*K*_a of each of the thiol components (*i.e.* **225** and **234**). Unfortunately, it has been reported that there are fewer than 30 thiols whose p*K*_a's have been experimentally determined (mostly due to their instability and low acidity) and these compounds were not amongst them. Instead of attempting to measure these values, I turned to the work of Hu and co-workers who have used quantum chemical (*i.e.* DFT) calculations to predict the p*K*_a's of a wide range of alkyl, amino, alkoxy and aryl thiols in DMSO.¹⁸⁹

Estimating the pK_a 's of these thiols by direct comparison to analogous structures disclosed in Hu's publication, I have predicted values of *ca.* 8-9 for cysteine **234** and *ca.* 16 for the mono-sulfhydryl calix[4]arene **225**. Using these values to compare the relative nucleophilicities of the thiolates of **234** and **225**, it can be seen that the thiolate of the mono-sulfhydryl calix[4]arene **225** is expected to be greater than that of cysteine **234**. In a similar way, it can be seen that the leaving group ability of the cysteine thiolate (pK_{aH} 8-9) is expected to be higher than that of the calix[4]arene thiolate (pK_{aH} 16). Indeed, these expectations correlate well with the observed course of events; the combination of the more nucleophilic calix[4]arene thiolate with the cystine disulfide **237** leads to a productive reaction (**Scheme 3.24**), whilst the opposite combination (**Scheme 3.23**) does not.

The outcome of these two reactions can also be rationalised by an examination of the steric effects; it seems reasonable to expect that the rate of thiol-disulfide interchange between **235** and **227** should be retarded by the presence of the two bulky calix[4]arene units about the disulfide bond in **227**. In contrast, the cystine disulfide **237** may present less of a steric impediment to the incoming thiolate nucleophile (**Scheme 3.26**).



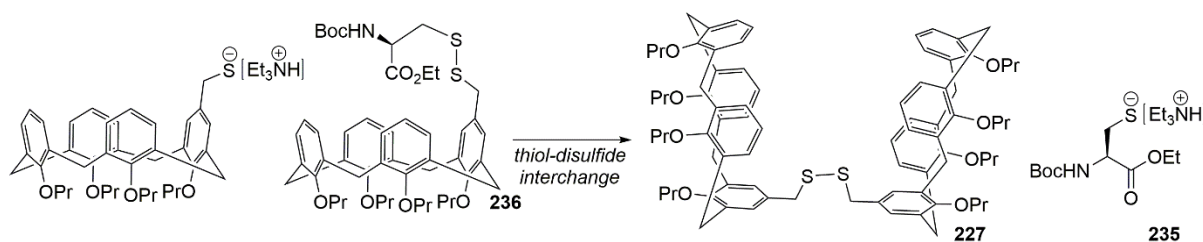
Scheme 3.26: Rationalisation of the outcome of the two thiol-disulfide interchange reactions

Satisfied that this combination of steric and electronic effects could explain the outcome of the two different reactions leading to **236**, I next wanted to be able to rationalise the production of small amounts of the homodimeric cavitand **227** (*c.a.* 10% in the reactions leading to peptidocalix[4]arenes **236** and **239**) and to understand why this compound was not produced in greater quantity.

A typical side reaction in disulfide exchange chemistry which leads to reduced yields is the formation

of disulfides *via* the oxidation of the thiol component by air.¹⁸⁸ Mindful of this fact, I had carried out all of the disulfide exchange chemistry in degassed solvents within gas tight NMR tubes, and was reasonably confident that air-oxidation could not account for the formation of small quantities of the homodimeric calix[4]arene **227**. Nevertheless, I felt it was important to rule out the possibility that advantageous oxygen might be responsible for the formation of **227**. Thus I treated a degassed solution of the mono-sulfhydryl calix[4]arene **225** in CDCl₃ with two equivalents of triethylamine, and subsequently monitored the composition of the mixture by ¹H-NMR spectroscopy over the course of four days at room temperature. I observed no trace of the homodimeric calix[4]arene **227** in the ¹H-NMR spectrum, with only unreacted starting material **225** and triethylamine present.

With this result firmly established, I was confident to propose that the small quantities of homodimeric cavitand **227** observed in the preparation of **236** and **239** had likely arisen from a thiol-disulfide interchange between the ‘mixed’ thiol product (illustrated for **236**), and the as yet unreacted mono-sulfhydryl calix[4]arene **225** (Scheme 3.27).



Scheme 3.27: Proposed thiolate-disulfide interchange pathway leading to formation of cavitand **227**

In thiol-disulfide exchange reactions with ‘mixed disulfides’ (*i.e.* such as **236**), it has been reported that their cleavage by a thiolate nucleophile typically proceeds with the release of the more acidic thiol, whilst the less acidic thiol is retained in the new mixed disulfide.¹⁹⁰ This expectation appears to correlate well with the observed course of events in this system; the more acidic thiol (*i.e.* cysteine) is released leading to the formation of **227**. However, since the opposite cleavage of the mixed disulfide by the calix[4]arene thiolate would lead to no net change, it is difficult to compare the relative rates of these two reactions.

The homodimeric cavitand **227** presumably represents a ‘thermodynamic sink’ for this system, since as has already been demonstrated, the reverse reaction (*i.e.* **227** into **226**) does not occur even after 144 hours at room temperature (Scheme 3.23). It is proposed that the explanation for the formation of only minimal quantities of cavitand **227** is kinetic in origin, and has to do with the steric demands placed on the thiol-disulfide interchange by the bulky calix[4]arene rings. Presumably then, these results – when taken together – suggest that the use of two equivalents of mono-sulfhydryl calix[4]arene **225** with one equivalent of the *N*-Boc (*S*)-cystine ethyl ester **237** would be likely to afford (after sufficient time) the homodimeric cavitand **227**, in preference to the mixed disulfide

calix[4]arene **236**. In this case, the cystine **237** might serve to ‘activate’ one half of the mono-sulfhydryl calix[4]arene **225** towards nucleophilic attack by the other.

3.10 Synthesis of orthogonally bonded supramolecular assemblies

Now that I had a good understanding of the factors involved in both CuAAC and DC_vC chemistries as applied to the calix[4]arenes, I wanted to see if it might be possible to employ both of these ‘orthogonal’ bonding approaches in the same system, to allow for the efficient construction of novel supramolecular assemblies. I was inspired in this endeavour by the work of Matile and co-workers, who have reported the use of orthogonal dynamic covalent bonds (*i.e.* disulfides and hydrazones) for the construction of orientated coaxial π -stacks (*e.g.* **240**) and their subsequent application as charge transporting pathways (**Figure 3.9**)¹⁹¹

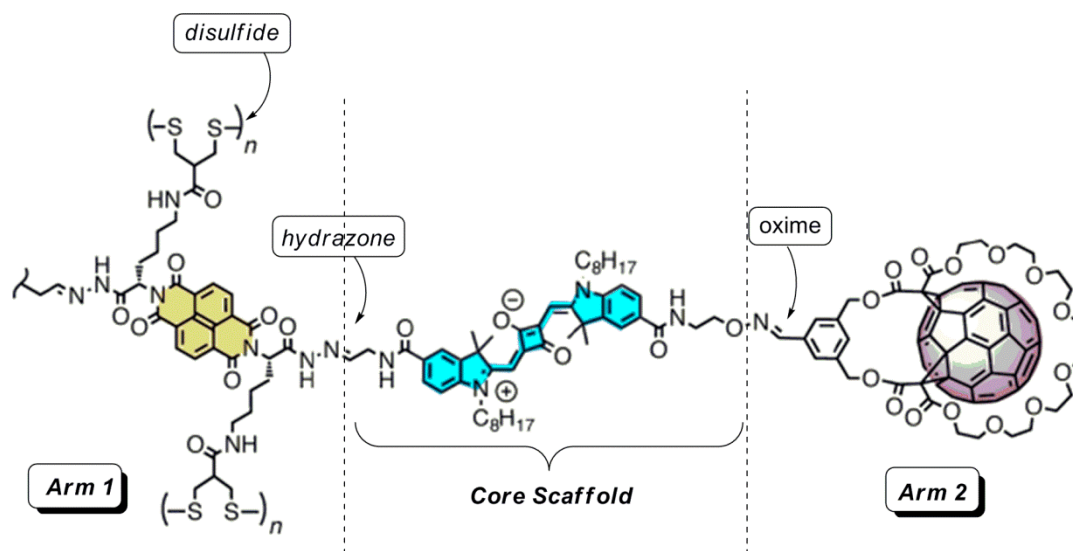


Figure 3.9: Matile’s synthesis of a complex supramolecular architecture optimised for the transportation of charge which exploits a synergistic combination of covalent (oxime), dynamic covalent (hydrazone) and redox (disulfide) chemistries¹⁹¹

Indeed, it is the exploitation of these orthogonal bonding interactions (in particular the disulfide linkages) which enable **240** to undergo the self-organising surface-initiated polymerisation required to form the coaxial π -stacks which confer the resulting assembly with its unique electrical properties. A closer examination of the structure of Matile’s compound **240** reveals that it can be considered to consist of a core scaffold functionalised at either side with two distinct ‘arms’. These arms are linked to the central core by means of either a covalent (oxime) or a dynamic covalent (hydrazone) bond. By constructing the material in this way, ‘Arm 1’ (linked by the dynamic hydrazone function) can then be readily exchanged with other units to generate a unique series of supramolecular

architectures with, presumably, modified electron transfer properties.

Inspired by the potential of this general design (*i.e.* Arm 1 – Core Scaffold – Arm 2) in combination with dynamic covalent chemistry (*i.e.* thiol-disulfide exchange) as a means of quickly accessing a range of novel supramolecular calix[4]arene arrays, I envisioned the synthesis of the first example of a redox active multicalix[4]arene array (*i.e.* **241**) (Figure 3.10).

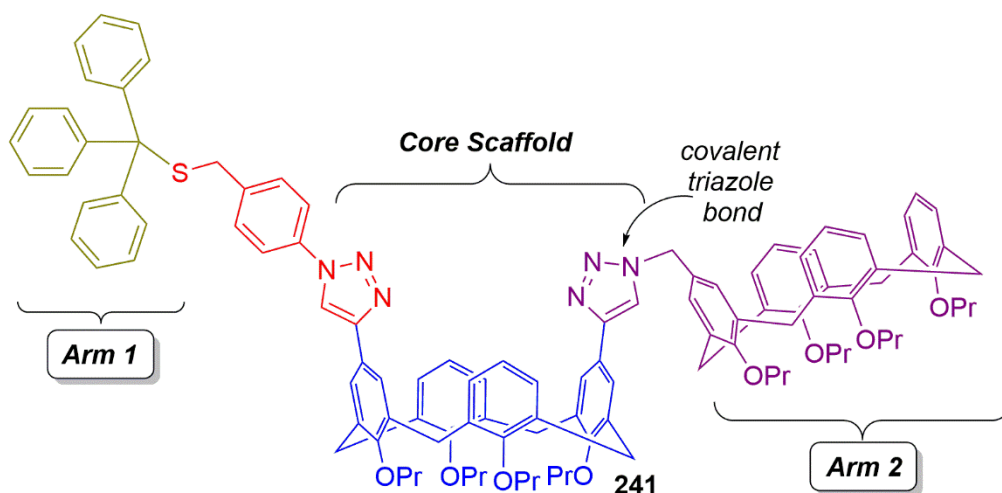
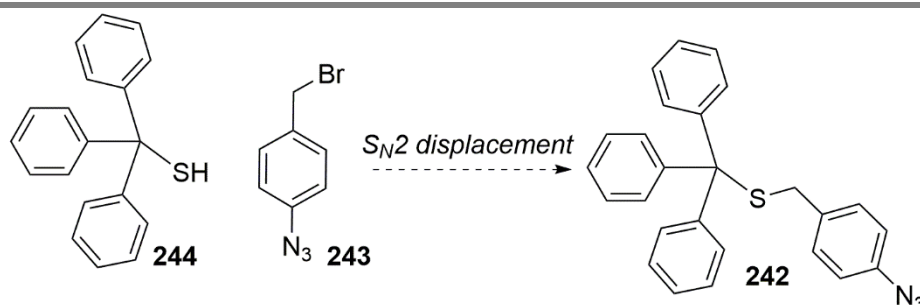


Figure 3.10: Proposed first example of a redox active multicalix[4]arene array **241**

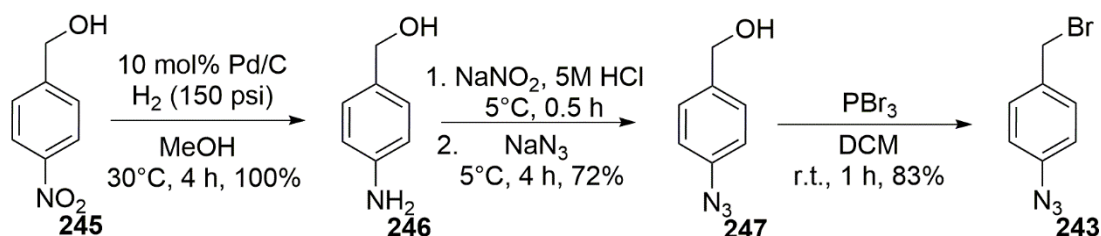
Whereas Matile and co-workers employed a squaraine dye derivative for their core scaffold, I opted for the use of an ABAC upper-rim functionalised calix[4]arene. This is a substitution pattern I anticipated could be readily generated *via* sequential CuAAC's onto the 1,3-*bis*-ethynyl calix[4]arene **209** synthesised previously. Indeed, in the previous investigations into the CuAAC chemistry of **209** with azidomethylene calix[4]arene **129** (Scheme 3.10) I had observed by TLC analysis an intermediate product which I suspected to be the product of a single addition. This result suggested the possibility of de-symmetrisation of the upper-rim of *bis*-ethynyl calix[4]arene **209** by performing two sequential CuAAC reactions with two different azides.

Considering the need to incorporate a redox active thiol within the design, whilst employing CuAAC chemistry to construct multicalix[4]arene array **241**, I proposed the synthesis of compound **242** which incorporates a trityl-protected thiol linked *via* a methylene spacer to a phenyl azide. The proposed synthesis of this compound leads back to the known 4-azidobenzyl bromide **243** and commercially available triphenylmethanethiol **244** (Scheme 3.28).



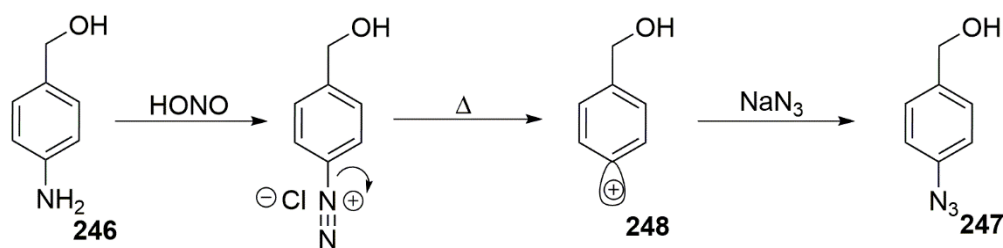
Scheme 3.28: Proposed synthesis of trityl-protected thiol **242**

A literature search for analogous bond-forming reactions with triphenylmethanethiol **244** (*i.e.* alkylation with a functionalised benzyl bromide) indicated that the use of potassium carbonate in acetone was a likely route to the synthesis of **242**.¹⁹² With this combination of reagents identified, I next needed to synthesise a sample of 4-azidobenzyl bromide **243** in order to conduct a test reaction. Opting to initiate its synthesis from 4-nitrobenzyl alcohol **245** – since this was the ‘closest’ starting material to hand – I began by reducing the nitro group of **245** to the corresponding aniline **246**. To affect this transformation, I stirred 4-nitrobenzyl alcohol **245** in methanol with 10 mol% Pd/C under hydrogen gas (150 psi) for three hours at 30 °C. This resulted in complete conversion to the desired aniline **246**, which was isolated in quantitative yield following filtration of the reaction mixture through Celite® to remove the heterogeneous catalyst (**Scheme 3.29**).



Scheme 3.29: Synthesis of 4-azidobenzyl bromide **243** from 4-nitrobenzyl alcohol **245**

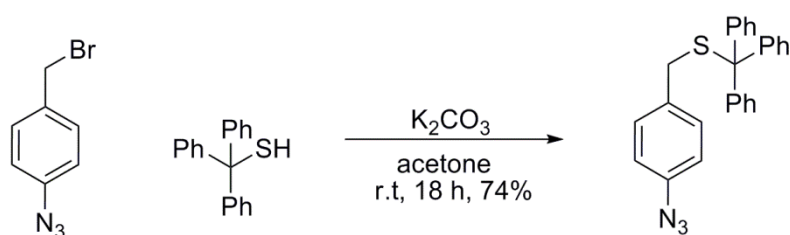
A subsequent Sandmeyer-type reaction (*i.e.* **246** to **247**) allowed for the efficient introduction of the azide functionality required for the CuAAC chemistry. The mechanism of this process is generally thought to involve diazotisation of the aniline *via* reaction with nitrous acid (formed *in situ* by the reaction of sodium nitrite with HCl) followed by loss of nitrogen gas to form an arene cation **248** which is then rapidly quenched by the azide anion (**Scheme 3.30**).¹⁹³



Scheme 3.30: Generally accepted mechanism for the reaction of aryl diazonium salts with nucleophiles (shown for N_3)¹⁹³

Performing this reaction under the conditions described by Spletstoser and co-workers, I was pleased to isolate **247** in 72% yield after flash column chromatography.¹⁹⁴ The introduction of the azide function was confirmed by FTIR spectroscopy, with the observation of a strong absorption band at 2104 cm^{-1} indicative of its presence. Finally, I needed to convert the ‘benzyl alcohol’ **247** into the corresponding ‘benzyl bromide’ **243** so that it could be coupled to triphenylmethanethiol **244** using S_N2 type chemistry. I opted to employ phosphorous tribromide in DCM for this transformation since I had previous success using this reagent, and was pleased to obtain a similarly positive result in this instance – the desired ‘benzyl bromide’ **243** was obtained in an 83% yield after one hour’ at room temperature.

With both components **243** and **244** in hand, I undertook the carbon-sulfur bond forming reaction under the conditions of Stoermer and co-workers (*i.e.* 0.2M in acetone, 1.2 equivalents of K_2CO_3).¹⁹⁵ After 18 hours at room temperature the reaction had gone to completion (as indicated by TLC analysis) and the trityl-protected thiol **242** was isolated in a 74% yield after purification by flash column chromatography on silica gel (**Scheme 3.31**).



Scheme 3.31: Synthesis of the trityl-protected thiol **242**

The identity of **242** was confirmed by a comprehensive physicochemical analysis, with, for example, a mass ion observed at 446.1087 in the HRMS analysis which corresponds to $[M+K]^+$. The mass ion at 832.3257 corresponds to $[2M+NH_4]^+$, whilst the mass ions at 243.1170 and 165.0698 presumably arise from fragmentation of the carbon-sulfur bond; the trityl group giving rise to the signal at 243.1170 corresponding to $[M]^+$ and the thiol group a signal at 165.0698 corresponding to $[M+H]^+$ (**Figure 3.11**).

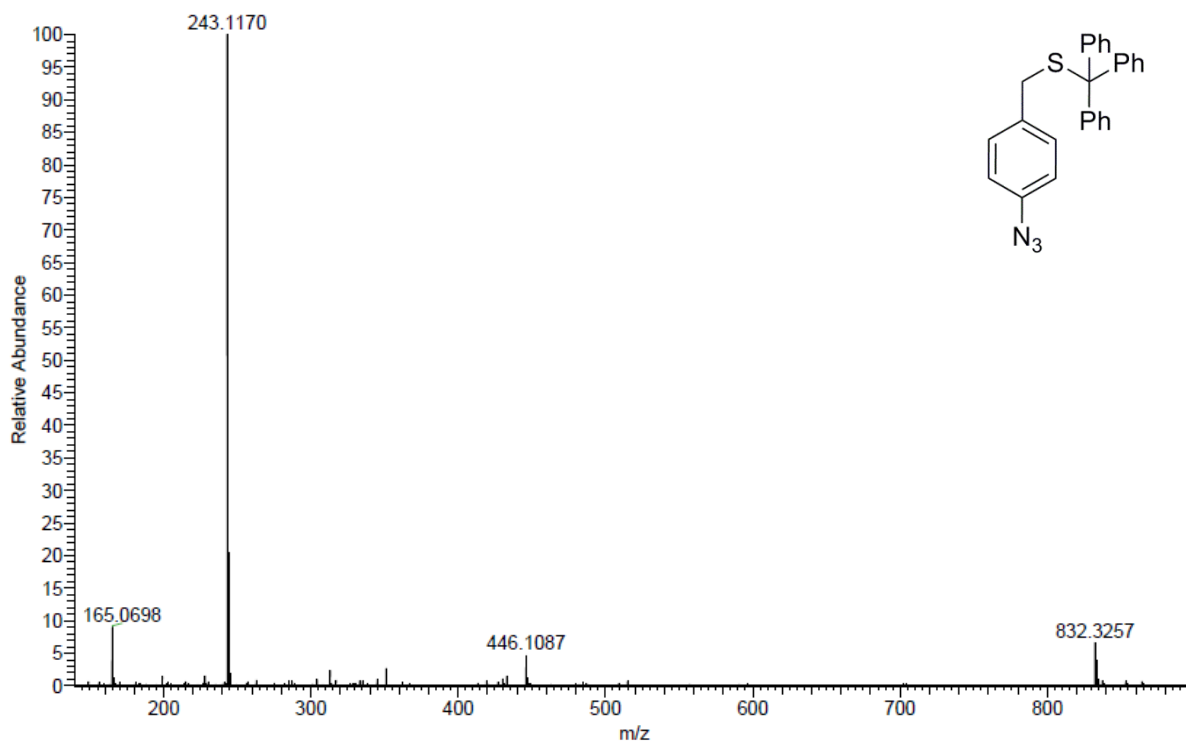
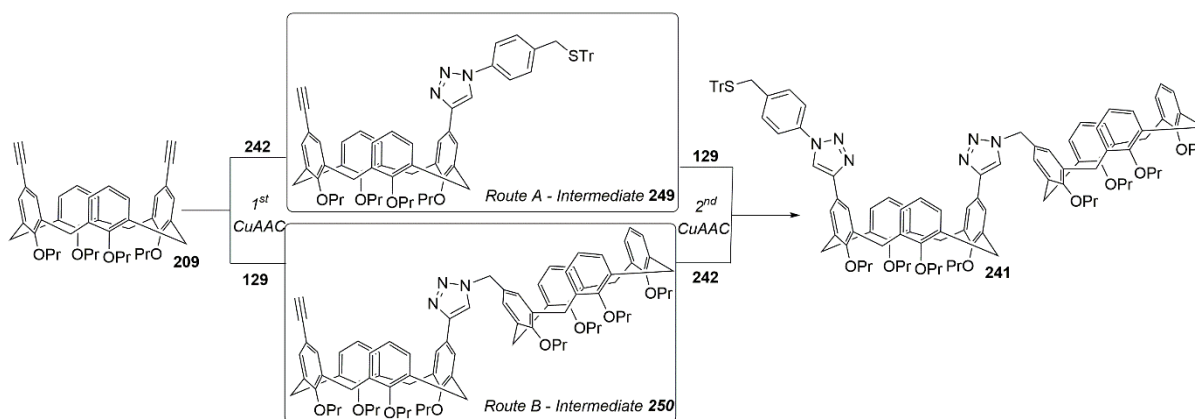


Figure 3.11: HRMS of trityl-protected thiol **242** showing mass ions at 165.0698, 243.1170, 446.1087 and 832.3257

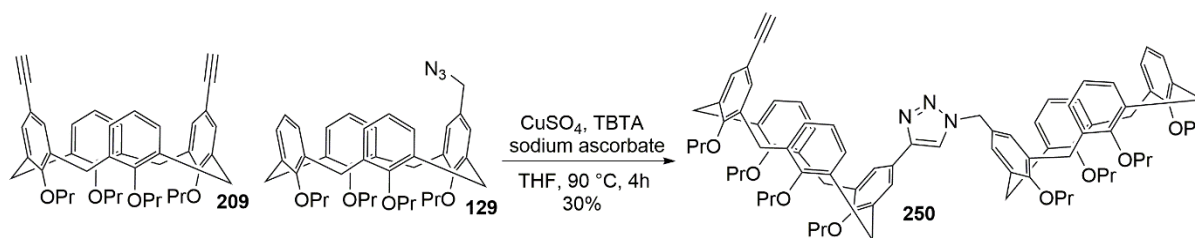
Satisfied that I had now established a reliable route towards the required ‘building blocks’ (*i.e.* **242**, **209** and **129**) I was in a position to begin the assembly of the first generation redox-active multicalix[4]arene array **241** via two different CuAAC reactions onto the 1,3-*bis*-ethynyl calix[4]arene scaffold **209**. Before proceeding I needed to consider which of the two azides (*i.e.* **242** or **209**) to employ first (**Scheme 3.32**).



Scheme 3.32: Two possible routes towards the desired multicalix[4]arene array **241**

I suspected that the ‘order of addition’ would largely depend on the ease of separating the resulting mixtures. It was anticipated that Route A might be preferable, since in my previous experience of this reaction (*i.e.* to form the triple calix[4]arene **208**) I had observed an easily separable, intermediate product, (by TLC analysis) that I suspected might correspond to the product of a *single*

CuAAC. Since I had no experience with the corresponding reaction (Route B – first step), I decided to begin by attempting the isolation of compound **250**. In order to promote the formation of **250**, equimolar quantities of *bis*-ethynyl calix[4]arene **209** and *mono*-azide calix[4]arene **129** were reacted under the conditions used previously for these CuAAC couplings (*i.e.* 10 mol% CuSO₄, 10 mol% sodium ascorbate, 20 mol% TBTA in tetrahydrofuran) (**Scheme 3.33**).

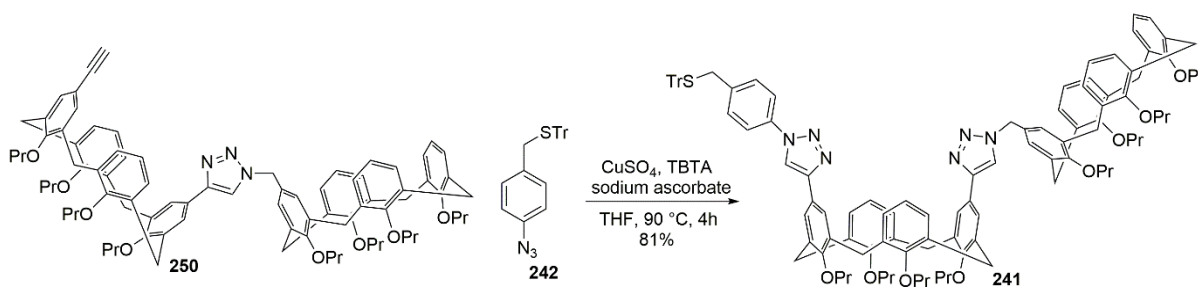


Scheme 3.33: The CuAAC reaction leading to the mono-substituted bis-calix[4]arene **250**

After four hours' reaction time, I was pleased to identify two new components by TLC analysis (in addition to unreacted **209**). Isolation of these by column chromatography and subsequent physicochemical analysis revealed the more polar component to be the triple calix[4]arene **208** which I had isolated previously, with, to some delight, the less polar component being the desired mono-substituted *bis*-calix[4]arene **250**. The presence of the single unreacted alkyne function was confirmed, in part, by ¹H- and ¹³C-NMR spectroscopy. In the ¹H-NMR spectrum of **250** a singlet was observed at 2.80 ppm which I have assigned to the alkyne CH proton, whilst in the ¹³C-NMR spectrum of **250** resonances observed at 84.4 and 77.1 ppm have been assigned to the internal and terminal alkynyl carbon atoms respectively.

I was reasonably satisfied with the apparently low isolated yield for this reaction (*i.e.* 30%) since the unreacted starting materials (*i.e.* **209** and **129**) could be readily isolated and recycled, in addition to the 'triple' calix[4]arene **208** by-product being a valuable compound in itself for complexation studies. On scaling this reaction up from 0.1 mmol to 0.3 mmol of each component, a comparable 31% isolated yield of **250** was obtained, thus illustrating the high reproducibility of this procedure.

Confident now in my ability to generate compound **250** in significant quantities (*i.e.* 130 mg), I looked towards its CuAAC coupling with the 'bespoke' trityl-protected azide **242**. To ensure the highest possible yield of multicalix[4]arene array **241**, I opted to use an excess of **242** in order to drive the reaction to completion (*i.e.* 1.5 equivalents). Performing the reaction under the standard CuAAC conditions allowed for the generation of **241** in a high 81% yield following isolation by flash column chromatography (**Scheme 3.34**).



Scheme 3.34: Synthesis of the multicalix[4]arene array **241**

For future applications of **241** it was clearly important to ensure that I had indeed isolated the expected trityl-protected compound, and not (for example) the free thiol **251** or the corresponding disulfide **252** (Scheme 3.35). For confirmation of this, I looked closely at the $^1\text{H-NMR}$ spectrum of **241** to ensure that all of the structural elements were present (Figure 3.12).

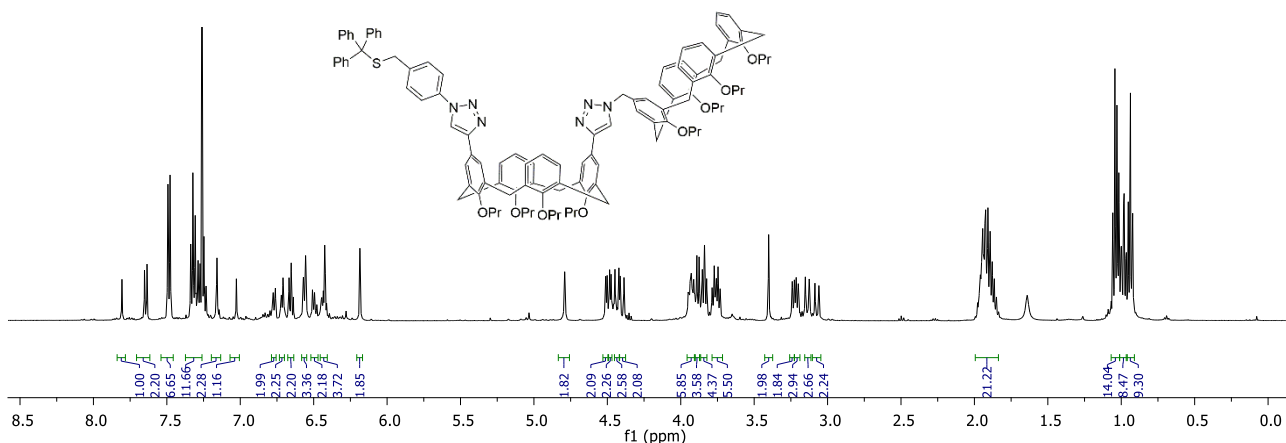
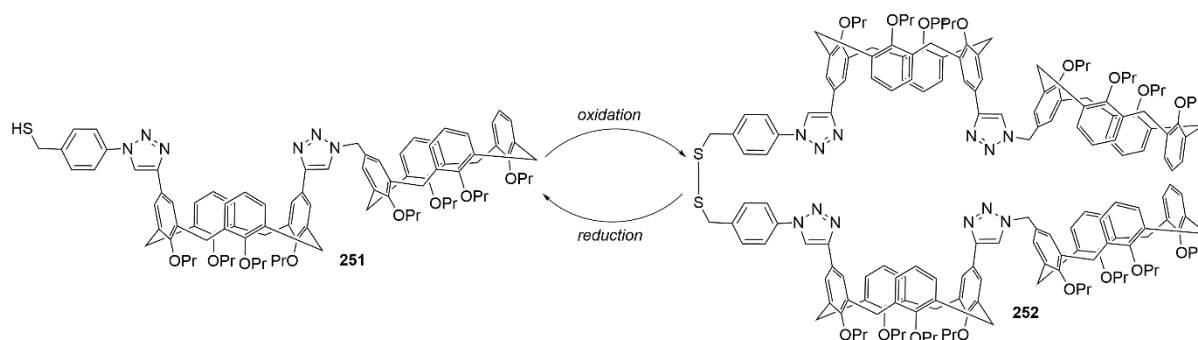


Figure 3.12: $^1\text{H-NMR}$ spectrum of the multicalix[4]arene array **241** (500 MHz, CDCl_3)

Whilst the $^1\text{H-NMR}$ spectrum of **241** is fairly complex, many of the signals can be assigned with some confidence from their chemical shift, integration and splitting patterns. Thus the singlets at 7.81 and 7.03 ppm which both integrate to one proton can be assigned to the triazole protons, with the lower field singlet presumably arising from the triazole ring carrying the trityl-protected thiol. The singlets at 4.79 and 3.40 ppm can be assigned to benzylic CH_2 's from the CH_2 -calix[4]arene and CH_2S -trityl protons respectively, whilst the presence of the trityl group is clearly indicated by the multiplets at 7.48, 7.32 and 7.24 ppm. Searching for further confirmation of the identity of **241** I looked towards its high resolution mass spectrum, and was pleased to observe a mass ion at 1696.8805 which corresponds to $[\text{M}+\text{H}]^+$.

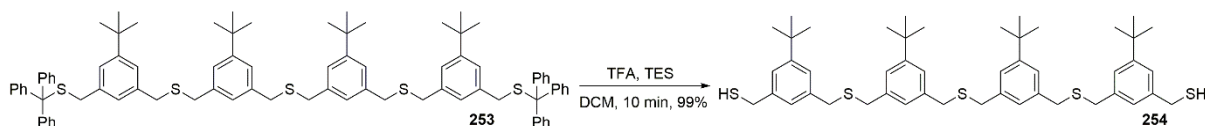
Confident that I had, in fact, isolated the desired multicalix[4]arene array **241** I was keen to investigate its redox properties. A number of experiments were envisioned based on the early investigations with **255** (Sections 3.8 and 3.9) which might afford insight into its versatile reactivity *via* the trityl-protected thiol **241**, and the corresponding unprotected thiol **251**. For example, I was

interested to see whether **241** or **251** would undergo the same kind of disulfide exchange chemistry that had been observed with **225** previously, or whether the pKa of **251** might disfavour these exchange processes. I was also interested to see if I could demonstrate the corresponding type of reversible cavitand formation with the unprotected thiol **251** as had been seen for the thiol calix[4]arene **225** (Section 3.8), thereby extending this ‘redox-switch’ approach into the multicalix[4]arene series for the first time (Scheme 3.35).



Scheme 3.35: Proposed extension of the ‘redox-switch’ approach to the multicalix[4]arene series using free thiol **251**

Suspecting that this second line of enquiry (*i.e.* the ‘redox switch’ to convert between **251** and **252**) would be synthetically less demanding, I opted to examine this process first. To access free thiol **251** from trityl-protected **241** I conducted a search of the literature to identify suitable conditions. Mayor and co-workers have reported the use of trifluoroacetic acid-triethylsilane for the unmasking of protected sulfide oligomers (*i.e.* **253** to **254**); compounds which later found application as the components of ‘carpet-like’ mono-layers on a gold (111) substrate (Scheme 3.36).¹⁹⁶



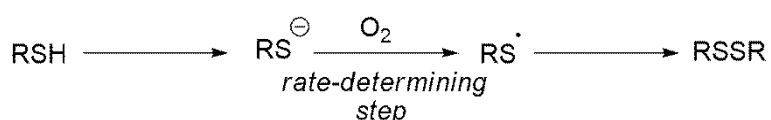
Scheme 3.36: Mayor’s use of a TFA-triethylsilane mediated deprotection to prepare oligomer **254**¹⁹⁶

The reaction of **253** with an excess of trifluoroacetic acid-triethylsilane in degassed DCM to afford **254** (and two equivalents of triphenylmethane by-product) was reported to proceed in near quantitative yield (*i.e.* 99%) and require only 10 minutes at room temperature. Encouraged by this report, and numerous others operating on a diverse range of substrates, I decided to employ these conditions in my system.

Wishing to avoid the possibility that aerial oxidation of **251** might lead to the isolation of disulfide **252**, I opted to thoroughly degas the reaction solvent (dichloromethane) using the freeze-pump-thaw method (3-cycles) before using this to carry out the deprotection (*i.e.* **241** to **251**) under an atmosphere of argon. The progress of the reaction was easily monitored by TLC analysis due to the

marked difference in polarity between **241** and **251**, and the desired product was isolated by column chromatography in a 49% yield. This modest yield was due to the low stability of **251** towards aerial oxidation, and indeed the disulfide **252** was also obtained in a 23% yield from this reaction. This susceptibility towards oxidation was also noted when attempting to record the ^1H - and ^{13}C -NMR spectra of **251**. Initially I attempted to record the ^1H -NMR spectrum of **251** under air, but a mixture of **251** and **252** was observed in the spectrum. Discarding this sample and switching to a gas-tight NMR tube with degassed CDCl_3 allowed satisfactory spectra of **251** to be obtained, thus confirming the suspicion that **251** was being rapidly oxidised in solution. A full physicochemical analysis confirmed the formation of **251** with, for example, a mass ion observed at 1476.8 which corresponds to $[\text{M}+\text{Na}]^+$ in the MALDI spectrum.

For future applications of multicalix[4]arene thiol **251** as a redox switchable cavitand, it was clearly important to understand this marked difference in reactivity towards advantageous oxygen when compared to the mono-thiol calix[4]arene **225** (which was shown to be stable for 1 week in CDCl_3 under air – **Section 3.8**). A first thought was to consider the relative acidities of **251** and **225** as a means of rationalising this behaviour. It was initially presumed that the rapid rate of oxidation observed for compound **251** was an indication of its greater acidity, as the thiolate anion required for this process would be present in a higher concentration. However this is not necessarily correct, since it has been experimentally determined that the rate determining step in such oxidations is the electron transfer from the thiolate anion to the oxygen atom, and not the initial ionic dissociation (**Equation 3.1**).¹⁹⁷ Thus this oxidation should favour the less acidic, more electron rich, thiols and may suggest that mono-calix[4]arene **225** is more acidic than the multicalix[4]arene **251**.



Equation 3.1: General equation for the oxidation of thiols ($R = \text{aryl or alkyl}$) by molecular oxygen¹⁹⁷

With experimental evidence to suggest that the disulfide-linked multicalix[4]arene **252** was the preferred form (under air) in this redox-switchable cavitand system, I was interested to see whether the reduction (*i.e.* **252** to **251**) could be performed as readily using dithiothreitol (as had been observed previously for disulfide-linked cavitand **227**). To answer this question, I first needed to oxidise all of compound **251** to **252** such that I had sufficient material to work with. Employing the reaction conditions previously used for the conversion of **225** into **227** (*i.e.* H_2O_2 and NaI in ethyl acetate, **Scheme 3.20**) afforded the disulfide-linked cavitand **252** in 79% isolated yield after 1 hour' reaction time. A full physicochemical analysis of this material indicated the oxidation had proceeded as expected. In the ^1H -NMR spectrum of **252** for example, the $\text{CH}_2\text{S-SCH}_2$ protons appear as a

characteristic singlet at 3.70 ppm (although somewhat obscured by the $-OCH_2-$ groups of the propyl chains) (**Figure 3.13**).

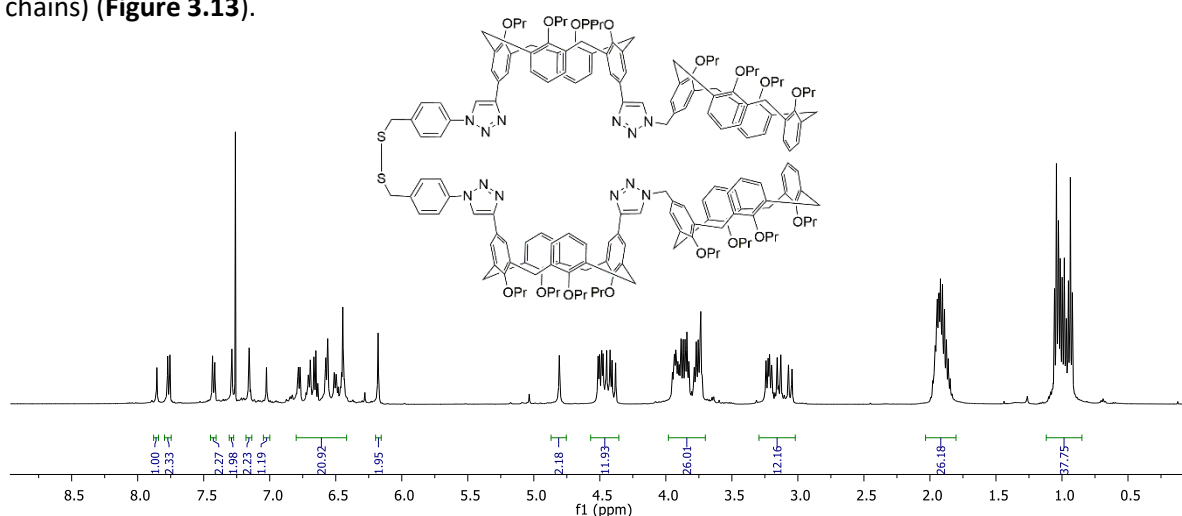


Figure 3.13: $^1\text{H-NMR}$ spectrum of the multicalix[4]arene disulfide **252** (500 MHz, CDCl_3)

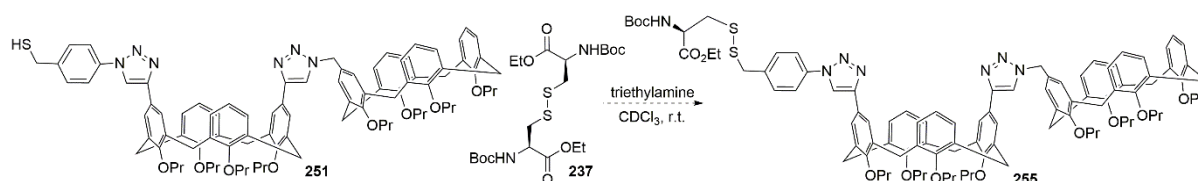
Satisfied that the $^1\text{H-NMR}$ spectrum corresponded to **252**, I looked towards mass spectrometry for further confirmation. In the HRMS analysis of **252**, a mass ion was observed at 1453.7676 for the doubly charged $[\text{M}+2\text{H}]^+$ species, whilst in the MALDI MS analysis, a mass ion corresponding to the sodiated species $[\text{M}+\text{Na}]^+$ was observed at 2928.2 thus providing further evidence to support this structural assignment.

I was delighted by the simplicity of the synthetic protocol furnishing **252**, and the fair overall yield obtained (*i.e.* 10% from **209** without taking in to account recovered starting materials) considering the complexity of **252**. Furthermore, since this synthesis was carried out on a milligram scale, the yield might be expected to improve if the process were to be scaled up.

With a sufficient quantity of multicalix[4]arene disulfide **252** in hand, I wanted to test its reduction using dithiothreitol **228** to afford the multicalix[4]arene thiol **251**; thereby completing the redox cycle (**Scheme 3.35**). I opted to do this by employing the same reaction conditions used previously for the reduction of disulfide-linked cavitanol **227** (**Scheme 3.22**) since these had performed well in that system. Thus I treated a degassed CDCl_3 solution of **252** with dithiothreitol **228** (1 eqⁿ) and a slight excess of triethylamine (1.2 eqⁿ) at room temperature for 18 hours. Analysis of an aliquot of this mixture by $^1\text{H-NMR}$ spectroscopy indicated complete conversion to multicalix[4]arene thiol **251**. However, subsequent purification by flash column chromatography (using degassed eluents) still afforded *ca.* 17% of the multicalix[4]arene disulfide **252** in addition to the desired multicalix[4]arene thiol **251** in a 65% yield; presumably sufficient oxygen was available at some stage during purification to affect this transformation. In any case, I was pleased to have been able to extend the 'redox switch' approach to this system (*i.e.* $\text{251} \leftrightarrow \text{252}$) even taking into account the practical

difficulties experienced with isolation of multicalix[4]arene thiol **251**.

Moving forward, I was keen to extend these studies with multicalix[4]arene thiol **251** to include its dynamic covalent chemistry with disulfides such as *N*-Boc cystine ethyl ester **237**. This was important to understand how the disparate reactivity of **251** (when compared against mono-thiol calix[4]arene **225**) would affect the outcome of such disulfide exchange processes. To examine this, I decided to repeat the disulfide exchange experiment affording **236** under identical conditions as had been used previously (Scheme 3.24) except in this case, employing multicalix[4]arene thiol **251** in place of mono-thiol calix[4]arene **225** (Scheme 3.37).



Scheme 3.37: Attempted disulfide exchange reaction between **251** and **237**

Performing the reaction in a gas tight NMR tube using degassed CDCl_3 under argon, I opted to employ $^1\text{H-NMR}$ spectroscopy to monitor the product distribution over time. After two hours at room temperature, I detected none of the desired peptidocalix[4]arene **255** by $^1\text{H-NMR}$ and instead observed complete conversion of thiol **251** into multicalix[4]arene disulfide **252**. The spectrum also indicated that cystine **237** had remained unchanged. This result was somewhat disappointing and may simply have arisen from aerial oxidation of **251** through inefficient degassing of the solvent. With only minimal amounts of material remaining, it was impractical to perform a subsequent reduction of **237** and repeat this experiment under modified conditions (*e.g.* using the freeze-pump-thaw method to degas the solvent).

3.11 Conclusions and outlook

In this chapter I have demonstrated how the application of modern (*i.e.* CuAAC chemistry) and cutting edge (*i.e.* DCvC) synthetic technologies to a small set of readily accessible calix[4] and [6]-arene ‘building blocks’ (**129**, **131**, **132**) has allowed for the rapid construction of a new family of redox-switchable multicalix[*n*]arene receptors. Based on my reading of the literature, it is proposed that that these receptors will have the potential to bind suitable guests with differing affinity between reduced and oxidised forms, and that this valuable property should open the way for their application and study in a wide range of nanoscale devices. Of particular interest might be the application of light or electrochemical stimuli to drive these redox reactions, since both obviate the need for additional reagents and would presumably allow a greater number of redox cycles to be performed before the material is lost or degraded.

In Section 3.9 of this chapter, I succeeded in demonstrating the dual utility of the mono-sulphydryl calix[4]arene **225** through the application of dynamic covalent chemistry for the synthesis of some structurally unusual peptidocalix[4]arenes. This work represents the first application of DC_vC to the calix[4]arenes, and should open the way for the synthesis and study of a new family of redox-active calix[4]arenes. For example, the highly functionalised mycothiol derived **256** and the γ -glutamylcysteine derived **257** might represent two interesting additional members (**Figure 3.14**).

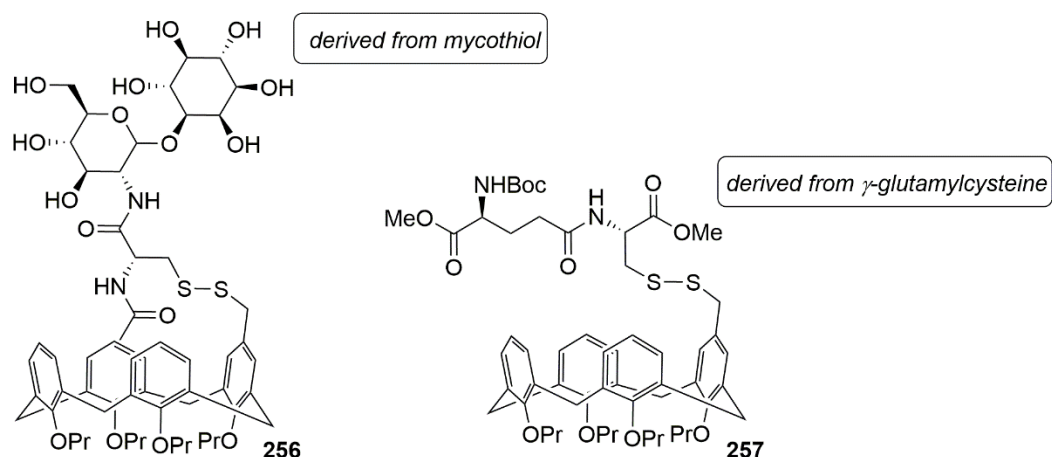


Figure 3.14: Redox-active calix[4]arenes which might be obtained via a DC_vC approach; **256** is derived from mycothiol and **257** from γ -glutamylcysteine.

Such compounds, obtained *via* a DC_vC approach, represent valuable targets as hosts for small organic molecules (for example the amino acids) due to the range of functional groups and chirality that could be readily installed. Indeed, a number of studies in the literature have focused on the application of peptidocalix[4]arenes as hosts for chiral molecules; some which operate with high stereoselectivity.¹⁹⁸ Taken together, these results hint at the possibility of performing the reversible binding of chiral molecules using redox-active peptidocalix[4]arenes (**Figure 3.15**).

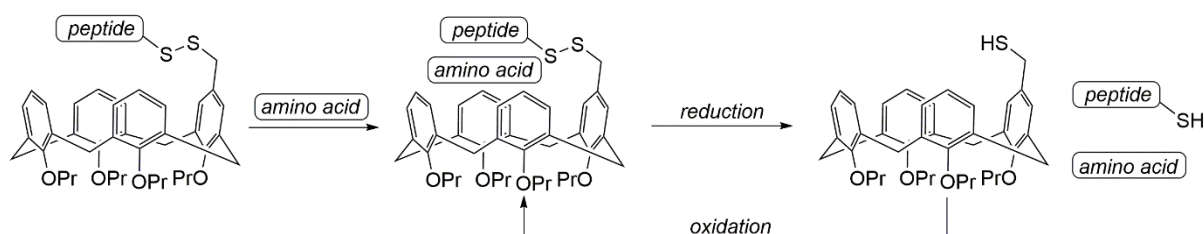


Figure 3.15: Reversible binding of chiral molecules as a possible future application of redox-active calix[4]arenes

Such a system might allow for the stereoselective binding and separation of chiral molecules – a research aim which has generated much interest in the calix[4]arene chemistry literature of late.¹⁹⁹ Indeed, many similar studies have been reported using cyclodextrins,²⁰⁰ crown ethers²⁰¹ and macrocyclic pseudo-peptides²⁰², thus highlighting the importance of this area to supramolecular

chemistry.

In the final section of this chapter, it was demonstrated how the combination of CuAAC and DC_vC to the same calix[4]arene scaffold could be used to access structurally unusual, redox active, multicalixarenes (**241**, **251** and **252**). The use of H₂O₂/NaI and dithiothreitol/TEA were then shown to be excellent reagent systems for the efficient conversion between thiol **251** and disulfide **252**; notwithstanding the practical difficulties encountered in isolation of thiol **251**.

Although I was unable to fully explore the redox chemistry of the multicalix[4]arene **251** with respect to forming the corresponding mixed disulfides with cysteine or glutathione, I am confident that further experimentation will allow these important compounds to be obtained, and ultimately, their host-guest properties to be studied.

Chapter 4: Results and Discussion

Synthesis and Physical Properties of Calix[4]arene- Based Dipole-Dipole NLOphores

4.1 Abstract

Synthetic methods for the production of second generation nonlinear optical (NLO) responsive chromophores ('NLOphores') based on upper-rim ABCC and ABCD functionalised calix[4]arenes are described. This chapter describes the synthesis of a new class of 'solvent switchable' NLOphore calix[4]arenes *via* a protocol previously optimised in the Bew group for the generation of inherently chiral, upper-rim functionalised, ABCD calix[4]arenes.¹ The key features of this protocol, which incorporates an intramolecular Cannizzaro reaction of upper-rim di-formyl functionalised calix[4]arenes as the central transformation, are discussed. Finally, preliminary physicochemical studies of these materials made using variable temperature ¹H-NMR spectroscopy, and, in collaboration with Professor Verbiest's research group, second-harmonic generation spectroscopy, are presented.

4.2 Methodology

The aim of this project was to develop a new class of 'switchable' calix[4]arene-based NLOphores which operate through a conformational response to changes in solvent polarity (**Section 1.7**). More simply stated, the aim was to develop a material where the NLO response to light could be turned 'on' or 'off' (or at least modulated) as desired. It was proposed that this could be achieved through the use of ABCB functionalised calix[4]arenes such as **260** and **261** which feature opposing CH₂OH and COOH groups at the upper-rim; calix[4]arenes which could, in turn, be accessed *via* an intramolecular Cannizzaro reaction optimised previously within the Bew group (**Figure 4.1**).

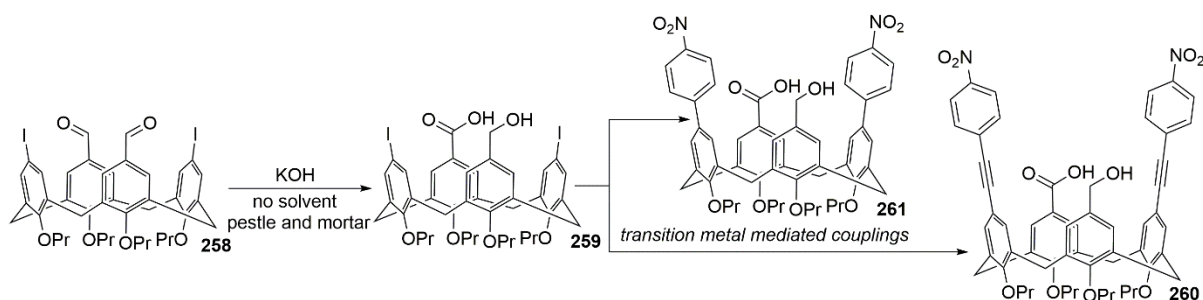


Figure 4.1: General synthetic scheme for the synthesis of proposed NLOphores **260** and **261**

The key interaction I hoped to exploit for the 'switch' was the hydrogen bonding arrangement observed between the CH₂OH and COOH groups of **259** *via* X-ray crystallography; this results in **259** adopting a pinched cone conformation which splays the aryl iodide rings (B and B) away from each other. It was anticipated that by installing (donor)-(π)-(acceptor) units at these positions *via* transition metal mediated couplings, a change in solvent polarity should favour one pinched cone conformation over the other, and therefore result in a different angle between the two opposing

(donor)-(π)-(acceptor) units. This change in opening angle would then affect the overall dipole moment of the molecule, and as a result, its NLO properties (**Figure 4.2**).

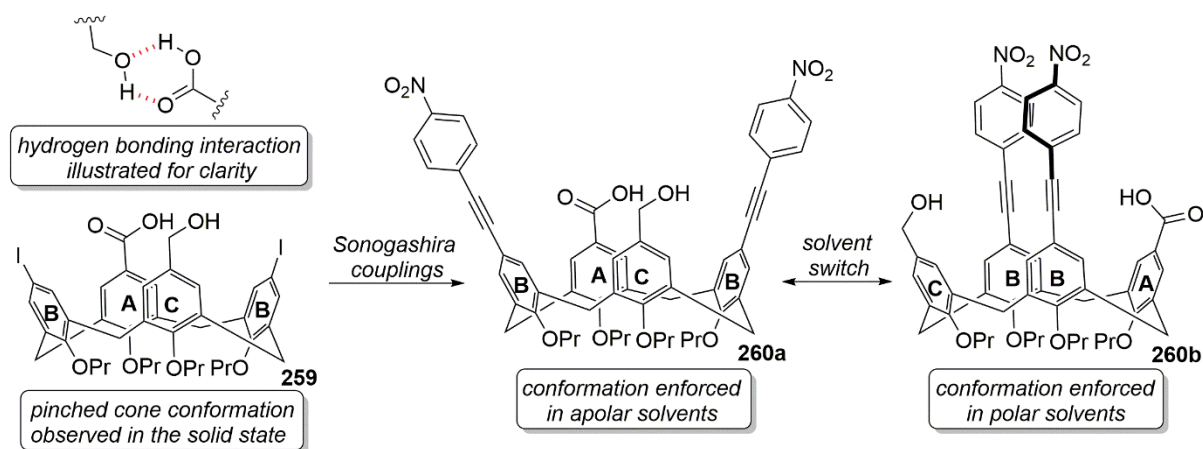


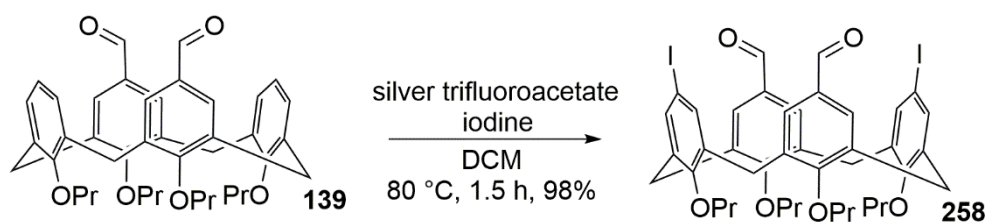
Figure 4.2: Principle of switchable NLOphore design **260**

In the right most structure **260b**, the hydrogen bonding has been disrupted by solvents which disfavour this interaction, and the time-averaged structure is anticipated to have both (donor)-(π)-(acceptor) units aligned with the central axis of the calix[4]arene, thereby resulting in a large net dipole moment. In contrast, the hydrogen bonding interaction in **260a** is expected to be promoted in apolar solvents and favour the pinched cone conformation **260a** which splays the two (donor)-(π)-(acceptor) units in opposite directions; thereby largely cancelling out the two dipoles. This type of cooperative movement acting between opposing calix[4]arene rings is well known, and has been termed a ‘breathing motion’ by a number of workers.^{46,204}

Thus in initiating this project, there were a clear set of challenges to address; a) what was the most efficient route towards the desired calix[4]arenes? b) could I functionalise **259** directly *via* Sonogashira couplings? c) how could the conformations of these calix[4]arenes in solution be determined? and d) could I employ the technique of second-harmonic generation spectroscopy and observe any ‘switchable’ NLO effects?

4.3 Synthesis of bis-iodo-bis-formyl calix[4]arene **258**

To address the first of these aims, I required a protocol for the reliable, scalable and high yielding synthesis of bis-iodo-bis-formyl calix[4]arene **258** as this compound was the key starting material for all of the proposed NLOphores (*e.g.* **260** and **261**). A review of the Bew groups’ work directed towards the synthesis of inherently chiral ABCD functionalised calix[4]arenes revealed a suitable procedure. Thus **258** can be generated in high yield (*i.e.* 98%) and purity (*i.e.* >95% by ¹H-NMR) by treatment of 1,3-diformyl calix[4]arene **139** with silver trifluoroacetate and iodine in DCM (**Scheme 4.1**).



Scheme 4.1: Synthesis of bis-iodo-bis-formyl calix[4]arene **258**²⁰³

Confident that this procedure would provide the most straightforward access to **258**, and with multigram quantities of **139** in hand from previous studies, I performed the *bis*-iodination reaction on a 1.5 g scale and obtained an excellent yield (*i.e.* 98%) of **258** after heating at 80 °C for 90 minutes under microwave irradiation. The ¹H-NMR spectrum of **258** corresponded exactly to that recorded previously, with the appearance of a singlet at 6.99 ppm arising from the four equivalent protons alpha to the iodine atoms being particularly characteristic. Further confirmation that this transformation had occurred as anticipated was sought from the ¹³C-NMR of **258**; as expected, a characteristic resonance was observed at 86.3 ppm arising from the two equivalent carbon atoms carrying the iodides (**Figure 4.3**).

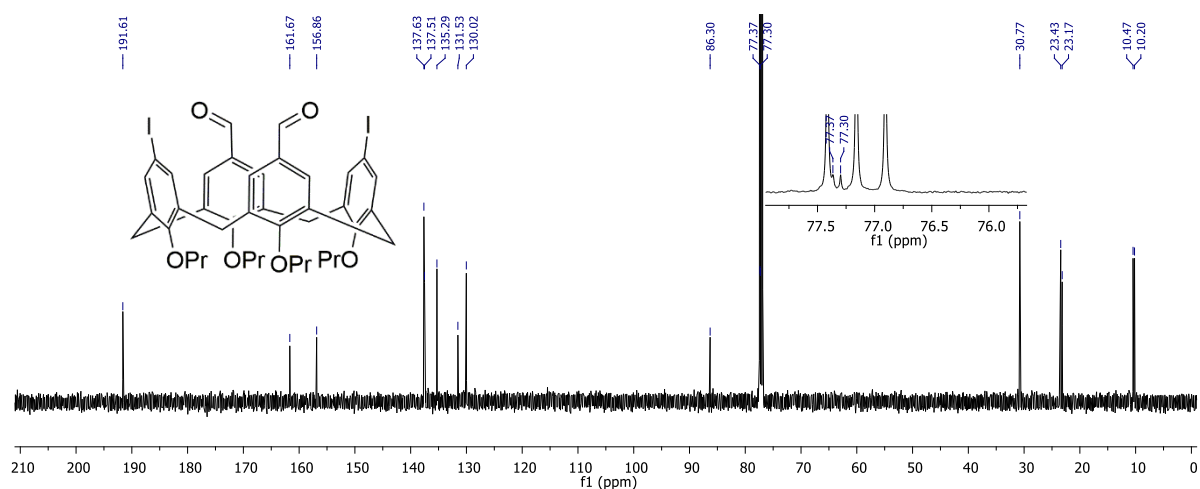
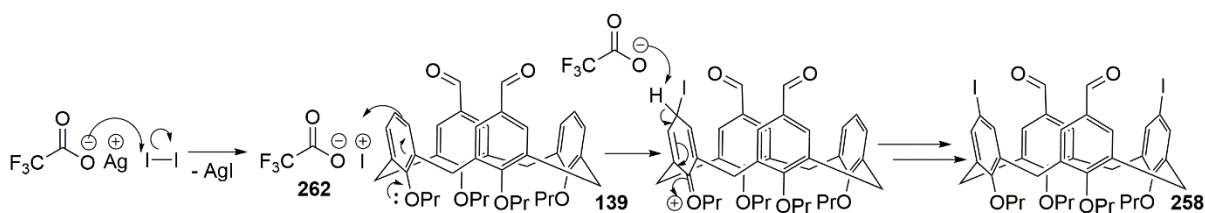


Figure 4.3: The ¹³C-NMR spectrum of bis-iodo-bis-formyl calix[4]arene **258** (124 MHz, CDCl₃)

A proposed mechanism for this transformation is outlined in **Scheme 4.2**. The active iodinating species **262** is generated by the reaction of silver trifluoroacetate and iodine in a step which produces one equivalent of silver iodide as the by-product. Following this, two sequential electrophilic aromatic substitution reactions occur at the upper-rim of **139** to afford *bis*-iodo functionalised **258**. Over-iodination is possible at the carbon atoms meta to the propoxy groups, but is prevented by the use of exactly two equivalents of silver trifluoroacetate in combination with the lower intrinsic reactivity of these positions (**Scheme 4.2**).

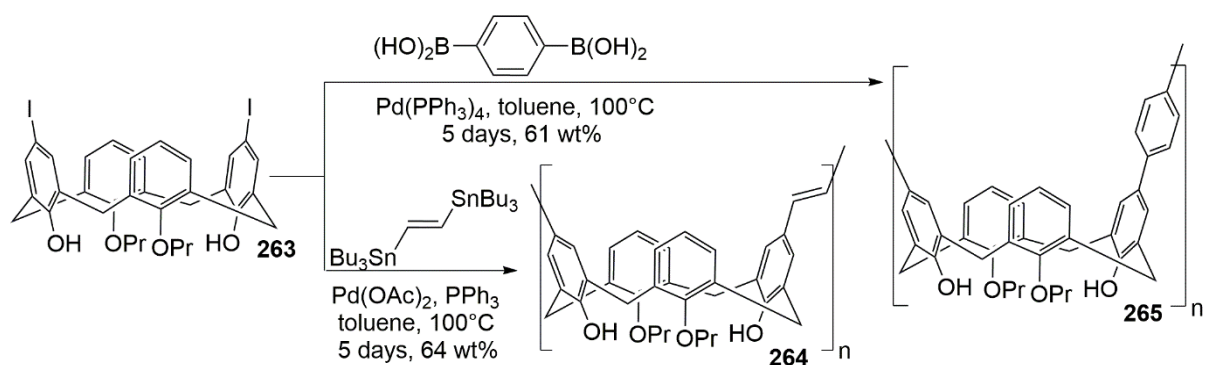


Scheme 4.2: Proposed reaction mechanism for the bis-iodination of **139**

With this protocol validated for the synthesis of multigram quantities of **258** (over several batches) I wanted to study its reactivity in transition metal mediated couplings (e.g. Sonogashira, Suzuki-Miyaura, Ullmann) before converting it into the Cannizzaro derived **259**, and finally the desired compounds. The aim of these experiments was to gain a fuller understanding of the reactivity of this class of ABAB functionalised calix[4]arenes, before subsequently applying this knowledge to the synthesis of the desired NLOphores.

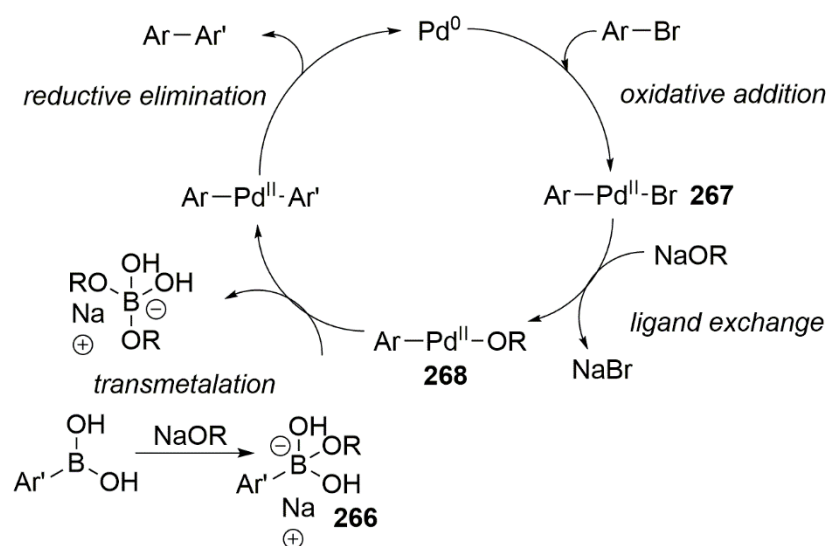
4.4 The reactivity of bis-iodo-bis-formyl calix[4]arene **258** in transition metal mediated couplings

As outlined above, I was keen to explore some transition metal mediated couplings using the readily available **258** to afford a better understanding of the reactivity of such ABCB functionalised systems. Indeed, as this project was carried out in parallel with the Bew groups' study of methods for the production of inherently chiral ABCD functionalised calix[4]arenes, some of this work was relevant to that project too. Thus I decided to continue with the NLOphore work by conducting a search of the literature for examples of cross-coupling reactions performed at the upper-rim of iodo- and bromo-functionalised calix[4]arenes. One of the earliest reports of such a transformation was disclosed by Dondoni and co-workers in 1998.²⁰⁵ In their communication, the Italian group demonstrated the application of Stille and Suzuki cross-coupling reactions using *bis*-iodide **263** for the generation of calix[4]arenylvinylene **264** and calix[4]arenylphenylene **265** oligomers (**Scheme 4.3**).



Scheme 4.3: Dondoni's synthesis of calix[4]arene based oligomers **264** and **265** using Stille and Suzuki cross-couplings²⁰⁵

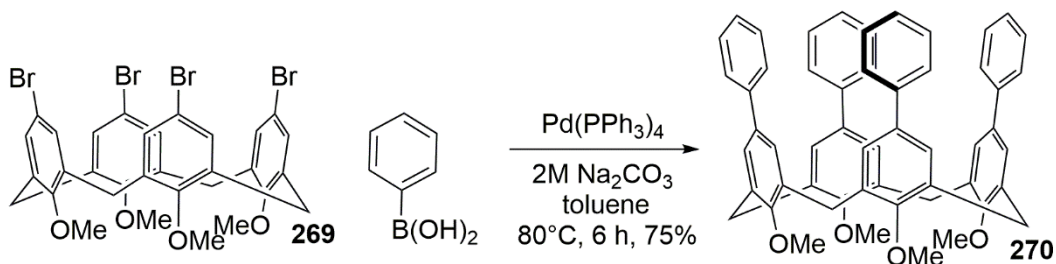
Interestingly, Dondoni's syntheses of **264** and **265** employed no additional base(s) but still produced moderate yields of the desired products (albeit after long reaction times). Generally however, an additional base is employed in most Suzuki reactions, and has been suggested to promote coupling *via* the formation of aryl hydroxyborates such as **266** (R = H) – species which are considered to be more nucleophilic than the corresponding boronic acids, and therefore more reactive towards transmetalation.²⁰⁶ A second hypothesis is that a ligand exchange reaction of an intermediate $[\text{ArPd}(\text{Br})(\text{L})_2]$ species **267** forms an $[\text{ArPd}(\text{OR})(\text{L})_2]$ species **268** which accelerates the subsequent transmetalation by virtue of the oxophilicity of boron.²⁰⁷ Until recently, these exact details were not fully understood. However, a recent kinetic study of the Suzuki reaction by Le Duc and co-workers has provided strong evidence for the catalytic cycle illustrated below (**Scheme 4.4**).²⁰⁸



Scheme 4.4: Catalytic cycle for the Suzuki coupling

In the catalytic cycle advocated in Le Duc's study, the base has three distinct roles; a) formation of the $[\text{ArPd}(\text{OR})(\text{L})_2]$ species **268** b) formation of the aryl borate **266** and c) acceleration of the reductive elimination step *via* reaction with the $[\text{ArPdAr}'(\text{L})_2]$ complex.

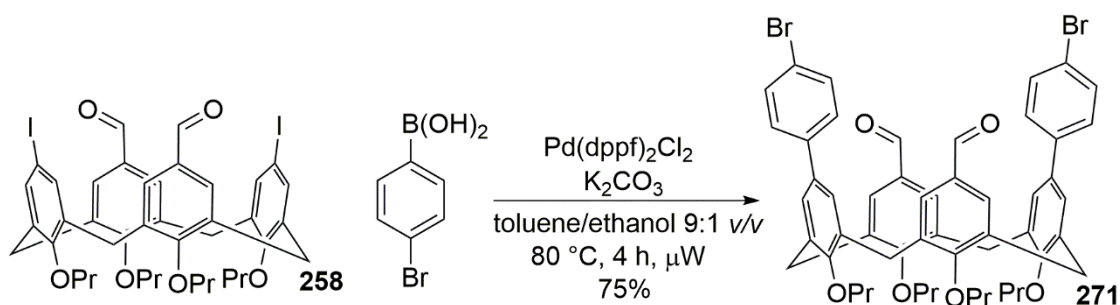
Thus after considering the importance of the base for this transformation, I sought to identify an alternative to Dondoni's seemingly base-free protocol (**Scheme 4.3**). Continuing the literature search, I identified a report from Atwood and co-workers which described the synthesis of rigid, deep cavity calix[4]arenes such as **270** *via* the Suzuki coupling of *tetra*-bromide **269** (**Scheme 4.5**).²⁰⁹



Scheme 4.5: Atwood's synthesis of rigid, deep-cavity calix[4]arene **270** via Suzuki coupling of **269**²⁰⁹

In this case, the American group employed sodium carbonate to promote the four-fold coupling of **269** and phenyl boronic acid; after six hours heating at 80 °C in toluene, an excellent yield (*i.e.* 75%) of **270** was obtained. Although not directly comparable to Dondoni's synthesis of **265** (Scheme 4.3) these results do seem to suggest that using an additional base has an accelerating effect on Suzuki couplings of calix[4]arene bromides and iodides have been reported – and most of these employ a base of some sort.^{210–212}

With a number of conditions identified for Suzuki couplings operating in calix[4]arene systems, I was keen to attempt some test reactions using the *bis*-iodo-*bis*-formyl calix[4]arene **258** to evaluate its reactivity. Thus I started by combining **258** with an excess (3 eqⁿ) of *para*-bromophenyl boronic acid under Pd(0) catalysis (20 mol%) using excess potassium carbonate (2 eqⁿ) as the base in a 9:1 v/v mixture of toluene and ethanol (which enhances the dielectric constant of the mixture to allow for microwave heating) (Scheme 4.6).

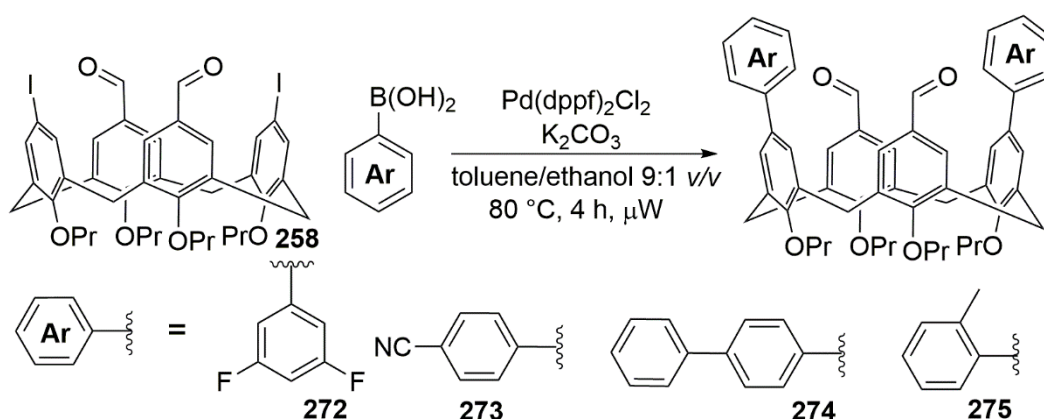


Scheme 4.6: Synthesis of Suzuki coupled **271** under microwave irradiation

After heating this mixture at 80 °C for 4 hours under microwave irradiation, I was pleased to observe complete conversion into the desired coupled product **271** by subsequent ¹H-NMR analysis of the crude mixture. Purification of the impure material *via* flash column chromatography on silica gel afforded **271** as an off-white solid in 75% yield, with a comprehensive physicochemical analysis confirming the structural assignment. In the ¹H-NMR spectrum of **271** the introduction of the *para*-bromo substituted aryl rings was confirmed by doublets at 7.27 (4H, *J* = 8.4 Hz) and 6.95 (4H, *J* = 8.4 Hz). Also, in the ¹³C-NMR spectrum of **271**, the loss of the carbon-iodine resonance at 86.3 ppm

present in the starting material **258** provided further confirmation that both of these positions had been substituted. Furthermore, a mass ion was observed at 974.2612 in the HRMS analysis of **271** which corresponds to $[M+NH_4]^+$ for this compound.

Pleased with the high yield (*i.e.* 75%) and short reaction time (*i.e.* four hours) required for the synthesis of **271**, I wanted to establish the generality of these reaction conditions when applied to **258** using a series of boronic acid coupling partners. Thus I performed the following Suzuki couplings on a 0.1 mmol scale, and observed the product distributions in each case *via* 1H -NMR spectroscopy of the impure mixtures (**Scheme 4.7**).

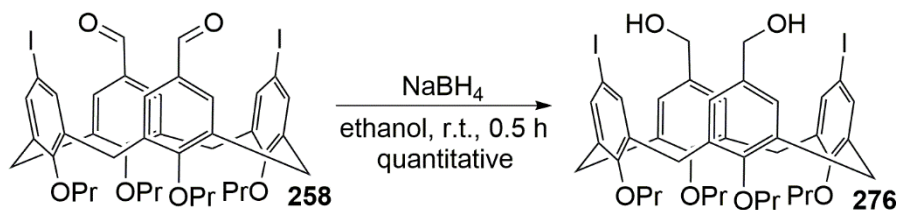


Scheme 4.7: Suzuki reactions of bis-iodide **258** with a range of boronic acid coupling partners

Of this set of boronic acids, only the reaction with biphenyl boronic acid gave full conversion to the corresponding *di*-substituted calix[4]arene **274**. No conversion was observed for the couplings with 2,5-difluorophenylboronic acid or 4-cyanophenylboronic acid, whilst the reaction *ortho*-tolylboronic acid resulted in only *ca.* 51% conversion to the corresponding *di*-substituted **275**.

4.5 The reactivity of bis-iodo-bis-hydroxymethylene calix[4]arene **276** in transition metal mediated couplings

Since the aim of these preliminary studies was to build an understanding of the reactivity of *tetra*-functionalised ABAB and ABAC calix[4]arenes (where A = iodide or bromide) in transition metal mediated couplings, before applying this knowledge to the synthesis of the NLOphore calix[4]arenes, I wanted to understand how the formyl groups present in **258** served to mediate its reactivity. It was proposed that the conversion of both formyl groups in **258** to primary alcohols by reduction would be a simple means of generating an analogue to test the effect of substitution at these 'B' positions. To affect this transformation, I treated an ethanolic solution of **258** with an excess of sodium borohydride at room temperature for 0.5 hours. After an aqueous work-up, I was pleased to obtain a quantitative yield of **276** as a high melting white solid (**Scheme 4.8**).

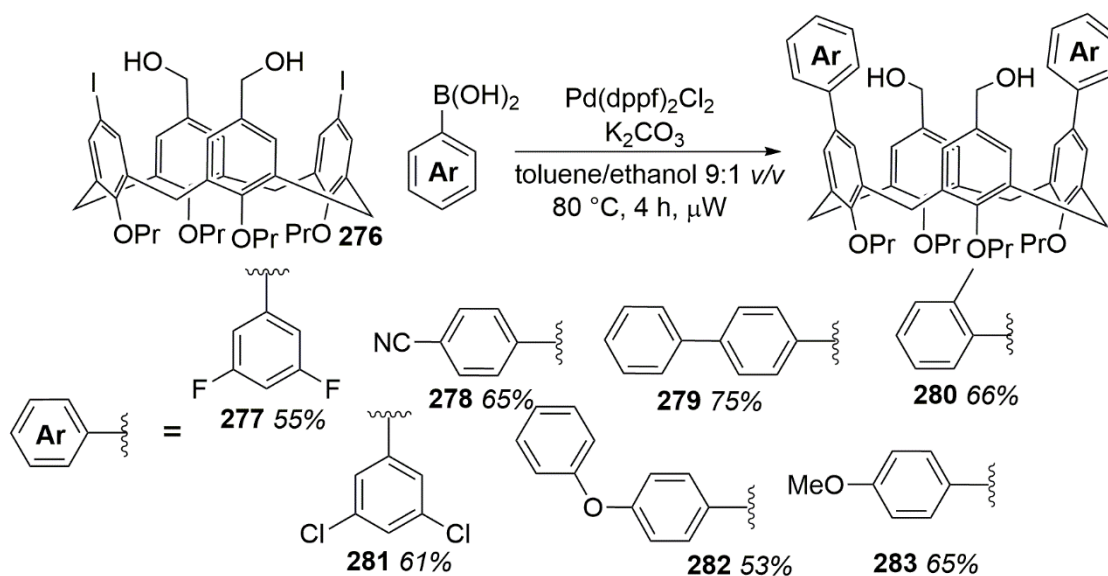


Scheme 4.8: Reduction of **258** with NaBH_4 in ethanol to afford bis-primary alcohol **276**

A comprehensive physicochemical analysis confirmed the structural assignment. In the $^1\text{H-NMR}$ spectrum of **276** I observed a singlet at 4.21 ppm arising from the four equivalent benzylic methylene protons, in addition to the disappearance of the formyl resonance observed at 9.51 ppm in the starting material **258**. The $^{13}\text{C-NMR}$ spectrum of **276** also confirmed the transformation had taken place as anticipated; a resonance was observed at 64.1 ppm arising from the two equivalent benzylic carbon atoms. Furthermore, a mass ion was observed at 922.2035 in the HRMS analysis which corresponds to $[\text{M}+\text{NH}_4]^+$ for **276**.

4.5.1 The reactivity of bis-iodo-bis-hydroxymethylene calix[4]arene **276** in Suzuki couplings

With bis-alcohol **276** in hand, I could compare its reactivity to bis-aldehyde **258** in Suzuki couplings to establish whether this functional group interconversion (*i.e.* CHO to CH_2OH) was at all significant. Opting to use identical reaction conditions as employed previously (**Scheme 4.7**) so I could make direct comparisons between the two systems, I reacted **276** with an expanded series of boronic acid coupling partners (**Scheme 4.9**).



Scheme 4.9: Suzuki reactions of bis-alcohol **276** with a range of boronic acid coupling partners

Interestingly, whilst the Suzuki coupling of 2,5-difluorophenylboronic acid and bis-aldehyde **258** failed to generate any of the desired product **272** (by $^1\text{H-NMR}$ analysis) the analogous reaction using

bis-alcohol **276** afforded the corresponding *di*-substituted product **277** in a 55% isolated yield after flash column chromatography. Similarly, whilst the reaction of *bis*-aldehyde **258** with 4-cyanophenylboronic acid failed to generate any **273**, the analogous reaction using *bis*-alcohol **276** afforded the *di*-substituted **277** in a 65% isolated yield after flash column chromatography. In all of the reactions illustrated in **Scheme 4.9**, full conversion was observed *via* $^1\text{H-NMR}$ spectroscopy of the impure mixtures. The modest yields arose from difficulties in isolation of these materials by column chromatography; closely eluting impurities and modest solubilities of the desired products were the main issues.

An inspection of the physicochemical data obtained for **277** to **283** revealed that each calix[4]arene was ABAB-substituted and fixed in the cone conformation. This was clearly indicated by the doublets (all *ca.* 13.5 Hz) observed in the $^1\text{H-NMR}$ spectra of these compounds at around 4.5 and 3.2 ppm which arise from the non-equivalent protons of the methylene bridges. A representative $^1\text{H-NMR}$ spectrum from this series is reproduced below (for the *bis*-substituted 2,5-difluorophenyl **277**) from which these characteristic doublets can clearly be discerned (**Figure 4.4**).

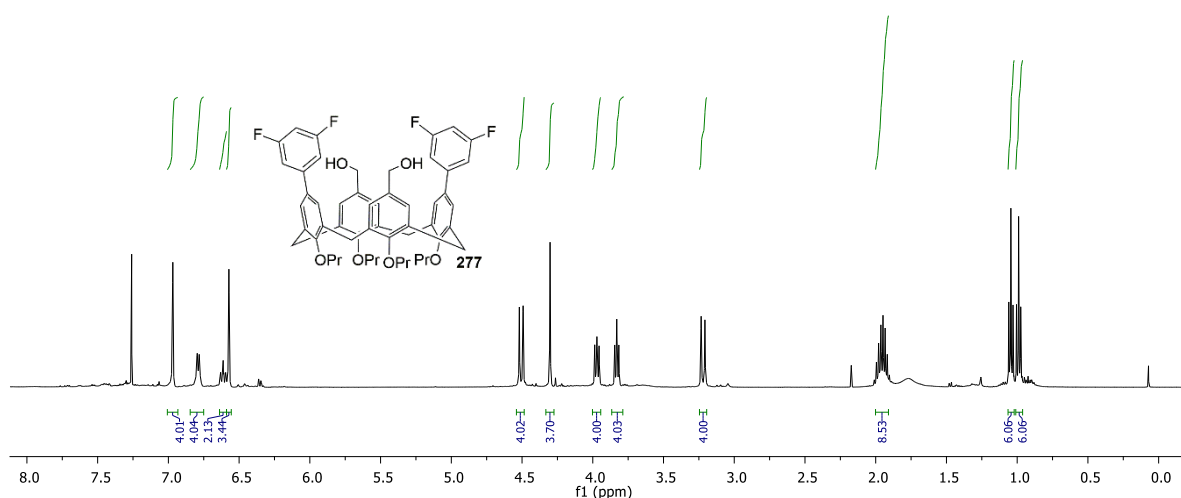


Figure 4.4: $^1\text{H-NMR}$ spectrum of 2,5-difluorophenyl substituted **277** (500 MHz, CDCl_3)

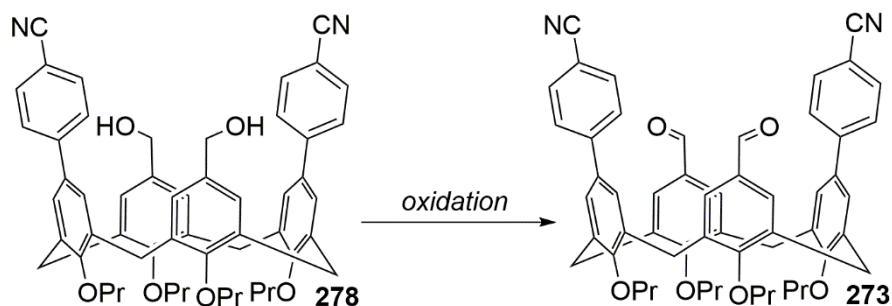
In the aromatic region, the 2,5-difluorophenyl rings are evidenced by a doublet at 6.79 ppm (4H, $J = 6.8$ Hz) and a triplet at 6.61 ppm (2H, $J = 8.9$ Hz); multiplets which arise from coupling to the fluorine atoms ($I = \frac{1}{2}$). The upper-rim ABAB substitution was further confirmed by the singlets at 6.97 and 6.57 ppm, which I have assigned to the two equivalent sets of arene protons carrying the 2,5-difluorophenyl and hydroxymethylene groups respectively.

From these preliminary studies then, it appeared that *bis*-alcohol **276** was a more reactive substrate than *bis*-aldehyde **258** in Suzuki couplings; and by extension, the nature of the substitution at the 'B' rings (*i.e.* CHO or CH_2OH) was playing an important role in mediating the reactivity observed. The

reasons for this are presumably electronic in origin, since the difference in steric bulk between CHO and CH₂OH groups might be expected to be minimal.

4.6 Synthesis of ABAB functionalised *bis*-aldehydes via the oxidation of ABAB functionalised *bis*-alcohols

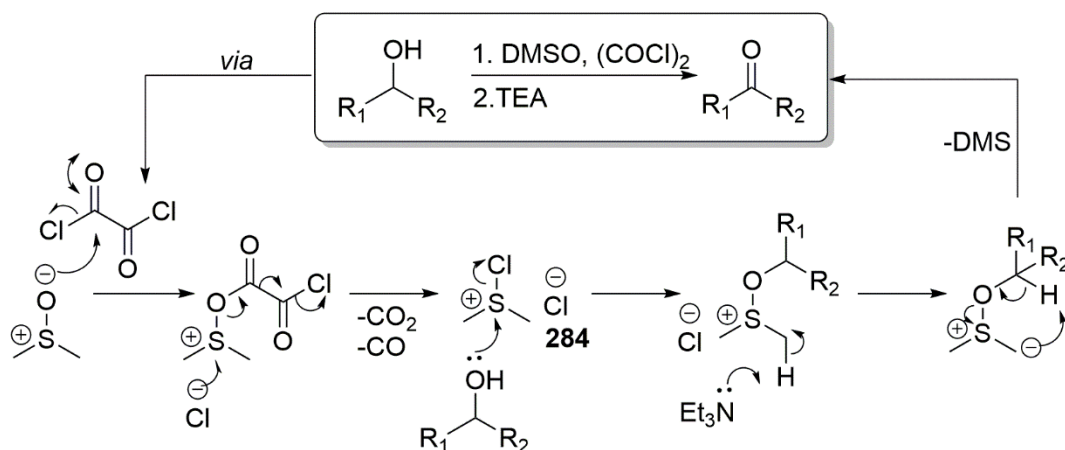
Since it was anticipated the target NLOphore calix[4]arenes (**260** and **261** in the first instance) would be derived from an intramolecular Cannizzaro reaction (**Section 4.8**), the presence of two opposing aldehydes at the upper-rim of the calix[4]arenes was critical. Thus whilst the reactivity of the *bis*-alcohol **276** appeared to be greater in Suzuki couplings, the resulting compounds (*i.e.* **277** to **283**) were in the wrong oxidation state for the subsequent transformation. In order to supplement the understanding of these systems and develop a possible second route to the target compounds, I considered the possibility of oxidising **278** to afford the previously inaccessible **273** (**Scheme 4.10**).



Scheme 4.10: Proposed synthesis of ABAB calix[4]arene **273** via oxidation of the corresponding primary *bis*-alcohol **278**

If such an approach were successful, this would enhance the options for the synthesis of a wide range of *bis*-aldehyde precursors (potentially derivatised with a set of acceptor functionalities). Thus I searched the literature to review methods for the oxidation of primary alcohols to aldehydes, and identified a number of potentially suitable protocols.

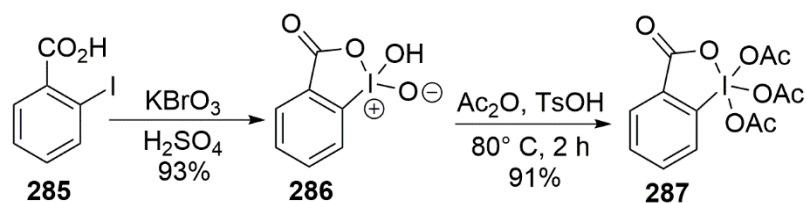
Several procedures for this transformation (CH₂OH to CHO) based on the activation of dimethyl sulfoxide have been described. One of the most widely used at present is the Swern oxidation, which involves the activation of DMSO with oxalyl chloride to generate chloro(dimethyl)sulfonium chloride **284** as the active species (**Scheme 4.11**).²¹³



Scheme 4.11: The mechanism of the Swern oxidation²¹³

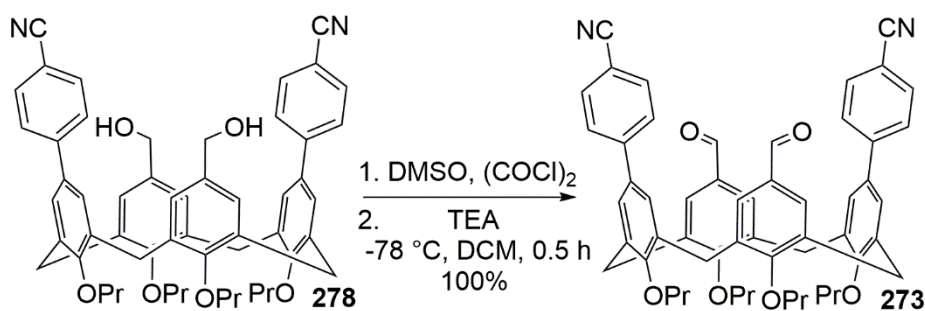
One of the principle advantages of the Swern oxidation is that all of the by-products (*i.e.* CO₂, CO and dimethyl sulfide) are volatile, and therefore the resulting aldehydes are typically obtained without recourse to column chromatography. This contrasts to some of the earlier variations of this type of activated DMSO oxidation (*i.e.* Pfitzner-Moffatt or Parikh-Doering) where an aqueous work-up is the minimum required to obtain pure products.

Besides activated DMSO oxidations, the Dess-Martin periodinane (DMP) **287** is a popular reagent for the transformation of primary alcohols to aldehydes.²¹⁴ This hypervalent iodine compound is derived from the oxidant 2-iodoxybenzoic acid (IBX) **286** by treatment with acetic anhydride in the presence of a catalytic amount (0.5 mol%) of tosylic acid, and is regarded to have a number of advantages over activated-DMSO based reagents.²¹⁵ These include high chemoselectivity, shorter reaction times and simplified work-ups (**Scheme 4.12**).



Scheme 4.12: Preparation of Dess-Martin periodinane **287** via the acylation of IBX **286**²¹⁵

The Dess-Martin periodinane **287** therefore appeared to be the ideal reagent for this transformation (*i.e.* **278** to **273**). However, without a sample of this oxidant immediately to hand, it was decided from a time efficiency point of view it would be prudent to test Swern's conditions in the first instance. Thus I performed a test reaction using 0.04 mmol of **278** in anhydrous DCM at -78 °C, and was pleased to observe (TLC analysis) complete conversion to the corresponding *bis*-aldehyde **273** after 0.5 hours (**Scheme 4.13**).



Scheme 4.13: Swern oxidation of diol **278** to bis-aldehyde **273**

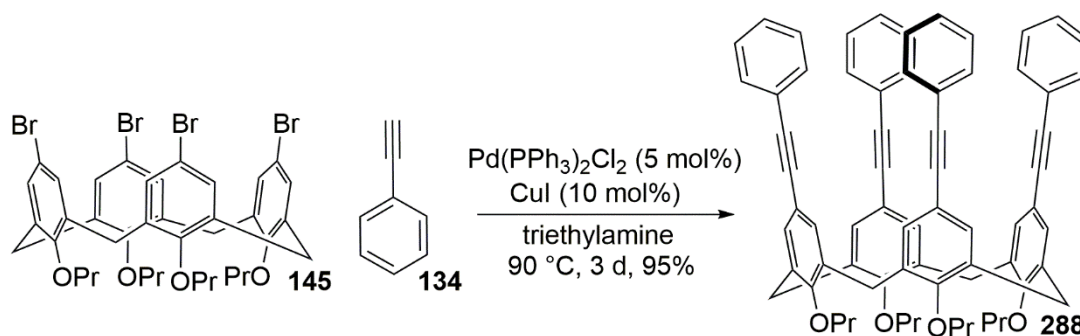
The low temperature employed (*i.e.* $-78\text{ }^{\circ}\text{C}$) was necessary to prevent the decomposition of the intermediate chloro(dimethyl)sulfonium chloride (**284** **Scheme 4.11**) and represents somewhat of a drawback in terms of operator convenience. However, this was a small consideration given the quantitative yield obtained of *bis*-aldehyde **273** isolated pure (>95% by $^1\text{H-NMR}$) after an aqueous work-up. A comprehensive physicochemical analysis indicated the oxidation had proceeded as expected on both primary alcohols; in the $^1\text{H-NMR}$ spectrum of **273** a singlet was observed at 9.51 ppm (2H) which I have assigned to the two equivalent formyl protons, whilst in the $^{13}\text{C-NMR}$ the formyl carbons were evidenced by a resonance at 191.64 ppm. Furthermore, a mass ion was observed at 873.4 in the MALDI-TOF analysis which corresponds to $[\text{M}+\text{Na}]^+$ for **273**.

Pleased to have validated this protocol as an efficient means of accessing the ABAB functionalised *bis*-aldehyde **273**, I was confident relying on this sequence of synthetic steps (*i.e.* reduction-coupling-oxidation) to enable the synthesis of a series of NLOphore calix[4]arenes carrying a range of acceptor units. Since one of the initial designs (*i.e.* **260**) would employ a Sonogashira reaction for its assembly, I needed to establish whether this type of coupling reaction would also favour the *bis*-alcohol **276** over the *bis*-aldehyde **258**.

4.7 The reactivity of *bis*-iodo-*bis*-formyl calix[4]arene **258** in Sonogashira couplings

Whilst the reduction-coupling-oxidation protocol established above proved to be an effective means of accessing Suzuki coupled ABAB functionalised calix[4]arenes (since the reduction and oxidation steps were high yielding), it was clearly not an ideal solution due to the two extra synthetic steps involved. Thus before yielding to a longer synthesis, I wanted to study whether the *bis*-aldehyde **258** would also show poor reactivity in Sonogashira couplings with a range of substituted acetylenes. To test this, I first conducted a search of the literature for examples of Sonogashira couplings operating on the upper-rim of bromide and iodide substituted calix[4]arenes, so I could identify a suitable set of reaction conditions for this system. Interestingly, compared to the Suzuki couplings (**Section 4.4**) a comparatively greater number of studies were identified.^{46,156,216–218}

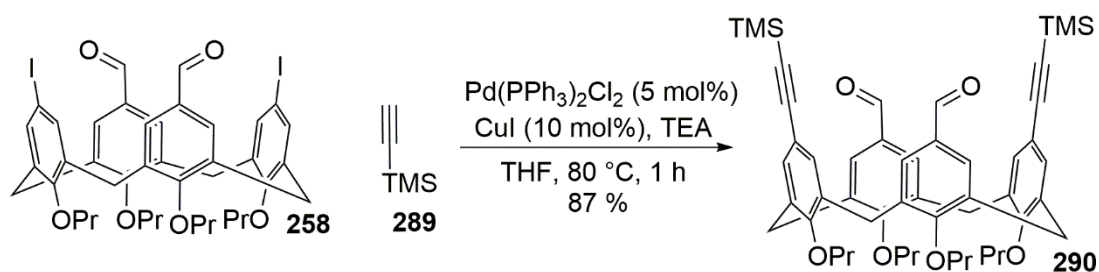
One of the earliest reports of such a transformation was disclosed by Dyker and co-workers in 2005.¹⁵⁶ In their communication, the German group described the four-fold Sonogashira coupling of *tetra*-bromo calix[4]arene **145** and phenylacetylene **134** under Pd(0) and Cu(I) catalysis to afford the electron-rich cavitand **288** in a 95% yield after purification by flash column chromatography (**Scheme 4.14**).



Scheme 4.14: Dyker's synthesis of the electron-rich cavitand **288** via a four-fold Sonogashira coupling

Interestingly, this 'classical' catalytic system was reported to be the only means of obtaining **288**; experiments employing DMF or THF as a co-solvent or copper-free conditions failed to generate any of the desired product, even under forcing conditions (*i.e.* elevated temperatures and/or increased catalyst loadings).

Whilst I was somewhat concerned about the long reaction time (*i.e.* 3 days) reported for the synthesis of **288**, I anticipated that *bis*-iodide **258** would be more reactive and, since the planned couplings were only two-fold, require less time to reach completion. Thus I opted to carry out a test reaction under Dyker's conditions, using *bis*-iodide substrate **258** and TMS-acetylene **289** (as I had more of this reagent to hand). However, due to the poor solubility of *bis*-iodide **258** in neat TEA, I was forced to employ THF as a co-solvent. Additionally, for added convenience, I opted to perform the coupling in a sealed vial under microwave irradiation (**Scheme 4.15**).

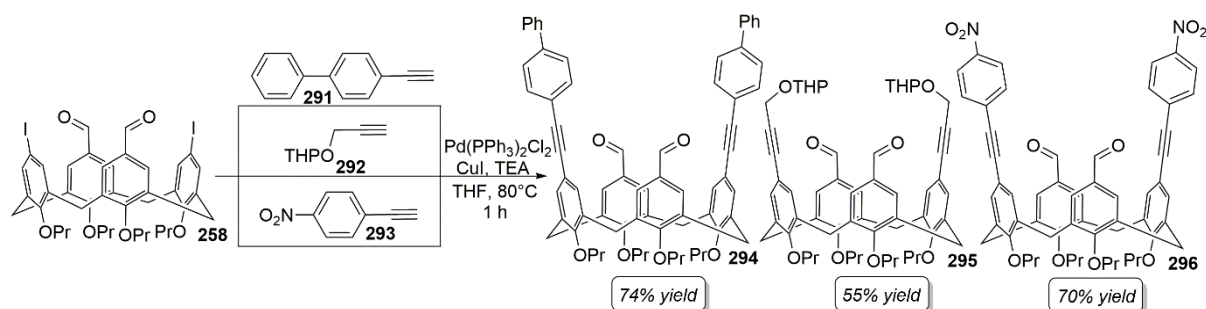


Scheme 4.15: Sonogashira coupling of *bis*-iodide **258** and TMS-acetylene **289**

Monitoring the reaction by TLC analysis, I was pleased to observe complete conversion into the desired TMS-acetylene adduct **290** after just one hour stirring at 80 °C. Subsequent isolation of this

material *via* flash column chromatography and a comprehensive physicochemical analysis confirmed the proposed structure. In the $^1\text{H-NMR}$ spectrum of **290** the TMS-acetylene units were evidenced by a singlet at 0.31 ppm (18H), whilst the presence of the aldehydes (inert to this transformation) was confirmed by a singlet at 9.21 ppm (2H).

To establish whether this catalytic system was as robust as it first appeared, I wanted to extend the range of substituted alkynes to substrates such as **291**, **292** and **293**. These alkynes were chosen principally to see if larger, more sterically encumbered, alkynes could be accommodated without a corresponding decrease in reaction rate or product yield (**Scheme 4.16**).



Scheme 4.16: Sonogashira couplings of bis-aldehyde **258** and substituted alkynes **291**, **292** and **293**

I was delighted to find that, in a similar fashion to TMS-acetylene adduct **290**, each of these reactions had reached completion after one hour stirring at 80 °C, and the corresponding products were obtained in 55 to 74% yields after flash column chromatography. Importantly for the NLO studies, the *para*-nitrophenyl substituted **296** was accessed in high yield (*i.e.* 70%) and purity (>95% by $^1\text{H-NMR}$). Indeed, this compound is only one synthetic step (*i.e.* a Cannizzaro reaction) from the desired NLOphore **260** (**Figure 4.1**) albeit changing the order of transformations I had originally planned to employ.

A subsequent comprehensive physicochemical analysis of **296** confirmed the structural assignment. For example, the $^{13}\text{C-NMR}$ spectrum of **296** displayed resonances at 96.3 and 87.2 ppm arising from the carbon-carbon triple bond, whilst the formyl carbon was evidenced by a signal at 191.7 ppm. In the $^1\text{H-NMR}$ spectrum of **296** the introduction of the equivalent *para*-nitrophenyl arenes was clearly evidenced by doublets at 8.09 (4H, $J = 8.9$ Hz) and 7.56 (4H, $J = 8.9$ Hz) ppm, whilst the presence of the *bis*-aldehydes on the opposing 'B'-rings was confirmed by a singlet (2H) at 9.47 ppm (**Figure 4.5**).

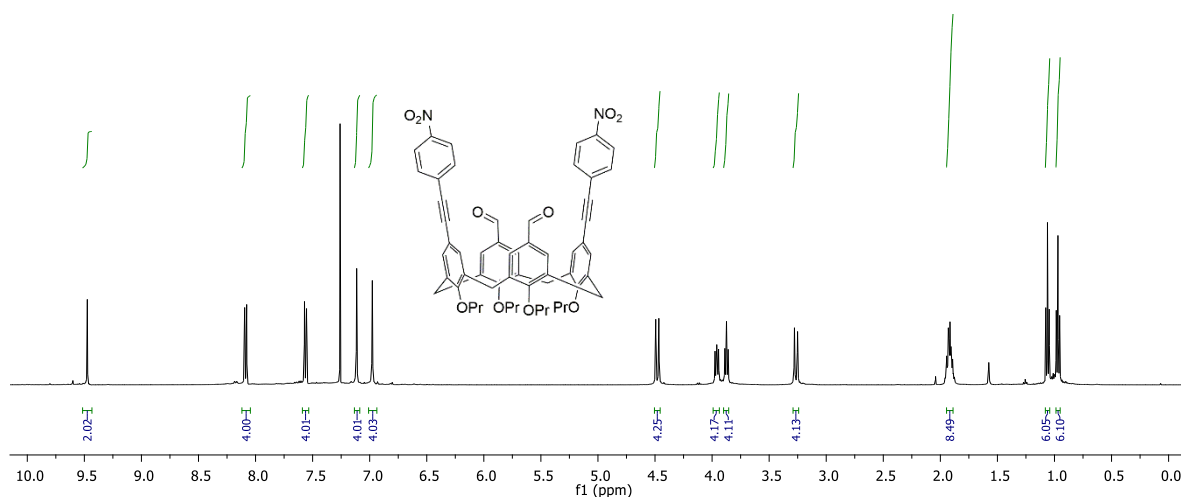
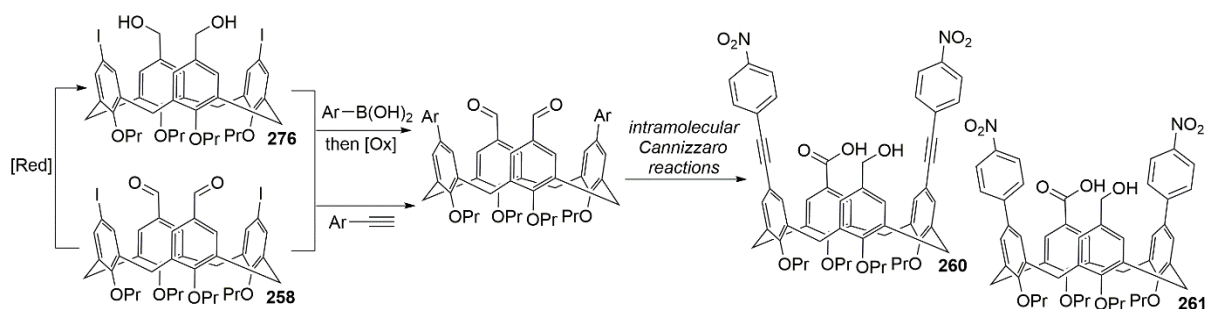


Figure 4.5: $^1\text{H-NMR}$ spectrum of *para*-nitrophenyl substituted **296** (500 MHz, CDCl_3)

Finally, a mass ion was observed at 961.2 in the MALDI-TOF analysis of **296** which corresponds to $[\text{M}+\text{Na}]^+$, thereby further confirming this structural assignment.

4.8 The Cannizzaro reaction of ABAB functionalised *bis*-aldehyde calix[4]arenes

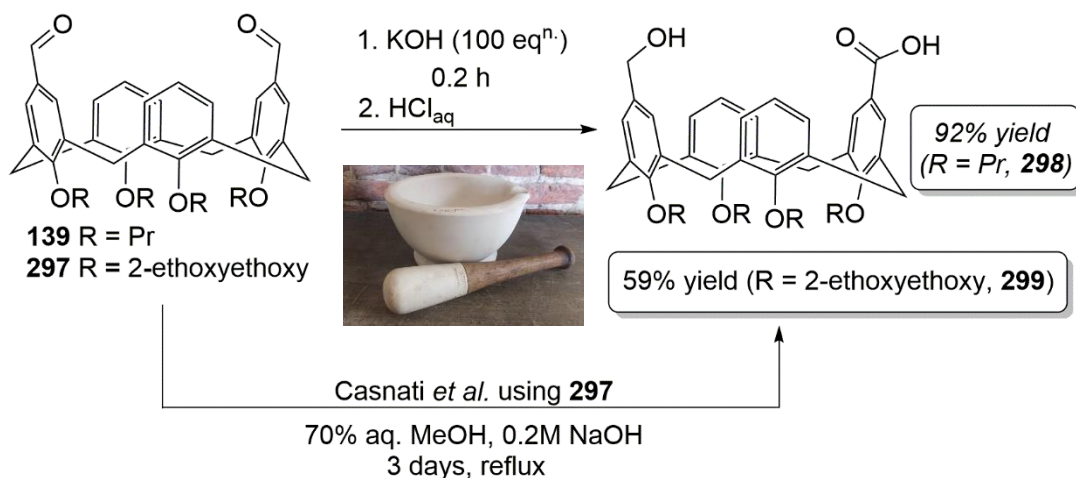
Given the results of the preliminary studies with *bis*-iodo-*bis*-hydroxymethylene calix[4]arene **276** and *bis*-iodo-*bis*-formyl calix[4]arene **258** in transition metal mediated couplings, I decided to reconsider the initial synthetic strategy towards NLOphore calix[4]arenes **260** and **261** (Figure 4.1). It became apparent that by varying the order of steps within this synthesis, it would likely be possible to avoid performing any coupling reactions on the, presumably highly polar, Cannizzaro derived **259**. This would be advantageous in terms of purification of the final products, and, also since I had already validated methods for the synthesis of Suzuki and Sonogashira derived *bis*-aldehydes (e.g. **273** and **296**). Thus based on the preliminary studies, I produced a revised synthetic plan (Scheme 4.17).



Scheme 4.17: Revised synthetic plan for the synthesis of NLOphore calix[4]arenes **260** and **261**

Before subjecting the sample of Sonogashira derived *bis*-aldehyde **296** to the Cannizzaro reaction however, I wanted to validate the experimental protocol (optimised previously within the Bew group) on a less valuable compound. Since the most abundant material I had available was the 1,3-

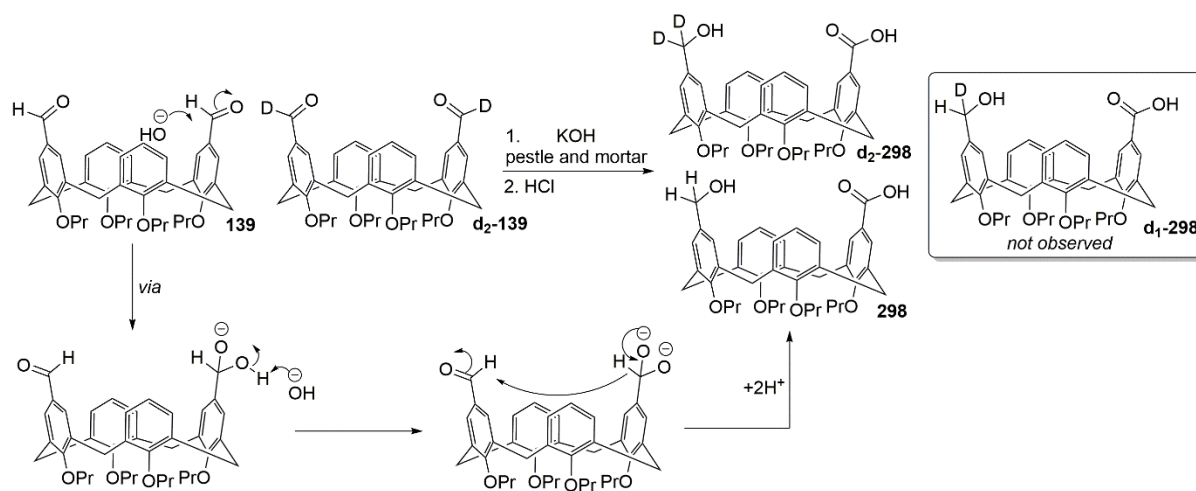
diformyl calix[4]arene **139**, I opted to attempt to reproduce the synthesis of the Cannizzaro derived **298** under the Bew group's mechanochemical conditions (**Scheme 4.18**).^{53,203}



Scheme 4.18: Above: Bew and Stephenson's protocol for the rapid intramolecular Cannizzaro reaction of 1,3-diformyl functionalised calix[4]arenes. Below: Casnati and co-workers original solution phase protocol.²¹⁹

The key enabling feature of this protocol is the use of a pestle and mortar to grind the materials (*i.e.* potassium hydroxide and 1,3-diformyl calix[4]arene **139**) in close contact; thereby increasing the reactants' surface area, obviating the need for solvent and – most importantly – increasing the reaction rate significantly (0.2 hours required instead of 3 days) compared to the analogous solution phase protocol, reported by Casnati and co-workers in 2012.²¹⁹

Mechanistic studies carried out within the Bew group previously confirmed the intramolecular nature of this process under these mechanochemical conditions. In a deuterium cross-over experiment, treatment of a 1:1 mixture of **139** and its deuterated analogue **d₂-139** with potassium hydroxide afforded an equimolar mixture of **298** and **d₂-298** after acidic work-up. None of singly deuterated **d₁-298** was observed by ²H-NMR spectroscopy or MALDI-TOF spectrometry, thereby confirming the proton/deuteron transfers were strictly intramolecular (**Scheme 4.19**).



Scheme 4.19: Deuterium cross-over experiment to demonstrate the intramolecular mechanism which operates under mechanochemical conditions

Confident I understood the mechanism involved, I decided to attempt a small scale reaction on 0.23 mmol of **139** to validate the method. Following the progress of the disproportionation by TLC analysis (DCM), I was pleased to observe complete consumption of **139** after grinding for a total of about 10 minutes. An acidic work-up and extraction with diethyl ether was sufficient to afford an excellent yield (*i.e.* 92%) of pure **298** without recourse to column chromatography. A subsequent physicochemical analysis of **298** revealed that the $^1\text{H-NMR}$, $^{13}\text{C-NMR}$ and MALDI-TOF analyses correlated exactly with those obtained previously in the Bew group for the same compound. Particularly characteristic was the presence of a singlet at 4.09 ppm in the $^1\text{H-NMR}$, which I have assigned to the equivalent methylene protons of the CH_2OH group. In the $^{13}\text{C-NMR}$ of **298** the CH_2OH carbon atom gave rise to a resonance at 64.3 ppm, whilst a resonance at 171.9 ppm confirmed the presence of the COOH group.

With some experience of this reaction in hand, I felt confident in subjecting Sonogashira derived *bis*-aldehyde **296** to these mechanochemical conditions. A slight concern was the possibility that the presence of the two aryl units might retard the rate of the intramolecular transfer, but as this required the experiment to be performed to find out, I proceeded in charging a mortar with **296** and potassium hydroxide (100 eqⁿ). After grinding the mixture vigorously for about half an hour, TLC analysis (DCM) indicated only a trace of starting material **296** remaining. Analysis of the crude reaction mixture by $^1\text{H-NMR}$ spectroscopy after an acidic work-up, however, indicated a complex mixture of products (**Figure 4.6**).

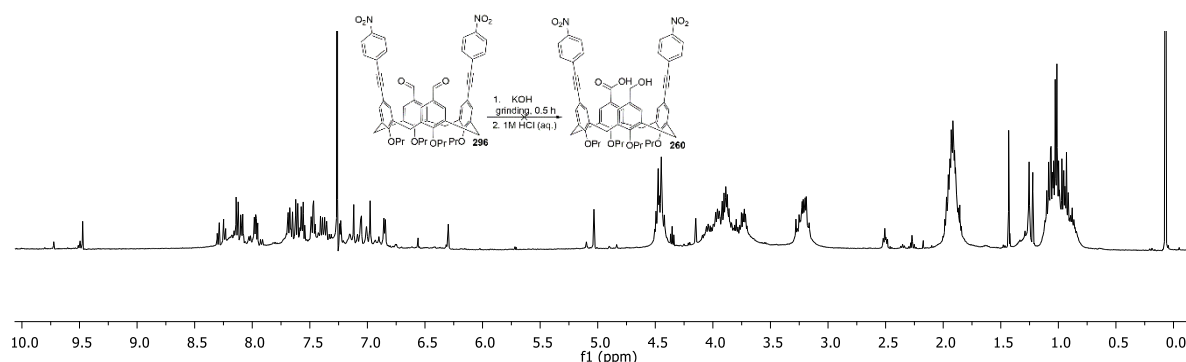
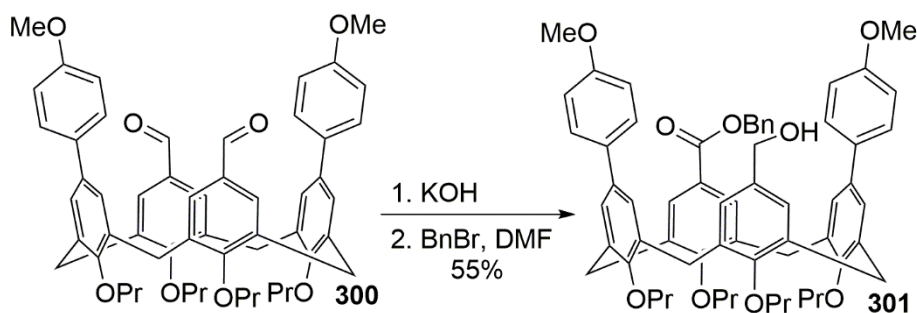


Figure 4.6: ¹H-NMR spectrum of attempted Cannizzaro reaction **296** to **260** (500 MHz, CDCl₃)

The broad resonances arising from the calix[4]arene core (e.g. methylene bridges at ca. 3.2 and 4.5 ppm) may suggest some polymerisation occurred under these conditions; possibly *via* the formation of intermolecular esters and/or through the reactivity of the alkyne functions. A few resonances around 9.5 ppm which presumably correspond to aldehyde protons can also be observed; however, since these only correspond to ca. 4 wt% of the mixture when integrated against the methylene bridge protons, these are not major components. In any case, TLC analysis confirmed the presence of several compounds, and all subsequent attempts at isolating a pure sample of **260** by flash column chromatography failed.

Somewhat disappointed by this result, I wanted to understand why the 1,3-diformyl calix[4]arene **139** readily afforded a pure sample of the corresponding Cannizzaro derived product **298** (Scheme 4.19), whilst *bis*-nitrophenyl substituted **296** returned a complex mixture. Indeed, this was all the more puzzling since in a related project running concurrently, the Bew group had demonstrated this mechanochemical Cannizzaro reaction could be performed successfully on *bis*-aryl functionalised calix[4]arenes such as **300**; albeit isolated as the benzyl esters (*i.e.* **301**) to enable a more straightforward purification (Scheme 4.20).



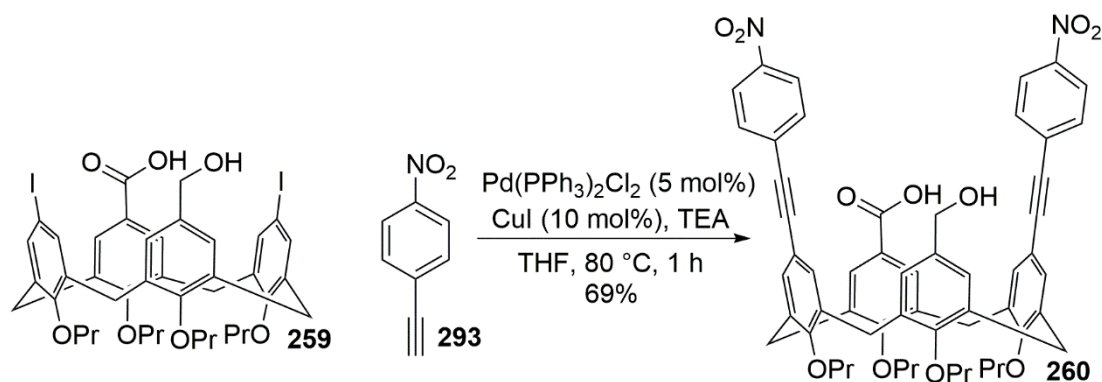
Scheme 4.20: Successful application of the intramolecular Cannizzaro reaction affording **301**

Since one of the principle differences between these two systems (*i.e.* **260** and **300**) was the presence of the carbon-carbon triple bonds, it was suspected these functions may be involved in some additional side reactions. To test if this effect was unique to the *para*-nitro substituted **269**, I

The physicochemical data of carboxylic acid **259** corresponded exactly to those obtained within the Bew group previously. In the $^1\text{H-NMR}$ spectrum, a singlet at 4.18 ppm was observed which has been assigned to the equivalent methylene protons of the CH_2OH group. In the $^{13}\text{C-NMR}$ spectrum, the ABAC substitution pattern at the upper-rim of **259** was confirmed by the presence of three sets of signals arising from the methyl groups of the propyl chains (9.98, 10.69 and 10.77 ppm) in addition to two resonances arising from the methylene bridge protons (30.75 and 30.86 ppm).

Since I required this material in a modest quantity (ideally around 1 g) for these studies, I needed to explore the scale at which this reaction could be performed. It was found that 1 g of **258** could indeed be converted into **259** in a comparable yield (*i.e.* 88%) although the reaction time was increased (to 1 hour); this was most likely due to the difficulty in grinding a larger mass of material equally. Nevertheless, even though some extra time and effort were required, this method did afford sufficient quantities of **259** for these studies.

With **259** in hand, I was keen to attempt some Sonogashira couplings using the biphenyl and *para*-nitrophenyl substituted alkynes **291** and **293**. Since the catalytic system I had employed previously (*i.e.* $\text{Pd}(\text{PPh}_3)_2\text{Cl}_2$, CuI and TEA in THF) for the couplings of *bis*-aldehyde **258** (Scheme 4.16) with **291** and **293** had already been demonstrated to perform well, I decided to employ this system here too. Thus a mixture of carboxylic acid **259** and *para*-nitrophenyl substituted alkyne **293** were treated with $\text{Pd}(\text{PPh}_3)_2\text{Cl}_2$, CuI and TEA in THF at 80 °C for 1 hour (Scheme 4.23).



Scheme 4.23: Test reaction between carboxylic acid **259** and *para*-nitro substituted alkyne **293**

Subsequent analysis of the impure mixture (by TLC) revealed that all of the starting material **259** had been consumed, and a new – somewhat more apolar – component had formed. Whilst the isolation of this material required two rounds of flash column chromatography, I was delighted to find that a sample of what was anticipated to be NLOphore calix[4]arene **260** could be obtained in high yield (*i.e.* 69%). A comprehensive physicochemical analysis of this material subsequently confirmed this structural assignment. Evidence for the substitution of both iodides with *para*-nitrophenyl units

came from the observation of doublets at 8.10 (4H, $J = 8.9$ Hz) and 7.60 (4H, $J = 8.9$ Hz) ppm in the $^1\text{H-NMR}$ spectrum (**Figure 4.7**).

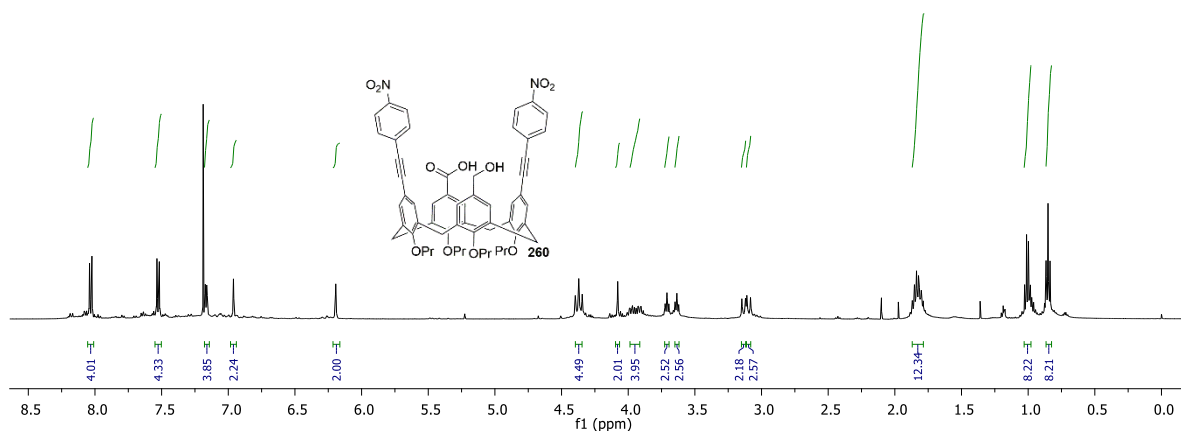


Figure 4.7: $^1\text{H-NMR}$ spectrum of NLOphore calix[4]arene **260** (500 MHz, CDCl_3)

The important combination of primary alcohol and carboxylic acid functions were, as anticipated, unaffected by this transformation. A signal at 4.08 ppm in the $^1\text{H-NMR}$ and 64.30 ppm in the $^{13}\text{C-NMR}$ confirms the presence of the primary alcohol, whilst a signal at 171.1 ppm in the $^{13}\text{C-NMR}$ has been assigned to the carbonyl carbon of the carboxylic acid. Further evidence for the formation of **260** was sought, and a HRMS analysis provided this with a mass ion observed at 979.3767 which corresponds to $[\text{M}+\text{Na}]^+$.

Pleased that this synthetic route had delivered a sample of NLOphore calix[4]arene **260** without too much difficulty, I began to think more closely about the materials required for the NLO studies (in light of my experience so far, and the reactions I perceived to be viable). From a time efficiency point of view, I decided to focus on generating a set of Sonogashira coupled analogues of **260** and omit the Suzuki derived **261** I had originally planned to synthesise. It became apparent that an important analogue would feature a combination of strongly polarised and weakly polarised (donor)-(π)-(acceptor) units at opposing sides of the calix[4]arene ring. Such a system would be anticipated to display a less pronounced dynamic NLO response to changes in conformation, since only a small change in overall dipole moment would be expected between the two pinched cone conformers. Thus compound **303** was conceived as an important control compound for the future studies using second harmonic generation spectroscopy (**Figure 4.8**).

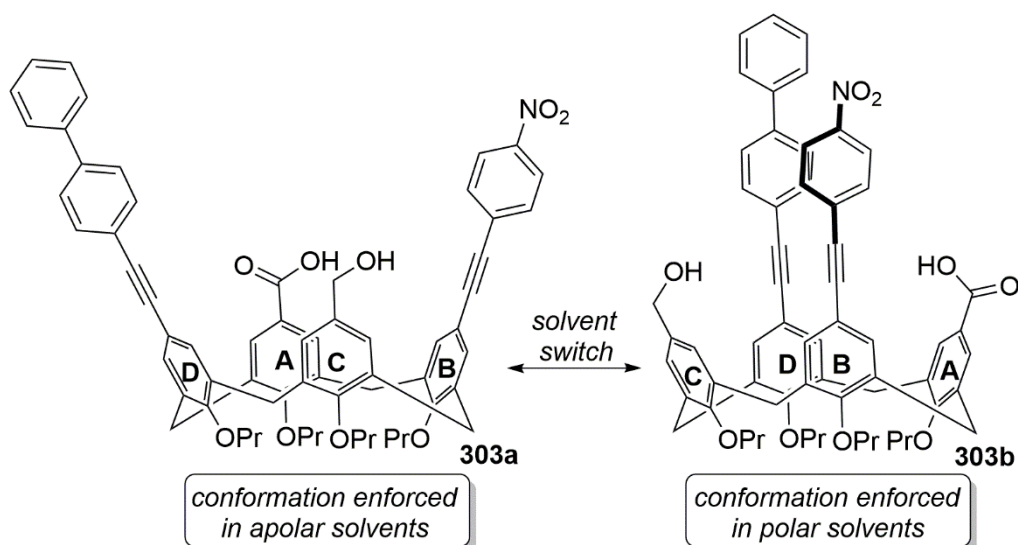
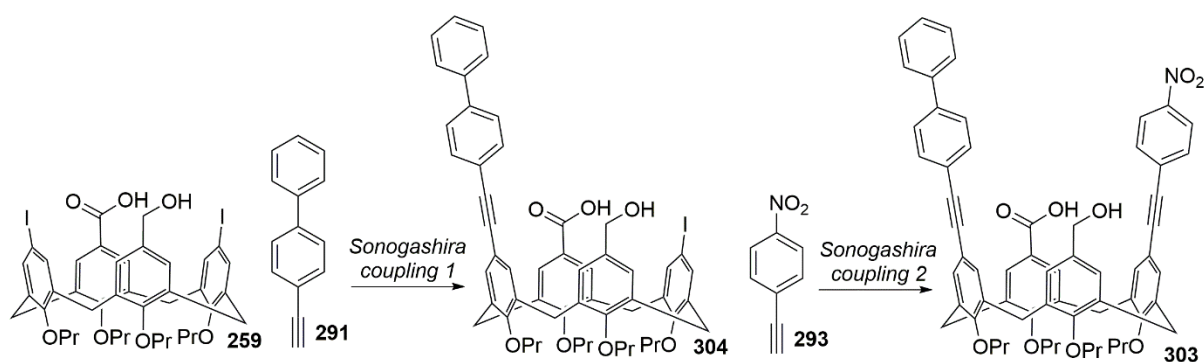


Figure 4.8: Proposed NLOphore calix[4]arene **303** featuring strongly and weakly polarised (donor)-(π)-acceptor units at opposing sides of the macrocyclic ring

It was proposed that this material could be synthesised *via* a stepwise approach starting from the carboxylic acid **259**. Thus, a Sonogashira coupling with one equivalent of biphenyl alkyne **291** was anticipated to furnish **304** from which **303** might be accessed by a subsequent Sonogashira coupling with *para*-nitro ethynylbenzene **293**. This order of addition (*i.e.* employing **291** instead of **293** first) was chosen to enable a more straightforward isolation of the corresponding intermediate **304**; it was anticipated that **291** might afford a more separable mixture (presumably comprising of **259**, **304** and the *bis*-substituted **302**) due to greater differences in polarity (**Scheme 4.24**).

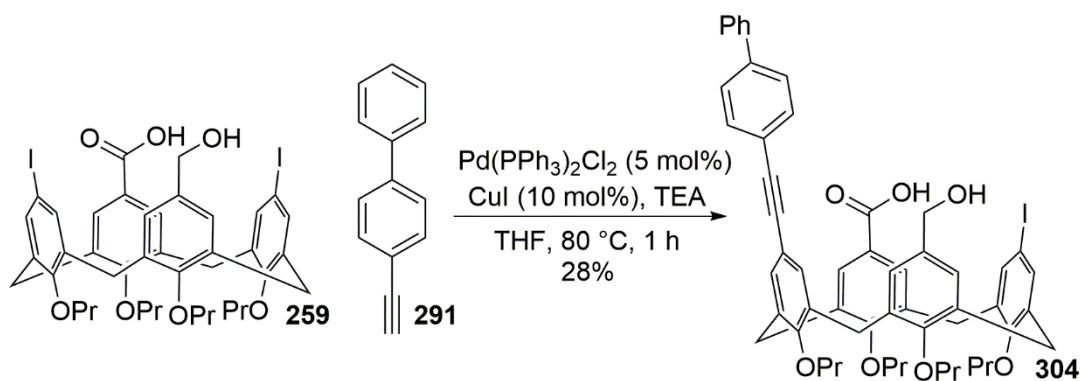


Scheme 4.24: Proposed synthetic route towards the NLOphore calix[4]arene **303**

It is noteworthy that, since compounds **304** and **303** carry four different groups their upper-rims, these C_1 symmetric calix[4]arenes display an *inherent chirality* (as coined by Böhmer *et al.* in 1994).²²⁰ As all of the starting materials and reagents were achiral and/or racemic, however, compounds **304** and **303** were expected to be furnished as racemic mixtures of (*M*)- and (*P*)-enantiomers. A separate study in the Bew group has been directed towards developing asymmetric

coupling reactions using **259**, but this was not the primary focus here; the absolute configuration of **303** being unimportant for the NLOphore studies.

Thus I initiated this synthetic route by attempting to couple carboxylic acid **259** with one equivalent of biphenyl alkyne **291** using the catalytic system already validated for the synthesis of NLOphore calix[4]arene **260** (Scheme 4.25).



Scheme 4.25: Synthesis of ABCD functionalised calix[4]arene **304** via a Sonogashira coupling

Monitoring the Sonogashira coupling by following the consumption of biphenyl alkyne **291** (TLC analysis), I observed that this reaction had reached completion after one hour. Isolation of the desired ABCD functionalised calix[4]arene **304** was achieved by flash column chromatography in moderate yield (*i.e.* 28%), with a comprehensive physicochemical analysis confirming the structural assignment. The substitution of only one iodide was confirmed, in part, by examination of the ¹³C-NMR spectrum of **304**; a resonance was observed at 86.9 ppm arising from the carbon-iodine function, whilst the presence of the internal alkyne was confirmed by resonances at 88.5 and 91.0 ppm. In the ¹H-NMR spectrum of **304**, the ABCD substitution pattern was evidenced by the doublets arising from the methylene bridges; since all of these methylene protons are inequivalent, a total of eight (albeit overlapped) doublets could be discerned. For further confirmation of this structural assignment, **304** was submitted for HRMS analysis. Pleasingly, a mass ion was observed at 986.3491 which corresponds to [M+NH₄]⁺ (Figure 4.9).

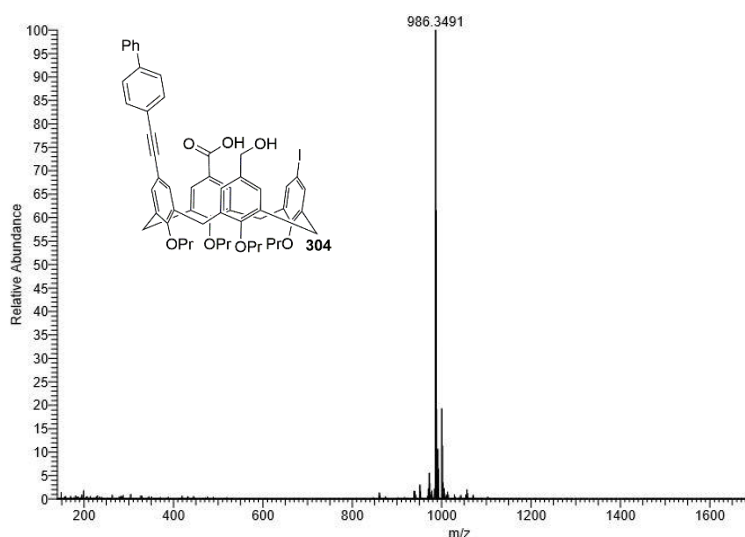
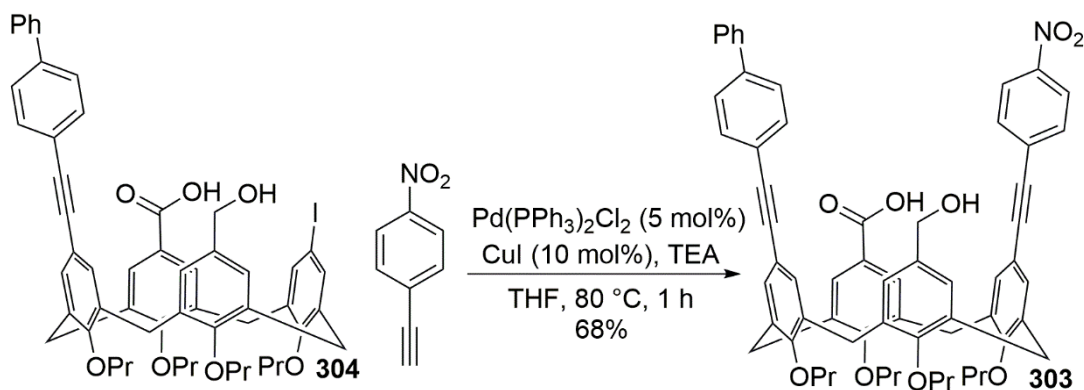


Figure 4.9: HRMS analysis of **304** showing a mass ion at 986.3491 which corresponds to [M+NH₄]⁺

Encouraged by the isolation of **304** in moderate yield from this coupling, I wanted to proceed with the synthesis of the mixed NLOphore calix[4]arene **303**. To obtain the highest possible yield of **303** I needed to ensure complete consumption of the starting material **304** in the Sonogashira coupling. Thus, in order to promote this, I opted to employ an excess (*i.e.* two equivalents) of *para*-nitro ethynylbenzene **293** in its preparation (Scheme 4.26).



Scheme 4.26: Synthesis of mixed NLOphore calix[4]arene **303** via a Sonogashira coupling

After heating the mixture to 80°C for one hour under microwave irradiation, TLC analysis indicated that all of **304** had been consumed. Satisfyingly, the ABCD-functionalised NLOphore calix[4]arene **303** was isolated from this impure mixture in 68% yield *via* flash column chromatography; a comprehensive physicochemical analysis confirming the structural assignment. The incorporation of the *para*-nitrophenyl alkyne moiety was evidenced, in part, by doublets at 8.08 (2H, $J = 8.9$ Hz) and 7.52 (2H, $J = 8.9$ Hz) in the $^1\text{H-NMR}$ spectrum of **303**. In the $^{13}\text{C-NMR}$ spectrum of **303**, the presence of two non-equivalent internal alkynes was confirmed by the resonances at 88.41, 88.44, 90.84 and 91.00 ppm. In addition, the loss of the resonance at 86.9 ppm observed in the starting material **304** confirmed that the carbon-iodine function was no longer present. For further confirmation of the structure of **303** a HRMS analysis was obtained; gratifyingly, a mass ion was observed at 1005.4685 which corresponds exactly to $[\text{M}+\text{NH}_4]^+$.

4.10 Variable temperature $^1\text{H-NMR}$ study of the conformation of Cannizzaro derived calix[4]arene **298**

At this stage of the project, I felt that I had sufficient materials (*i.e.* **259**, **260**, **298**, **303** and **304**) to begin to study the conformational changes proposed to occur in different solvent environments (*e.g.* pinched cone **260a** to pinched cone **260b** Figure 4.2). It became apparent that a useful preliminary study would involve measuring the $^1\text{H-NMR}$ spectra of one of these 'switchable' systems in a number of solvents of disparate polarity, to see if any differences might be observed. As an extension to this,

I considered whether heating or cooling the NMR sample might also provide a means of ‘operating’ this conformational switch.

To enable the most straightforward analysis of these effects, I chose to study ABCB functionalised calix[4]arene **298** as this had the least complicated $^1\text{H-NMR}$ spectrum (of the set of final compounds I had prepared) (**Figure 4.10**).

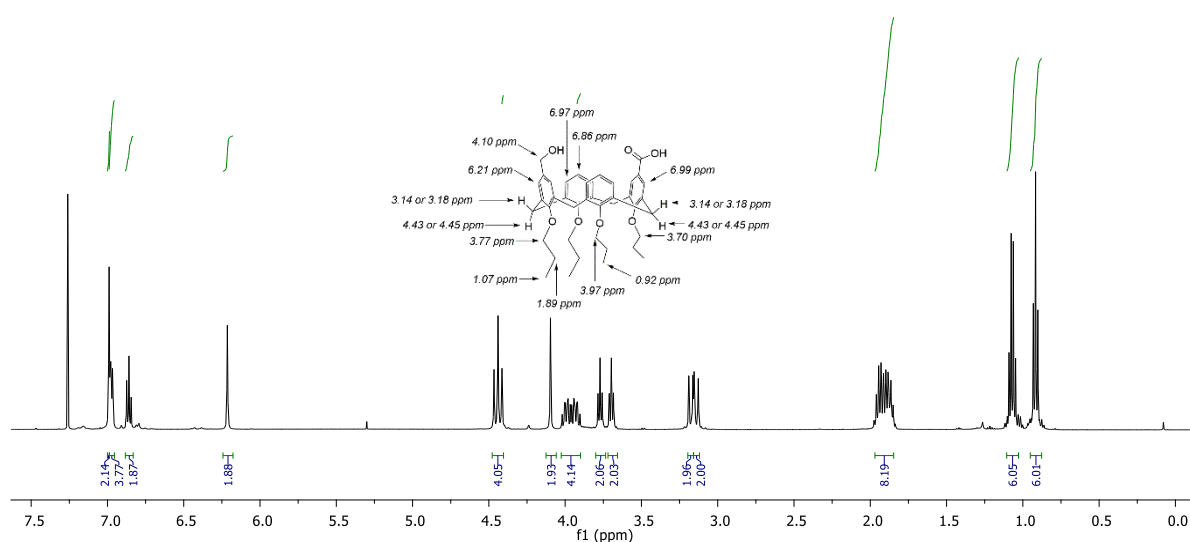


Figure 4.10: $^1\text{H-NMR}$ spectrum of calix[4]arene **298** (500 MHz, CDCl_3 , 40 mM, 298K)

As a starting point, it was important to be able to assign the ambient temperature $^1\text{H-NMR}$ spectrum of **298** to enable the interpretation of the VT and solvent dependent data that I wanted to obtain. Thus I made the assignment on the basis of the chemical shifts and multiplicities (illustrated above). The doublets arising from the methylene bridge protons, however, could not be confidently assigned; the equatorial protons flanking the CH_2OH functionalised arene ring may resonate at either 3.14 or 3.18 ppm, and *vice versa* for the equatorial protons flanking the COOH functionalised arene. The assignment of the axial doublets (albeit overlapped) is similarly uncertain. Unfortunately, at this stage, I was unable to identify a suitable NMR technique to assign these signals unambiguously.

Hypothesising that the ambient temperature $^1\text{H-NMR}$ spectrum of **298** in CDCl_3 represented a time averaged structure wherein the hydrogen bonding interaction between COOH and CH_2OH units had been disrupted (*via* interactions with the solvent), I wanted to test the effect of switching the solvent to the significantly less polar d_8 -toluene. It was hypothesised that this solvent would promote the different time averaged structure wherein the hydrogen bonding interaction would enforce the pinched cone conformation splaying the functionalised aryl units inwards. Interestingly, recording the ambient temperature $^1\text{H-NMR}$ spectrum of **298** in d_8 -toluene afforded significantly

different data to that obtained in CDCl_3 under the same conditions (*i.e.* temperature and concentration) (**Figure 4.11**).

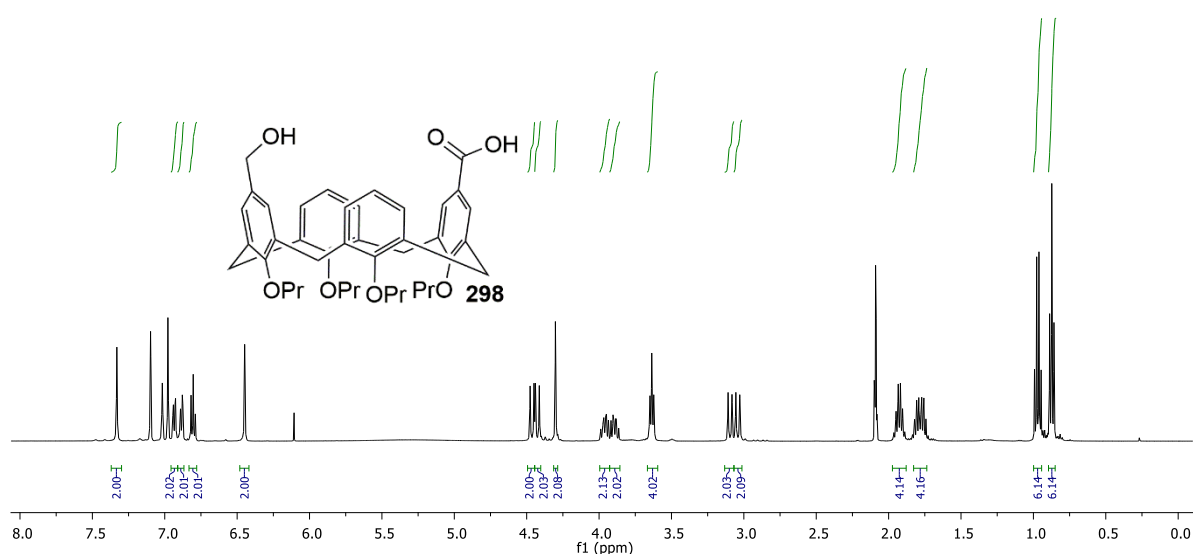


Figure 4.11: $^1\text{H-NMR}$ spectrum of calix[4]arene **298** (500 MHz, d_8 -toluene, 40 mM, 298K)

One clear difference is the triplet at 3.64 ppm (4H) which had previously appeared as a pair of triplets at 3.70 (2H) and 3.77 (2H) ppm in the CDCl_3 spectrum (**Figure 4.10**). Since I had previously assigned this pair of triplets to the OCH_2 groups on the CH_2O and COOH functionalised arenes, I was surprised to observe these protons resonating at the same chemical shift when the spectrum was recorded in d_6 -toluene. One possible interpretation might be that, in d_6 -toluene, a switch in conformation affords the hydrogen bonded structure **298b** wherein the two sets of OCH_2 protons are now in indistinguishable chemical environments (**Figure 4.12**).

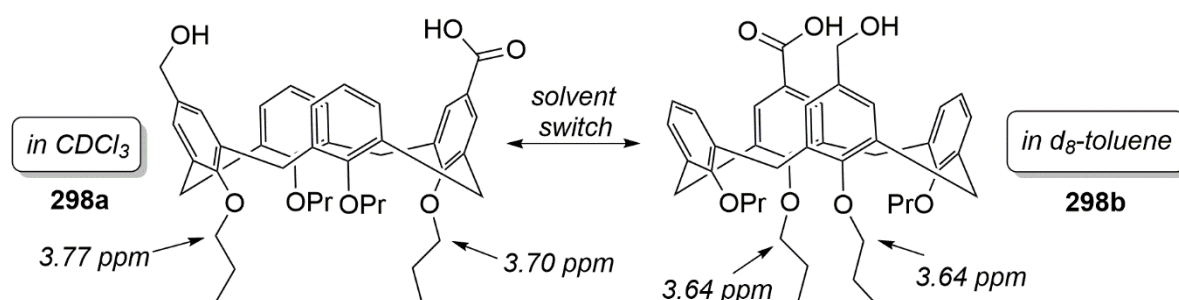


Figure 4.12: Rationalisation of the changes between $^1\text{H-NMR}$ spectra of **298** resulting from a 'solvent switch' (CDCl_3 to d_8 -toluene)

To probe the idea that stark differences in chemical shifts observed for the OCH_2 protons could be directly related to a conformational change, I considered the use of variable temperature $^1\text{H-NMR}$. It was hypothesised if the ambient temperature spectrum of **298** in d_8 -toluene represented time averaged structure **298b**, the spectrum could be 'transformed' to appear more like the ambient

temperature spectrum of **298** in d-chloroform by heating the sample (*i.e.* to overcome the supposed hydrogen bonding interaction). Similarly, it was anticipated that cooling the d-chloroform sample of **298** might produce a ^1H -NMR spectrum which appeared more like the ambient temperature d_8 -toluene spectrum (*i.e.* by promoting hydrogen bonding).

Since recording ^1H -NMR spectra at elevated temperatures was somewhat more practical than at depressed temperatures, I began these VT-NMR studies by obtaining spectra of **298** in d_8 -toluene at 313, 333, 353 and 373 K (**Figure 4.13**).

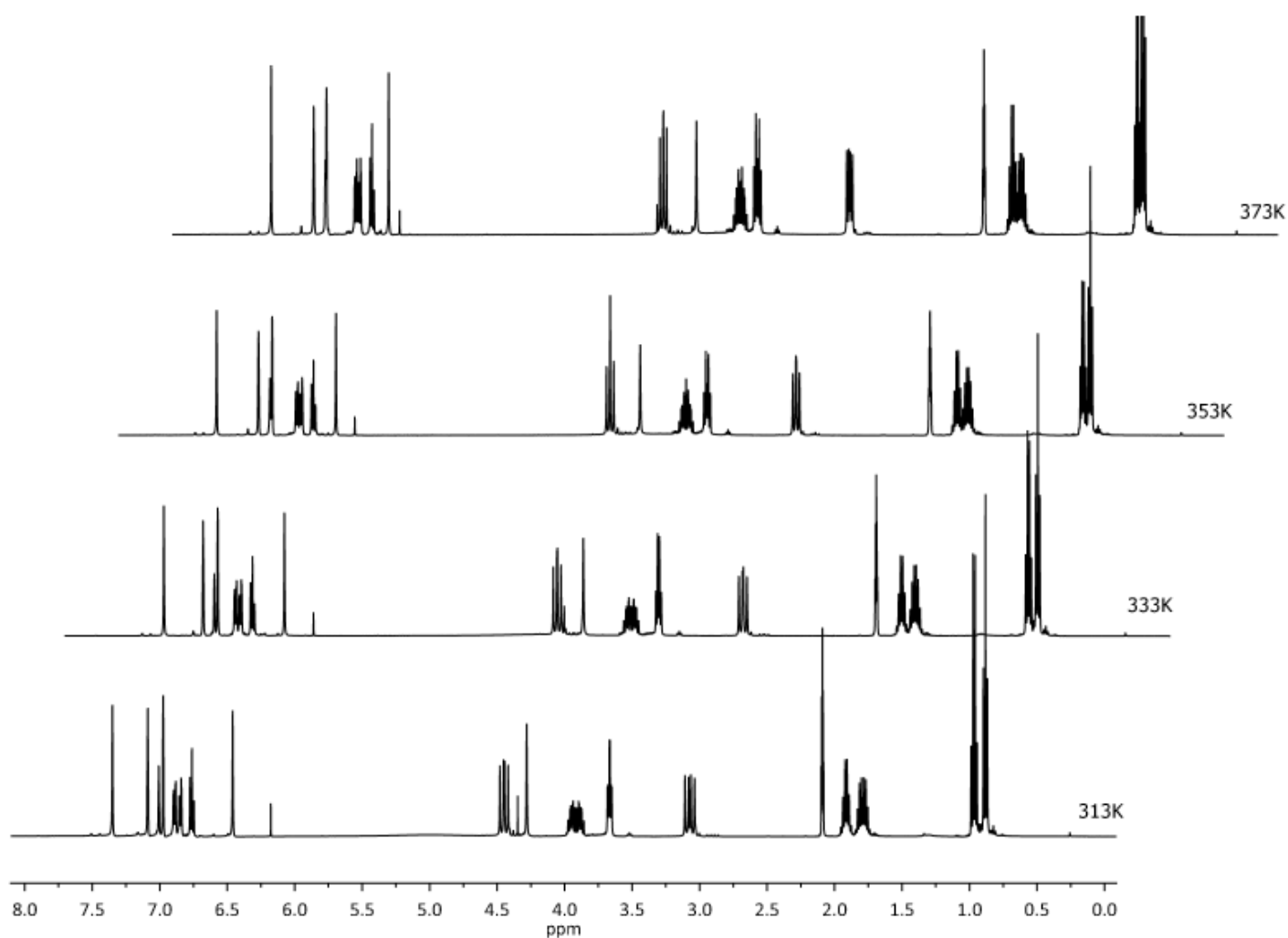


Figure 4.13: Stacked ^1H -NMR spectra of **298** at 313, 333, 353 and 373 K (500 MHz, d_8 -toluene, 40 mM)

Focusing in on the region between 3.6 and 3.7 ppm, it can be seen that the triplet (4H) present in the ambient temperature ^1H -NMR spectrum of **298** in d_8 -toluene (**Figure 4.1**) starts to be resolved into a pair of triplets (2H) as the sample is heated. If this trend could be continued (d_8 -toluene boils at 383K) then a fully resolved pair of triplets would be anticipated, affording a ^1H -NMR spectrum which is qualitatively similar (in this regard) to that obtained in ambient temperature d-chloroform.

To study whether this trend towards the 298 K d-chloroform spectrum was mirrored elsewhere, I examined the aromatic region of this series of d₈-toluene VT-spectra. I focused on the group of signals arising from the unsubstituted propoxy-arenes (*i.e.* triplet at 6.76 ppm and doublet of doublets at 6.85 and at 6.89 ppm) and observed that the doublet of doublets at 6.85 and at 6.89 ppm began to coalesce as the sample is heated, whilst the triplet at 6.76 ppm (313 K) shifted upfield to 6.62 ppm. In a similar way to the changes observed for the OCH₂ protons discussed previously, a continuation of this trend would be expected to afford a set of resonances similar to that obtained in ambient temperature d-chloroform (*viz.* the multiplet at 6.97 ppm in **Figure 4.10**).

With this preliminary study adding some weight to the hypothesis, I realised it would be important to continue the VT-NMR work and record low temperature spectra of **298** in d-chloroform. In this case, I was interested to see whether any trends towards the ambient temperature d₈-toluene spectrum might be observed (*i.e. via* the promotion of intramolecular hydrogen bonding). Although CDCl₃ freezes at 207 K, I could not record spectra below about 230 K due to the cooling system available and therefore could not exploit the full range of temperatures possible. Nevertheless, I was interested to see if some trends could still be observed within this temperature range, and recorded ¹H-NMR spectra of **298** in d-chloroform at 298, 273, 253 and 233 K (**Figure 4.14**).

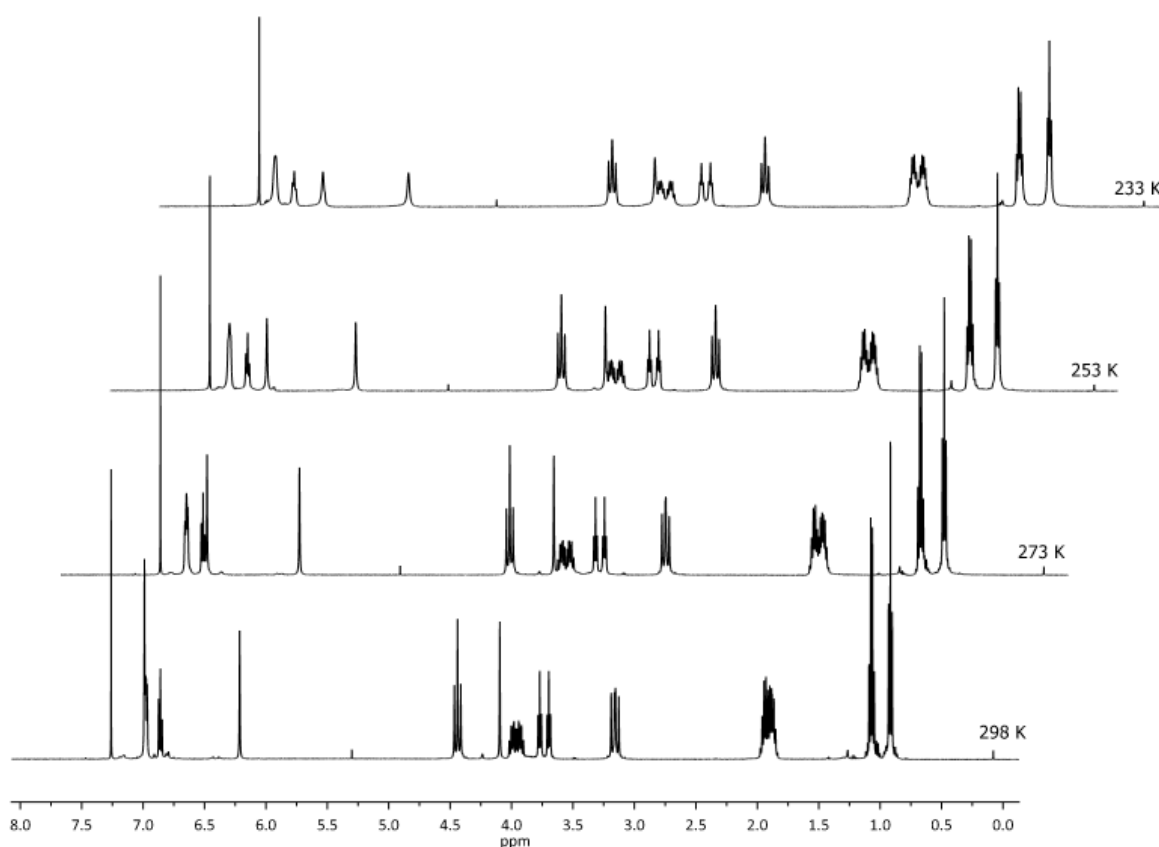


Figure 4.14: Stacked ¹H-NMR spectra of **298** at 298, 273, 253 and 233 K (500 MHz, CDCl₃, 40 mM)

Interestingly, for the low temperature d-chloroform series, the coalescence of the triplets at 3.70 and 3.77 ppm (observed at 298 K) I had anticipated was not observed; although a gradual upfield shift occurred for both triplets upon cooling, these signals never start to coalesce and remained separated by 0.07 ppm in all spectra.

Instead, the most significant spectral changes were observed in the aromatic region. The singlet arising from the aryl protons alpha to the COOH group, for example, undergoes a dramatic upfield shift upon cooling. At 298 K this resonance was displayed at 6.99 ppm, whilst at 233 K the same resonance was observed at 6.74 ppm. This behaviour is quite different from the d_8 -toluene series where the corresponding resonance (*i.e.* 7.33 ppm at 298 K) does not shift significantly throughout the temperature range. These d-chloroform data suggest that this simple model of comparing the qualitative appearance of the two data sets (*i.e.* d_8 -toluene and d-chloroform) was too simplistic, and additional variables were involved.

To proceed, I clearly needed a more reliable way of relating the $^1\text{H-NMR}$ spectra of **298** to its conformation. A thorough search of the literature returned only a small number of studies regarding the interconversion of pinched-cone conformations, all of which involved upper-rim AAAA and ABAB substituted systems, arguably making the interpretation of the solvent and temperature dependent $^1\text{H-NMR}$ spectra somewhat easier than for the ABAC substituted **298**.^{44,221,222} For example, Reinhoudt and co-workers reported that the ABAB substituted *bis*-urea **305** exists predominantly as its pinched-cone conformer **305a** in ambient temperature d-chloroform and the time-averaged C_{4v} cone-conformer **305b** in ambient temperature d_6 -DMSO (Figure 4.15).

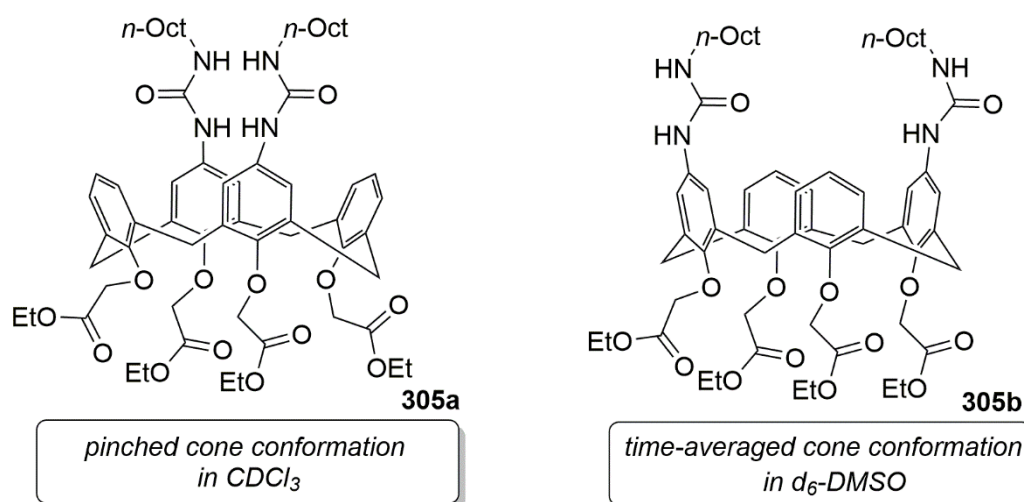


Figure 4.15: Conformational switching between C_{2v} pinched-cone **305a** and C_{4v} cone-conformer **305b**

These conformational assignments were made primarily on the basis of distance measurements between the equatorial protons of the methylene bridges and the two adjacent aromatic protons,

obtained *via* quantitative NOESY spectroscopy. In the time averaged C_{4v} cone-conformer **305b** these distances are equal, whilst in the pinched-cone conformer **305a** they are significantly different (**Figure 4.16**).

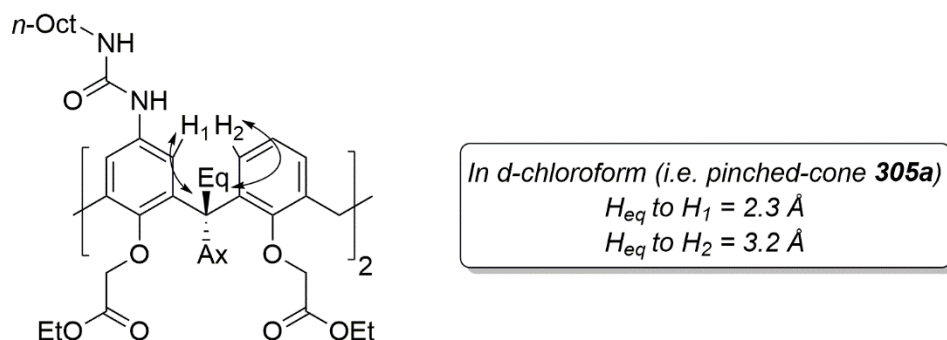


Figure 4.16: Reinhoudt's assignment of solution phase conformation using NOESY spectroscopy²²¹

When the NOESY spectrum of **305** was obtained in d-chloroform, the equatorial methylene protons were calculated to be 0.9 Å closer to H_1 than to H_2 , thereby allowing the conformation to be confidently assigned as pinched-cone **305a**. Motivated by the possibility of using this method in my system, I decided to record the NOESY spectrum of **298** in d-chloroform to study whether any NOE interactions could be observed in the first instance (**Figure 4.17**).

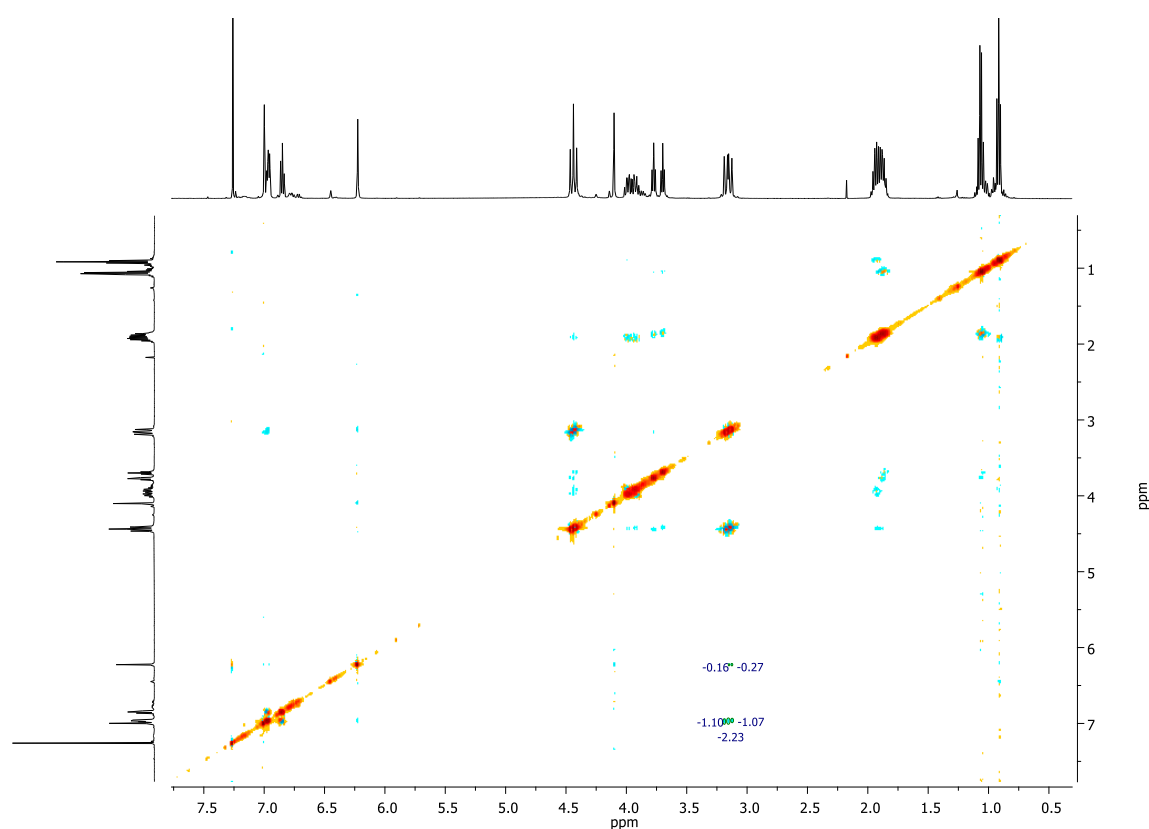


Figure 4.17: NOESY spectrum of **298** (500 MHz, $CDCl_3$, 40 mM)

In accordance with Reinhoudt and co-workers study of the analogous **305a**, I observed cross peaks between both sets of equatorial protons and the *meta* protons of the unsubstituted propyloxy-arenes. I also observed cross peaks between the higher field set of equatorial protons (*ca.* 3.14 ppm) and the singlet at 6.21 ppm which corresponds to the protons alpha to the hydroxymethylene function (**Figure 4.18**).

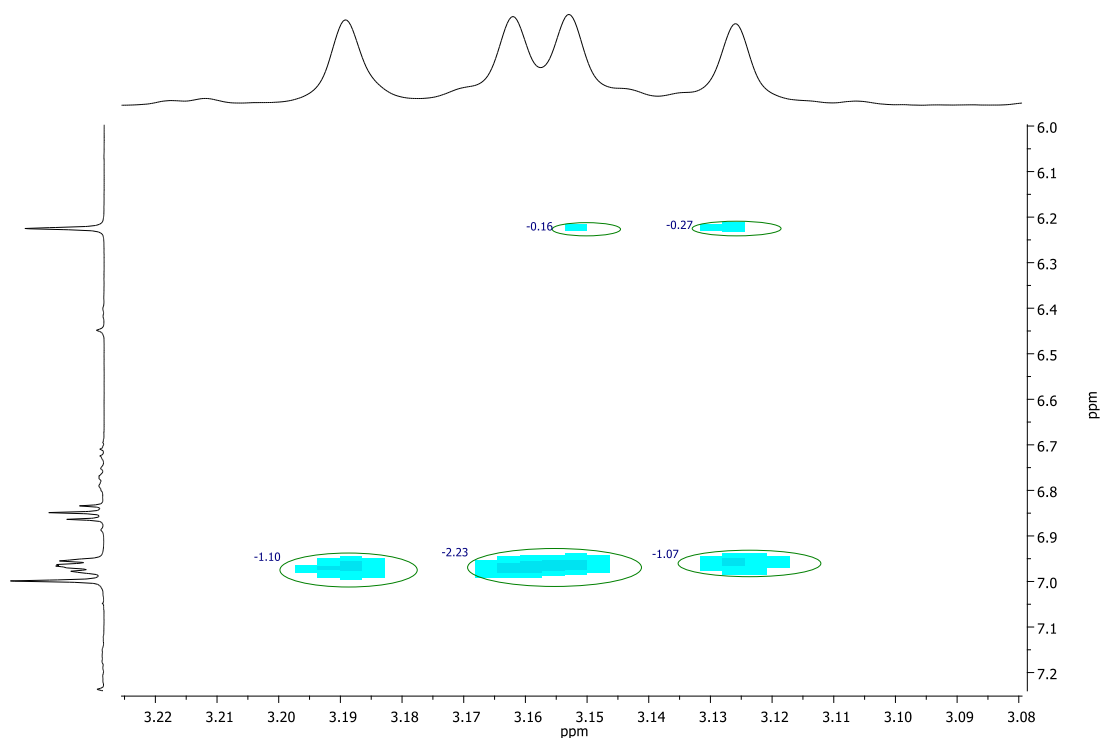


Figure 4.18: Expansion of the NOESY spectrum of **298** (500 MHz, CDCl₃, 40 mM)

Interestingly however, no nuclear Overhauser effect was observed between the lower field set of equatorial protons (*ca.* 3.18 ppm) and the protons alpha to the carboxylic acid functional group at 6.99 ppm as I had anticipated; the reasons for which remain unclear.

Although this spectrum was not acquired under strictly quantitative conditions, it was encouraging to observe that the intensities of the nOe interactions (**Figure 4.18**) between the higher field set of equatorial protons (3.14 ppm) and the *meta* protons of the unsubstituted propyloxy-arenes were noticeably greater than those to the protons alpha to the hydroxymethylene function. Since the intensity of an nOe interaction decreases with $1/r^6$ where r is equal to the inter-nuclear separation, these results might suggest that **298** adopts a time-averaged pinched cone conformation which, in *d*-chloroform, splay the functionalised aryl units apart in space. With time constraints at the end of this project, I was unable to investigate further and instead switched my focus to studying the NLO properties of these novel materials by SHG spectroscopy (**Section 4.10**).

4.11 SHG photophysics study of NLOphore calix[4]arenes **260** and **121**

With the results of the $^1\text{H-NMR}$ studies using **298** difficult to interpret fully, I wanted to exploit a more direct spectroscopic method to study the NLO properties of the second generation designs. Crucially, I wanted to understand whether these NLO properties might be ‘solvent-switchable’ as had been anticipated. To do this, I turned to the literature to review previous work in this area.

In one of the earliest studies made of NLOphore calix[4]arenes (**Section 1.5.5**), Hennrich and co-workers reported the application of second harmonic generation (SHG) spectroscopy as a powerful analytical tool to measure the first hyperpolarizabilities, β , of a series of *para*-nitroethynyl substituted calix[4]arenes (**Figure 4.19**).

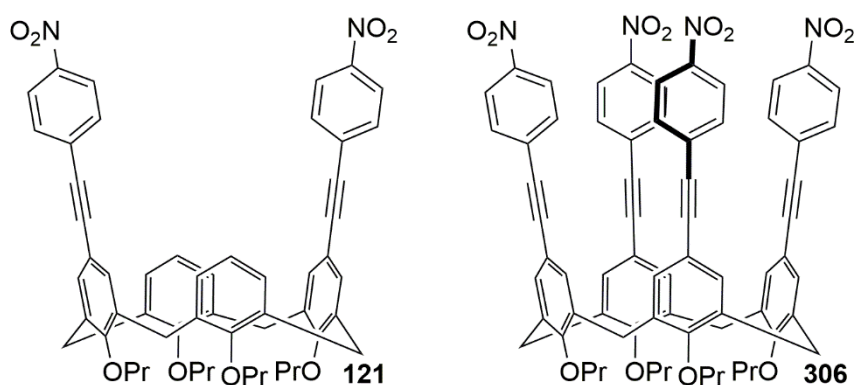


Figure 4.19: Structures of NLOphore calix[4]arenes **121** and **306** studied by Hennrich and co-workers

The magnitude of β (in basic terms) reflects the non-linearity of the transition between ground and excited states, a parameter which, in turn, relates to the difference in dipole moment between ground and excited states.⁴⁶ Notably, through mathematical analysis, the Spanish group were able to relate the dipole moments of the NLOphore calix[4]arenes **306** and **121** to the opening angle θ of the calix[4]arene cavities.

This spectroscopic technique was therefore exactly what I required to test the calix[4]arene based NLOphores (*e.g.* **260**). However, as these SHG measurements require specialised equipment and techniques to obtain, the Bew and Stephenson groups initiated a collaboration with Professor Verbiest and co-workers in Leuven; a group with much expertise in this area.^{110,223} To initiate these studies, I needed to consider which compounds would provide the most information regarding the switching capability of the second generation designs. Since Hennrich and co-workers had already reported their results on the NLO properties of the *bis*-nitrophenyl substituted **121**, which lacks any ‘switchable’ element, it was proposed that a direct comparison with the CH_2OH , NO_2 , COOH , NO_2 functionalised **260** would yield an appropriate set of data.

The experimental set-up employed was the same as that used by Hennrich and co-workers in their 2007 publication, with the added complexity that the series of SHG measurements of **121** and **260** obtained were recorded in DCM with increasing volumes of DMSO added (from 0 to 80%). For the reference compound **121** (synthesised *via* the literature procedure) I anticipated that no trend in first hyperpolarizability would be observed with increasing concentration of DMSO. Whilst for the ‘switchable’ **260** I anticipated that a disruption in hydrogen bonding at the upper-rim would manifest as a clear trend in first hyperpolarizability (by promoting a conformational change which increases the dipole moment of **260**). Additionally, as I wanted to be able to discern *intramolecular* hydrogen bonding from any *intermolecular* effects, these measurements were made at two concentration regimes (*i.e.* 1×10^{-5} M and 5×10^{-6} M). The data for these two compounds are illustrated below (Figure 4.20).

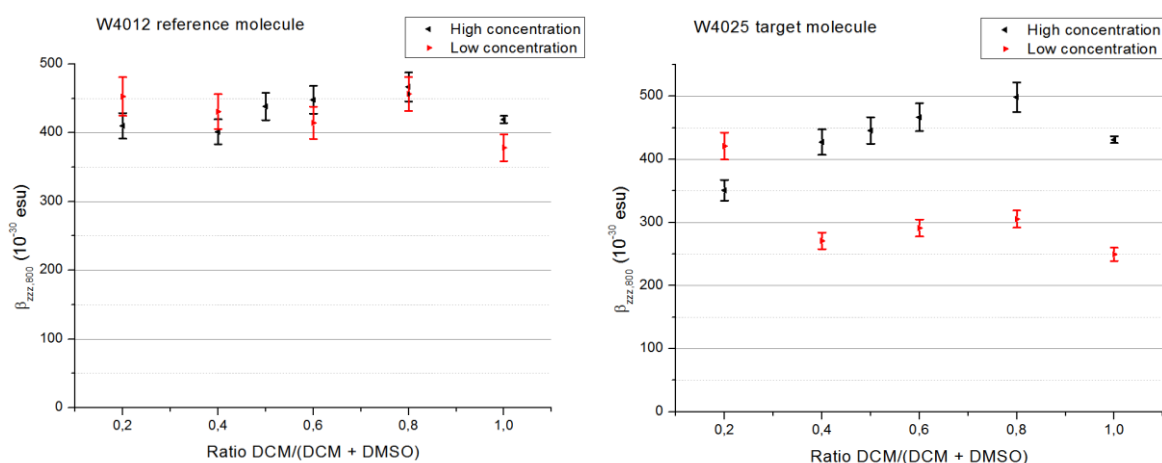


Figure 4.20: Left: first hyperpolarizabilities of reference compound **121** at two concentrations with increasing concentration of DMSO. Right: first hyperpolarizabilities of reference compound **260** at two concentrations with increasing concentration of DMSO. Data obtained by Verbiest and co-workers.

For the reference compound *bis*-nitrophenyl substituted **121** (Figure 4.20, left) no significant change in the first hyperpolarizability β was observed with increasing concentration of DMSO, for either low or high concentration series. Auspiciously, the magnitude of β in neat DCM at 1×10^{-6} M (*i.e.* 419×10^{-30} esu) was in close agreement with the value reported by Hennrich and co-workers for **121** ($480 \pm 20 \times 10^{-30}$ esu). These results suggest that the opening angle θ of **121** (calculated to be $27 \pm 5^\circ$ by Hennrich *et al.* in neat DCM) is not affected by the polarity of the solvent; therefore, as I had anticipated, the NLO properties of **121** are not solvent switchable.

In contrast, the value of first hyperpolarizability for ‘second generation’ **260** changes significantly upon the addition of DMSO, for both high and low concentration series. For the high concentration series (1×10^{-5} M) an increase in the first hyperpolarizability was observed upon the addition of 20 volume percent DMSO, which then gradually decreases with increasing volumes of DMSO. A similar trend is observed for the low concentration series (5×10^{-6} M) although the magnitudes of β are significantly lower (about 200×10^{-30} esu) consistent with some contribution from *intermolecular* hydrogen bonding. Although neither series (high or low concentration) displays a clear trend in β over the full range of solvent polarities, the high concentration series does show a linear relationship between increasing solvent polarity and β , following the initial addition of 20 volume percent DMSO.

However, this relationship is not what I had anticipated based on the model of conformation switching proposed at the outset of this project (**Figure 4.21**).

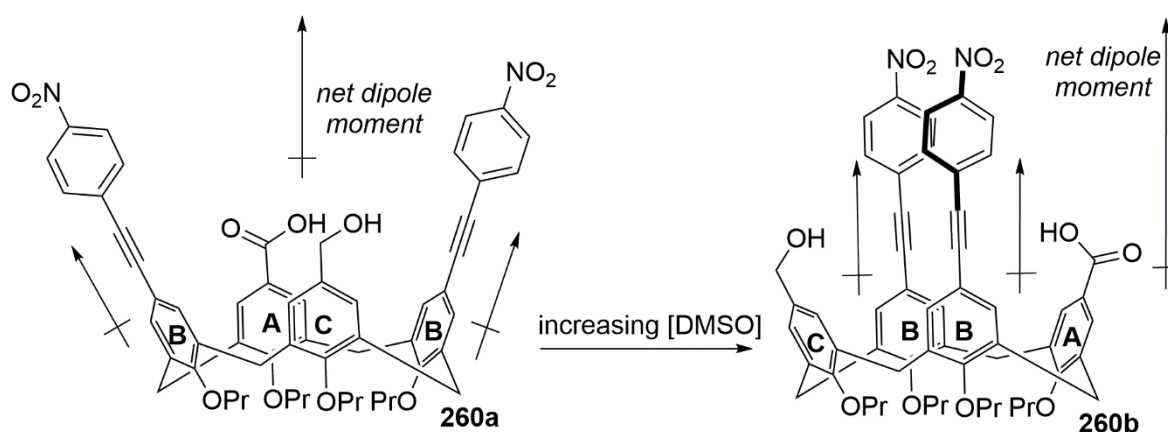


Figure 4.21: Conformational switching anticipated for **260** upon increasing [DMSO]

I had expected that, with increasing solvent polarity, **260** would adopt the pinched cone conformation **260b** which places the (donor)-(π)-(acceptor) units along the central axis of the calix[4]arene core; a conformational change that would increase the net dipole moment (over **260a**) and consequently, increase the magnitude of second harmonic generation. Clearly then, this model does not satisfactorily explain the measured data (**Figure 4.20**) which, after an initial increase in β of about 60×10^{-30} esu, displays a gradual decrease in the magnitude of β . This could be a result of *intramolecular* effects (the presence of which was revealed by the low concentration series) but more work is required to fully understand these results.

Attempts at obtaining SHG data for the ABCD functionalised **303** (**Scheme 4.26**) were hampered by the presence of a high fluorescence contribution which could not be compensated for using standard protocols (*i.e.* the ‘chopper’ and ‘demodulation’ techniques). Thus it was not possible to compare the effect of modifying solvent polarity on **303**, to the corresponding data obtained for **260**.

4.12 Conclusions and outlook

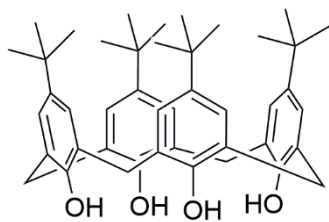
In this project I have developed synthetic methods which allow for the generation of upper-rim ABAC and ABCD functionalised calix[4]arenes (*i.e.* **260** and **303**) *via* a protocol which employs the mechanochemical Cannizzaro reaction (**Section 4.8**) as a key enabling step. Preliminary studies into their application as solvent switchable NLOphores were encouraging, with SHG spectroscopic investigations indicating that changes in the magnitude of first hyperpolarizability β could be promoted by modulations in solvent polarity. However, a strong model which fully explains these data is still lacking and further work should be directed towards gaining a fuller understanding of the physicochemical properties (particularly in regards to conformation) of these new materials.



Experimental Section

General Information

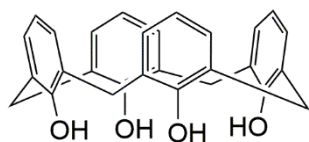
All air and water sensitive reactions were carried out in flame-dried apparatus under an atmosphere of argon with magnetic stirring unless otherwise indicated. Analytical thin-layer chromatography (TLC) was performed on Merck Millipore F₂₅₄ silica gel sheets and visualisation was achieved by irradiation with UV light (254 nm), and/or staining with potassium permanganate, ninhydrin or anisaldehyde followed by heating. Flash column and automated column chromatography was performed using Material Harvest silica gel 60 (40 – 63 μm) with either standard glass columns or a Biotage Isolera SP1 purification system. ¹H- and ¹³C-NMR spectra were recorded on either a Bruker Avance 500 (500 MHz) or Bruker Avance 400 (400 MHz) spectrometer. Chemical shifts are reported in δ (ppm) and are referenced to the residual solvent signals (¹H NMR: CDCl₃ at 7.26 ppm, (CD₃)₂SO at 2.50 ppm and C₆D₆ at 7.16 ppm; ¹³C NMR: CDCl₃ at 77.16 ppm, (CD₃)₂SO at 39.52 ppm and C₆D₆ at 128.06 ppm). Signal multiplicities are described as: s = singlet, d = doublet, t = triplet, q = quartet, m = multiplet, br = broad, and coupling constants are reported in Hertz (Hz). FT-IR spectra were recorded on a Perkin Elmer Spectrum 100 series spectrometer on sodium chloride plates as thin films, and are reported in wavenumbers (cm⁻¹). Low resolution mass spectrometry (LRMS) was carried out on a Shimadzu Axima MALDI-TOF instrument. High resolution mass spectrometry (HRMS) was carried out by the EPSRC National Mass Spectrometry Service at the University of Swansea. Ion mass/charge (*m/z*) ratios are reported as values in atomic mass units. Melting points of crystalline solids were recorded on a Stuart Scientific SMP1 apparatus in open-ended capillary tubes and are uncorrected. Microwave reactions were carried out using an Emerys Creator microwave reactor (300 W) in sealed vessels. Dichloromethane and methanol were distilled from calcium hydride under an atmosphere of argon. Tetrahydrofuran and diethyl ether were distilled from sodium benzophenone ketyl under an atmosphere of argon. All other solvents and reagents were purchased from commercial sources and used as received.



Synthesis of 33⁷: To a three-necked 5 L RBF was added *p*-tert-butylphenol (500 g, 3.3 mol), formaldehyde (332 mL, 38% solution in water, 4.1 mol) and 10 M aqueous sodium hydroxide (15 mL, 0.15 mol). The flask was equipped with an overhead mechanical stirrer and an inlet for nitrogen, then stirred and heated under a strong flow of

nitrogen gas at 100 °C until the mixture expanded into a viscous mass (*ca.* 1 h). At this point the heat source was removed, and the material was allowed to cool to room temperature. Diphenyl ether (2.5 L) and toluene (100 mL) were then added, and after fitting a still head and removing the mechanical stirrer, the mixture was heated to 150 °C until all of the remaining water had been collected. The mixture was then heated at reflux for 6 h, and allowed to cool to 60 °C before the addition of ethyl acetate (1.5 L). Upon cooling to room temperature, the precipitate was collected by suction filtration and washed with acetone (500 mL). Drying to constant weight in a vacuum oven at 60 °C overnight afforded **33** as an off-white solid which was used without further purification (297 g, 0.45 mol, 55%). Analysis revealed the solid to be the title compound. Spectral data were in accordance with literature values.⁷

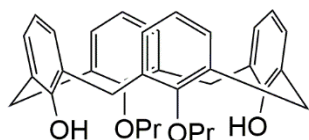
¹H-NMR (500 MHz, CDCl₃) δ 10.3 (s, 4H), 7.0 (s, 8H), 4.2 (d, 4H, *J* = 14 Hz), 3.5 (d, 4H, *J* = 14 Hz), 1.2 (s, 36H) ppm; ¹³C-NMR (126 MHz, CDCl₃) δ 146.9, 144.5, 127.7, 126.1, 34.2, 32.7, 31.6 ppm; FTIR (thin film) 3172 (OH) cm⁻¹



Synthesis of 37²²⁴: A 1 L RBF was charged with a suspension of **33** (50 g, 77 mmol) and phenol (34.8 g, 370 mmol) in toluene (300 mL). Aluminium chloride (53.9 g, 405 mmol) was added and the mixture

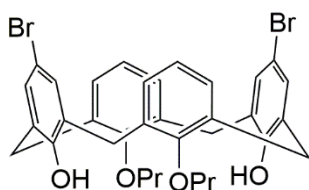
stirred for 1 h at room temperature under an atmosphere of nitrogen. The mixture was then poured onto crushed ice (*ca.* 300 g) and extracted with dichloromethane (300 mL). The dichloromethane was removed by rotary evaporation, and the product was precipitated by the addition of methanol (200 mL) to afford a white solid which was collected by suction filtration. The precipitate was washed with pentane (40 mL) and dried in a vacuum oven overnight to afford **37** as a white solid (27.8 g, 65.5 mmol, 85%). Analysis revealed the solid to be the title compound. Spectral data were in accordance with literature values.²²⁴

¹H-NMR (500 MHz, CDCl₃) δ 10.2 (s, 4H), 7.0 (d, 8H, *J* = 7.7 Hz), 6.7 (t, 4H, *J* = 7.7 Hz), 4.2 (brs, 4H), 3.5 (brs, 4H) ppm; ¹³C-NMR (126 MHz, CDCl₃) δ 145.1, 129.2, 128.4, 122.4, 31.7 ppm; FTIR (thin film) 3142 (OH) cm⁻¹



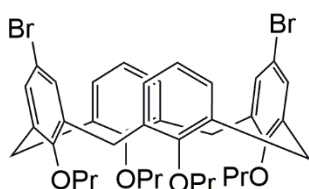
Synthesis of 38²²⁵: A 500 mL RBF was charged with a mixture of **37** (9.82 g, 23.1 mmol) and potassium carbonate (3.58 g, 25.9 mmol) in acetonitrile (150 mL). *n*-Propyl iodide (5.1 mL, 52.1 mmol) was added *via* syringe, and the mixture heated at reflux for 18 h under an atmosphere of nitrogen. The reaction mixture was allowed to cool to room temperature, and the solvent was removed *in vacuo*. The residue was partitioned between dichloromethane (100 mL) and 1M HCl (100 mL), and the organic phase separated, dried over magnesium sulfate, filtered and concentrated *in vacuo* to afford an off-white solid. Trituration with methanol (50 mL) afforded **38** as a white solid (10.2 g, 20.1 mmol, 87%). Analysis revealed the solid to be the title compound. Spectral data were in accordance with literature values.²²⁵

¹H-NMR (500 MHz, CDCl₃) δ 8.28 (s, 2H), 7.02 (d, 4H, *J* = 7.4 Hz), 6.92 (d, 4H, *J* = 7.4 Hz), 6.72 (t, 2H, *J* = 7.4 Hz), 6.63 (t, 2H, *J* = 7.4 Hz), 4.29 (d, 4H, *J* = 13.0 Hz), 3.99 (t, 4H, *J* = 7 Hz), 3.38 (d, *J* = 13.0 Hz, 4H), 2.12 – 2.02 (m, 4H), 1.32 (t, *J* = 7.4 Hz, 6H) ppm; **¹³C-NMR** (126 MHz, CDCl₃) δ 153.0, 151.7, 133.9, 128.7, 128.3, 128.0, 125.2, 118.9, 78.3, 31.4, 23.6, 11.0 ppm; **FTIR** (thin film) 3370 (OH) cm⁻¹



Synthesis of 146a³⁷: A 250 mL RBF was charged with a solution of **38** (6.18 g, 12.2 mmol) in dichloromethane (80 mL) under an atmosphere of nitrogen. Bromine (1.88 mL, 36.4 mmol) was added dropwise *via* syringe, and the mixture stirred at room temperature for 2 h. The mixture was cooled in ice, and the precipitate collected by suction filtration and washed with dichloromethane (20 mL) to afford **146a** as an off-white solid (7.29 g, 10.9 mmol, 90%). Analysis revealed the solid to be the title compound. Spectral data were in accordance with literature values.³⁷

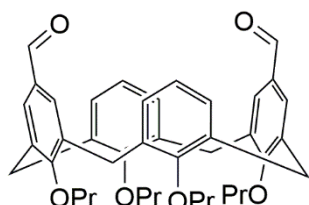
¹H-NMR (500 MHz, CDCl₃) δ 8.36 (s, 2H), 7.14 (s, 4H), 6.91 (d, 4H, *J* = 7.0 Hz), 6.78 (t, 2H, *J* = 7.0 Hz), 4.22 (d, 4H, *J* = 12 Hz), 3.92 (t, 4H, *J* = 6.0 Hz), 3.29 (d, 4H, *J* = 12 Hz), 2.03 (m, 4H), 1.26 (t, 6H, *J* = 8 Hz) ppm; **FTIR** (thin film) 3275 (OH) cm⁻¹



Synthesis of 146³⁷: A 250 mL RBF was charged with a suspension of **146a** (3.88 g, 5.83 mmol) in anhydrous *N,N*-dimethylformamide (50 mL) under an atmosphere of nitrogen. Sodium hydride (60% in mineral oil, 0.893 g, 23.3 mmol) was added in one portion, and the mixture stirred at room temperature for 0.5 h before the addition of *n*-propyl iodide (2.8 mL, 29.1 mmol) *via* syringe. The mixture was stirred at room temperature for 18 h and then quenched by the addition of 1M HCl (80 mL). The precipitate was collected by suction filtration and washed with methanol (30

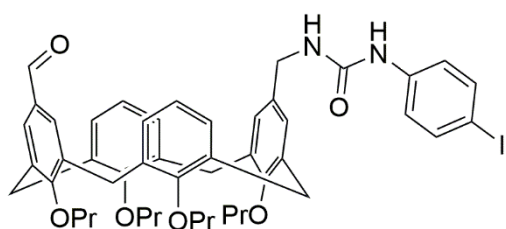
mL) to afford **146** as a white solid (4.03 g, 5.36 mmol, 92%). Analysis revealed the solid to be the title compound. Spectral data were in accordance with literature values.³⁷

¹H-NMR (500 MHz, CDCl₃) δ 6.77 (s, 4H), 6.64 (s, 4H), 4.40 (d, *J* = 13.4 Hz, 4H), 3.86 – 3.79 (m, 8H), 3.11 (d, *J* = 13.4 Hz, 4H), 1.96 – 1.86 (m, 6H), 1.04 – 0.91 (m, 12H) ppm; ¹³C-NMR (126 MHz, CDCl₃) δ 156.2, 155.8, 132.7, 134.0, 130.8, 128.4, 122.5, 115.0, 76.5, 30.9, 23.2, 10.2 ppm.



Synthesis of 139⁵¹: A 250 mL RBF was charged with a suspension of **146** (10.01 g, 13.3 mmol) in anhydrous tetrahydrofuran (80 mL) at -78 °C under an atmosphere of nitrogen. *n*-Butyl lithium (2.0 M in hexanes, 26 mL, 53.3 mmol) was added *via* syringe in one portion, and the mixture stirred at this temperature for 15 minutes before the addition of anhydrous *N,N*-dimethylformamide (21 mL, 226 mmol) *via* syringe in one portion. After stirring for a further 0.5 h at -78 °C, the reaction mixture was poured into ice cold 4 M HCl (100 mL), and extracted with chloroform (2 x 150 mL). The organic extracts were combined and washed with a saturated solution of sodium hydrogen carbonate 150 mL) and water (4 x 150 mL), then dried over magnesium sulfate, filtered, and concentrated to afford an off white solid. Recrystallisation of this material from *n*-hexane (100 mL) afforded **139** as a white solid (5.62 g, 8.66 mmol, 65 %). Analysis revealed the solid to be the title compound. Spectral data was in accordance with literature values.⁵¹

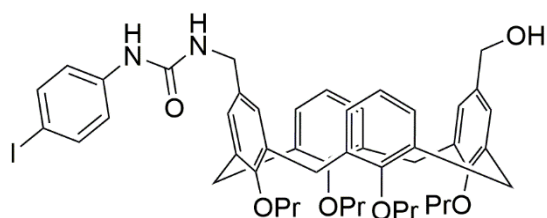
¹H-NMR (500 MHz, CDCl₃) δ 9.44 (s, 2H), 6.97 (s, 4H), 6.69 (m, 6H), 4.44 (d, 4H, *J* = 13.6 Hz), 3.85 (m, 8H), 3.20 (d, 4H, *J* = 13.6 Hz), 1.88 (m, 8H), 1.00 (t, 6H, *J* = 7.4 Hz), 0.94 (t, 6H, *J* = 7.4 Hz) ppm; ¹³C-NMR (126 MHz, CDCl₃) δ 192.1, 162.4, 156.8, 132.1, 134.9, 131.4, 130.1, 129.0, 122.8, 77.4, 77.0, 31.1, 23.7, 23.5, 10.6, 10.3 ppm; FTIR (thin film) 1682 (C=O) cm⁻¹



Synthesis of 141¹¹⁶: A 20 mL capacity vial was charged with a mixture of **139** (1.5 g, 2.31 mmol) and *p*-iodophenyl urea (1 g, 3.81 mmol) in anhydrous toluene (10 mL) under an atmosphere of argon. Trifluoroacetic acid (1.51 mL, 19.7 mmol) and triethylsilane (3.5 mL, 21.96 mmol) were then added in succession *via* syringe. The mixture was allowed to stir in the dark for 18 h at room temperature, after which time TLC analysis (30% ethyl acetate in petrol) indicated **139** had formed as the major product. The reaction mixture was diluted with ethyl acetate (30 mL) and then washed with a saturated solution of sodium hydrogen carbonate (20 mL) and brine (20 mL). The organic phase was separated, dried over magnesium sulfate, filtered and concentrated to

afford a pale purple solid. Purification by column chromatography on silica gel (25% ethyl acetate in petrol) afforded **139** as a white solid (1.12 g, 1.25 mmol, 54%). Analysis revealed the solid to be the title compound. Spectral data was in accordance with literature values.¹¹⁶

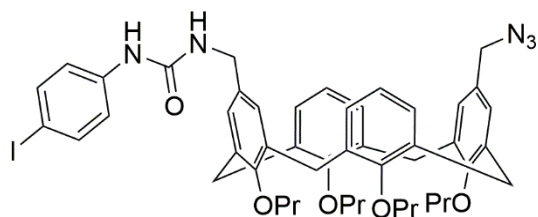
¹H-NMR (500 MHz, CDCl₃) δ 9.42 (s, 1H), 7.57 (d, *J* = 8.8 Hz, 2H), 7.29 (d, *J* = 8.8 Hz, 2H), 7.05 (d, *J* = 7.5 Hz, 4H), 6.83 (s, 2H), 6.80 (t, *J* = 7.5 Hz, 2H), 6.19 (s, 2H), 4.50 (d, *J* = 13.3 Hz, 2H), 4.40 (d, *J* = 13.2 Hz, 2H), 4.10 – 4.04 (m, 2H), 3.99 – 3.92 (m, 2H), 3.80 (m, 4H), 3.65 (t, *J* = 6.9 Hz, 2H), 3.22 (d, *J* = 13.4 Hz, 2H), 3.13 (d, *J* = 13.2 Hz, 2H), 2.02 – 1.83 (m, 8H), 1.11 (t, *J* = 7.4 Hz, 3H), 1.06 (t, *J* = 7.4 Hz, 3H), 0.91 (t, *J* = 7.5 Hz, 6H) ppm; **¹³C-NMR** (126 MHz, CDCl₃) δ 193.2, 157.2, 155.1, 154.7, 138.9, 137.1, 136.0, 135.6, 134.6, 133.4, 131.8, 130.3, 130.1, 129.1, 128.3, 126.6, 122.2, 120.6, 84.2, 77.0, 76.2, 43.0, 30.3, 22.9, 22.5, 10.2, 9.3 ppm; **FTIR** (thin film) 1685 (C=O), 1664 (urea C=O) cm⁻¹



Synthesis of 162: To a solution of **141** (400 mg, 0.45 mmol) in isopropanol (12 mL) was added sodium borohydride (25 mg, 0.67 mmol) in one portion. The mixture was stirred at room temperature for 0.5 h under an atmosphere of nitrogen. TLC analysis (30 %

ethyl acetate in petrol) indicated that the starting material **141** had been consumed. The mixture was diluted with ethyl acetate (25 mL), and then washed with water (15 mL) and brine (15 mL). The organics were dried over magnesium sulfate, filtered and concentrated to afford **162** (392 mg, 0.44 mmol, 98 %) as a white solid.

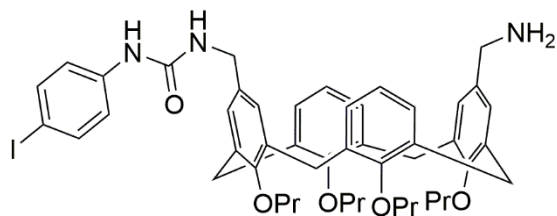
¹H-NMR (500 MHz, CDCl₃) δ 7.54 (d, *J* = 8.3 Hz, 2H), 7.12 (d, *J* = 8.1 Hz, 2H), 7.07 (brs, 1H), 6.97 (d, *J* = 7.5 Hz, 4H), 6.72 (t, *J* = 7.4 Hz, 2H), 6.35 (s, 2H), 6.27 (s, 2H), 4.77 (brs, 1H), 4.46 (d, *J* = 13.0 Hz, 2H), 4.42 (d, *J* = 13.0 Hz, 2H), 4.24 (s, 2H), 3.99 (m, 4H), 3.85 (d, *J* = 4.5 Hz, 2H), 3.69 (m, 4H), 3.15 (d, *J* = 12.4 Hz, 2H), 3.13 (d, *J* = 12.4 Hz, 2H), 2.00 (m, 2H), 1.89 (m, 2H), 1.07 (m, 6H), 0.92 (t, *J* = 7.5 Hz, 6H) ppm; **¹³C-NMR** (126 MHz, CDCl₃) δ 157.3, 155.4, 155.1, 139.6, 137.8, 136.4, 136.2, 134.1, 133.9, 132.1, 128.9, 128.7, 127.0, 126.0, 122.3, 121.2, 84.9, 76.7, 64.6, 43.5, 31.11, 31.16, 23.6, 23.1, 10.8, 10.8, 10.1 ppm; **FT-IR** (neat) 3333, 2960, 2927, 2874, 1661, 1586, 1543, 1463, 1390, 1306, 1260, 1217, 1006, 965, 801 cm⁻¹; **MS** (MALDI) *m/z* 919.88 [M + Na]⁺; **HRMS** [M + NH₄]⁺ Calculated for C₄₉H₆₁IN₃O₆: 914.3600; Found: 914.3596



Synthesis of 158: To a solution of **162** (200 mg, 0.22 mmol) in anhydrous toluene (8 mL) was added diphenylphosphoryl azide (96 μ L, 0.45 mmol) followed by DBU (67 μ L, 0.45 mmol) under an atmosphere of nitrogen, and the mixture stirred at

room temperature for 18 h. TLC analysis (30 % ethyl acetate in petrol) indicated that the starting material **162** had been consumed. The mixture was diluted with ethyl acetate (20 mL), and then washed with water (15 mL) and brine (15 mL). The organics were dried over magnesium sulfate, filtered and concentrated to afford a brown solid. Purification by column chromatography on silica gel (40% ethyl acetate in petrol) afforded **158** as a white solid (180 mg, 0.19 mmol, 86 %).

¹H-NMR (500 MHz, CDCl₃) δ 7.56 (d, J = 8.8 Hz, 2H), 7.05 (d, J = 8.8 Hz, 2H), 6.56 (m, 10H), 4.87 (t, J = 5.4 Hz, 1H), 4.45 (d, J = 13.7 Hz, 2H), 4.42 (d, J = 13.7 Hz, 2H), 4.09 (d, J = 5.4 Hz, 2H), 4.01 (s, 2H), 3.84 (m, 8H), 3.15 (d, J = 13.3 Hz, 2H), 3.12 (d, J = 13.3 Hz, 2H), 1.92 (m, 8H), 0.99 (m, 12H) ppm; **¹³C-NMR** (126 MHz, CDCl₃) δ 156.9, 156.5, 156.4, 155.2, 138.8, 138.1, 135.8, 135.6, 134.9, 134.8, 128.6, 128.4, 128.3, 128.2, 127.5, 122.4, 122.2, 86.3, 77.1, 77.1, 54.6, 44.3, 31.1, 23.4, 23.3, 10.4 ppm; **FT-IR** (neat) 3339, 2961, 2931, 2874, 2096, 1650, 1586, 1545, 1486, 1475, 1390, 1307, 1282, 1219, 1196, 1135, 1082, 1066, 1037, 1006, 966, 908, 855, 820, 758 cm⁻¹; **MS** (MALDI) m/z 917.8 [M - N₂ + Na]⁺; **HRMS** [M + NH₄]⁺ Calculated for C₄₉H₆₀N₆O₅: 939.3664; Found: 939.3661

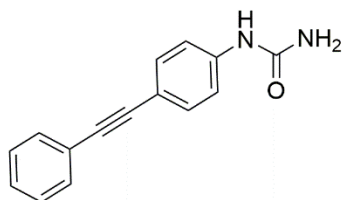


Synthesis of 142: To a solution of **158** (50 mg, 0.054 mmol) in THF (1 mL) was added triphenylphosphine (29 mg, 0.11 mmol) and water (98 μ L, 5.42 mmol). The mixture was stirred at room temperature for 18 h under an atmosphere of nitrogen. TLC analysis (30

% ethyl acetate in petrol) indicated that the starting material **158** had been consumed. The mixture was diluted with ethyl acetate (5 mL), then washed with water (2 mL) and brine (2 mL). The organics were dried over magnesium sulfate, filtered and concentrated to afford a white solid. Purification by column chromatography on silica gel (gradient elution: 1 to 20 % methanol in dichloromethane) afforded **142** as a white solid (35 mg, 0.039 mmol, 72 %).

¹H-NMR (500 MHz, CDCl₃) δ 7.52 (d, J = 8.7 Hz, 2H), 7.13 (d, J = 8.7 Hz, 2H), 7.01 (m, 4H), 6.71 (t, J = 7.4 Hz, 2H), 6.25 (s, 2H), 6.15 (s, 2H), 4.45 (d, J = 13.1 Hz, 2H), 4.40 (d, J = 13.0 Hz, 2H), 4.01 (m, 4H), 3.71 (s, 2H), 3.67 (t, J = 6.9 Hz, 2H), 3.63 (t, J = 7.0 Hz, 2H), 3.42 (s, 2H), 3.14 (d, J = 8.1 Hz, 2H), 3.11 (d, J = 8.0 Hz, 2H), 2.00 (m, 4H), 1.89 (m, 4H), 1.07 (m, 6H), 0.90 (t, J = 7.5 Hz, 6H) ppm; **¹³C-NMR** (126 MHz, CDCl₃) δ 157.5, 156.2, 155.5, 154.8, 139.8, 137.7, 136.7, 136.2, 134.5, 133.6, 131.9, 129.2,

128.8, 126.7, 125.7, 122.4, 121.0, 84.6, 76.6, 43.8, 42.8, 31.1, 23.6, 23.1, 10.8, 10.8, 10.0 ppm; **FT-IR** (neat) 3314, 2960, 2932, 2874, 1663, 1586, 1547, 1485, 1462, 1390, 1307, 1282, 1218, 1134, 1038, 1005, 965, 908, 820, 759, 733 cm^{-1} ; **MS** (MALDI) m/z 918.46 $[\text{M}+\text{Na}]^+$; **HRMS** $[\text{M}+\text{H}]^+$ Calculated for $\text{C}_{49}\text{H}_{59}\text{N}_3\text{O}_5$: 896.3494; Found: 896.3494



Synthesis of 143: A flame-dried microwave vial was charged with a mixture of *para*-iodophenyl urea **140** (0.5 g, 1.91 mmol), $\text{Pd}(\text{PPh}_3)\text{Cl}_2$ (100 mg, 0.95 mmol) and copper(I)iodide (36 mg, 0.19 mmol) in anhydrous DMF (10 mL) under an atmosphere of argon. Triethylamine (610 μL , 3.8 mmol) and phenylacetylene **134** (838 μL , 7.63 mmol) were added, and the mixture heated to 120 $^\circ\text{C}$ in the microwave synthesiser for 1 hour. The solvents were removed *in vacuo* and the residue taken up in ethyl acetate (30 mL) then washed with 5% aqueous citric acid (20 mL) and brine (20 mL). The organic phase was separated, dried (MgSO_4), filtered and concentrated *in vacuo* to afford a brown solid. Trituration of this material with diethyl ether afforded **143** as a light brown solid (390 mg, 1.65 mmol, 87%).

$^1\text{H-NMR}$ (d_6 -DMSO, 500 MHz) δ 8.76 (s, 1H), 7.51 (m, 2H), 7.46 (d, 2H, $J = 8.6$ Hz), 7.40 (m, 5H), 5.95 (s, 2H) ppm; **$^{13}\text{C-NMR}$** (d_6 -DMSO, 126 MHz) 155.7, 141.2, 132.1, 131.1, 128.7, 128.3, 122.8, 117.5, 114.8, 89.9, 87.9 ppm; **FT-IR** (neat) 3484, 3386, 3219, 3055, 2190, 1623, 1608, 1515, 1440, 1299, 1179, 829, 739, 616 cm^{-1} ; **MS** (MALDI) m/z 259.23 $[\text{M}+\text{Na}]^+$; **HRMS** $[\text{M} + \text{H}]^+$ Calculated for $\text{C}_{15}\text{H}_{13}\text{N}_2\text{O}$: 237.0924; Found: 237.0927



Synthesis of 189: A flame-dried microwave vial was charged with a mixture of TMS-protected **185** (542 mg, 2.66 mmol), $\text{Pd}(\text{PPh}_3)_4$ (140 mg, 0.12 mmol), 4-iodoaniline (471 mg, 2.66 mmol), K_2CO_3 (1 g, 7.24 mmol) and copper(I)iodide (46 mg, 0.24 mmol) in anhydrous THF (8 mL) and MeOH (2 mL). The mixture was degassed with nitrogen before the addition of *N,N*-diisopropylethylamine (0.63 mL, 3.62 mmol) *via* syringe, then heated at 70 $^\circ\text{C}$ under microwave irradiation for 4 hours. The reaction mixture was absorbed directly onto silica. Purification by column chromatography on silica gel (gradient 15 to 100% ethyl acetate in petrol) afforded **189** (480 mg, 2.15 mmol, 81%) as a yellow solid. Spectral data was in accordance with literature values.²²⁶

$^1\text{H-NMR}$ (500 MHz, CDCl_3) δ 7.43 (d, $J = 8.9$ Hz, 2H), 7.32 (d, $J = 8.6$ Hz, 2H), 6.86 (d, $J = 8.9$ Hz, 2H), 6.63 (d, $J = 8.6$ Hz, 2H), 3.82 (s, 3H) ppm; **$^{13}\text{C-NMR}$** (CDCl_3 , 126 MHz) δ 159.3, 146.5, 132.9, 132.9, 114.9, 114.0, 55.4 ppm; **FT-IR** (neat) 3475, 3381, 3212, 3055, 2202, 1620, 1605, 1584, 1574, 1514, 1396, 1293, 1176, 827, 799 cm^{-1}



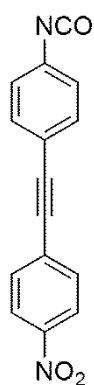
Synthesis of 190: A flame-dried microwave vial was charged with a mixture of TMS-protected **186** (582 mg, 2.66 mmol), Pd(PPh₃)₄ (140 mg, 0.12 mmol), 4-iodoaniline (471 mg, 2.66 mmol), K₂CO₃ (1 g, 7.24 mmol) and copper(I)iodide (46 mg, 0.24 mmol) in anhydrous THF (8 mL) and MeOH (2 mL). The mixture was degassed with nitrogen before the addition of *N,N*-diisopropylethylamine (0.63 mL, 3.62 mmol) *via* syringe, then heated at 70 °C under microwave irradiation for 4 hours. The reaction mixture was absorbed directly onto silica. Purification by column chromatography on silica gel (gradient 15 to 100 % ethyl acetate in petrol) afforded **190** (430 mg, 1.81 mmol, 68%) as a yellow solid. Spectral data was in accordance with literature values.²²⁷

¹H-NMR (500 MHz, CDCl₃) δ 8.16 (d, *J* = 8.9 Hz, 2H), 7.60 (d, *J* = 8.9 Hz, 2H), 7.36 (d, *J* = 8.6 Hz, 2H), 6.66 (d, *J* = 8.6 Hz, 2H) ppm; **¹³C-NMR** (CDCl₃, 126 MHz) δ 147.7, 146.5, 136.3, 133.6, 131.9, 131.3, 123.8, 114.8, 96.4, 86.3 ppm; **FT-IR** (neat) 2267, 2198, 1675, 1600, 1520, 1262, 1103, 1022, 835, 736 cm⁻¹



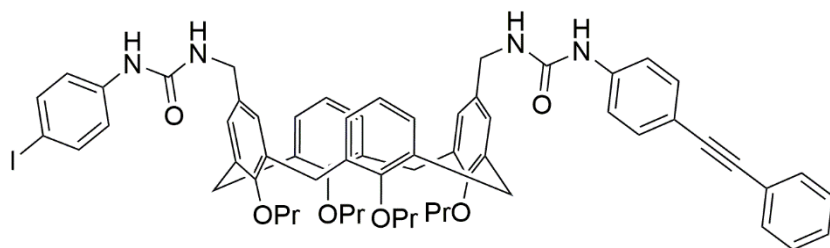
Synthesis of 183: A flame dried 25 mL flask was charged with a mixture of **189** (116 mg, 0.52 mmol) and triphosgene (60 mg, 0.2 mmol) in anhydrous toluene (8 mL) under an atmosphere of nitrogen. Triethylamine (86 μL, 0.62 mmol) was added *via* syringe, and the mixture heated at reflux for 2 h. After cooling to room temperature, the mixture was filtered and concentrated to afford **183** as an orange waxy solid (119 mg, 0.48 mmol, 92%).

¹H-NMR (CDCl₃, 500 MHz) δ 7.46 (m, 4H), 7.05 (m, 2H), 6.88 (m, 2H), 3.83 (s, 3H) ppm; **FT-IR** (neat) 3062, 2972, 2936, 2841, 2284, 1694, 1608, 1557, 1531, 1506, 1456, 1289, 1266, 1251, 1174, 1146, 1109, 1030, 832, 737, 704 cm⁻¹



Synthesis of 184: A flame dried 25 mL flask was charged with a mixture of **190** (124 mg, 0.52 mmol) and triphosgene (60 mg, 0.2 mmol) in anhydrous toluene (8 mL) under an atmosphere of nitrogen. Triethylamine (86 μL, 0.62 mmol) was added *via* syringe, and the mixture heated at reflux for 2 h. After cooling to room temperature, the mixture was filtered and concentrated to afford **184** as a dark red solid (119 mg, 0.45 mmol, 87%).

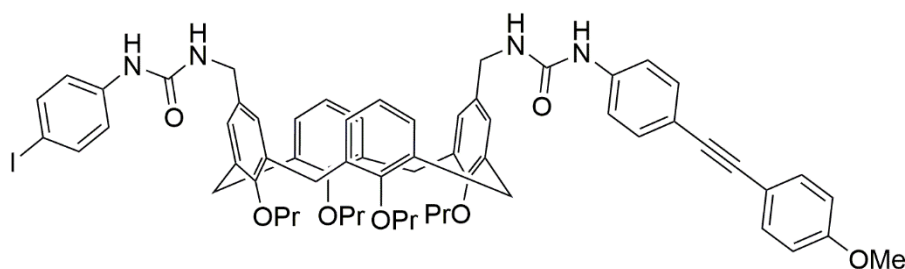
¹H-NMR (CDCl₃, 500 MHz) δ 8.16 (m, 2H), 7.59 (m, 2H), 7.45 (m, 2H), 7.04 (m, 2H) ppm; **FT-IR** (neat) 2266, 2213, 1591, 1514, 1340, 1109, 839, 751, 668 cm⁻¹



Synthesis of 137: A microwave vial was charged with a solution of **142** (20 mg, 0.022 mmol) and **144** (5 mg, 0.022 mmol) in d-

chloroform (1 mL). The vial was sealed with a PTFE-lined crimp cap and heated in the microwave synthesiser at 75 °C for 4 h. $^1\text{H-NMR}$ analysis indicated that the starting material **142** had been consumed. The solvent was removed *in vacuo* and the residue purified by flash column chromatography (40% ethyl acetate in petrol) to afford **137** as a pale yellow solid (19 mg, 0.17 mmol, 77%).

$^1\text{H-NMR}$ (500 MHz, CDCl_3) δ 7.99 (s, 1H), 7.94 (s, 1H), 7.58 (m, 4H), 7.34 (m, 6H), 6.99 (m, 5H), 6.79 (t, $J = 7.3$ Hz, 2H), 6.74 (d, $J = 8.7$ Hz, 2H), 6.42 (s, 2H), 6.08 (s, 2H), 6.07 (s, 2H), 4.41 (d, $J = 13.0$ Hz, 4H), 4.00 (m, 4H), 3.71 (s, 4H), 3.64 (t, $J = 6.7$ Hz, 4H), 3.10 (d, $J = 13.3$ Hz, 4H), 1.98 (m, 4H), 1.86 (m, 4H), 1.08 (t, $J = 7.4$ Hz, 6H), 0.89 (t, $J = 7.5$ Hz, 6H) ppm; $^{13}\text{C-NMR}$ (126 MHz, CDCl_3) δ 157.7, 156.9, 154.6, 139.3, 139.0, 137.73, 136.66, 133.5, 132.59, 132.56, 132.44, 132.39, 132.11, 132.03, 131.9, 131.8, 131.7, 131.6, 131.1, 128.97, 128.91, 128.87, 128.4, 128.1, 125.1, 123.7, 121.9, 119.7, 118.9, 117.2, 89.6, 88.8, 85.5, 77.3, 76.6, 42.4, 31.0, 23.6, 23.1, 10.9, 9.9 ppm; **FT-IR** (neat) 3331, 2962, 2932, 2875, 1652, 1589, 1539, 1486, 1464, 1391, 1308, 1283, 1217, 1006, 965, 909, 755, 733, 691 cm^{-1} ; **MS** (MALDI) m/z 1137.74 $[\text{M} + \text{Na}]^+$; **HRMS** $[\text{M} + \text{NH}_4]^+$ Calculated for $\text{C}_{64}\text{H}_{70}\text{N}_6\text{O}_8$: 1132.4444; Found: 1132.4455

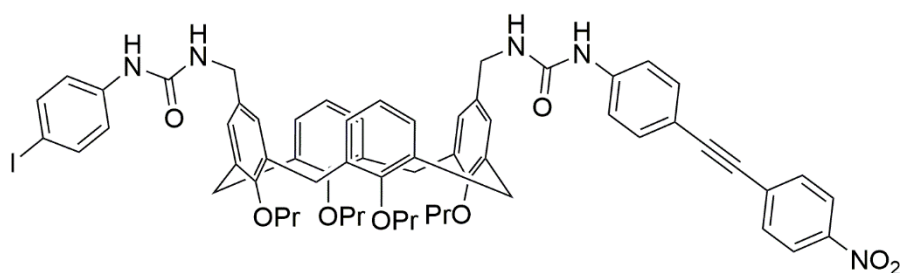


Synthesis of 190: A microwave vial was charged with a solution of **142** (60 mg, 0.067 mmol) **183** (20 mg, 0.07 mmol) in

anhydrous THF (2 mL). The vial was sealed with a PTFE-lined crimp cap and heated in the microwave synthesiser at 75 °C for 4 h. TLC analysis (10% methanol in dichloromethane / visualisation with ninhydrin stain) indicated that the starting material **142** had been consumed. The solvent was removed to afford a light brown solid which was triturated with diethyl ether to afford **190** as a pale yellow solid (55 mg, 0.047 mmol, 70 %).

$^1\text{H-NMR}$ (500 MHz, CDCl_3) δ 8.01 (br s, 2H), 7.51 (d, $J = 8.7$ Hz, 2H), 7.33 (d, $J = 8.6$ Hz, 2H), 7.24 (d, $J = 8.5$ Hz, 2H), 6.98 (m, 4H), 6.89 (d, $J = 8.8$ Hz, 2H), 6.76 (m, 3H), 6.42 (br s, 2H), 6.08 (s, 4H), 4.40 (d, $J =$

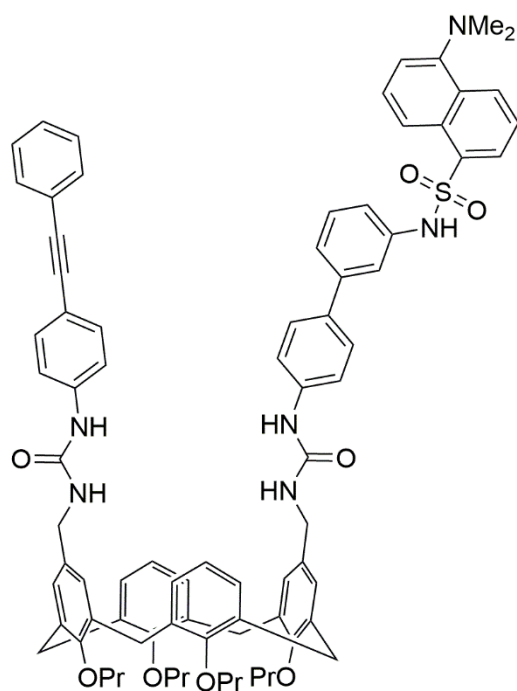
13.0 Hz, 4H), 4.00 (m, 4H), 3.83 (s, 3H), 3.70 (d, $J = 7.0$ Hz, 4H), 3.63 (t, $J = 6.5$ Hz, 4H), 3.10 (d, $J = 13.2$ Hz, 4H), 1.99 (m, 4H), 1.86 (m, 4H), 1.08 (t, $J = 7.4$ Hz, 6H), 0.89 (t, $J = 7.4$ Hz, 6H) ppm; ^{13}C NMR (126 MHz, CDCl_3) δ 158.4, 156.5, 155.8, 155.8, 153.4, 137.9, 137.9, 136.5, 135.5, 132.4, 132.0, 131.1, 130.7, 128.2, 127.8, 123.9, 120.9, 120.7, 118.6, 116.4, 114.7, 113.2, 112.9, 87.5, 87.1, 84.2, 76.1, 75.5, 54.3, 41.2, 29.9, 22.5, 21.9, 9.8, 8.8 ppm; FT-IR (neat) 3323, 2961, 2932, 2875, 2246, 1652, 1588, 1548, 1519, 1463, 1390, 137, 1284, 1247, 1217, 1172, 1034, 965, 909, 831, 763, 732 cm^{-1} ; MS (MALDI) m/z 1167.45 $[\text{M}+\text{Na}]^+$; HRMS $[\text{M}+\text{NH}_4]^+$ Calculated for $\text{C}_{65}\text{H}_{73}\text{N}_5\text{O}_7\text{I}_1$: 1162.4549; Found: 1162.4559



Synthesis of 191: A microwave vial was charged with a solution of **142** (60 mg, 0.067 mmol) **184** (18 mg, 0.07 mmol) in

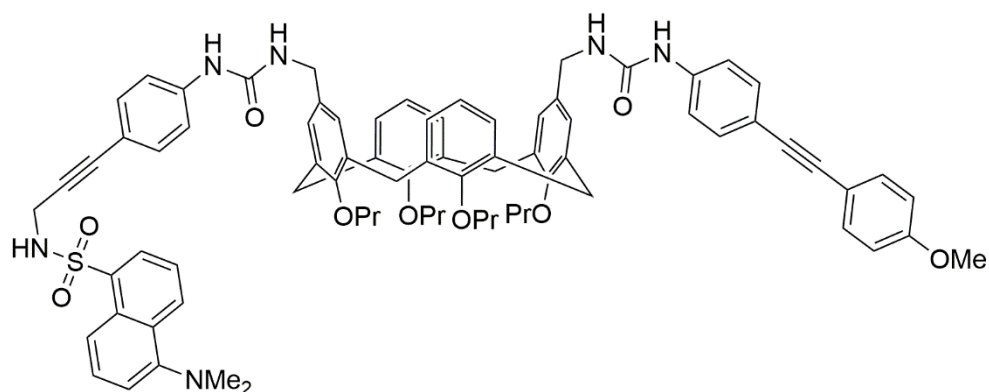
anhydrous THF (2 mL). The vial was sealed with a PTFE-lined crimp cap and heated in the microwave synthesiser at 75 °C for 4 h. TLC analysis (10% methanol in dichloromethane / visualisation with ninhydrin stain) indicated that the starting material **142** had been consumed. The solvent was removed to afford a dark brown solid which was triturated with diethyl ether to afford **191** as a light brown solid (69 mg, 0.060 mmol, 90 %).

^1H -NMR (500 MHz, CDCl_3) δ 8.21 (d, $J = 8.9$ Hz, 2H), 7.97 (s, 1H), 7.77 (s, 1H), 7.66 (d, $J = 8.9$ Hz, 2H), 7.40 (d, $J = 8.5$ Hz, 2H), 7.31 (d, $J = 8.4$ Hz, 2H), 7.07 (d, $J = 8.4$ Hz, 2H), 7.02 (m, 4H), 6.82 (m, 4H), 6.09 (s, 2H), 6.08 (s, 2H), 4.42 (d, $J = 13.1$ Hz, 4H), 4.01 (m, 4H), 3.74 (d, $J = 12.5$ Hz, 4H), 3.63 (t, $J = 6.7$ Hz, 4H), 3.10 (d, $J = 13.3$ Hz, 4H), 1.99 (m, 3H), 1.86 (m, 4H), 1.08 (t, $J = 7.4$ Hz, 6H), 0.89 (t, $J = 7.5$ Hz, 6H) ppm; ^{13}C -NMR (126 MHz, CDCl_3) δ 157.6, 156.9, 156.8, 154.6, 146.8, 140.6, 139.1, 137.7, 136.6, 133.6, 132.8, 132.6, 132.2, 132.1, 132.0, 131.8, 130.8, 128.9, 128.9, 125.1, 123.8, 122.0, 121.9, 119.4, 115.5, 9.5, 87.1, 85.5, 77.3, 76.6, 42.4, 31.0, 23.6, 23.1, 10.9, 9.9 ppm; FT-IR (neat) 3323, 2961, 2931, 2874, 2213, 1656, 1587, 1518, 1485, 1463, 1390, 1341, 1308, 1282, 1217, 1179, 1106, 1006, 820, 731 cm^{-1} ; MS (MALDI) m/z 1182.65 $[\text{M}+\text{Na}]^+$; HRMS $[\text{M}+\text{NH}_4]^+$ Calculated for $\text{C}_{64}\text{H}_{70}\text{N}_6\text{O}_8\text{I}_1$: 1177.4294; Found: 1177.4302



yellow solid (10 mg, 8 μ mol, 18%).

¹H-NMR (500 MHz, CDCl₃) δ 8.44 (d, J = 8.5 Hz, 1H), 8.31 (d, J = 8.7 Hz, 1H), 8.14 (d, J = 7.3 Hz, 1H), 7.52 (t, J = 8.1 Hz, 2H), 7.45 (m, 2H), 7.36 (m, 2H), 7.30 (m, 4H), 7.00 (m, 18H), 6.12 (s, 4H), 5.85 (s, 1H), 5.78 (s, 1H), 4.52 (d, J = 13.1 Hz, 4H), 4.01 (m, 4H), 3.79 (m, 4H), 3.63 (t, J = 6.8 Hz, 4H), 3.12 (d, J = 13.1 Hz, 2H), 3.09 (d, J = 13.1 Hz, 2H), 2.81 (s, 6H), 1.98 (m, 4H), 1.86 (m, 4H), 1.07 (m, 6H), 0.89 (t, J = 7.5 Hz, 6H) ppm; **¹³C-NMR** (126 MHz, CDCl₃) δ 157.7, 156.6, 156.5, 154.7, 141.7, 139.5, 136.9, 136.7, 134.2, 134.1, 133.6, 133.6, 132.5, 131.9, 131.8, 131.6, 130.9, 130.5, 129.8, 129.6, 129.0, 128.8, 128.5, 128.2, 127.5, 125.3, 125.2, 123.9, 123.6, 123.2, 122.1, 120.5, 120.4, 120.3, 119.7, 118.6, 117.1, 115.4, 89.7, 88.8, 45.5, 42.7, 31.1, 23.6, 23.1, 10.9, 9.8 ppm; **FT-IR** (neat) 3332, 2960, 2939, 2874, 1654, 1588, 1513, 1463, 1311, 1217, 1143, 1064, 1006, 964, 835 cm⁻¹; **HRMS** [M+H]⁺ Calculated for C₈₂H₈₅N₆O₈S: 1313.6132 ; Found: 1313.6141



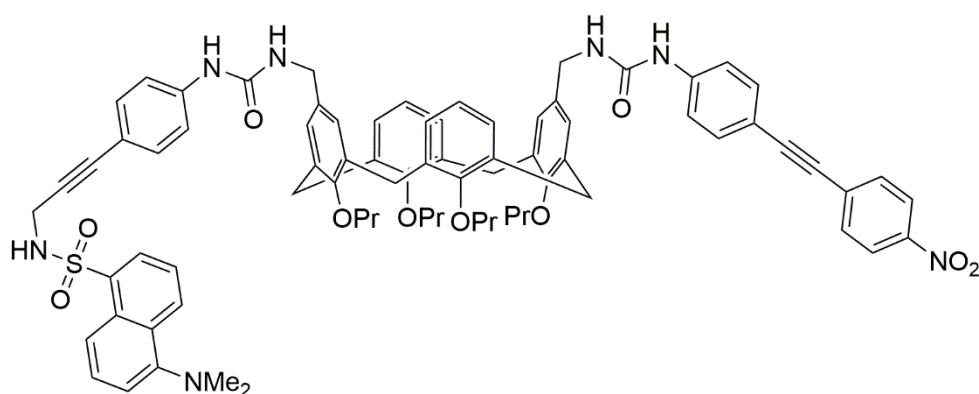
tetrakis(triphenylphosphine)palladium(0) (5 mg, 4.37 μ mol, 0.2 eq.) and piperidine (21 μ L, 0.22

Synthesis of 114: A microwave vial was charged with a mixture of **137** (50 mg, 0.044 mmol), **135** (19, 0.053 mmol), tri-*tert*-butylphosphine (1M in toluene, 9 μ L, 9 μ mol), PdCl₂(PPh₃)₂ (3 mg, 4 μ mol) and K₂CO₃ (12 mg, 0.88 mmol) in dry DMF (1 mL). The vial was sealed with a PTFE-lined crimp cap and heated in the microwave synthesiser at 70 °C for 18 h. The solvent was removed *in vacuo* and the residue partitioned between ethyl acetate (10 mL) and water (10 mL). The organic phase was separated, dried (MgSO₄), filtered and concentrated to afford a brown solid. Purification of this impure material by flash column chromatography (40% ethyl acetate in petrol) afforded **114** as a light

Synthesis of 126: To a solution of **190** (25 mg, 0.022 mmol) in anhydrous THF (0.5 mL) was added

mmol, 10 eq.) under an atmosphere of nitrogen. The mixture was degassed with nitrogen for 3 minutes before the addition of **178** (8 mg, 0.026 mmol, 1.2 eq.) in anhydrous THF (0.5 mL), and finally CuI (1.6 mg, 0.009 mmol). The mixture was stirred at room temperature for 4 h. TLC analysis (ethyl acetate-petrol, 1:1 v/v) indicated that **190** had been consumed. The reaction mixture was diluted with ethyl acetate (8 mL), and then washed with water (4 mL) and brine (4 mL). The organics were dried over magnesium sulfate, filtered and concentrated to afford an orange solid. Purification by column chromatography (ethyl acetate-petrol, 1:1 v/v) afforded **126** as an orange solid (20 mg, 0.015 mmol, 70 %).

¹H-NMR (500 MHz, CDCl₃) δ 8.45 (d, *J* = 8.5 Hz, 1H), 8.25 (dd, *J* = 7.3, 1.1 Hz, 1H), 8.22 (d, *J* = 8.6 Hz, 1H), 7.59 (s, *J* = 7.0 Hz, 1H), 7.54 (s, 1H), 7.51 (m, 1H), 7.45 (m, 3H), 7.28 (d, *J* = 8.6 Hz, 2H), 7.09 (d, *J* = 7.4 Hz, 1H), 7.02 (m, 6H), 6.88 (m, 4H), 6.80 (t, *J* = 7.4 Hz, 2H), 6.69 (d, *J* = 8.6 Hz, 2H), 6.08 (s, 4H), 6.01 (s, 1H), 5.89 (s, 1H), 5.06 (t, *J* = 5.9 Hz, 1H), 4.42 (d, *J* = 2.1 Hz, 2H), 4.40 (d, *J* = 2.0 Hz, 2H), 4.00 (m, 4H), 3.95 (d, *J* = 6.0 Hz, 2H), 3.83 (s, 3H), 3.76 (d, *J* = 5.5 Hz, 2H), 3.73 (d, *J* = 3.6 Hz, 2H), 3.62 (t, *J* = 6.3 Hz, 4H), 3.09 (d, *J* = 11.8 Hz, 4H), 2.77 (s, 6H), 1.98 (m, 4H), 1.86 (m, 4H), 1.07 (t, *J* = 7.4 Hz, 6H), 0.89 (7, *J* = 7.5 Hz, 6H) ppm; ¹³C-NMR (126 MHz, CDCl₃) δ 159.7, 157.7, 156.56, 156.44, 154.6, 152.2, 139.7, 138.9, 136.73, 136.69, 134.5, 133.57, 133.47, 133.09, 132.34, 132.30, 131.9, 130.96, 130.00, 129.99, 129.94, 128.97, 128.95, 128.73, 125.29, 125.19, 123.4, 122.0, 119.8, 118.96, 118.62, 117.7, 115.62, 115.48, 115.29, 114.2, 88.87, 88.29, 84.7, 82.0, 55.5, 45.5, 42.5, 34.1, 31.01, 27.3, 23.64, 23.07, 10.9, 9.9 ppm; FT-IR (neat) 3341, 2961, 2941, 2878, 1653, 1589, 1518, 1463, 1311, 1290, 1250, 1218, 1143, 1042, 833, 732 cm⁻¹; MS (MALDI) *m/z* 1328.8 [M + Na]⁺; HRMS [M + H]⁺ Calculated for C₈₀H₈₅N₆O₉S₁: 1305.6093; Found: 1305.6093



Synthesis of **127**:

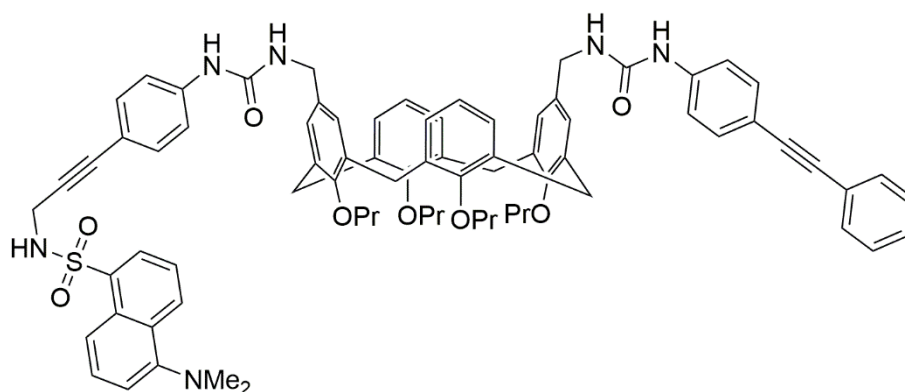
To a solution of **191** (40 mg, 0.034 mmol) in anhydrous THF (0.5 mL) was added

tetrakis(triphenyl

phosphine)palladium(0) (8 mg, 6.90 μmol, 0.2 eq.) and piperidine (34 μL, 0.34 mmol, 10 eq.) under an atmosphere of nitrogen. The mixture was degassed with nitrogen for 3 minutes before the addition of **178** (12 mg, 0.041 mmol, 1.2 eq.) in anhydrous THF (0.5 mL), and finally CuI (2.6 mg, 0.014 mmol). The mixture was stirred at room temperature for 4 h. TLC analysis (ethyl acetate-

petrol, 1:1 v/v) indicated that **191** had been consumed. The reaction mixture was diluted with ethyl acetate (8 mL), and then washed with water (4 mL) and brine (4 mL). The organics were dried over magnesium sulfate, filtered and concentrated to afford an orange solid. Purification by column chromatography (ethyl acetate-petrol, 1:1 v/v) afforded **127** as a light brown solid (30 mg, 0.02 mmol, 66 %)

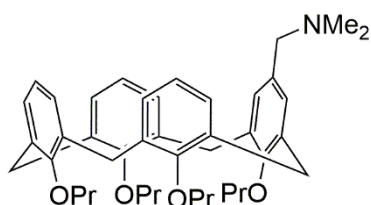
¹H-NMR (500 MHz, CDCl₃) δ 8.46 (d, *J* = 8.5 Hz, 1H), 8.24 (t, *J* = 9.1 Hz, 2H), 8.16 (d, *J* = 7.6 Hz, 2H), 7.72 (s, 1H), 7.60 (d, *J* = 7.6 Hz, 2H), 7.51 (d, *J* = 7.9 Hz, 2H), 7.45 (m, 1H), 7.30 (d, *J* = 7.8 Hz, 2H), 7.09 (m, 3H), 7.01 (m, 4H), 6.96 (d, *J* = 7.9 Hz, 2H), 6.81 (m, 3H), 6.11 (s, 2H), 6.10 (s, 2H), 6.03 (s, 1H), 5.87 (s, 1H), 5.18 (s, 1H), 4.42 (d, *J* = 13.0 Hz, 4H), 4.01 (m, 4H), 3.94 (d, *J* = 5.5 Hz, 2H), 3.78 (s, 2H), 3.75 (s, 2H), 3.63 (t, *J* = 6.2 Hz, 4H), 3.09 (d, *J* = 12.6 Hz, 4H), 2.80 (s, 6H), 1.98 (m, 4H), 1.86 (m, 4H), 1.07 (t, *J* = 7.2 Hz, 6H), 0.89 (t, *J* = 7.1 Hz, 6H) ppm; **¹³C-NMR** (126 MHz, CDCl₃) δ 157.7, 156.45, 156.37, 154.7, 152.2, 146.8, 140.6, 139.5, 136.71, 136.66, 134.4, 133.64, 133.59, 132.83, 132.41, 132.18, 131.70, 131.01, 130.63, 130.59, 130.00, 129.94, 129.86, 128.97, 128.75, 125.30, 125.22, 123.80, 123.42, 122.0, 119.45, 119.19, 118.6, 115.96, 115.56, 115.34, 95.4, 89.7, 87.2, 82.5, 45.5, 42.7, 42.6, 34.1, 31.1, 23.6, 23.1, 10.9, 9.9 ppm; **FT-IR** (neat) 3344, 2961, 2933, 2876, 2218, 1658, 1588, 1517, 1464, 1342, 1310, 1217, 1142, 1010, 835, 751 cm⁻¹; **MS** (MALDI) *m/z* 1342.27 [M + Na]⁺; **HRMS** [M + H]⁺ Calculated for C₇₉H₈₂N₇O₁₀S₁: 1320.5838; Found: 1320.5828



Synthesis of 182: To a solution of **137** (20 mg, 0.018 mmol) in anhydrous THF (0.5 mL) was added tetrakis(triphenylphosphine)palladium(0) (4 mg, 3.6 μmol, 0.2 eq.)

and piperidine (18 μL, 0.18 mmol, 10 eq.) under an atmosphere of nitrogen. The mixture was degassed with nitrogen for 3 minutes before the addition of **178** (6 mg, 0.022 mmol, 1.2 eq.) in anhydrous THF (0.5 mL), and finally CuI (1.3 mg, 0.007 mmol). The mixture was stirred at room temperature for 4 h. TLC analysis (ethyl acetate-petrol, 1:1 v/v) indicated that **137** had been consumed. The reaction mixture was diluted with ethyl acetate (8 mL), and then washed with water (4 mL) and brine (4 mL). The organics were dried over magnesium sulfate, filtered and concentrated to afford an orange solid. Purification by column chromatography (ethyl acetate-petrol, 1:1 v/v) afforded **182** as an orange solid (15 mg, 0.012 mmol, 66 %)

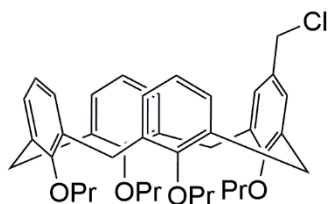
¹H-NMR (500 MHz, CDCl₃) δ 8.45 (d, *J* = 8.5 Hz, 1H), 8.25 (dd, *J* = 7.3, 1.1 Hz, 1H), 8.22 (d, *J* = 8.6 Hz, 1H), 7.57 (s, 2H), 7.51 (m, 4H), 7.45 (dd, *J* = 8.5, 7.4 Hz, 1H), 7.33 (m, 3H), 7.29 (d, *J* = 8.5 Hz, 3H), 7.09 (d, *J* = 7.4 Hz, 1H), 7.05 (d, *J* = 8.6 Hz, 2H), 7.01 (m, 4H), 6.89 (d, *J* = 8.6 Hz, 2H), 6.80 (t, *J* = 7.4 Hz, 2H), 6.70 (d, *J* = 8.6 Hz, 2H), 6.08 (s, 2H), 6.07 (s, 2H), 6.01 (s, 1H), 5.91 (s, 1H), 5.00 (t, *J* = 6.0 Hz, 1H), 4.43 (d, *J* = 1.9 Hz, 2H), 4.40 (d, *J* = 1.8 Hz, 2H), 4.01 (m, 4H), 3.94 (d, *J* = 6.0 Hz, 2H), 3.74 (m, 4H), 3.63 (t, *J* = 6.4 Hz, 4H), 3.11 (d, *J* = 2.6 Hz, 2H), 3.08 (d, *J* = 2.5 Hz, 2H), 2.77 (s, *J* = 10.0 Hz, 6H), 1.98 (m, 4H), 1.86 (m, 4H), 1.07 (t, *J* = 7.4 Hz, 6H), 0.89 (t, *J* = 7.5 Hz, 6H) ppm; **¹³C-NMR** (126 MHz, CDCl₃) δ 157.7, 156.55, 156.47, 154.6, 152.2, 139.60, 139.29, 136.7, 134.5, 133.58, 133.49, 132.51, 132.31, 131.81, 131.65, 130.97, 130.04, 129.99, 129.94, 128.96, 128.74, 128.55, 128.47, 128.31, 125.26, 125.17, 123.56, 123.39, 122.0, 119.70, 119.05, 118.6, 115.58, 115.29, 89.7, 88.9, 84.6, 82.1, 45.5, 42.6, 34.1, 31.1, 23.64, 23.08, 10.9, 9.9 ppm; **FT-IR** (neat) 3345, 2956, 2933, 2878, 1653, 1589, 1541, 1513, 1463, 1310, 1217, 1143, 1070, 1007, 963, 912, 837, 756 cm⁻¹; **MS** (MALDI) *m/z* 1298.15 [M + Na]⁺; **HRMS** [M + H]⁺ Calculated for C₇₉H₈₃N₆O₈S₁: 1275.5988; Found: 1275.5988



Synthesis of 198⁵³: A 20 mL capacity microwave vial was charged with a solution of **51** (0.500 g, 1.038 mmol) in anhydrous *N,N*-dimethylformamide (17 mL) under an atmosphere of argon. Sodium hydride (0.208 g, 5.19 mmol, 60% in mineral oil) was added in one portion, and the vial sealed with a PTFE lined crimp cap. The

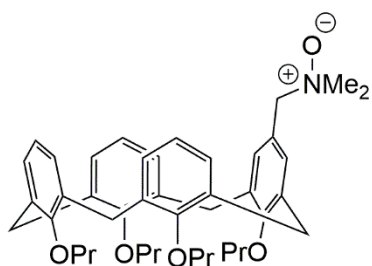
resulting suspension was stirred for 0.5 h at room temperature, before the addition of *n*-propyl methanesulphonate (0.660 g, 4.780 mmol) *via* syringe in one portion. The reaction mixture was then heated to 90 °C under microwave irradiation for 1.5 hours. Upon cooling to room temperature, the reaction mixture was poured into water (50 mL) and extracted with diethyl ether (3 x 30 mL). The combined organic extracts were then washed with water (4 x 30 mL) and brine (30 mL), dried over magnesium sulfate, then filtered and concentrated to afford a pale yellow oil. Purification by column chromatography on silica gel (dichloromethane then dichloromethane-methanol 9:1 *v/v*) afforded **198** as a pale yellow foam (0.469 g, 0.718 mmol, 70%). Analysis revealed the foam to be the title compound. Spectral data were in accordance with those reported previously for this compound.⁵³

¹H-NMR (CDCl₃, 500 MHz) δ 6.66 – 6.53 (m, 11H), 4.46 (d, *J* = 11.3 Hz, 2H), 4.43 (d, *J* = 11.3 Hz, 2H), 3.85 (t, *J* = 7.3 Hz, 8H), 3.19 – 3.11 (m, 4H), 2.08 (s, 6H), 1.98 – 1.84 (m, 8H), 1.01 – 0.98 (m, 12H) ppm; **¹³C-NMR** (CDCl₃, 126 MHz) δ 156.92, 156.71, 156.29, 135.55, 135.51, 135.22, 135.03, 129.77, 128.46, 128.22, 122.26, 122.05, 77.03, 76.81, 44.15, 31.01, 30.96, 23.32, 23.24, 10.41, 10.39, 10.30 ppm; **FT-IR** (thin film) 2960, 2930, 2872, 1450, 1380, 1257, 1210, 1191, 1078, 1062, 1033, 1003, 944, 911, 768, 733 cm⁻¹



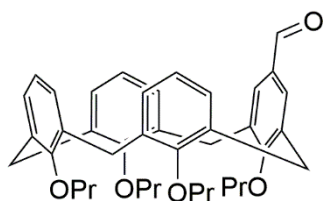
Synthesis of 199⁵³: A 20 mL RBF was charged with a solution of **198** (0.35 g, 0.53 mmol) in chloroform (5 mL). Ethyl chloroformate (125 μ L, 1.19 mmol) was added in one portion *via* syringe, and the mixture stirred at room temperature for 2 h. The mixture was then filtered through a short plug of silica gel using dichloromethane as the eluent. The solvents were then removed *in vacuo* to afford **199** as a white foam (0.26 g, 0.43 mmol, 74 %). Spectral data were in accordance with those reported previously for this compound.⁵³

¹H-NMR (CDCl₃, 500 MHz) δ 6.72 – 6.59 (m, 6H), 6.39 – 6.32 (m, 5H), 4.38 (d, J = 3.9 Hz, 2H), 4.35 (d, J = 4.0 Hz, 2H), 4.11 (s, 2H), 3.86 – 3.77 (m, 4H), 3.76 – 3.68 (m, 4H), 3.08 (d, J = 3.1 Hz, 2H), 3.06 (d, J = 3.2 Hz, 2H), 1.90 – 1.76 (m, 8H), 0.97 – 0.93 (m, 6H), 0.88 (t, J = 7.5 Hz, 6H) ppm; **¹³C-NMR** (CDCl₃, 126 MHz) δ 157.11, 156.66, 156.34, 135.80, 135.46, 135.19, 134.70, 130.64, 128.55, 128.40, 128.32, 127.84, 121.95, 121.61, 76.72, 76.65, 76.56, 46.78, 30.88, 23.18, 23.01, 10.33, 10.27, 10.02 ppm; **FT-IR** (thin film) 2969, 2924, 2921, 2870, 1450, 1285, 1213, 1190, 1082, 1066, 1033, 1002, 967, 909, 787, 762 cm⁻¹

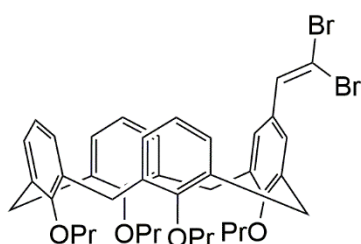


Synthesis of 205: A 10 mL RBF was charged with a solution of **198** (0.19 g, 0.30 mmol) in chloroform (5 mL). 3-chloroperbenzoic acid (70 wt%, 0.30 g, 0.60 mmol) was added in one portion and the mixture stirred at room temperature for 4 h. The organic phase was then washed with aqueous NaOH (1M) (3 x 5 mL) followed by water (3 x 5 mL) and dried over magnesium sulfate. After filtering the suspension and removing the solvent *in vacuo*, the product was purified by column chromatography on silica gel (chloroform-methanol 95:5 v/v) to afford **205** as a pale yellow oil (0.140 g, 0.21 mmol, 70%). Spectral data were in accordance with those reported previously for this compound.⁵³

¹H-NMR (CDCl₃, 500 MHz) δ 7.01 (d, 4H, J = 7.5 Hz), 6.82 (t, 2H, J = 7.5 Hz), 6.40 (m, 5H), 4.45 (d, 2H, J = 13 Hz), 4.46 (d, 2H, J = 13 Hz), 4.02 (m, 4H), 3.94 (s, 2H), 3.73 (t, 2H, J = 7.5 Hz), 3.67 (t, 2H, J = 7.5 Hz), 3.18 (d, 2H, J = 13.1 Hz), 3.16 (d, 2H, J = 13.1 Hz), 2.26 (s, 6H), 2.05 (m, 4H), 1.87 (m, 4H), 1.08 (t, 3H, J = 7.4 Hz), 1.04 (t, 3H, J = 7.4 Hz), 0.94 (t, 6H, J = 7.5 Hz) ppm; **¹³C-NMR** (CDCl₃, 100 MHz) δ 157.21, 156.87, 155.61, 136.71, 136.26, 134.74, 134.04, 131.80, 129.20, 128.74, 127.68, 123.68, 122.63, 122.43, 99.21, 77.71, 76.81, 76.52, 58.49, 56.30, 30.96, 23.63, 23.19, 13.87, 10.86, 10.84, 10.08 ppm; **FT-IR** (thin film) 2960, 2932, 2874, 1455, 1384, 1300, 1282, 1247, 1218, 1208, 1195, 1171, 1131, 1105, 1087, 1066, 1037, 1005, 964, 942, 905, 885, 843, 836, 758 cm⁻¹

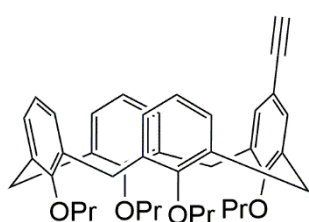


Synthesis of 60: A 20 mL capacity microwave vial was charged with a solution of **205** (672 mg, 1 mmol) in dichloromethane (10 mL) and acetic anhydride (0.95 mL, 10.1 mmol) was added. The vial was sealed with a PTFE lined crimp cap and the mixture heated in the microwave synthesiser at 80 °C for 1 h. The mixture was allowed to cool to room temperature, and then absorbed directly onto silica gel. Purification *via* column chromatography on silica gel (20% diethyl ether in pentane) afforded **60** as a white solid (430 mg, 0.69 mmol, 69 %). Spectral data was in accordance with literature values.²²⁸ R_f 0.34 (20% diethyl ether in pentane); $^1\text{H NMR}$ (CDCl_3 , 500 MHz) δ 9.56 (s, 1H), 6.99 (s, 2H), 6.80 – 6.63 (m, 6H), 6.50 – 6.33 (m, 3H), 4.48 (d, $J = 13.6$, 2H), 4.43 (d, $J = 13.5$, 2H), 3.96 – 3.76 (m, 8H), 3.22 (d, $J = 13.6$ Hz, 2H), 3.15 (d, $J = 13.5$ Hz, 2H), 1.96 – 1.86 (m, 8H), 1.03 (m, 6H), 0.96 (t, $J = 7.5$ Hz, 6H) ppm; $^{13}\text{C NMR}$ (CDCl_3 , 126 MHz) δ 191.90, 162.17, 156.96, 156.37, 136.15, 135.95, 134.84, 134.81, 131.05, 130.12, 128.97, 128.45, 128.04, 122.36, 122.01, 77.04, 76.85, 76.83, 31.11, 23.53, 23.46, 23.32, 10.59, 10.54, 10.32 ppm;



Synthesis of 200: A solution of triphenylphosphine (210 mg, 0.8 mmol) in dry dichloromethane (4 mL) was added dropwise to a solution of **60** (166 mg, 0.27 mmol) and carbon tetrabromide (266 mg, 0.8 mmol) in dry dichloromethane (8 mL) at 0°C. The mixture was stirred at 0°C for 0.5 h, then at room temperature for 1 h. TLC analysis (15% ethyl acetate in petrol) indicated that the starting material **60** had been consumed. The mixture was filtered through a short plug of silica gel with dichloromethane as the eluent, and concentrated to afford **200** as a pale orange solid (198 mg, 0.26 mmol, 95 %).

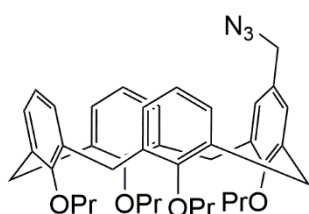
$^1\text{H-NMR}$ (CDCl_3 , 500 MHz) δ 7.05 (s, 1H), 6.82 – 6.76 (m, 4H), 6.73 – 6.66 (m, 4H), 6.48 – 6.43 (m, 3H), 4.46 (d, $J = 13.4$ Hz, 4H), 3.97 – 3.76 (m, 8H), 3.17 (d, $J = 13.4$ Hz, 2H), 3.16 (d, $J = 13.4$ Hz, 2H), 1.99 – 1.87 (m, 8H), 1.05 (m, 6H), 0.97 (t, $J = 7.5$ Hz, 6H) ppm; $^{13}\text{C-NMR}$ (CDCl_3 , 126 MHz) δ 157.18, 156.81, 156.20, 136.97, 136.06, 135.59, 134.85, 134.51, 128.78, 128.71, 128.53, 128.48, 128.10, 122.10, 122.04, 85.91, 77.36, 76.88, 76.85, 76.75, 31.13, 31.11, 23.50, 23.49, 23.29, 10.65, 10.62, 10.29 ppm; **FT-IR** (thin-film) 2961, 2933, 2874, 1588, 1456, 1384, 1246, 1216, 1194, 1127, 1086, 1066, 1006, 966 cm^{-1} ; **MS** (MALDI) m/z 798.96 $[\text{M}+\text{Na}]^+$; **HRMS** $[\text{M} + \text{Na}]^+$ Calculated for: $\text{C}_{42}\text{H}_{49}\text{Br}_2\text{O}_4$; 777.1976 Found: 777.1982



Synthesis of 131: A 10 mL RBF was charged with a solution of **200** (200 mg, 0.26 mmol) in dry tetrahydrofuran (5 mL) at -78°C under an atmosphere of argon. n -Butyllithium (1 mL, 2.1 mmol, 2M in hexanes) was added dropwise *via* syringe and the mixture stirred at -78°C for 1 h.

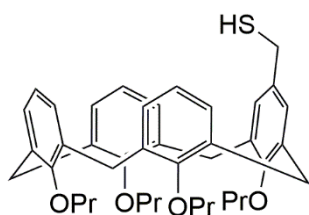
TLC analysis (10% diethyl ether in petrol) indicated the starting material **131** had been consumed. The mixture was allowed to warm to room temperature and then quenched with a saturated solution of ammonium chloride (aq.) (5 mL). The mixture was transferred to a 25 mL separating funnel and extracted with diethyl ether (2 x 10 mL). The combined organics were dried over magnesium sulphate, filtered and concentrated to afford an orange oil (148 mg, 0.24 mmol, 51 %)

¹H-NMR (CDCl₃, 500 MHz) δ 6.72 (s, 2H), 6.67 – 6.52 (m, 9H), 4.45 (d, *J* = 13.5 Hz, 2H), 4.42 (d, *J* = 13.5 Hz, 2H), 3.89 – 3.79 (m, 8H), 3.16 (d, *J* = 13.5 Hz, 2H), 3.11 (d, *J* = 13.5 Hz, 2H), 2.87 (s, 1H), 1.95 – 1.85 (m, 8H), 1.03 – 0.95 (m, 12H) ppm; **¹³C-NMR** (CDCl₃, 126 MHz) δ 157.61, 156.78, 156.59, 135.55, 135.13, 134.73, 132.20, 128.62, 128.29, 128.21, 122.19, 122.17, 115.31, 84.75, 82.32, 76.82, 76.76, 75.06, 31.14, 30.94, 23.41, 23.39, 23.36, 10.51, 10.48, 10.42 ppm; **FT-IR** (thin-film) 3312, 2960, 2932, 2874, 1586, 1455, 1384, 1246, 1214, 1194, 1086, 1006, 966, 888 cm⁻¹; **MS** (MALDI) *m/z* 637.9 [M+Na]⁺; **HRMS** [M + H]⁺ Calculated for: C₄₂H₄₉O₄; 617.3625 Found: 617.3627



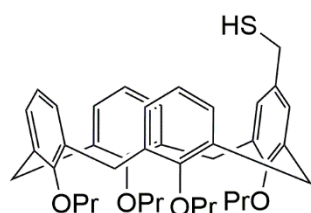
Synthesis of 129: A 5 mL capacity microwave vial was charged with a solution of **199** (124 mg, 0.19 mmol) in *N,N*-dimethylformamide (3 mL) and sodium azide (14 mg, 0.195 mmol) was added. The vial was sealed with a PTFE lined crimp cap and the mixture heated in the microwave synthesiser at 100 °C for 1 h. The mixture was allowed to cool to room temperature, then diluted with dichloromethane (15 mL) and washed with water (3 x 15 mL). After drying over magnesium sulphate and removing the solvent under reducer pressure, the desired product was obtained as a pale yellow oil (0.106 g, 84% yield).

¹H-NMR (CDCl₃, 400 MHz) δ 6.59 (m, 6H), 6.40 (m, 3H), 6.33 (s, 2H), 4.46 (d, 2H, *J* = 13.4 Hz), 4.45 (d, 2H, *J* = 13.4 Hz), 3.84 (s, 2H), 3.80 (m, 4H), 3.73 (q, 4H, *J* = 8 Hz), 3.16 (d, 4H, *J* = 13.4 Hz), 1.84 (m, 8H), 0.94 (m, 6H), 0.89 (t, 6H, *J* = 8 Hz); **¹³C-NMR** (CDCl₃, 100 MHz) δ 157.02, 156.68, 156.59, 135.74, 135.50, 135.39, 135.01, 128.61, 128.45, 128.23, 128.11, 122.17, 121.72, 76.86, 58.49, 54.86, 31.17, 23.51, 23.39, 13.94, 10.64, 10.43 ppm; **FT-IR** (thin-film) 2961, 2932, 2920, 2875, 2092, 1455, 1384, 1301, 1282, 1246, 1214, 1194, 1129, 1086, 1067, 1038, 1006, 966, 759 cm⁻¹.



Synthesis of 225: A 5 mL capacity microwave vial was charged with a solution of **199** (160 mg, 0.25 mmol) in tetrahydrofuran (1.5 mL) and thiourea (23 mg, 0.29 mmol) was added. The vial was sealed with a PTFE lined crimp cap and the mixture heated in the microwave synthesiser at 90 °C for 1 h. The mixture was allowed to cool to room temperature, and the solvent removed *in vacuo*. The crude thiuronium salt was transferred to a 5 mL capacity

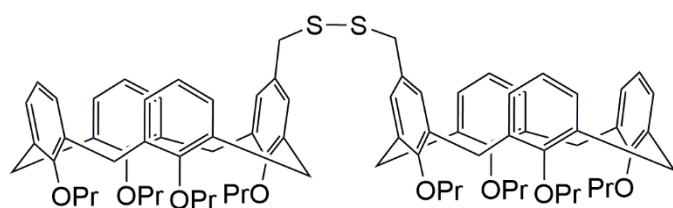
microwave vial and taken up in degassed 1M KOH_(aq) (2 mL) and tetrahydrofuran (2 mL). The vial was sealed with a PTFE lined crimp cap and the mixture heated in the microwave synthesiser at 90 °C for 1 h. The mixture was allowed to cool to room temperature, diluted with 1M HCl (10 mL) and extracted with dichloromethane (2 x 10 mL). The organics were dried over magnesium sulphate, filtered and concentrated *in vacuo* to afford a clear oil. Purification *via* column chromatography on silica gel (30% dichloromethane in pentane) afforded **225** as a clear oil (105 mg, 0.16 mmol, 82 %).



Synthesis of 225 via the reduction of 227: To a stirred solution of **227** (70 mg, 0.055 mmol) in dry degassed dichloromethane (2 mL) under an atmosphere of nitrogen was added dithiothreitol (22mg, 0.14 mmol) and triethylamine (23 μ L, 0.17 mmol). The mixture was stirred at room temperature for 18 h. The reaction mixture was absorbed directly onto silica.

Purification *via* column chromatography on silica gel (30% dichloromethane in pentane) afforded **225** as a clear oil (30 mg, 0.047 mmol, 86 %).

¹H-NMR (CDCl₃, 500 MHz) δ 6.74 – 6.70 (m, 4H), 6.68 – 6.63 (m, 2H), 6.52 – 6.45 (m, 3H), 6.40 (s, 2H), 4.45 (d, J = 13.3 Hz, 2H), 4.43 (d, J = 13.3 Hz, 2H), 3.88 (m, 4H), 3.80 (m, 4H), 3.35 (d, J = 7.2 Hz, 2H), 3.13 (t, J = 12.8 Hz, 4H), 1.97 – 1.85 (m, 8H), 1.01 (td, J = 7.4, 0.8 Hz, 6H), 0.96 (t, J = 7.5 Hz, 6H) ppm; **¹³C-NMR** (CDCl₃, 126 MHz) δ 157.03, 156.51, 155.60, 135.69, 135.53, 135.07, 134.92, 134.29, 128.49, 128.47, 128.03, 127.63, 122.05, 121.81, 76.86, 76.77, 31.12, 28.76, 23.45, 23.31, 10.58, 10.35 ppm; **FT-IR** (neat) 2960, 2932, 2874, 1585, 1455, 1384, 1246, 1213, 1194, 1086, 1006, 966, 759 cm⁻¹; **MS** (MALDI) m/z 661.4 [M+Na]⁺; **HRMS** [M + NH₄]⁺ Calculated for: C₄₁H₅₄NO₄S; 656.3801 Found: 656.3740

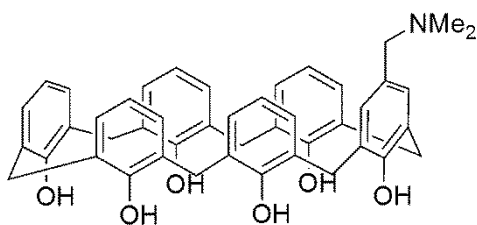


Synthesis of 227: To a solution of **225** (15 mg, 0.023 mmol) in ethyl acetate (0.5 mL) was added sodium iodide (1 mg, 7 μ mol) then hydrogen peroxide (3 μ L, 0.023 mmol) *via* syringe. The mixture was

stirred at room temperature for 1 h. The mixture was diluted with ethyl acetate (8 mL), then washed with a saturated solution of aqueous sodium thiosulfate (5 mL) and water (5 mL). The organics were dried over magnesium sulphate, filtered and concentrated *in vacuo* to afford **227** as a clear oil (15 mg, 0.023 mmol, 100%)

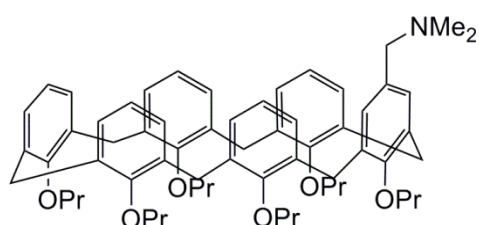
¹H-NMR (CDCl₃, 500 MHz) δ 6.71 – 6.47 (m, 22H), 4.44 (dd, J = 13.3, 7.1 Hz, 8H), 3.88 – 3.77 (m, 16H), 3.43 (s, 4H), 3.14 (dd, J = 13.4, 6.1 Hz, 8H), 1.96 – 1.85 (m, 16H), 1.01 – 0.92 (m, 24H) ppm; **¹³C-NMR** (CDCl₃, 126 MHz) δ 156.94, 156.56, 135.54, 135.07, 134.86, 130.40, 129.30, 128.30, 128.22, 122.11,

121.83, 76.84, 76.77, 43.80, 31.14, 29.85, 23.41, 23.36, 10.51, 10.42 ppm; **FT-IR** (neat) 2961, 2923, 2875, 1732, 1586, 1462, 1455, 1263, 1210, 1195, 1086, 1007, 966, 758, 739 cm^{-1} ; **MS** (MALDI) m/z 1298.66 $[\text{M}+\text{Na}]^+$; **HRMS** $[\text{M} + \text{NH}_4]^+$ Calculated for: $\text{C}_{82}\text{H}_{102}\text{NO}_8\text{S}_2$; 1292.7041 Found: 1292.7005



Synthesis of 213: To a solution of calix[6]arene (2.23 g, 3.5 mmol) in tetrahydrofuran (50 mL) was added dimethylamine (1.2 mL, 5.53 mmol, 25 % aq. solution) and formaldehyde (0.4 mL, 5.25 mmol, 37% aq. solution). The mixture was stirred at room temperature for 6 h, after which time the

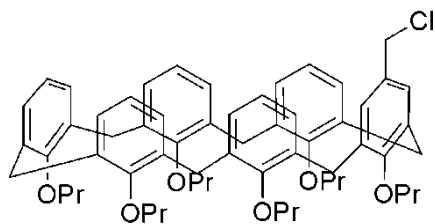
fine white precipitate was collected by suction filtration to afford **213** as a white solid (1.23 g, 1.77 mmol, 50 %). The extremely low solubility of **213** in a wide range of organic solvents required its characterisation as the propyl ether **214**, described below.



Synthesis of 214: A 20 mL capacity microwave vial was charged with solution of **213** (0.500 g, 0.721 mmol) in anhydrous *N,N*-dimethylformamide (15 mL) under nitrogen, and sodium hydride (0.221 g, 5.77 mmol, 60% in mineral oil) was added. The resulting suspension was

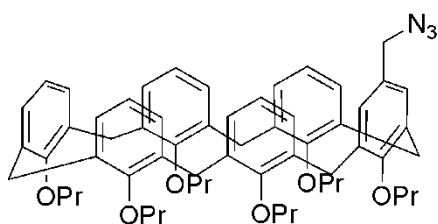
stirred for 30 minutes at room temperature before the addition of *n*-propyl methanesulphonate (747 μL , 6.13 mmol) *via* syringe. The vial was sealed with a PTFE lined crimp cap and the mixture heated in the microwave synthesiser at 90 $^{\circ}\text{C}$ for 1.5 h. On cooling to room temperature, the aqueous layer was extracted with diethyl ether (3 x 30 mL), and the combined organic solution washed with 1% potassium carbonate aqueous solution, dried over magnesium sulphate and the solvent removed under reduced pressure to afford a pale yellow oil. The oil was dissolved in 5 mL of dichloromethane and filtered through silica gel (dichloromethane first to remove the excess of electrophile and then dichloromethane / methanol = 9:1 V/V) to yield the desired product as a pale yellow oil (0.400 g, 0.423 mmol, 59 %).

¹H-NMR (C_6D_6 , 500 MHz) δ 7.24 (brs, 9H), 7.10 (brs, 2H), 6.89 – 6.85 (m, 5H), 4.07 (s, 12H), 3.39 (brs, 8H), 3.29 (s, 2H), 3.23 (brs, 4H), 2.10 (brs, 6H), 1.49 (brs, 6H), 1.32 (brs, 6H), 0.82 (t, $J = 6.1$ Hz, 6H), 0.78 – 0.70 (m, 12H) ppm; **¹³C-NMR** (C_6D_6 , 126 MHz) δ 156.0, 155.8, 155.6, 155.3, 135.2, 135.0, 134.7, 123.88, 123.78, 74.84, 74.76, 63.61, 44.8, 31.2, 31.01, 30.97, 23.95, 23.94, 23.86, 23.84, 10.88, 10.83, 10.77 ppm; **FT-IR** (neat) 3361, 2963, 2935, 2875, 2281, 1750, 1588, 1454, 1385, 1250, 1215, 1194, 1084, 1063, 1042, 1006, 963, 889 cm^{-1} ; **MS** (MALDI) m/z 988.02 $[\text{M}+\text{CO}_2]^+$; **HRMS** $[\text{M} + \text{H}]^+$ Calculated for: $\text{C}_{63}\text{H}_{80}\text{N}_1\text{O}_6$; 946.5980 Found: 946.5978



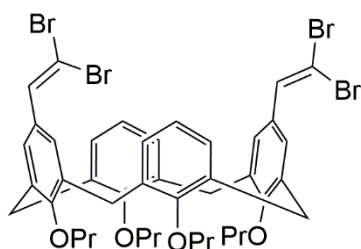
Synthesis of 215: A solution of **214** (0.150 g, 0.159 mmol) and freshly distilled ethyl chloroformate (61 μ L, 0.634 mmol) in chloroform (0.5 mL) was stirred at room temperature for 3 hours. After this time, the solvent was removed under reduced pressure and the residue filtered through silica gel (dichloromethane) to afford the desired compound as a pale yellow oil (77 mg, 0.082 mmol, 52 %).

$^1\text{H-NMR}$ (CDCl_3 , 400 MHz) δ 7.08 – 6.68 (m, 17H), 4.11 (s, 2H), 3.94 (s, 12H), 3.58 – 3.14 (m, 12H), 1.64 – 1.16 (m, 12H), 0.92 – 0.52 (m, 18H) ppm; **$^{13}\text{C-NMR}$** (CDCl_3 , 75 MHz) δ 155.4, 155.24, 155.19, 155.0, 135.0, 134.82, 134.75, 134.7, 134.6, 134.2, 132.4, 129.4, 128.9, 123.6, 123.47, 123.41, 74.9, 74.7, 74.6, 46.5, 30.7, 30.6, 30.4, 23.7, 23.64, 23.60, 23.5, 10.7, 10.66, 10.62, 10.5 ppm; **FT-IR** (neat) 2961, 2935, 2876, 1730, 1589, 1449, 1385, 1249, 1214, 1193, 1080, 1006, 962 cm^{-1} ; **MS** (MALDI) m/z 960.17 $[\text{M}+\text{Na}]^+$; **HRMS** $[\text{M} + \text{NH}_4]^+$ Calculated for: $\text{C}_{61}\text{H}_{77}\text{Cl}_1\text{N}_1\text{O}_6$; 954.5434 Found: 954.5433



Synthesis of 132: A 1 mL capacity microwave vial was charged with a solution of **215** (26 mg, 0.028 mmol) in *N,N*-dimethylformamide (0.5 mL) and sodium azide (18 mg, 0.277 mmol) was added. The vial was sealed with a PTFE lined crimp cap and the mixture heated in the microwave

synthesiser at 90 $^\circ\text{C}$ for 3 h. The mixture was allowed to cool to room temperature, then diluted with diethyl ether (5 mL) and washed with water (3 x 5 mL). After drying over magnesium sulphate and removing the solvent under reduced pressure, the desired product was obtained as a pale yellow oil (22 mg, 0.023 mmol, 84 %). **$^1\text{H-NMR}$** (CDCl_3 , 400 MHz) δ 7.11 – 6.68 (m, 17H), 3.94 (brs, 12H), 3.85 (brs, 2H), 3.53 – 3.08 (m, 12H), 1.60 – 1.24 (m, 12H), 0.76 (m, 18H) ppm; **$^{13}\text{C-NMR}$** (CDCl_3 , 100 MHz) δ 155.4, 155.2, 155.1, 135.0, 134.8, 134.76, 134.69, 134.56, 134.2, 130.2, 129.3, 128.9, 123.6, 123.46, 123.40, 74.82, 74.77, 74.69, 74.65, 54.6, 30.66, 30.60, 30.4, 23.6, 23.5, 10.71, 10.66, 10.5 ppm; **FT-IR** (neat) 3070, 3030, 2962, 2934, 2875, 2094, 1723, 1587, 1449, 1250, 1216, 1194, 1081, 1062, 1007, 963 cm^{-1} ; **MS** (MALDI) m/z 983.16 $[\text{M}+\text{K}]^+$; **HRMS** $[\text{M} + \text{NH}_4]^+$ Calculated for: $\text{C}_{61}\text{H}_{77}\text{N}_4\text{O}_6$; 961.5838 Found: 961.5832

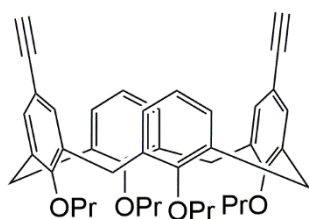


Synthesis of 211: A solution of triphenylphosphine (970 mg, 3.7 mmol) in dry dichloromethane (8 mL) was added dropwise to a solution of **139** (400 mg, 0.62 mmol) and carbon tetrabromide (1.227 g, 3.7 mmol) in dry dichloromethane (15 mL) at 0 $^\circ\text{C}$. The mixture was stirred at 0 $^\circ\text{C}$ for 0.5 h, then at room temperature for 1

h. TLC analysis (15% ethyl acetate in petrol) indicated that the starting material **139** had been

consumed. The mixture was filtered through a short plug of silica gel with dichloromethane as the eluent, and concentrated to afford **211** as a pale orange solid (570 mg, 0.59 mmol, 96 %).

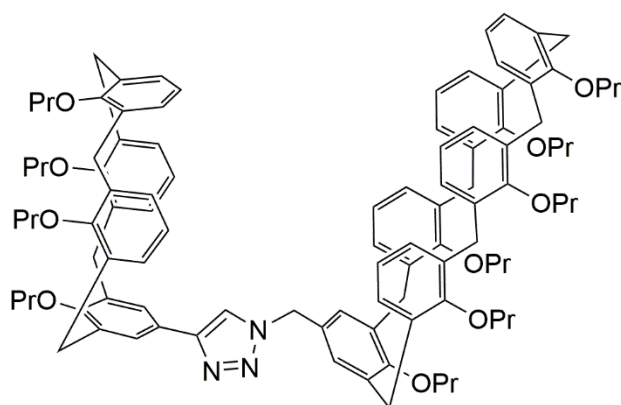
¹H-NMR (CDCl₃, 500 MHz) δ 7.09 (s, 2H), 6.79 – 6.67 (m, 10H), 4.45 (d, *J* = 13.3 Hz, 4H), 3.95 – 3.90 (m, 4H), 3.82 (t, *J* = 7.3 Hz, 4H), 3.17 (d, *J* = 13.4 Hz, 4H), 2.01 – 1.88 (m, 8H), 1.05 (t, *J* = 7.2 Hz, 6H), 0.98 (t, *J* = 7.5 Hz, 6H) ppm; **¹³C-NMR** (CDCl₃, 126 MHz) δ 156.9, 156.7, 136.8, 135.5, 134.6, 128.9, 128.7, 128.6, 122.4, 86.9, 77.0, 76.8, 31.1, 23.5, 23.3, 10.6, 10.3 ppm; **FT-IR** (neat) 2952, 2921, 2870, 1422, 1396, 1245, 1237, 1197, 1046, 1013, 1002, 966 cm⁻¹; **MS** (MALDI) *m/z* 982.6 [M+Na]⁺; **HRMS** [M+Na]⁺ Calculated for: C₄₄H₅₂Br₄O₄N₁; 978.0585 Found: 978.0588



Synthesis of 209: A 10 mL RBF was charged with a solution of **211** (296 mg, 0.31 mmol) in dry tetrahydrofuran (5 mL) at -78°C under an atmosphere of argon. ⁿbutyllithium (1.5 mL, 3.1 mmol, 2M in hexanes) was added dropwise *via* syringe and the mixture stirred at -78°C for 1 h. TLC analysis (10% diethyl ether in petrol) indicated the starting material

211 had been consumed. The mixture was allowed to warm to room temperature and then quenched with a saturated solution of ammonium chloride (aq.) (5 mL). The mixture was transferred to a 25 mL separating funnel and extracted with diethyl ether (2 x 10 mL). The combined organics were dried over magnesium sulphate, filtered and concentrated to afford an orange oil. Purification *via* column chromatography on silica gel (5% diethyl ether in petrol) afforded **209** as a pale orange solid (100 mg, 0.16 mmol, 51 %)

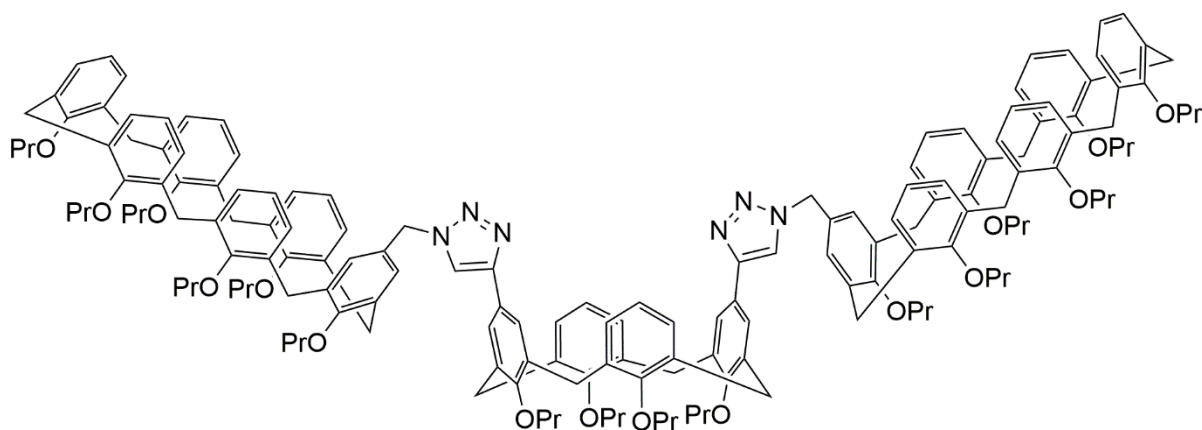
¹H-NMR (CDCl₃, 500 MHz) δ 7.08 (s, 4H), 6.46 – 6.31 (m, 6H), 4.41 (d, *J* = 13.4 Hz, 4H), 3.97 – 3.93 (m, 4H), 3.74 (t, *J* = 7.1 Hz, 4H), 3.13 (d, *J* = 13.4 Hz, 4H), 2.96 (s, 2H), 1.96 – 1.83 (m, 8H), 1.04 (t, *J* = 7.4 Hz, 6H), 0.94 (t, *J* = 7.5 Hz, 6H) ppm; **¹³C-NMR** (CDCl₃, 126 MHz) δ 158.4, 155.8, 136.5, 133.5, 132.6, 128.1, 122.5, 115.3, 84.5, 77.0, 76.9, 75.7, 30.9, 23.5, 23.3, 10.7, 10.2 ppm; **FT-IR** (neat) 3310, 2961, 2933, 2875, 2104, 1589, 1456, 1384, 1305, 1224, 1195, 1004, 966 cm⁻¹; **MS** (MALDI) *m/z* 663.48 [M+Na]⁺; **HRMS** [M + H]⁺ Calculated for: C₄₄H₄₉O₄; 641.3625 Found: 641.3637



Synthesis of 133: A microwave vial was charged with a solution of **132** (19 mg, 0.02 mmol), **131** (18 mg, 0.03 mmol), copper(II) sulphate (1 mg, 0.004 mmol), tris(benzyltriazolylmethyl)amine (3 mg, 0.006 mmol) and sodium ascorbate (6 mg, 0.03 mmol) in tetrahydrofuran (0.5 mL). The vial

was sealed with a PTFE lined crimp cap and the mixture heated in the microwave synthesiser at 90 °C for 3 h. TLC analysis (10% diethyl ether in pentane) indicated that the starting material **132** had been consumed. The solvent was removed *in vacuo* and the residue purified by column chromatography on silica gel (2% diethyl ether in dichloromethane) to afford **133** as a pale orange solid (27 mg, 0.017 mmol, 86 %)

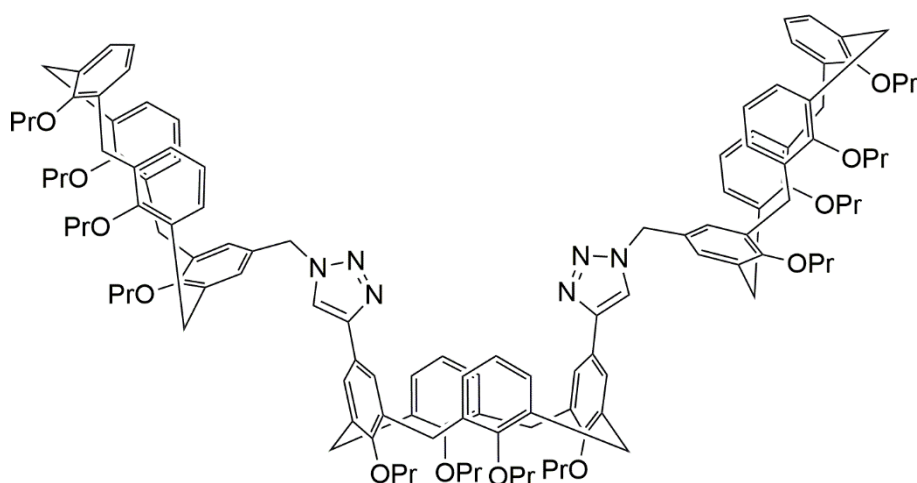
¹H-NMR (CDCl₃, 500 MHz) δ 7.15 – 6.33 (m, 29H), 4.97 (brs, 2H), 4.46 (m, 4H), 4.04 – 3.85 (m, 16H), 3.79 (t, *J* = 7.2 Hz, 4H), 3.44 (brs, 12H), 3.20 (brd, *J* = 13.2 Hz, 2H), 3.14 (d, *J* = 13.2 Hz, 2H), 1.93 (m, 8H), 1.66 – 1.43 (m, 12H), 1.04 (t, *J* = 7.4 Hz, 6H), 0.99 – 0.93 (m, 6H), 0.85 – 0.53 (m, 18H) ppm;
¹³C-NMR (CDCl₃, 126 MHz) δ 157.6, 157.2, 156.2, 155.4, 155.3, 136.5, 135.9, 135.3, 134.9, 134.8, 134.66, 134.62, 134.55, 134.3, 133.9, 128.9, 128.4, 128.2, 128.1, 126.0, 123.7, 123.5, 122.1, 121.9, 76.77, 76.69, 74.9, 74.7, 31.1, 30.7, 30.6, 30.4, 23.6, 23.5, 23.3, 10.7, 10.6, 10.5, 10.34, 10.30 ppm;
FT-IR (neat) 2961, 2931, 2880, 1589, 1455, 1385, 1248, 1214, 1194, 1086, 1042, 1006, 964, 911 cm⁻¹;
MS (MALDI) *m/z* 1582.96 [M+Na]⁺; **HRMS** [M+H]⁺ Calculated for: C₁₀₃H₁₂₂N₃O₁₀; 1561.9157 Found: 1561.9144



Synthesis of 217: A microwave vial was charged with a solution of **209** (12 mg, 0.019 mmol), **132** (53 mg, 0.056 mmol), copper(II) sulphate (1.8 mg, 0.007 mmol), tris(benzyltriazolylmethyl)amine (3 mg, 0.006 mmol) and sodium ascorbate (7 mg, 0.04 mmol) in tetrahydrofuran (0.7 mL). The vial was sealed with a PTFE lined crimp cap and the mixture heated in the microwave synthesiser at 90 °C for 3 h. TLC analysis (30% diethyl ether in pentane) indicated that the starting material **209** had been consumed. The solvent was removed *in vacuo* and the residue purified by column chromatography on silica gel (50% diethyl ether in pentane) to afford **217** as a pale orange solid (38 mg, 0.015 mmol, 86 %)

¹H-NMR (CDCl₃, 500 MHz) δ 7.35 (s, 2H), 6.99 – 6.59 (m, 40H), 6.21 (s, 4H), 4.96 (s, 4H), 4.38 (d, *J* = 13.2 Hz, 4H), 3.96 – 3.78 (m, 28H), 3.64 (t, *J* = 6.9 Hz, 4H), 3.34 (brs, 16H), 3.11 (d, *J* = 13.4 Hz, 4H), 1.91 – 1.78 (m, 8H), 1.44 (brs, 24H), 1.01 (t, *J* = 7.4 Hz, 6H), 0.87 – 0.82 (m, 6H), 0.68 (brs, 32H) ppm;

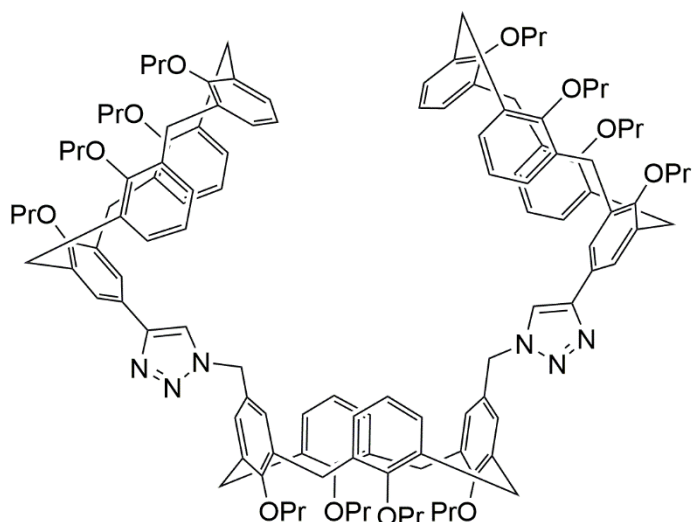
¹³C-NMR (CDCl₃, 126 MHz) δ 155.37, 155.31, 155.24, 155.20, 137.14, 135.28, 135.02, 134.94, 134.82, 134.80, 134.76, 134.69, 134.66, 134.55, 134.23, 134.03, 133.48, 130.20, 129.59, 129.27, 128.95, 127.92, 126.11, 123.69, 123.62, 123.52, 123.40, 122.28, 118.88, 74.85, 74.82, 74.77, 74.74, 74.65, 54.57, 53.85, 31.12, 30.72, 30.63, 30.51, 30.43, 29.84, 29.07, 23.89, 23.66, 23.62, 23.49, 23.19, 23.13, 11.10, 10.85, 10.73, 10.66, 10.53, 10.15 ppm; FT-IR (neat) 2962, 2934, 2875, 2094, 1728, 1588, 1455, 1385, 1249, 1216, 1195, 1084, 1006, 964, 766 cm⁻¹; MS (MALDI) *m/z* 1582.96 [M+Na]⁺; HRMS [M + H]⁺ Calculated for: C₁₀₃H₁₂₂N₃O₁₀; 1561.9157 Found: 1561.9144



Synthesis of 208: A 5 mL capacity microwave vial was charged with a solution of **209** (15 mg, 0.02 mmol), **129** (45 mg, 0.07 mmol), copper(II) sulphate pentahydrate (2 mg, 0.09 mmol), sodium ascorbate (9 mg, 0.05 mmol) and

tris(benzyltriazolylmethyl)amine (5 mg, 0.09 mmol) in tetrahydrofuran (1 mL). The vial was sealed with a PTFE lined crimp cap and heated to 90°C in the microwave synthesiser for 2 h. TLC analysis (dichloromethane) indicated the starting material **209** had been consumed. The solvent was removed *in vacuo* and the residue purified by column chromatography on silica gel (30 % diethyl ether in petrol) to afford **208** as a clear oil (34 mg, 0.018 mmol, 75 %)

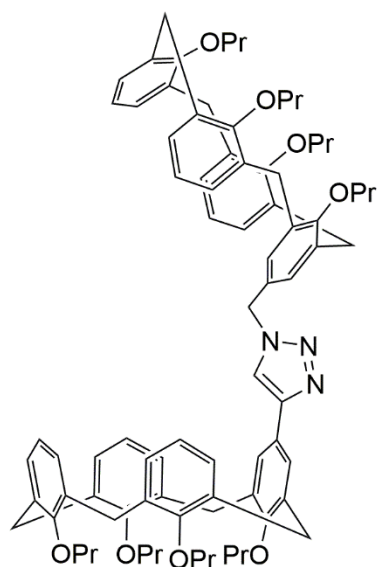
¹H-NMR (CDCl₃, 500 MHz) δ 7.36 (s, 4H), 7.22 (s, 2H), 6.79 (m, 8H), 6.69 (t, *J* = 7.4 Hz, 4H), 6.47 (s, 6H), 6.38 – 6.29 (m, 10H), 5.06 (s, 4H), 4.50 – 4.40 (m, 12H), 4.01 – 3.72 (m, 24H), 3.24 – 3.08 (m, 12H), 1.98 – 1.86 (m, 24H), 1.10 – 1.01 (m, 18H), 0.97 – 0.92 (m, 18H) ppm; ¹³C-NMR (CDCl₃, 126 MHz) δ 157.87, 157.16, 156.58, 156.31, 155.80, 136.88, 136.06, 135.56, 135.41, 134.63, 133.75, 128.76, 128.56, 128.05, 127.98, 127.71, 126.07, 122.35, 122.24, 121.60, 118.94, 77.41, 77.16, 77.00, 76.91, 76.77, 54.06, 31.16, 31.11, 31.07, 23.58, 23.50, 23.49, 23.25, 10.77, 10.66, 10.63, 10.25, 10.23 ppm; FT-IR (neat); 2961, 2933, 2875, 1587, 1456, 1384, 1247, 1215, 1195, 1087, 1006. 966, 911 cm⁻¹; MS (MALDI) *m/z* 1959.6 [M+Na]⁺; HRMS [M+H]⁺ Calculated for: C₁₂₆H₁₄₇N₆O₁₂; 1937.1102 Found: 1937.1128



Synthesis of 207: A 5 mL capacity microwave vial was charged with a solution of **161** (20 mg, 0.03 mmol), **131** (53 mg, 0.09 mmol), copper(II) sulphate pentahydrate (3 mg, 0.11 mmol), sodium ascorbate (11 mg, 0.06 mmol) and tris(benzyltriazolylmethyl)amine (6 mg, 0.11 mmol) in tetrahydrofuran (1 mL). The vial was sealed with a PTFE lined crimp cap and heated to 90°C in

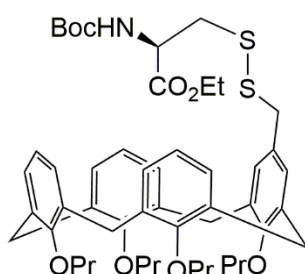
the microwave synthesiser for 3 h. TLC analysis (10% diethyl ether in petrol) indicated the starting material **161** had been consumed. The solvent was removed *in vacuo* and the residue purified by column chromatography on silica gel (50 % diethyl ether in pentane) to afford **207** as a clear oil (38 mg, 0.02 mmol, 69 %).

¹H-NMR (CDCl₃, 500 MHz) δ 7.32 (s, 2H), 7.15 (s, 4H), 6.66 – 6.43 (m, 28H), 5.21 (s, 4H), 4.53 – 4.41 (m, 16H), 3.95 – 3.76 (m, 24H), 3.20 (d, *J* = 13.5 Hz, 4H), 3.15 (d, *J* = 13.5 Hz, 8H), 1.99 – 1.86 (m, 24H), 1.03 (t, *J* = 7.4 Hz, 12H), 1.01 – 0.93 (m, 24H) ppm; ¹³C-NMR (CDCl₃, 126 MHz) δ 157.35, 157.15, 157.01, 156.59, 156.37, 148.48, 136.26, 136.02, 135.67, 134.87, 134.81, 134.49, 128.45, 128.31, 128.21, 128.14, 128.09, 125.90, 124.37, 122.49, 122.12, 121.84, 118.75, 77.37, 77.01, 76.91, 76.76, 76.69, 54.01, 31.14, 31.11, 31.07, 23.45, 23.35, 23.31, 10.58, 10.40, 10.37, 10.34 ppm; FT-IR (neat) 2961, 2933, 2875, 1586, 1455, 1384, 1354, 1246, 1213, 1195, 1006, 966, 759 cm⁻¹; MS (MALDI) *m/z* 1959.2 [M+Na]⁺; HRMS [M + H]⁺ Calculated for: C₁₂₆H₁₄₇N₆O₁₂; 1937.1102 Found: 1937.1079



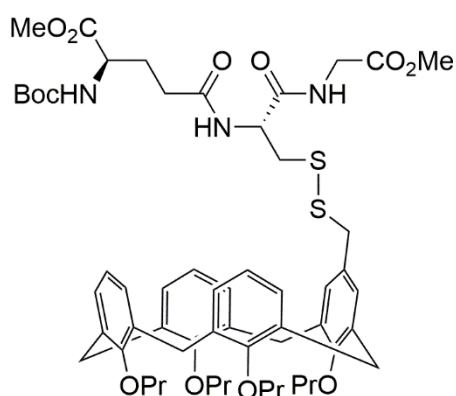
Synthesis of 206: A 5 mL capacity microwave vial was charged with a solution of **131** (30 mg, 0.05 mmol), **129** (38 mg, 0.06 mmol), copper(II) sulphate pentahydrate (4 mg, 0.19 mmol), sodium ascorbate (19 mg, 0.1 mmol) and tris(benzyltriazolylmethyl)amine (10 mg, 0.02 mmol) in tetrahydrofuran (1 mL). The vial was sealed with a PTFE lined crimp cap and heated to 90°C in the microwave synthesiser for 2 h. TLC analysis (dichloromethane) indicated the starting material **131** had been consumed. The solvent was removed *in vacuo* and the residue purified by column chromatography on silica gel (30 % diethyl ether in petrol) to afford **206** as a clear oil (52 mg, 0.04 mmol, 85 %).

¹H-NMR (CDCl₃, 500 MHz) δ 7.15 (s, 2H), 7.14 (s, 1H), 6.84 (dd, *J* = 7.4, 1.4 Hz, 4H), 6.81 – 6.78 (m, 4H), 6.71 (t, *J* = 7.4 Hz, 2H), 6.67 (d, *J* = 7.5 Hz, 2H), 6.51 (dd, *J* = 6.4, 2.8 Hz, 2H), 6.47 – 6.42 (m, 6H), 6.37 (t, *J* = 7.5 Hz, 1H), 6.28 (s, 2H), 5.03 (s, 2H), 4.50 – 4.42 (m, 8H), 3.97 – 3.86 (m, 8H), 3.82 – 3.72 (m, 8H), 3.24 – 3.08 (m, 8H), 1.98 – 1.86 (m, 16H), 1.06 – 1.00 (m, 12H), 0.98 – 0.91 (m, 12H) ppm; **¹³C-NMR** (CDCl₃, 126 MHz) δ 157.44, 157.25, 157.14, 156.56, 156.27, 136.35, 136.16, 135.84, 135.67, 135.36, 134.68, 134.56, 134.36, 128.81, 128.60, 128.40, 128.16, 128.09, 127.97, 127.92, 127.79, 126.01, 124.43, 122.21, 122.13, 121.87, 121.57, 118.80, 77.00, 76.76, 76.70, 54.04, 31.16, 31.12, 23.50, 23.48, 23.30, 23.24, 10.68, 10.62, 10.36, 10.31, 10.22 ppm; **FT-IR** (neat) 2960, 2932, 2874, 1586, 1456, 1384, 1246, 1214, 1194, 1006, 966 cm⁻¹; **MS** (MALDI) *m/z* 1287.32 [M+Na]⁺; **HRMS** [M+H]⁺ Calculated for: C₈₃H₉₈N₃O₈; 1263.7348 Found: 1263.7348



Synthesis of 236: A 5 mL capacity vial was charged with a solution of **225** (130 mg, 0.2 mmol) and **237** (76 mg, 0.153 mmol) in anhydrous degassed deuteriochloroform (2 mL). Triethylamine (57 μL, 0.41 mmol) was added, and the mixture stirred at room temperature in the dark under an atmosphere of argon for 48 h. An aliquot (200 μL) was taken, and the solvent removed. Purification by column chromatography on silica gel (dichloromethane) afforded **236** as a clear oil (12 mg, 0.014 mmol, 67 % based on quantity removed).

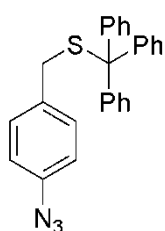
¹H-NMR (CDCl₃, 500 MHz) δ 6.66 – 6.48 (m, 11H), 5.28 (d, *J* = 7.7 Hz, 1H), 4.45 (d, *J* = 11.0 Hz, 2H), 4.42 (d, *J* = 10.8 Hz, 2H), 4.24 – 4.16 (m, 2H), 3.90 – 3.79 (m, 8H), 3.60 (s, 2H), 3.15 (d, *J* = 9.3 Hz, 2H), 3.12 (d, *J* = 9.3 Hz, 2H), 2.89 (qd, *J* = 13.9, 5.3 Hz, 2H), 1.97 – 1.86 (m, 8H), 1.45 (s, 9H), 1.29 (t, *J* = 7.1 Hz, 3H), 1.03 – 0.95 (m, 12H) ppm; **¹³C-NMR** (CDCl₃, 126 MHz) δ 170.9, 156.8, 156.7, 156.5, 155.2, 135.5, 135.3, 135.0, 130.4, 129.7, 129.29, 129.26, 129.18, 128.37, 128.28, 128.26, 128.21, 122.1, 121.8, 80.2, 77.7, 76.8, 61.8, 53.2, 43.8, 41.1, 31.12, 31.10, 28.5, 23.4, 14.3, 10.5, 10.47, 10.45 ppm; **FT-IR** (neat) 3436, 2962, 2932, 2874, 2245, 1718, 1585, 1458, 1384, 1367, 1247, 1210, 1086, 1007, 966, 760, 734 cm⁻¹; **MS** (MALDI) *m/z* 908.81 [M+Na]⁺; **HRMS** [M + NH₄]⁺ Calculated for: C₅₁H₇₁N₂O₈S₂; 903.4646 Found: 903.4646



Synthesis of 239: A 1 mL capacity vial was charged with a solution of **225** (130 mg, 0.2 mmol) and **238** (133 mg, 0.153 mmol) in anhydrous degassed deuteriochloroform (2 mL). Triethylamine (57 μL, 0.41 mmol) was added, and the mixture stirred at room temperature in the dark under an atmosphere of argon for 48 h. An aliquot (200 μL) was

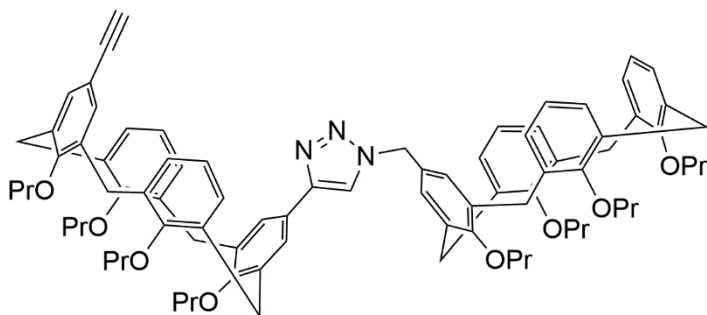
taken, and the solvent removed. Purification by column chromatography on silica gel (dichloromethane) afforded **239** as a clear oil (13 mg, 0.012 mmol, 60 % based on quantity removed).

¹H-NMR (CDCl₃, 500 MHz) δ 8.44 (s, 1H), 6.61 – 6.38 (m, 11H), 5.45 (s, 1H), 5.25 (d, *J* = 7.3 Hz, 1H), 4.59 (dd, *J* = 13.3, 7.3 Hz, 1H), 4.41 – 4.28 (m, 5H), 4.11 – 3.87 (m, 4H), 3.80 – 3.73 (m, 4H), 3.71 – 3.64 (m, 10H), 3.55 (d, *J* = 5.0 Hz, 2H), 3.07 (d, *J* = 9.7 Hz, 2H), 3.05 (d, *J* = 9.7 Hz, 2H), 2.99 (dd, *J* = 14.7, 3.9 Hz, 1H), 2.90 – 2.75 (m, 1H), 2.38 – 2.24 (m, 2H), 2.17 – 2.08 (m, 4H), 1.88 – 1.77 (m, 8H), 1.37 (s, 9H), 0.95 – 0.88 (m, 12H) ppm; **¹³C-NMR** (CDCl₃, 126 MHz) δ 173.0, 172.6, 170.8, 170.1, 156.5, 135.5, 135.3, 135.1, 129.3, 129.2, 128.6, 128.5, 128.42, 128.40, 128.32, 128.30, 128.2, 127.9, 122.1, 121.8, 53.2, 52.6, 52.5, 41.5, 32.5, 31.1, 28.5, 23.4, 23.39, 23.36, 10.5, 10.48, 10.44, 10.42, 10.3 ppm; **FT-IR** (neat) 3310, 2961, 2932, 2875, 1744, 1713, 1656, 1527, 1454, 1383, 1367, 1247, 1211, 1168, 1086, 1036, 1007, 966, 759 cm⁻¹; **MS** (MALDI) *m/z* 1094.72 [M+Na]⁺; **HRMS** [M+NH₄]⁺ Calculated for: C₅₈H₈₁N₄O₁₂S₂; 1089.5372 Found: 1089.5370



Synthesis of 242: A 50 mL round bottomed flask was charged with a mixture of 4-azidobenzyl bromide (429 mg, 2.02 mmol), triphenylmethyl mercaptan (615 mg, 2.23 mmol) and potassium carbonate (336 mg, 2.43 mmol) in acetone (10 mL). The mixture was stirred at room temperature overnight. The potassium carbonate was removed by filtration and the filtrate concentrated. Purification by column chromatography on silica gel (15 % dichloromethane in petrol) afforded **242** (610 mg, 1.5 mmol, 74 %) as an orange oil.

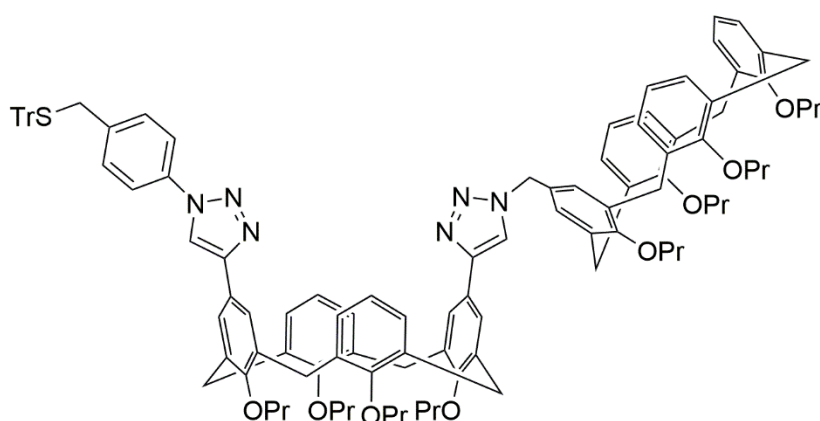
¹H-NMR (CDCl₃, 500 MHz) δ 7.49 – 7.44 (m, 6H), 7.34 – 7.28 (m, 6H), 7.26 – 7.21 (m, 3H), 7.10 (d, *J* = 8.5 Hz, 2H), 6.89 (d, *J* = 8.5 Hz, 2H), 3.29 (s, 2H) ppm; **¹³C-NMR** (CDCl₃, 126 MHz) δ 144.8, 138.9, 133.9, 130.6, 129.7, 128.1, 126.9, 119.2, 67.7, 36.5 ppm; **FT-IR** (neat) 3227, 3056, 3030, 2926, 2409, 2255, 2108, 1955, 1896, 1595, 1579, 1505, 1444, 1303, 1283, 1182, 1128, 1082, 1034, 833, 741, 699 cm⁻¹; **MS** (MALDI) *m/z* 430.27 [M+Na]⁺; **HRMS** [M+H]⁺ Calculated for: C₂₆H₂₂N₃S; 408.1569 Found: 408.1571



Synthesis of 250: A 5 mL capacity microwave vial was charged with a solution of **129** (100 mg, 0.156 mmol), **209** (101 mg, 0.156 mmol), copper(II) sulphate pentahydrate (8 mg, 0.031 mmol), sodium ascorbate (6 mg, 0.031

mmol) and tris(benzyltriazolylmethyl)amine (33 mg, 0.062 mmol) in tetrahydrofuran (2 mL). The vial was sealed with a PTFE lined crimp cap and heated to 90°C in the microwave synthesiser for 3 h. The solvent was removed *in vacuo* and the residue purified by column chromatography on silica gel (dichloromethane then 4 % ether in dichloromethane) to afford **250** as a clear oil (61 mg, 0.047 mmol, 30 %).

¹H-NMR (CDCl₃, 500 MHz) δ 7.41 (s, 2H), 7.29 (s, 1H), 7.11 (s, 2H), 6.87 – 6.23 (m, 17H), 5.06 (s, 2H), 4.50 – 4.41 (m, 8H), 4.03 – 3.89 (m, 8H), 3.83 – 3.69 (m, 8H), 3.25 – 3.10 (m, 8H), 2.80 (s, 1H), 1.98 – 1.85 (m, 16H), 1.11 – 1.02 (m, 12H), 0.98 – 0.89 (m, 12H) ppm; **¹³C-NMR** (CDCl₃, 126 MHz) δ 158.67, 157.87, 157.23, 157.18, 156.59, 156.27, 155.63, 148.23, 136.94, 136.83, 136.14, 135.92, 135.82, 135.63, 135.39, 134.89, 134.75, 134.57, 133.63, 133.20, 132.65, 128.80, 128.63, 128.60, 128.08, 127.92, 127.85, 127.17, 126.24, 124.54, 122.36, 122.22, 122.10, 121.56, 121.49, 118.92, 115.12, 84.37, 77.06, 77.01, 76.76, 75.53, 65.50, 54.07, 31.16, 31.11, 31.08, 30.94, 23.57, 23.50, 23.24, 23.20, 10.79, 10.68, 10.65, 10.62, 10.26, 10.22, 10.17, 10.12 ppm; **FT-IR** (neat) 3311, 2962, 2933, 2875, 2244, 1587, 1455, 1384, 1281, 1195, 1216, 1086, 1006, 966, 909, 759, 733 cm⁻¹; **MS** (MALDI) *m/z* 1310.32 [M+Na]⁺; **HRMS** [M+H]⁺ Calculated for: C₈₅H₉₈N₃O₈; 1288.7348 Found: 1288.7346

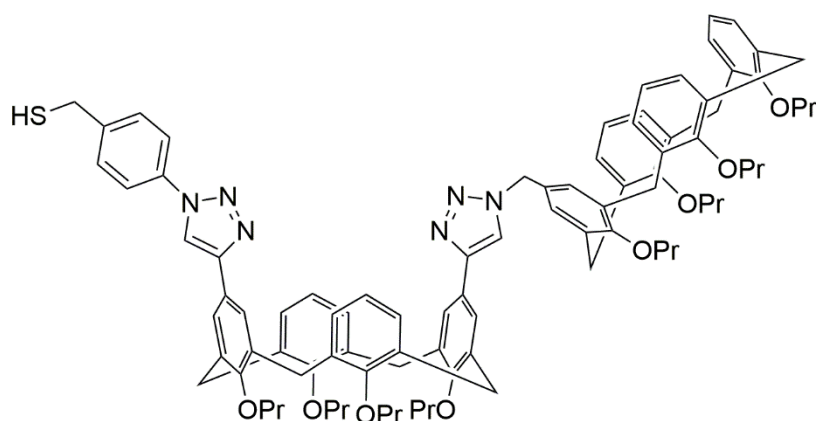


Synthesis of 241: A 5 mL capacity microwave vial was charged with a solution of **250** (50 mg, 0.039 mmol), **242** (24 mg, 0.058 mmol), copper(II) sulphate pentahydrate (2 mg, 0.007 mmol), sodium ascorbate (3 mg, 0.016 mmol) and

tris(benzyltriazolylmethyl)amine (4 mg, 0.007 mmol) in tetrahydrofuran (2 mL). The vial was sealed with a PTFE lined crimp cap and heated to 90°C in the microwave synthesiser for 6 h. The solvent was removed *in vacuo* and the residue purified by column chromatography on silica gel (5 % ether in dichloromethane) to afford **241** as a clear oil (53 mg, 0.031 mmol, 81 %).

¹H-NMR (CDCl₃, 500 MHz) δ 7.81 (s, 1H), 7.64 (d, *J* = 8.5 Hz, 2H), 7.52 – 7.47 (m, 8H), 7.32 (m, 6H), 7.17 – 7.12 (m, 2H), 7.02 (s, 1H), 6.88 – 6.16 (m, 21H), 4.78 (s, 2H), 4.55 – 4.37 (m, 8H), 4.20 (s, 2H), 4.00 – 3.72 (m, 16H), 3.40 (s, 2H), 3.27 – 3.05 (m, 8H), 1.98 – 1.84 (m, 16H), 1.10 – 0.91 (m, 24H) ppm; **¹³C-NMR** (CDCl₃, 126 MHz) 157.18, 157.10, 156.44, 156.28, 148.45, 144.68, 138.00, 136.12, 135.96, 135.82, 135.50, 135.32, 134.89, 134.75, 134.61, 130.45, 129.74, 128.69, 128.66, 128.64,

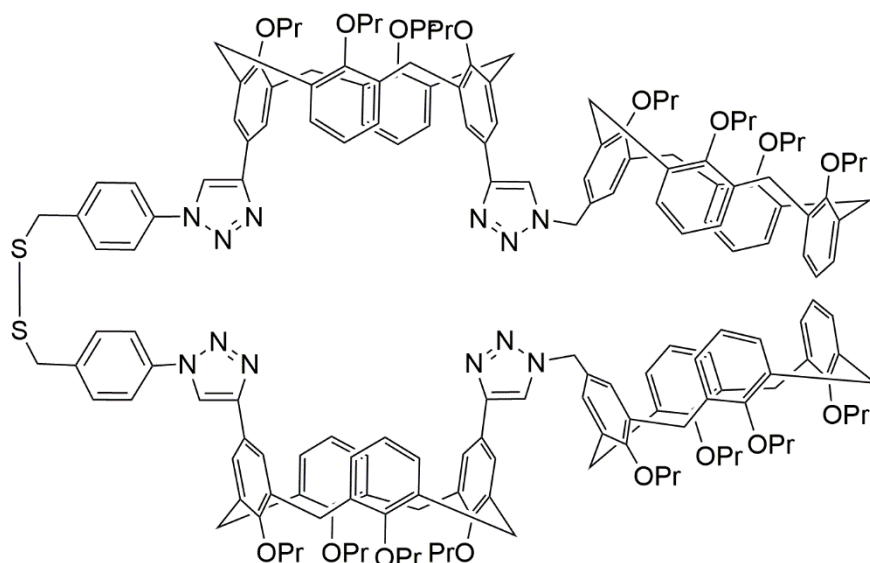
128.55, 128.41, 128.17, 128.07, 127.94, 127.56, 127.40, 127.17, 126.97, 125.79, 123.76, 122.42, 122.20, 122.10, 121.59, 120.66, 118.83, 118.74, 116.81, 115.54, 67.83, 65.50, 53.96, 36.57, 31.17, 31.16, 31.10, 31.08, 31.01, 23.48, 23.44, 23.37, 23.35, 23.24, 10.65, 10.62, 10.61, 10.54, 10.44, 10.42, 10.26, 10.24, 10.22 ppm; **FT-IR** (neat) 2961, 2933, 2874, 2243, 2109, 1590, 1518, 1456, 1384, 1215, 1085, 1037, 1006, 966, 909, 760, 733, 701 cm^{-1} ; **MS** (MALDI) m/z 1718.08 $[\text{M}+\text{Na}]^+$; **HRMS** $[\text{M} + \text{NH}_4]^+$ Calculated for: $\text{C}_{111}\text{H}_{122}\text{N}_6\text{O}_8\text{S}$; 1712.9142 Found: 1712.9145



Synthesis of 251: To a solution of **241** (52 mg, 0.031 mmol) in anhydrous degassed dichloromethane (0.5 mL) was added triethylsilane (50 μL , 0.31 mmol) and trifluoroacetic acid (24 μL , 0.31 mmol). The mixture was

stirred at room temperature for 1 h under an atmosphere of argon. The solvents were removed *in vacuo* and the residue purified by column chromatography on silica gel (dichloromethane then 4% diethyl ether in dichloromethane) to afford **251** as a clear oil (22 mg, 0.015 mmol, 49 %).

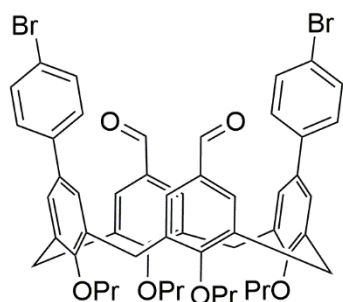
$^1\text{H-NMR}$ (CDCl_3 , 500 MHz) δ 7.93 (s, 1H), 7.77 (d, $J = 8.6$ Hz, 2H), 7.48 (d, $J = 8.6$ Hz, 2H), 7.07 (d, $J = 8.2$ Hz, 2H), 7.05 (d, $J = 7.4$ Hz, 2H), 6.96 (d, $J = 3.4$ Hz, 1H), 6.90 (m, 2H), 6.77 (s, 2H), 6.75 (m, 2H), 6.68 – 6.56 (m, 7H), 6.43 – 6.30 (m, 4H), 6.05 (s, 2H), 4.57 (s, 2H), 4.50 (m, 4H), 4.42 (d, $J = 13.3$ Hz, 2H), 4.35 (m, 2H), 4.06 – 3.98 (m, 4H), 3.91 – 3.66 (m, 14H), 3.22 (d, $J = 6.4$ Hz, 2H), 3.19 (d, $J = 6.6$ Hz, 2H), 3.14 (d, $J = 13.3$ Hz, 2H), 3.02 (d, $J = 13.3$ Hz, 2H), 2.00 – 1.81 (m, 16H), 1.09 (m, 6H), 1.05 – 0.97 (m, 6H), 0.93 (m, 12H) ppm; **$^{13}\text{C-NMR}$** (CDCl_3 , 126 MHz) 157.35, 157.24, 157.05, 157.00, 156.87, 156.71, 156.31, 147.73, 142.05, 135.94, 135.88, 135.77, 135.69, 135.58, 135.51, 135.47, 135.38, 135.31, 135.25, 134.70, 134.66, 130.77, 129.45, 129.06, 128.71, 128.53, 127.89, 127.54, 126.92, 125.44, 125.15, 122.95, 122.55, 122.23, 121.51, 120.84, 120.61, 119.50, 117.28, 76.81, 76.74, 54.69, 31.18, 31.08, 30.96, 29.84, 28.58, 23.52, 23.48, 23.42, 23.28, 23.22, 10.72, 10.64, 10.58, 10.23, 10.19 ppm; **FT-IR** (neat) 2962, 2933, 2875, 2109, 1770, 1608, 1519, 1462, 1455, 1384, 1214, 1196, 1006, 966, 890, 838, 761, 736, 703 cm^{-1} ; **MS** (MALDI) m/z 1476.8 $[\text{M}+\text{Na}]^+$; **HRMS** $[\text{M} + \text{NH}_4]^+$ Calculated for: $\text{C}_{92}\text{H}_{108}\text{N}_7\text{O}_8\text{S}$; 1470.8384 Found: 1470.8379



Synthesis of 252: To a solution of **251** (80 mg, 0.055 mmol) in ethyl acetate (1 mL) was added sodium iodide (20 mg, 0.14 mmol) then hydrogen peroxide (30% w/w in water, 50 μ L, 0.55 mmol) dropwise. The mixture was stirred at room temperature for

1 h. Ethyl acetate (5 mL) and water (5 mL) were added, and the organic layer separated. The solvents were removed *in vacuo* and the residue purified by column chromatography on silica gel (7% ether in dichloromethane) to afford **252** as a white solid (65 mg, 0.022 mmol, 79 %).

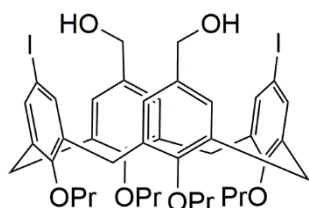
$^1\text{H-NMR}$ (CDCl_3 , 500 MHz) δ 7.85 (s, 2H), 7.76 (d, $J = 8.5$ Hz, 4H), 7.42 (d, $J = 8.5$ Hz, 4H), 7.28 (s, 4H), 7.15 (s, 4H), 7.02 (s, 2H), 6.79 – 6.41 (m, 30H), 6.17 (s, 4H), 4.80 (s, 4H), 4.52 – 4.37 (m, 16H), 3.96 – 3.71 (m, 26H), 3.25 – 3.02 (m, 34H), 1.99 – 1.83 (m, 32H), 1.06 – 0.90 (m, 48H) ppm; $^{13}\text{C-NMR}$ (CDCl_3 , 126 MHz) 157.66, 157.33, 157.08, 156.48, 156.33, 156.30, 148.66, 147.93, 137.97, 136.45, 136.39, 136.19, 135.93, 135.46, 135.33, 134.68, 134.49, 134.36, 130.74, 128.67, 128.51, 128.37, 128.29, 128.10, 127.96, 127.51, 125.89, 125.75, 123.76, 122.36, 122.19, 121.59, 120.64, 118.59, 116.69, 53.73, 42.71, 31.18, 31.09, 31.01, 23.47, 23.44, 23.35, 23.32, 23.24, 10.63, 10.60, 10.40, 10.37, 10.25 ppm; **FT-IR** (neat) 2961, 2933, 2875, 1519, 1455, 1384, 1214, 1195, 1126, 1037, 1006, 966, 889, 759 cm^{-1} ; **MS** (MALDI) m/z 2928.2 $[\text{M}+\text{Na}]^+$; **HRMS** $[\text{M} + 2\text{H}]^{2+}$ Calculated for: $\text{C}_{184}\text{H}_{208}\text{N}_{12}\text{O}_{16}\text{S}_2$; 1453.7662 Found: 1453.7676



Synthesis of 271: A microwave vial was charged with a solution of **258** (50 mg, 0.06 mmol), $\text{Pd}(\text{dppf})\text{Cl}_2$ (8 mg, 0.01 mmol), potassium carbonate (15 mg, 0.11 mmol) and *para*-bromophenyl boronic acid (36 mg, 0.18 mmol) in a mixture of toluene (0.9 mL) and ethanol (0.1 mL). The vial was then sealed with a PTFE lined crimp cap, and the mixture heated and stirred in the microwave synthesiser at 80°C for 4

h. The solvent was removed *in vacuo* to afford a brown solid. Purification by flash column chromatography afforded **271** as an off-white solid (43 mg, 0.045 mmol, 75%)

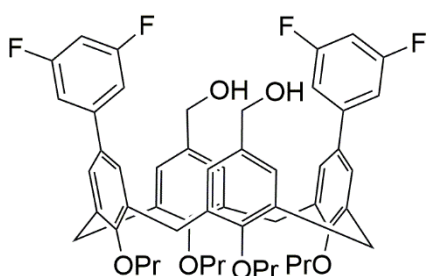
¹H-NMR (500 MHz, CDCl₃) δ 9.58 (s, 2H), 7.27 (d, *J* = 8.4 Hz, 4H), 7.20 (s, 4H), 6.95 (d, *J* = 8.4 Hz, 4H), 6.83 (s, 4H), 4.53 (d, *J* = 13.5 Hz, 4H), 4.03 – 3.99 (m, 4H), 3.91 – 3.87 (m, 4H), 3.31 (d, *J* = 13.6 Hz, 4H), 1.99 – 1.91 (m, 8H), 1.06 – 1.00 (m, 12H) ppm; **¹³C-NMR** (CDCl₃, 126 MHz) δ 191.8, 162.9, 156.4, 139.3, 136.2, 134.9, 134.4, 132.6, 131.6, 131.3, 130.2, 128.3, 127.1, 121.1, 117.4, 31.3, 23.5, 23.4, 10.4 ppm; FTIR (thin film) 2962, 2931, 2874, 1690, 1586, 1474, 1465, 1383, 1277, 1123, 1072, 1003, 961, 821, 809 cm⁻¹; **MS** (MALDI) *m/z* 996.62 [M+K]⁺; **HRMS** [M+NH₄]⁺ Calculated for C₅₄H₅₈Br₂O₆: 974.2612 Found: 974.2609.



Synthesis of 276: To a solution of **258** (400 mg, 0.44 mmol) in ethanol (4 mL) was added sodium borohydride (50 mg, 1.33 mmol) in one portion. The mixture was stirred at room temperature for 0.5 h under an atmosphere of nitrogen. TLC analysis (30% ethyl acetate in petrol) indicated that the starting material **258** had been consumed. The solvent was removed *in vacuo* and the residue partitioned between dichloromethane (15 mL) and water (15 mL). The organics were dried over magnesium sulfate, filtered and concentrated to afford **276** as a white solid (398 mg, 0.44 mmol, 99 %).

¹H-NMR (CDCl₃, 500 MHz) δ 7.29 (s, 4H), 6.35 (s, 4H), 4.37 (d, *J* = 13.3 Hz, 4H), 4.21 (s, 4H), 3.99 – 3.93 (m, 4H), 3.68 (t, *J* = 7.1 Hz, 4H), 3.08 (d, *J* = 13.4 Hz, 4H), 1.97 – 1.81 (m, 8H), 1.04 (t, *J* = 7.4 Hz, 6H), 0.90 (t, *J* = 7.5 Hz, 6H) ppm; **¹³C-NMR** (CDCl₃, 126 MHz) δ 157.45, 155.4, 138.8, 137.4, 134.9, 133.4, 126.6, 85.7, 77.3, 76.9, 64.1, 30.9, 23.49, 23.05, 10.7, 10.1 ppm; **FT-IR** (neat) 3343, 2961, 2931, 2874, 1564, 1480, 1384, 1281, 1214, 1126, 1004, 963 cm⁻¹; **MS** (MALDI) *m/z* 927.52 [M+Na]⁺; **HRMS** [M + NH₄]⁺ Calculated for C₄₂H₅₄O₆N₁I₂: 922.2035; Found: 922.2035.

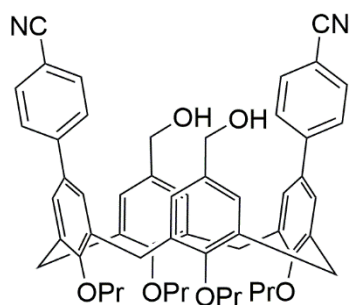
GP1: A microwave vial was charged with a solution of **276** (100 mg, 0.11 mmol), Pd(dppf)Cl₂ (12 mg, 0.02 mmol), potassium carbonate (30 mg, 0.22 mmol) and the appropriate aryl boronic acid (0.33 mmol) in toluene/ethanol (9:1, 1.5 mL). The vial was sealed with a PTFE lined crimp cap, and the mixture heated and stirred in the microwave synthesiser for 4 h at 80° C. The solvents were removed *in vacuo* and the impure mixture purified *via* column chromatography on silica gel to afford (**277** to **283**).



Synthesis of 277: Synthesis employing **GP1**. Purification *via* column chromatography on silica gel (5% diethyl ether in dichloromethane) afforded **277** as an orange oil (53 mg, 0.061 mmol, 55%)

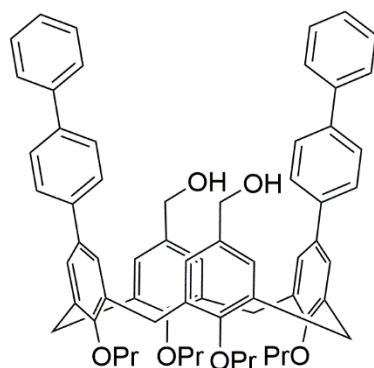
¹H-NMR (CDCl₃, 500 MHz) δ 6.97 (s, 4H), 6.79 (d, *J* = 6.8 Hz, 4H),

6.61 (tt, $J = 8.9, 2.2$ Hz, 2H), 6.57 (s, 4H), 4.51 (d, $J = 13.3$ Hz, 4H), 4.30 (s, 4H), 4.00 – 3.94 (m, 4H), 3.83 (t, $J = 7.3$ Hz, 4H), 3.22 (d, $J = 13.4$ Hz, 4H), 2.02 – 1.89 (m, 8H), 1.04 (t, $J = 7.4$ Hz, 6H), 0.99 (t, $J = 7.5$ Hz, 6H) ppm; $^{13}\text{C-NMR}$ (CDCl_3 , 126 MHz) δ 164.26, 164.16, 162.30, 162.19, 157.6, 156.0, 144.5, 144.4, 144.3, 136.2, 134.8, 134.5, 132.6, 128.1, 127.0, 126.9, 109.41, 109.36, 109.3, 109.2, 102.0, 101.7, 101.6, 64.9, 31.4, 23.5, 23.3, 10.6, 10.3 ppm; **FT-IR** (neat) 3309, 2961, 2933, 2875, 1623, 1595, 1455, 1402, 1386, 1280, 1217, 1116, 1037, 1011 cm^{-1} ; **MS** (MALDI) m/z 899.85 $[\text{M}+\text{Na}]^+$; **HRMS** $[\text{M}+\text{NH}_4]^+$ Calculated for $\text{C}_{54}\text{H}_{60}\text{F}_4\text{O}_6\text{N}_1$: 894.4351; Found: 894.4336.



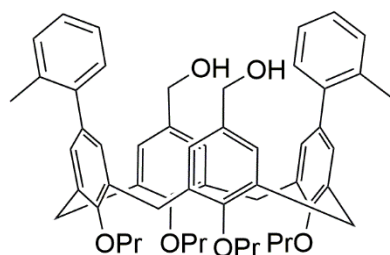
Synthesis of 278: Synthesis employing **GP1**. Purification *via* column chromatography on silica gel (15% diethyl ether in dichloromethane) afforded **278** as an orange oil (61 mg, 0.072 mmol, 65%).

$^1\text{H-NMR}$ (CDCl_3 , 500 MHz) δ 7.61 (d, $J = 8.5$ Hz, 4H), 7.56 (d, $J = 8.5$ Hz, 4H), 7.21 (s, 4H), 6.39 (s, 4H), 4.52 (d, $J = 13.3$ Hz, 4H), 4.15 (s, 4H), 4.09 – 4.03 (m, 4H), 3.77 (t, $J = 7.1$ Hz, 4H), 3.24 (d, $J = 13.4$ Hz, 4H), 2.04 – 1.89 (m, 8H), 1.09 (t, $J = 7.4$ Hz, 6H), 0.96 (t, $J = 7.5$ Hz, 6H) ppm; $^{13}\text{C-NMR}$ (CDCl_3 , 126 MHz) δ 158.4, 155.6, 145.5, 137.0, 134.8, 133.8, 132.9, 132.5, 127.6, 127.4, 126.5, 119.2, 110.2, 64.8, 31.4, 23.6, 23.2, 10.8, 10.1 ppm; **FT-IR** (neat) 3402, 2962, 2933, 2876, 2226, 1605, 1464, 1385, 1307, 1228, 1158, 1036, 1005, 964, 909, 834 cm^{-1} ; **MS** (MALDI) m/z 877.17 $[\text{M}+\text{Na}]^+$; **HRMS** $[\text{M} + \text{H}]^+$ Calculated for $\text{C}_{56}\text{H}_{62}\text{N}_3\text{O}_6$: 872.4633; Found: 872.4619.



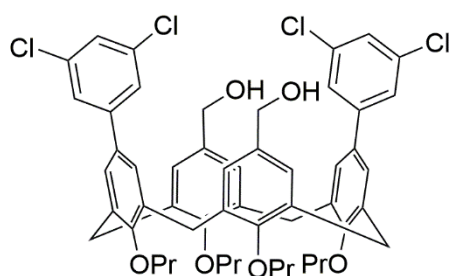
Synthesis of 279: Synthesis employing **GP1**. Purification *via* column chromatography on silica gel (5% diethyl ether in dichloromethane) afforded **279** as a brown oil (79 mg, 0.083 mmol, 75%).

$^1\text{H-NMR}$ (CDCl_3 , 500 MHz) δ 7.66 – 7.59 (m, 12H), 7.43 (m, 4H), 7.37 – 7.30 (m, 6H), 6.41 (s, 4H), 4.54 (d, $J = 13.2$ Hz, 4H), 4.14 (s, 4H), 4.11 – 4.06 (m, 4H), 3.77 (t, $J = 7.0$ Hz, 4H), 3.26 (d, $J = 13.3$ Hz, 4H), 2.09 – 2.00 (m, 4H), 1.99 – 1.91 (m, 4H), 1.11 (t, $J = 7.4$ Hz, 6H), 0.97 (t, $J = 7.5$ Hz, 6H) ppm; $^{13}\text{C-NMR}$ (CDCl_3 , 126 MHz) δ 157.4, 155.5, 141.0, 140.2, 139.6, 136.7, 134.8, 134.5, 133.9, 128.9, 127.49, 127.45, 127.39, 127.3, 127.1, 126.5, 64.9, 31.4, 23.6, 23.2, 10.8, 10.1 ppm; **FT-IR** (neat) 3344, 2960, 2932, 2874, 1743, 1599, 1466, 1384, 1277, 1006, 909 cm^{-1} ; **MS** (MALDI) m/z 979.19 $[\text{M}+\text{Na}]^+$; **HRMS** $[\text{M} + \text{H}]^+$ Calculated for $\text{C}_{66}\text{H}_{72}\text{O}_6\text{N}_1$: 974.5354; Found: 974.5352.



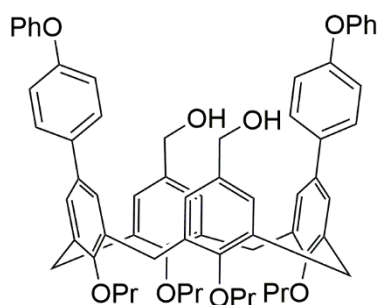
Synthesis of 280: Synthesis employing **GP1**. Purification *via* column chromatography on silica gel (5% diethyl ether in dichloromethane) afforded **280** as an orange oil (60 mg, 0.073 mmol, 66%).

$^1\text{H-NMR}$ (CDCl_3 , 500 MHz) δ 7.17 (m, 6H), 7.03 (m, 2H), 6.83 (s, 4H), 6.57 (s, 4H), 4.52 (d, $J = 13.0$ Hz, 4H), 4.24 (s, 4H), 4.02 – 3.96 (m, 4H), 3.84 (t, $J = 7.3$ Hz, 4H), 3.19 (d, $J = 13.1$ Hz, 4H), 2.08 – 1.95 (m, 8H), 1.81 (s, 6H), 1.07 (t, $J = 7.4$ Hz, 6H), 1.02 (t, $J = 7.5$ Hz, 6H) ppm; $^{13}\text{C-NMR}$ (CDCl_3 , 126 MHz) δ 155.9, 155.8, 141.9, 135.7, 135.6, 135.1, 134.8, 134.7, 130.6, 129.8, 129.6, 126.7, 126.68, 125.7, 65.1, 31.2, 23.5, 23.4, 20.5, 10.6, 10.3 ppm; **FT-IR** (neat) 3335, 2960, 2874, 2932, 1603, 1465, 1384, 1228, 1126, 1037, 1007, 65, 875, 758, 727 cm^{-1} ; **MS** (MALDI) m/z 871.31 $[\text{M}+\text{K}]^+$; **HRMS** $[\text{M} + \text{NH}_4]^+$ Calculated for $\text{C}_{56}\text{H}_{68}\text{O}_6\text{N}_1$: 850.5041; Found: 850.5027.



Synthesis of 281: Synthesis employing **GP1**. Purification *via* column chromatography on silica gel (2.5% diethyl ether in dichloromethane) afforded **281** as an orange oil (63 mg, 0.067 mmol, 61%).

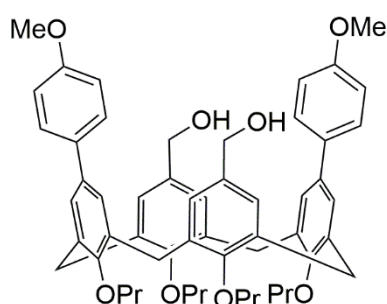
$^1\text{H-NMR}$ (CDCl_3 , 500 MHz) δ 7.19 – 7.14 (m, 6H), 6.98 (s, 4H), 6.55 (s, 4H), 4.50 (d, $J = 13.3$ Hz, 4H), 4.28 (s, 4H), 4.01 – 3.96 (m, 4H), 3.82 (t, $J = 7.3$ Hz, 4H), 3.22 (d, $J = 13.4$ Hz, 4H), 2.02 – 1.90 (m, 8H), 1.05 (t, $J = 7.4$ Hz, 6H), 0.98 (t, $J = 7.5$ Hz, 6H) ppm; $^{13}\text{C-NMR}$ (CDCl_3 , 126 MHz) δ 157.6, 155.8, 143.9, 143.4, 136.2, 135.0, 134.7, 134.3, 132.2, 130.5, 129.0, 128.4, 127.1, 126.8, 126.3, 125.1, 64.8, 31.2, 23.4, 23.2, 10.5, 10.1 ppm; **FT-IR** (neat) 3313, 2962, 2932, 2875, 1585, 1467, 1429, 1385, 1218, 1126 cm^{-1} ; **MS** (MALDI) m/z 964.92 $[\text{M}+\text{Na}]^+$; **HRMS** $[\text{M}+\text{H}]^+$ Calculated for $\text{C}_{54}\text{H}_{60}\text{Cl}_4\text{O}_6\text{N}_1$: 958.3169; Found: 958.3159.



Synthesis of 282: Synthesis employing **GP1**. Purification *via* column chromatography on silica gel (2.5% diethyl ether in dichloromethane) afforded **282** as a brown oil (52 mg, 0.058 mmol, 53%).

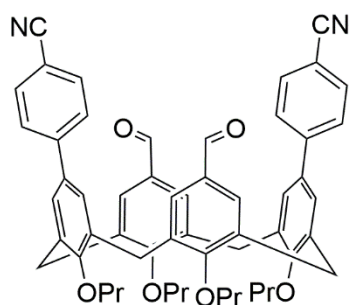
$^1\text{H-NMR}$ (CDCl_3 , 500 MHz) δ 7.58 – 7.53 (m, 4H), 7.39 – 7.34 (m, 4H), 7.28 (s, 4H), 7.14 – 7.10 (m, 2H), 7.09 – 7.04 (m, 8H), 6.35 (s, 4H), 4.52 (d, $J = 13.2$ Hz, 4H), 4.12 – 4.06 (m, 8H), 3.74 (t, $J = 7.0$ Hz, 4H), 3.23 (d, $J = 13.3$ Hz, 4H), 2.07 – 1.98 (m, 4H), 1.97 – 1.89 (m, 4H), 1.11 (t, $J = 7.4$ Hz, 6H), 0.95 (t, $J = 7.5$ Hz, 6H) ppm; $^{13}\text{C-NMR}$ (CDCl_3 , 126 MHz) δ 157.58, 157.17, 156.3, 155.4, 136.8, 136.4, 134.7, 134.3, 133.7, 129.9, 128.3, 127.4, 126.4, 123.3, 119.3, 118.9, 64.8, 31.4, 23.6, 23.2, 10.9, 10.1 ppm; **FT-IR** (neat) 3328, 2961,

2932, 2874, 1589, 1489, 1384, 1231, 1005 cm^{-1} ; **MS** (MALDI) m/z 1011.27 $[\text{M}+\text{Na}]^+$; **HRMS** $[\text{M}+\text{H}]^+$ Calculated for $\text{C}_{66}\text{H}_{72}\text{N}_1$: 1006.5252; Found: 1006.5236.



Synthesis of 283: Synthesis employing **GP1**. Purification *via* column chromatography on silica gel (10% diethyl ether in dichloromethane) afforded **283** as a clear oil (59 mg, 0.072 mmol, 65%).

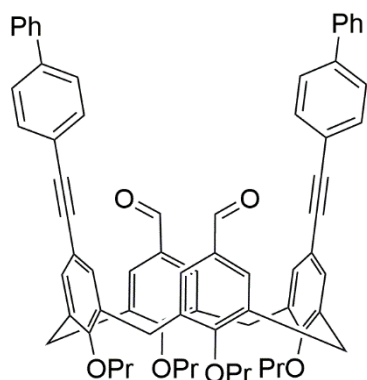
$^1\text{H-NMR}$ (CDCl_3 , 500 MHz) δ 7.46 (d, $J = 8.7$ Hz, 4H), 7.20 (s, 4H), 6.92 (d, $J = 8.7$ Hz, 4H), 6.39 (s, 4H), 4.51 (d, $J = 13.2$ Hz, 4H), 4.13 (s, 4H), 4.08 – 4.02 (m, 4H), 3.85 (s, 6H), 3.75 (t, $J = 7.0$ Hz, 4H), 3.22 (d, $J = 13.3$ Hz, 4H), 2.06 – 1.98 (m, 4H), 1.98 – 1.90 (m, 4H), 1.09 (t, $J = 7.4$ Hz, 6H), 0.95 (t, $J = 7.5$ Hz, 6H) ppm; **$^{13}\text{C-NMR}$** (CDCl_3 , 126 MHz) δ 158.8, 156.7, 155.5, 136.5, 134.69, 134.6, 134.0, 133.86, 128.0, 127.1, 126.4, 114.2, 64.9, 55.5, 31.4, 23.6, 23.2, 10.8, 10.1 ppm; **FT-IR** (neat) 3375, 2960, 2933, 2874, 1609, 1516, 1464, 1384, 1230, 1179, 1125, 1035, 1007, 964, 909, 828 cm^{-1} ; **MS** (MALDI) m/z 887.64 $[\text{M}+\text{Na}]^+$; **HRMS** $[\text{M} + \text{NH}_4]^+$ Calculated for $\text{C}_{56}\text{H}_{64}\text{O}_8\text{N}_1$: 882.4939; Found: 882.4934.



Synthesis of 273: To a solution of oxalyl chloride (19 μL , 0.22 mmol) in anhydrous dichloromethane (0.5 mL) at -78°C under an atmosphere of nitrogen was added anhydrous dimethyl sulfoxide (31 μL , 0.44 mmol) *via* syringe. The mixture was stirred for 15 minutes before the addition of a solution of **278** (32 mg, 0.04 mmol) in anhydrous dichloromethane (0.5 mL) dropwise *via* syringe. After 0.5 h stirring, triethylamine (92 μL , 0.66 mmol) was added and the mixture stirred for a further 0.5 h at -78°C , and then 2 h at room temperature. The mixture was diluted with dichloromethane (8 mL) and washed with water (3 x 5 mL). The organic phase was dried over magnesium sulfate, filtered and concentrated to afford **273** as an off-white solid (32 mg, 0.04 mmol, quant.)

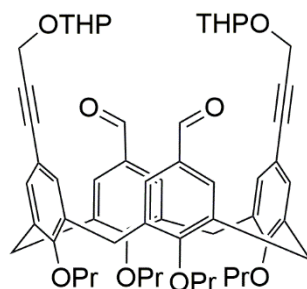
$^1\text{H-NMR}$ (CDCl_3 , 500 MHz) δ 9.51 (s, 2H), 7.47 (d, $J = 8.4$ Hz, 4H), 7.27 (d, $J = 8.4$ Hz, 4H), 7.10 (s, 4H), 6.97 (s, 4H), 4.55 (d, $J = 13.7$ Hz, 4H), 3.95 (m, 8H), 3.33 (d, $J = 13.7$ Hz, 4H), 1.94 (m, 8H), 1.06 (t, $J = 7.5$ Hz, 6H), 1.00 (t, $J = 7.5$ Hz, 6H) ppm; **$^{13}\text{C-NMR}$** (CDCl_3 , 126 MHz) δ 191.6, 162.1, 157.6, 144.8, 136.8, 136.7, 133.4, 132.4, 131.1, 130.1, 127.5, 127.2, 118.9, 110.4, 77.4, 77.3, 31.3, 23.5, 23.3, 10.5, 10.3 ppm; **FT-IR** (neat) 2962, 2932, 2875, 2727, 1692, 1597, 1465, 1383, 1275, 1231, 1121, 1065, 1035, 1004, 961, 885, 836 cm^{-1} ; **MS** (MALDI) m/z 874.2 $[\text{M}+\text{Na}]^+$; **HRMS** $[\text{M}+\text{NH}_4]^+$ Calculated for $\text{C}_{56}\text{H}_{64}\text{O}_8\text{N}_1$: 882.4939; Found: 882.4934.

GP2: A microwave vial was charged with a solution of **258** (80 mg, 0.09 mmol) and Pd(PPh₃)₂Cl₂ (20 mg, 0.02 mmol) in anhydrous tetrahydrofuran (2 mL). The solution was degassed by sparging with nitrogen for 5 minutes, before the addition of the appropriate alkyne (0.18 mmol), triethylamine (125 μ L, 0.90 mmol) and finally copper(I)iodide (7 mg, 0.04 mmol). The vial was sealed with a PTFE lined crimp cap, and the mixture heated and stirred in the microwave synthesiser for 1 h at 80° C. The solvents were removed *in vacuo* and the impure mixture purified *via* column chromatography on silica gel to afford (**294** to **296**).



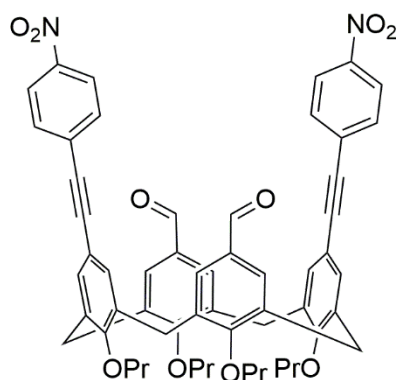
Synthesis of 294: Synthesis employing **GP2**. Purification *via* column chromatography on silica gel (dichloromethane) afforded **294** as a white solid (66 mg, 0.067 mmol, 74%).

¹H-NMR (CDCl₃, 500 MHz) δ 9.44 (s, 2H), 7.44 (m, 18H), 7.19 (s, 4H), 6.93 (s, 4H), 4.47 (d, J = 13.6 Hz, 4H), 3.97 (m, 4H), 3.85 (t, J = 7.1 Hz, 4H), 3.26 (d, J = 13.6 Hz, 4H), 1.92 (m, 8H), 1.08 (t, J = 7.5 Hz, 4H), 0.95 (t, J = 7.5 Hz, 4H) ppm; ¹³C-NMR (CDCl₃, 126 MHz) δ 191.8, 161.4, 157.6, 140.7, 140.5, 135.8, 135.1, 132.5, 132.0, 131.6, 129.9, 128.9, 127.6, 127.2, 127.1, 127.0, 122.6, 117.6, 90.4, 88.7, 77.3, 77.1, 31.0, 23.5, 23.3, 10.6, 10.2 ppm; FT-IR (neat) 2962, 2931, 2875, 1693, 1597, 1487, 1462, 1277, 1218, 1126 cm⁻¹; MS (MALDI) m/z 1024.6 [M+Na]⁺; HRMS [M+NH₄]⁺ Calculated for C₇₀H₆₈O₆N₁: 1018.5047; Found: 1018.5047



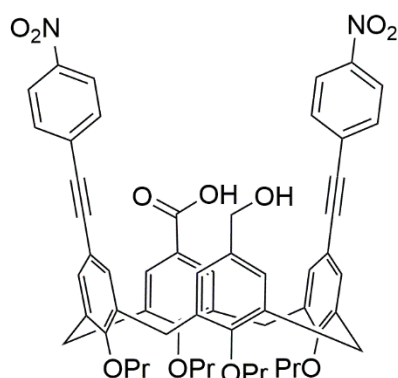
Synthesis of 295: Synthesis employing **GP2**. Purification *via* column chromatography on silica gel (6% diethyl ether in dichloromethane) afforded **295** as an off-white solid (53 mg, 0.057 mmol, 65%).

¹H-NMR (CDCl₃, 500 MHz) δ 9.27 (s, 2H), 7.22 (s, 4H), 6.68 (s, 4H), 4.95 (t, J = 3.4 Hz, 2H), 4.56 (d, J = 15.6 Hz, 2H), 4.48 (d, J = 15.6 Hz, 2H), 4.42 (d, J = 13.6 Hz, 4H), 3.94 (m, 8H), 1.88 (m, 8H), 1.69 (m, 12H), 1.07 (t, J = 7.5 Hz, 6H), 0.88 (t, J = 7.5 Hz, 6H) ppm; ¹³C-NMR (CDCl₃, 126 MHz) δ 191.6, 160.9, 157.9, 136.2, 134.6, 132.9, 131.5, 129.6, 116.9, 97.0, 86.0, 84.6, 77.3, 62.2, 55.0, 30.9, 30.5, 25.6, 23.6, 23.1, 19.3, 10.7, 9.9 ppm; FT-IR (neat) 2937, 2875, 2236, 1693, 1596, 1463, 1383, 1275, 1120, 1036, 1022, 1002, 961, 903, 872 cm⁻¹; MS (MALDI) m/z 948.2 [M+Na]⁺; HRMS [M+NH₄]⁺ Calculated for C₅₈H₇₂O₁₀N₁: 942.5157; Found: 942.5154.



Synthesis of 296: Synthesis employing **GP2**. Purification *via* column chromatography on silica gel (1% ethyl acetate in dichloromethane) afforded **296** as a brown solid (59 mg, 0.063 mmol, 70%).

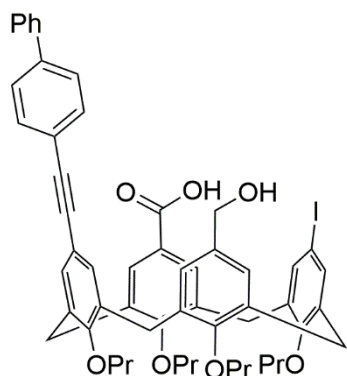
¹H-NMR (500 MHz, CDCl₃) δ 9.47 (s, 2H), 8.09 (d, *J* = 8.9 Hz, 4H), 7.56 (d, *J* = 8.9 Hz, 4H), 7.11 (s, 4H), 6.98 (s, 4H), 4.48 (d, *J* = 13.8 Hz, 4H), 3.95 (m, 4H), 3.87 (t, *J* = 7.2 Hz, 4H), 3.26 (d, *J* = 13.8 Hz, 4H), 1.92 (m, 8H), 1.06 (t, *J* = 7.5 Hz, 6H), 0.97 (t, *J* = 7.5 Hz, 6H) ppm; **¹³C-NMR** (CDCl₃, 126 MHz) δ 191.7, 161.6, 158.2, 146.7, 135.8, 135.2, 132.7, 132.1, 132.0, 131.5, 130.6, 129.9, 123.6, 116.4, 95.3, 87.2, 30.9, 23.5, 23.3, 10.6, 10.2 ppm; **FT-IR** (neat) 2964, 2933, 2876, 2206, 1692, 1590, 1518, 1493, 1460, 1341, 1277, 1126, 999, 855, 733 cm⁻¹; **MS** (MALDI) *m/z* 940.5 [M+H]⁺; **HRMS** [M + NH₄]⁺ Calculated for C₅₈H₅₈N₂O₁₀: 956.4117; Found: 979.4110.



Synthesis of 260: A microwave vial was charged with a solution of **259** (200 mg, 0.22 mmol) and Pd(PPh₃)₂Cl₂ (50 mg, 0.04 mmol) in anhydrous tetrahydrofuran (3 mL). Triethylamine (190 μL, 1.09 mmol) was added *via* syringe, and the mixture degassed by sparging with nitrogen for 5 minutes before the addition of 4-nitroethynylbenzene (96 mg, 0.65 mmol) and finally copper(I)iodide (16 mg, 0.09 mmol). The vial was sealed with a PTFE lined crimp cap, and the mixture heated and stirred in the

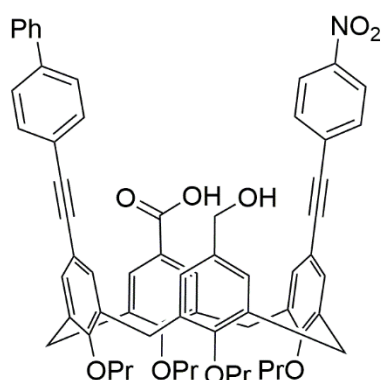
microwave synthesiser at 80 °C for 1 h. The solvent was removed *in vacuo* to afford a brown oil. Purification *via* column chromatography on silica gel (15% diethyl ether in dichloromethane) afforded **260** as a brown solid (143 mg, 0.15 mmol, 69%).

¹H-NMR (500 MHz, CDCl₃) δ 8.10 (d, *J* = 8.9 Hz, 4H), 7.60 (d, *J* = 8.9 Hz, 4H), 7.24 (m, 4H), 7.03 (s, 2H), 6.27 (s, 2H), 4.43 (m, 4H), 4.15 (s, 2H), 4.08 – 3.95 (m, 4H), 3.78 (t, *J* = 7.0 Hz, 2H), 3.71 (t, *J* = 6.9 Hz, 2H), 3.21 (d, *J* = 13.7 Hz, 2H), 3.17 (d, *J* = 13.8 Hz, 2H), 1.96 – 1.85 (m, 8H), 1.07 (m, 6H), 0.92 (t, *J* = 7.5 Hz, 6H) ppm; **¹³C-NMR** (CDCl₃, 126 MHz) δ 171.13, 160.74, 158.86, 155.30, 146.68, 136.97, 136.30, 134.67, 134.11, 133.33, 132.95, 132.53, 132.31, 132.15, 130.92, 130.22, 128.73, 126.17, 123.59, 123.11, 115.83, 95.92, 87.01, 64.30, 31.07, 30.96, 23.55, 23.21, 10.78, 10.71, 10.06 ppm; **FT-IR** (neat) 2962, 2936, 2877, 2209, 1689, 1591, 1518, 1461, 1341, 1216, 1106, 1002, 962, 854, 750, 694 cm⁻¹; **MS** (MALDI) *m/z* 979.78 [M+Na]⁺; **HRMS** [M+Na]⁺ Calculated for C₅₈H₅₆N₂O₁₁Na₁: 979.3776; Found: 979.3767.



Synthesis of 304: A microwave vial was charged with a solution of **259** (800 mg, 0.89 mmol) and Pd(PPh₃)₂Cl₂ (125 mg, 0.18 mmol) in anhydrous tetrahydrofuran (4 mL). Triethylamine (776 μL, 4.44 mmol) was added *via* syringe, and the mixture degassed with nitrogen before the addition of **291** (158 mg, 0.89 mmol) and finally copper(I)iodide (68 mg, 0.36 mmol). The vial was sealed with a PTFE lined crimp cap, and the mixture heated and stirred in the microwave synthesiser at 80 °C for 1 h. The solvent was removed *in vacuo* to afford a brown oil. Purification *via* column chromatography on silica gel (dichloromethane) afforded **304** as a pale brown solid (240 mg, 0.25 mmol, 28%).

¹H-NMR (500 MHz, CDCl₃) δ 7.73 – 7.29 (m, 13H), 7.11 – 6.78 (m, 2H), 6.32 – 6.20 (m, 2H), 4.46 – 4.32 (m, 4H), 4.17 (s, 2H), 4.03 – 3.88 (m, 4H), 3.78 – 3.64 (m, 4H), 3.23 – 3.05 (m, 4H), 1.94 – 1.79 (m, 8H), 1.13 – 1.02 (m, 6H), 0.95 – 0.84 (m, 6H) ppm; **¹³C-NMR** (CDCl₃, 126 MHz) δ 171.08, 160.58, 158.04, 157.53, 155.18, 140.64, 140.61, 139.12, 138.40, 137.84, 137.40, 136.72, 136.04, 134.76, 134.14, 133.92, 133.38, 133.15, 132.70, 132.19, 132.14, 130.33, 130.08, 128.95, 127.62, 127.18, 127.09, 126.34, 126.13, 123.17, 122.92, 117.10, 91.02, 88.50, 85.92, 64.25, 31.06, 30.97, 30.87, 30.76, 23.53, 23.17, 23.03, 10.80, 10.72, 10.07, 10.00 ppm; **FT-IR** (neat) 3435, 2962, 2933, 2875, 1687, 1601, 1463, 1384, 1308, 1283, 1202, 1126, 1003, 963, 839, 763, 697 cm⁻¹; **MS** (MALDI) *m/z* 967.98 [M+H]⁺; **HRMS** [M + NH₄]⁺ Calculated for C₅₆H₆₁N₁O₇I₁: 986.3487; Found: 986.3491.



Synthesis of 303: A microwave vial was charged with a solution of **304** (110 mg, 0.11 mmol) and Pd(PPh₃)₂Cl₂ (26 mg, 0.02 mmol) in anhydrous tetrahydrofuran (3 mL). Triethylamine (99 μL, 0.57 mmol) was added *via* syringe, and the mixture degassed with nitrogen before the addition of 4-nitroethynylbenzene (25 mg, 0.11 mmol) and finally copper(I)iodide (8 mg, 0.05 mmol). The vial was sealed with a PTFE lined crimp cap, and the mixture heated and stirred in the microwave synthesiser at 80 °C for 1 h. The

solvent was removed *in vacuo* to afford a brown oil. Purification *via* column chromatography on silica gel (15% diethyl ether in dichloromethane) afforded **260** as a brown solid (77 mg, 0.08 mmol, 68%).

¹H-NMR (500 MHz, CDCl₃) δ 8.08 (d, *J* = 8.9 Hz, 2H), 7.63 – 7.30 (m, 15H), 7.06 – 6.98 (m, 2H), 6.30 – 6.21 (m, 2H), 4.49 – 4.32 (m, 4H), 4.17 (s, 2H), 4.07 – 3.94 (m, 4H), 3.81 – 3.65 (m, 4H), 3.25 – 3.04 (m, 4H), 1.88 (m, 8H), 1.12 – 1.03 (m, 6H), 0.95 – 0.86 (m, 6H) ppm; **¹³C-NMR** (CDCl₃, 126 MHz) δ

171.54, 160.61, 158.89, 158.03, 157.52, 155.19, 146.64, 140.57, 140.46, 139.10, 138.39, 137.81, 137.38, 137.02, 136.70, 136.35, 136.03, 134.67, 134.23, 134.14, 133.92, 133.38, 133.14, 132.94, 132.67, 132.50, 132.31, 132.19, 132.08, 132.03, 130.97, 130.29, 130.08, 128.93, 127.61, 127.12, 127.07, 127.04, 126.97, 126.34, 126.13, 123.60, 123.22, 122.87, 122.77, 117.05, 115.82, 95.94, 91.00, 90.84, 88.44, 88.41, 87.04, 85.88, 64.23, 31.05, 30.95, 30.85, 30.74, 23.54, 23.51, 23.20, 23.14, 23.01, 10.78, 10.71, 10.05, 9.98 ppm; **FT-IR** (neat) 2954, 2920, 2865, 1631, 1452, 1394, 1318, 1283, 1253, 1226, 1001, 980, 842, 618 cm^{-1} ; **MS** (MALDI) m/z 1027.84 $[\text{M}+\text{K}]^+$; **HRMS** $[\text{M}+\text{Na}]^+$ Calculated for $\text{C}_{64}\text{H}_{61}\text{N}_1\text{O}_9\text{Na}_1$: 1010.4239; Found: 1010.4239.

References

- (1) Gutsche, C. D. *Calixarenes - An Introduction*, 2nd Edition; Monographs in Supramolecular Chemistry; The Royal Society of Chemistry, 2008.
- (2) Zinke, A.; Ziegler, E.; Martinowitz, E.; Pichelmayer, H.; Tomio, M.; Wittmann-Zinke, H.; Zwanziger, S. *Ber. Dtsch. Chem. Ges.* **1944**, 77B, 264–272.
- (3) Baeyer, A. *Ber. Dtsch. Chem. Ges.* **1868**, 5, 1094–1100.
- (4) Baekeland, L. H. *J. Ind. Eng. Chem.* **1909**, 1, 149–161.
- (5) Ziegler, E.; Kaufmann, W.; Klementschnitz, W. *Monatsh. Chem.* **1952**, 83, 1334–1343.
- (6) Cornforth, J. W.; D'Arcy Hart, P.; Nicholls, G. A.; Rees, R. J. W.; Stock, J. A. *Br. J. Pharmacology. Chem.* **1955**, 10, 73–86.
- (7) Gutsche, C. D. *J. Org. Chem.* **1986**, 51, 742–745.
- (8) Gutsche, C. D.; Muthukrisnan, R. *J. Org. Chem.* **1978**, 43, 4905–4906.
- (9) Hayes, B. T.; Hunter, R. F. *J. Appl. Chem.* **1958**, 8, 743–748.
- (10) Kwang, H. N.; Gutsche, C. D. *J. Org. Chem.* **1982**, 47, 2713–2719.
- (11) Vocanson, F.; Lamartine, R. *Supramol. Chem.* **1996**, 7, 19–25.
- (12) Gutsche, C. D. *Acc. Chem. Res.* **1983**, 16, 161–170.
- (13) Gutsche, C.; Jr, D. J.; Stewart, D. *J. Org. Chem.* **1999**, 64, 3747–3750.
- (14) Gutsche, C. D.; Dhawan, B.; Leonis, M.; Stewart, D. *Org. Synth.* **1990**, 68, 238–242.
- (15) Stewart, D. R.; Gutsche, C. D. *Org. Prep. Proced. Int.* **1993**, 25, 137–139.
- (16) Vocanson, F.; Lamartine, R.; Lanteri, P.; Longerey, R.; Gauvrit, J. Y. *New J. Chem.* **1995**, 19, 825–829.
- (17) Stewart, D. R.; Gutsche, C. D. *J. Am. Chem. Soc.* **1999**, 121, 4136–4146.
- (18) Bew, S. P.; Sharma, S. V. *Chem. Commun.* **2007**, No. 9, 975–977.
- (19) Böhmer, V.; Marschollek, F.; Zettat, L. *J. Org. Chem.* **1987**, 52, 3200–3205.
- (20) Böhmer, V.; Merkel, L.; Kunz, U. *J. Chem. Soc. Chem. Commun.* **1987**, 4, 4–5.

-
- (21) de Mendoza, J.; Nieto, P. M.; Prados, P.; Sanchez, C. *Tetrahedron* **1990**, *46*, 671–682.
- (22) Usul, S.; Deyama, K.; Kinoshita, R.; Odagaki, Y.; Fakazawa, Y. *Tetrahedron Lett.* **1993**, *34*, 8127–8130.
- (23) Tsue, H.; Enyo, K.; Hirao, K. *Org. Lett.* **2000**, *2*, 3071–3074.
- (24) Gopalsamuthiram, V.; Wulff, W. D. *J. Am. Chem. Soc.* **2004**, *126*, 13936–13937.
- (25) Wang, C.-C.; Wang, Y.; Liu, H.-J.; Lin, K.-J.; Chou, L.-K.; Chan, K.-S. *J. Phys. Chem. A* **1997**, *101*, 8887–8901.
- (26) Dötz, K. H.; Tomuschat, P. *Chem. Soc. Rev.* **1999**, *28*, 187–198.
- (27) Schlosser, M.; Editor. *Organometallics in Synthesis, Third Manual.*; John Wiley & Sons, Inc., 2013.
- (28) Kaemmerer, H.; Happel, G.; Caesar, F. *Makromol. Chemie* **1972**, *162*, 179–197.
- (29) Gutsche, D. D.; Bauer, L. J. *J. Am. Chem. Soc.* **1985**, *107*, 6059–6063.
- (30) Andretti, G. D.; Ungaro, R.; Pochini, A. *J. Chem. Soc. Chem. Commun.* **1979**, 1005–1007.
- (31) Harada, T.; Ohseto, F.; Shinkai, S. *Tetrahedron* **1994**, *50*, 13377–13394.
- (32) Thondorf, I.; Brenn, J.; Brandta, W.; Böhmer, V. *Tetrahedron Lett.* **1995**, *36*, 6665–6668.
- (33) Gutsche, C.; Levine, J. *J. Am. Chem. Soc.* **1982**, 2652–2653.
- (34) Gutsche, D. C.; Dhawan, B.; Levine, J. A.; Hyun No, K.; Bauer, L. J. *Tetrahedron* **1983**, *39*, 409–426.
- (35) Jaime, C.; De Mendoza, J.; Prados, P.; Nieto, P. M.; Sanchez, C. *Sect. Title Phys. Org. Chem.* **1991**, *56*, 3372–3376.
- (36) Shu, C.; Liu, W.; Ku, M.; Tang, F.; Yeh, M.; Lin, L. *J. Org. Chem.* **1991**, *56*, 3730–3733.
- (37) Casnati, A.; Fochi, M.; Minari, P.; Pochint, A.; Reggiani, M.; Ungaro, R.; Reinhoudt, D. N. *Gazz. Chim. Ital.* 1996, pp 99–106.
- (38) Sharma, S. K.; Gutsche, C. D. *Tetrahedron* **1994**, *50*, 4087–4104.
- (39) Van Loon, J. D.; Arduini, A.; Coppi, L.; Verboom, W.; Pochini, A.; Ungaro, R.; Harkema, S.; Reinhoudt, D. N. *J. Org. Chem.* **1990**, *55*, 5639–5646.

-
- (40) Verboom, W.; Durie, A.; Egberink, R. J. M.; Asfari, Z.; Reinhoudt, D. N. *J. Org. Chem.* **1992**, *57*, 1313–1316.
- (41) Kumar, S.; Kurur, N. D.; Chawla, H. M.; Varadarajan, R. *Synth. Commun.* **2001**, *31*, 775–779.
- (42) Van Loon, J. D.; Arduini, A.; Verboom, W.; Ungaro, R.; Van Hummel, G. J.; Harkema, S.; Reinhoudt, D. N. *Tetrahedron Lett.* **1989**, *30*, 2681–2684.
- (43) Gutsche, C. D. *Calixarenes - An introduction*; 2008; Vol. 34.
- (44) Lazzarotto, M.; Sansone, F.; Baldini, L.; Casnati, A.; Cozzini, P.; Ungaro, R. *European J. Org. Chem.* **2001**, 595–602.
- (45) Nakamura, Y.; Tanaka, S.; Serizawa, R.; Morohashi, N.; Hattori, T. *J. Org. Chem.* **2011**, 2168–2179.
- (46) Hennrich, G.; Murillo, M. T.; Prados, P.; Al-Saraierh, H.; El-Dali, A.; Thompson, D. W.; Collins, J.; Georghiou, P. E.; Teshome, A.; Asselberghs, I.; Clays, K. *Chem. - A Eur. J.* **2007**, *13*, 7753–7761.
- (47) Deng, Z.; Liu, J.; Hu, C.; Yang, L.; Du, H.; Hu, K.; Huang, Y.; Yang, X.; Jiang, Q.; Zhang, S. *J. Sep. Sci.* **2014**, *37*, 3268–3275.
- (48) Schazmann, B.; Alhashimy, N.; Diamond, D. *J. Am. Chem. Soc.* **2006**, *128*, 8607–8614.
- (49) Gutsche, C. D.; Lin, L.-G. *Tetrahedron* **1986**, *42*, 1633–1640.
- (50) Stanstny, V.; Lhota, P.; Michlova, V. *Tetrahedron* **2002**, *58*, 7207–7211.
- (51) Larsen, M.; Jørgensen, M. *J. Org. Chem.* **1996**, *61*, 6651–6655.
- (52) Alam, I.; Sharma, S. K.; Gutsche, C. D. *J. Org. Chem.* **1994**, *59*, 3716–3720.
- (53) Martinez, L. Investigation of Artificial Malonyl Group Carriers and Multifunctional Cyclic Scaffolds Towards the Mimicry of PKS, PhD thesis, UEA Digital Repository, 2015.
- (54) Oizumi, H.; Kumise, T.; Itani, T. *J. Photopolym. Sci. Technol.* **2008**, *21*, 443–449.
- (55) Bügler, J.; Engbersen, J. F. J.; Reinhoudt, D. N. *J. Org. Chem.* **1998**, *63*, 5339–5344.
- (56) Radu, A.; Peper, S.; Gonczy, C.; Runde, W.; Diamond, D. *Electroanalysis* **2006**, *18*, 1379–1388.
- (57) Gruber, T.; Fischer, C.; Felsmann, M.; Seichter, W.; Weber, E. *Org. Biomol. Chem.* **2009**, *7*,

-
- 4904.
- (58) Arena, G.; Casnati, A.; Contino, A.; Mirone, L.; Sciotto, D.; Ungaro, R. *Chem. Commun.* **1996**, 2277–2278.
- (59) Brown, F.; Hall, G. R.; Walter, A. J. *J. Inorg. Nucl. Chem.* **1955**, *1*, 241–247.
- (60) Mokhtari, B.; Pourabdollah, K.; Dallali, N. *J. Radioanal. Nucl. Chem.* **2011**, *287*, 921–934.
- (61) Fanning, J. C. *Coord. Chem. Rev.* **1995**, *140*, 27–36.
- (62) Talanov, V. S.; Talanova, G. G.; Gorbunova, M. G.; Bartsch, R. A. *J. Chem. Soc. Perkin Trans. 2* **2002**, 209–215.
- (63) Fanni, S.; Arnaud-Neu, F.; McKerverey, M. A.; Schwing-Weill, M. J.; Ziat, K. *Tetrahedron Lett.* **1996**, *37*, 7975–7978.
- (64) Sameni, S.; Jeunesse, C.; Matt, D.; Harrowfield, J. *Chem. Soc. Rev.* **2009**, *38*, 2117–2146.
- (65) Araki, K.; Hisaichi, K.; Kanai, T.; Shinkai, S. *Chem. Lett.* **1995**, No. 7, 569–570.
- (66) Neri, P.; Bottino, A.; Cunsolo, F.; Piattelli, M.; Gavuzzo, E. *Angew. Chemie Int. Ed.* **1998**, *37*, 166–169.
- (67) Bottino, A.; Cunsolo, F.; Piattelli, M.; Neri, P. *Tetrahedron Lett.* **1998**, *39*, 9549–9552.
- (68) Iglesias-sa, C.; Fragoso, A.; de Mendoza, J. De. *Org. Lett.* **2006**, *8*, 2572–2574.
- (69) Arduini, A.; Pochini, A.; Secchi, A. *European J. Org. Chem.* **2000**, 2325–2334.
- (70) Liu, J. M.; Zheng, Y. S.; Zheng, Q. Y.; Xie, J.; Wang, M. X.; Huang, Z. T. *Tetrahedron* **2002**, *58*, 3729–3736.
- (71) Higler, I.; Timmerman, P.; Verboom, W.; Reinhoudt, D. N. *J. Org. Chem.* **1996**, *3263*, 5920–5931.
- (72) Mogck, O.; Parzuehowski, P.; Nissinen, M.; Biihmer, V.; Rokicki, G.; Rissanen, K. *Tetrahedron* **1998**, *54*, 10053–10068.
- (73) Oude Wolbers, M. P.; Van Veggel, F. C. J. M.; Heeringa, R. H. M.; Hofstraat, J. W.; Geurts, F. A. J.; Van Hummel, G. J.; Harkema, S.; Reinhoudt, D. N. *Liebigs Ann.* **1997**, No. 12, 2587–2600.
- (74) Calvo-Flores, F. G.; Isac-García, J.; Hernández-Mateo, F.; Pérez-Balderas, F.; Calvo-Asín, J. A;

-
- Sánchez-Vaquero, E.; Santoyo-González, F. *Org. Lett.* **2000**, *2*, 2499–2502.
- (75) Rostovtsev, V. V.; Green, L. G.; Fokin, V. V.; Sharpless, K. B. *Angew. Chemie - Int. Ed.* **2002**, *41*, 2596–2599.
- (76) Morales-Sanfrutos, J.; Ortega-Mun, M.; Lopez-Jaramillo, J.; Hernandez-Mateo, F.; Santoyo-Gonzalez, F. *J. Org. Chem.* **2008**, *73*, 7772–7774.
- (77) Meldal, M.; Tornøe, C. W. *Chem. Soc. Rev.* **2008**, *108*, 2952–3015.
- (78) Schulze, B.; Schubert, U. S. *Chem. Soc. Rev.* **2014**, *43*, 2522.
- (79) McDonald, K. P.; Qiao, B.; Twum, E. B.; Lee, S.; Gamache, P. J.; Chen, C.-H.; Yi, Y.; Flood, A. H. *Chem. Commun.* **2014**, *50*, 13285–13288.
- (80) Diamond, D. J. *Incl. Phenom. Mol. Recognit. Chem.* **1994**, *19*, 149–166.
- (81) Yamamoto, H.; Ueda, K.; Sandanayake, K. R. A. S.; Shinkai, S. *Chem. Lett.* **1995**, No. 7, 497–498.
- (82) Shimizu, H.; Iwamoto, K.; Fujimoto, K.; Shinkai, S. *Chem. Lett.* **1991**, No. 12, 2147–2150.
- (83) Kubo, Y.; Tokita, S.; Kojima, Y.; Osano, Y. T.; Matsuzaki, T. **1996**, *3263*, 3758–3765.
- (84) Formica, M.; Fusi, V.; Giorgi, L.; Micheloni, M. *Coord. Chem. Rev.* **2012**, *256*, 170–192.
- (85) Aoki, I.; Toru, S.; Shinkai, S. *J. Chem. Soc. Chem. Commun.* **1992**, *9*, 730–732.
- (86) Ji, H.-F.; Dabestani, R.; Brown, G. M.; Sachleben, R. A. *Chem. Commun.* **2000**, *1*, 833–834.
- (87) Talanova, G. G.; Talanov, V. S. *Supramol. Chem.* **2010**, *22*, 838–852.
- (88) World Health Organization. *Guidelines for Drinking-water Quality*; 2006; Vol. 1.; www.who.int/water_sanitation_health/dwq/gdwq0506.pdf; Accessed 01/12/2016
- (89) Leray, I.; Valeur, B. *Eur. J. Inorg. Chem.* **2009**, No. 24, 3525–3535.
- (90) Talanova, G. G.; Elkarim, N. S.; Talanov, V. S.; Bartsch, R. A. *Anal. Chem.* **1999**, *71*, 3106–3109.
- (91) Métivier, R.; Leray, I.; Valeur, B. *Chem. - A Eur. J.* **2004**, *10*, 4480–4490.
- (92) Métivier, R.; Leray, I.; Lebeau, B.; Valeur, B. *J. Mater. Chem.* **2005**, *15*, 2965.
- (93) Zhang, J. F.; Zhou, Y.; Yoon, J.; Kim, J. S. *Chem. Soc. Rev.* **2011**, *40*, 3416.

-
- (94) Hadrup, N.; Lam, H. R. *Regul. Toxicol. Pharmacol.* **2014**, *68*, 1–7.
- (95) Preisser, G.; Schollmeyer, W. *Arch. fuer Toxikologie* **1965**, *20*, 327–333.
- (96) Goyer, R. A.; Cherian, M. G.; *Met. Toxicol.*; Academic Press, 1995; pp 389–412.
- (97) Shamsipur, M.; Alizadeh, K.; Hosseini, M.; Caltagirone, C.; Lippolis, V. *Sensors Actuators B Chem.* **2006**, *113*, 892–899.
- (98) Chen, T.; Zhu, W.; Xu, Y.; Zhang, S.; Zhang, X.; Qian, X. *Dalton Trans.* **2010**, *39*, 1316–1320.
- (99) Xu, Z.; Zheng, S.; Yoon, J.; Spring, D. R. *Analyst.* **2010**, *135*, 2554–2559.
- (100) Kim, J. S.; Shon, O. J.; Rim, J. A.; Kim, S. K.; Yoon, J. *J. Org. Chem.* **2002**, *67*, 2348–2351.
- (101) Joseph, R.; Ramanujam, B.; Acharya, A.; Rao, C. P. *J. Org. Chem.* **2009**, *74*, 8181–8190.
- (102) Debrouwer, W.; Heugebaert, T. S. A.; Roman, B. I.; Stevens, C. V. *Adv. Synth. Catal.* **2015**, *357*, 2975–3006.
- (103) Jou, M. J.; Chen, X.; Swamy, K. M.; Kim, H. N.; Kim, H. J.; Lee, S. G.; Yoon, J. *Chem Commun* **2009**, No. 46, 7218–7220.
- (104) Egorova, O. a; Seo, H.; Chatterjee, A.; Ahn, K. H. *Org. Lett.* **2010**, *12*, 401–403.
- (105) Do, J. H.; Kim, H. N.; Yoon, J.; Kim, J. S.; Kim, H. J. *Org. Lett.* **2010**, *12*, 932–934.
- (106) Chinapang, P.; Ruangpornvisuti, V.; Sukwattanasinitt, M.; Rashatasakhon, P. *Dye. Pigment.* **2015**, *112*, 236–238.
- (107) Memon, S.; Bhatti, A. A.; Bhatti, A. A.; Ocak, Ü.; Ocak, M. *J. Fluoresc.* **2015**, 1507–1515.
- (108) Bew, S. P.; Sharma, S. V. 2008. Unpublished Results.
- (109) Reinhoudt, D. N.; Kelderman, E.; Verboom, W. *Angew. Chemie Int. Ed. English* **1992**, *31*, 1075–1077.
- (110) Reinhoudt, D. N.; Verboom, W.; Heesink, G.; Derhaeg, L.; Verbiest, T. *Adv. Mater.* **1993**, *5*, 925–930.
- (111) Kenis, P. J. A; Noordman, O. F. J.; Houbrechts, S.; Van Hummel, G. J.; Harkema, S.; Van Veggel, F. C. J. M.; Clays, K.; Engbersen, J. F. J.; Persoons, A.; Van Hulst, N. F.; Reinhoudt, D. N. *J. Am. Chem. Soc.* **1998**, *120*, 7875–7883.

-
- (112) Datta, A.; Pati, S. K. *Chemistry* **2005**, *11*, 4961–4969.
- (113) Singh, C. P.; Sharma, R.; Shukla, V.; Khundrakpam, P.; Misra, R.; Bindra, K. S.; Chari, R. *Chem. Phys. Lett.* **2014**, *616*, 189–195.
- (114) Chemla, D. S. *Nonlinear Optical Properties of Organic Molecules and Crystals*; Volume 1; Chapter 1; Elsevier Science, London, 2012.
- (115) Messier, J.; Kajzar, F.; Prasad, P. *Organic Molecules for Nonlinear Optics and Photonics*; Chapter 2; Nato Science Series E; Springer Netherlands, 2012.
- (116) Bew, S. P.; Brimage, R. a; Hiatt-Gipson, G.; Sharma, S. V; Thurston, S. *Org. Lett.* **2009**, *11*, 2483–2486.
- (117) Zhan, W.; Li, Y.; Huang, W.; Zhao, Y.; Yao, Z.; Yu, S.; Yuan, S.; Jiang, F.; Yao, S.; Li, S. *Bioorg. Med. Chem.* **2012**, *20*, 4323–4329.
- (118) Rudzevich, Y.; Vysotsky, M. O.; Böhmer, V.; Brody, M. S.; Rebek, J.; Broda, F.; Thondorf, I. *Org. Biomol. Chem.* **2004**, *2*, 3080–3084.
- (119) Sansone, F.; Barbosa, S.; Casnati, A.; Fabbi, M.; Pochini, A.; Ugozzoli, F.; Ungaro, R. *European J. Org. Chem.* **1998**, 897–905.
- (120) Dubé, D.; Scholte, A. A. *Tetrahedron Lett.* **1999**, *40*, 2295–2298.
- (121) Tao, Z.-F.; Li, G.; Tong, Y.; Stewart, K. D.; Chen, Z.; Bui, M.-H.; Merta, P.; Park, C.; Kovar, P.; Zhang, H.; Sham, H. L.; Rosenberg, S. H.; Sowin, T. J.; Lin, N.-H. *Bioorg. Med. Chem. Lett.* **2007**, *17*, 5944–5951.
- (122) Zdanovich, V.; Kudryavtsev, R.; Kursanov, D. *Izv. Akad. Nauk SSSR* **1970**, No. 2, 472–473.
- (123) Medda, F.; Joseph, T. L.; Pirrie, L.; Higgins, M.; Slawin, A. M. Z.; Lain, S.; Verma, C.; Westwood, N. J. *Medchemcomm* **2011**, *2*, 611.
- (124) Gomez, R.; Seoane, C.; Segura, J. L. *J. Org. Chem.* **2010**, *75*, 5099–5108.
- (125) Moreno, E.; Plano, D.; Lamberto, I.; Font, M.; Encio, I.; Palop, J. A.; Sanmartin, C. *Eur. J. Med. Chem.* **2012**, *47*, 83–298.
- (126) Ernest, I.; Kalvoda, J.; Rihs, G.; Mutter, M. *Tetrahedron Lett.* **1990**, *31*, 4011–4014.
- (127) Pedras, M. S. C.; Sarma-Mamillapalle, V. K. *J. Agric. Food Chem.* **2012**, *60*, 7792–7798.

-
- (128) Sarodnick, G.; Linker, T.; Heydenreich, M.; Koch, A.; Starke, I.; Furstenberg, S.; Kleinpeter, E. *J. Org. Chem.* **2009**, *74*, 1282–1287.
- (129) Xia, C.; Xu, J.; Wu, W.; Liang, X. *Catal. Commun.* **2004**, *5*, 383–386.
- (130) Hoffman, C.; Tanke, R. S.; Miller, M. J. *J. Org. Chem.* **1989**, No. 54, 3750–3751.
- (131) Baldini, L.; Sansone, F.; Casnati, A.; Ugozzoli, F.; Ungaro, R. *J. Supramol. Chem.* **2003**, *2*, 219–226.
- (132) Hayakawa, I.; Nakamura, T.; Ohno, O.; Suenaga, K.; Kigoshi, H. *Org. Biomol. Chem.* **2015**, *13*, 9969–9976.
- (133) Albert, S. K.; Thelu, H. V. P.; Golla, M.; Krishnan, N.; Chaudhary, S.; Varghese, R. *Angew. Chemie, Int. Ed.* **2014**, *53*, 8352–8357.
- (134) Putey, A.; Popowycz, F.; Do, Q.-T.; Bernard, P.; Talapatra, S. K.; Kozielski, F.; Galmarini, C. M.; Joseph, B. *J. Med. Chem.* **2009**, *52*, 5916–5925.
- (135) Liu, S.; Edgar, K. J. *Biomacromolecules* **2015**, *16*, 2556–2571.
- (136) Tian, W. Q.; Wang, Y. A. *J. Org. Chem.* **2004**, *69*, 4299–4308.
- (137) Lindsley, C. W.; Zhao, Z.; Newton, R. C.; Leister, W. H.; Strauss, K. A. *Tetrahedron Lett.* **2002**, *43*, 4467–4470.
- (138) Mahdavi, H.; Amani, J. *Org. Lett.* **2007**, *2*, 3777–3779.
- (139) Collman, J. P.; Wang, Z.; Straumanis, A. *J. Org. Chem.* **1998**, *63*, 2424–2425.
- (140) Hogarth, G.; Humphrey, D. G.; Kaltsoyannis, N.; Kim, W.-S.; Lee, M.; Norman, T.; Redmond, S. *P. J. Chem. Soc. Dalton Trans. Inorg. Chem.* **1999**, 2705–2723.
- (141) Belger, C.; Plietker, B. *Chem. Commun.*, **2012**, *48*, 5419–5421.
- (142) Ozensoy, E.; Hess, C.; Goodman, D. W. *J. Am. Chem. Soc.* **2002**, *124*, 8524–8525.
- (143) Delebecq, E.; Pascault, J. P.; Boutevin, B.; Ganachaud, F. *Chem. Rev.* **2013**, *113*, 80–118.
- (144) Samuelsson, K.; Bergstrom, M. A.; Jonsson, C. A.; Westman, G.; Karlberg, A.-T. *Chem. Res. Toxicol.* **2011**, *24*, 35–44.
- (145) Elfeky, S. *Curr. Org. Synth.* **2011**, *8*, 872–880.

-
- (146) Mendel, A. J. *Chem. Eng. Data* **1970**, *15*, 340–341.
- (147) Li, X.; Wang, M.; Wang, G. *Appl. Chem. Ind.*, **2006**, *35*, 45–47.
- (148) Chui, C.-H.; Wang, Q.; Chow, W.-C.; Yuen, M. C.-W.; Wong, K.-L.; Kwok, W.-M.; Cheng, G. Y.-M.; Wong, R. S.-M.; Tong, S.-W.; Chan, K.-W.; Lau, F.-Y.; Lai, P. B.-S.; Lam, K.-H.; Fabbri, E.; Tao, X.-M.; Gambari, R.; Wong, W.-Y. *Chem. Commun.* **2010**, *46*, 3538.
- (149) Melissaris, A. P.; Litt, M. H. *J. Org. Chem.* **1994**, *59*, 5818–5821.
- (150) Rubinshtein, M.; James, C. R.; Young, J. L.; Ma, Y. J.; Kobayashi, Y.; Gianneschi, N. C.; Yang, J. *Org. Lett.* **2010**, *12*, 3560–3563.
- (151) Chinchilla, R.; Nájera, C. *Chem. Soc. Rev.* **2011**, *40*, 5084.
- (152) Lakowicz, J. R.; *Principles of Fluorescence Spectroscopy*; Springer, Baltimore, **2006**; pp 27–61.
- (153) Holmes-Farley, S. R.; Whitesides, G. M. *Langmuir* **1986**, *2*, 266–281.
- (154) Galindo, F.; Luis, S. V. *Org. Biomol. Chem.* **2015**, *13*, 7736–7749.
- (155) Camilleri, M. Preparation of Asymmetric Capsules Using Calixarenes as Primary Scaffolds, MSc Thesis, University of East Anglia, 2012.
- (156) Dyker, G.; Mastalerz, M.; Müller, I. M. *European J. Org. Chem.* **2005**, No. 17, 3801–3812.
- (157) Takemura, H.; Iwanaga, T.; Shinmyozu, T. *Tetrahedron Lett.* **2005**, *46*, 6687–6690.
- (158) Leonard, N. J.; Morrow, D. F.; Rogers, M. T. *J. Am. Chem. Soc.* **1957**, *79*, 5476–5479.
- (159) Buergi, H. B.; Dunitz, J. D.; Shefter, E. *Nat. New Biol.* **1973**, *244*, 186–188.
- (160) Wu, X.; Zhang, D.; Zhou, S.; Gao, F.; Liu, H. *Chem. Commun.*, **2015**, *51*, 12571–12573.
- (161) Carpino, L. A.; Padykula, R. E.; Barr, D. E.; Hall, F. H.; Krause, J. G.; Dufresne, R. F.; Thoman, C. *J. J. Org. Chem.* **1988**, *53*, 2565–2572.
- (162) Bell, T. W.; Anti-viral triaza compounds and compositions.; US Patent 6342492 B1, January 29, 2002.
- (163) Wang, Z. In *Comprehensive Organic Name Reactions and Regents*; John Wiley and Sons; 2009; pp 2251–2255.
- (164) Kelderman, E.; Derhaeg, L.; Verboom, W.; Engbersen, J. F. J.; Harkema, S.; Persoons, A.;

-
- Reinhoudt, D. N. *Supramol. Chem.* **1993**, *2*, 183–190.
- (165) Habrant, D.; Rauhala, V.; Koskinen, A. M. P. *Chem. Soc. Rev.* **2010**, *39*, 2007–2017.
- (166) Chan, T. R.; Hilgraf, R.; Sharpless, K. B.; Fokin, V. V. *Org. Lett.* **2004**, *6*, 2853–2855.
- (167) Bew, S. P.; Brimage, R. A.; L'Hermite, N.; Sharma, S. V. *Org. Lett.* **2007**, *9*, 3713–3716.
- (168) Berg, R.; Straub, B. F. *Beilstein J. Org. Chem.* **2013**, *9*, 2715–2750.
- (169) Percec, V.; Bera, T. K.; De, B. B.; Sanai, Y.; Smith, J.; Holerca, M. N.; Barboiu, B.; Grubbs, R. B.; Frechet, J. M. J. *J. Org. Chem.* **2001**, *66*, 2104–2117.
- (170) van Duynhoven, J. P. M.; Janssen, R. G.; Verboom, W.; Franken, S. M.; Casnati, A.; Pochini, A.; Ungaro, R.; de Mendoza, J.; Nieto, P. M.; et al. *J. Am. Chem. Soc.* **1994**, *116*, 5814–5822.
- (171) Pochorovski, I.; Diederich, F. *Acc. Chem. Res.* **2014**, *47*, 2096–2105.
- (172) Pochorovski, I.; Ebert, M. O.; Gisselbrecht, J. P.; Boudon, C.; Schweizer, W. B.; Diederich, F. *J. Am. Chem. Soc.* **2012**, *134*, 14702–14705.
- (173) Ruiz-Botella, S.; Vidossich, P.; Ujaque, G.; Vicent, C.; Peris, E. *Chem. - A Eur. J.* **2015**, *21*, 10558–10565.
- (174) Kirihaara, M.; Asai, Y.; Ogawa, S.; Noguchi, T.; Hatano, A.; Hirai, Y. *Synthesis (Stuttg.)* **2007**, *21*, 3286–3289.
- (175) Singh, R.; Lamoureux, G. V.; Lees, W. J.; Whitesides, G. M. *Methods Enzymol.* **1995**, *251* (Biothiols, Part A), 167–173.
- (176) Hofbauer, F.; Frank, I. *Chem. - A Eur. J.* **2010**, *16*, 5097–5101.
- (177) Schuster, M. C.; Mann, D. A.; Buchholz, T. J.; Johnson, K. M.; Thomas, W. D.; Kiessling, L. L. *Org. Lett.* **2003**, *5*, 1407–1410.
- (178) Black, S. P.; Sanders, J. K.; Stefankiewicz, A. R. *Chem. Soc. Rev.* **2014**, *43*, 1861–1872.
- (179) Jin, Y.; Wang, Q.; Taynton, P.; Zhang, W. *Acc. Chem. Res.* **2014**, *47*, 1575–1586.
- (180) Jin, Y.; Yu, C.; Denman, R. J.; Zhang, W. *Chem. Soc. Rev.* **2013**, *42*, 6634–6654.
- (181) Seebach, D. *Angew. Chemie Int. Ed. English* **1990**, *29*, 1320–1367.
- (182) Sisco, S. W.; Larson, B. M.; Moore, J. S. *Macromol. Chem.*, **2014**, *47*, 3829–3836.

-
- (183) Szymanski, M.; Wierzbicki, M.; Gilski, M.; Jedrzejewska, H.; Sztylko, M.; Cmoch, P.; Shkurenko, A.; Jaskolski, M.; Szumna, A. *Chem. - A Eur. J.* **2016**, *22*, 3148–3155.
- (184) Furusho, Y.; Oku, T.; Rajkumar, G. A.; Takata, T. *Chem. Lett.* **2004**, *33*, 52–53.
- (185) Ten Cate, A. T.; Dankers, P. Y. W.; Sijbesma, R. P.; Meijer, E. W. *J. Org. Chem.* **2005**, *70*, 5799–5803.
- (186) Namyslo, J. C.; Stanitzek, C. *Synthesis (Stuttg.)* **2006**, No. 20, 3367–3369.
- (187) Pompella, A.; Visvikis, A.; Paolicchi, A.; De Tata, V.; Casini, A. F. *Biochem. Pharmacol.* **2003**, *66*, 1499–1503.
- (188) Singh, R.; Whitesides, G. M. (1993) Thiol-disulfide interchange, in *The Chemistry of Sulphur-Containing Functional Groups*; (eds S. Patai and Z. Rappoport), John Wiley and Sons, Inc., Chichester, UK.
- (189) Yu, H.; Yang, Y.; Zhang, L.; Dang, Z.; Hu, G. *J. Phys. Chem. A* **2014**, *118*, 606–622.
- (190) Freter, R.; Pohl, E. R.; Wilson, J. M.; Hupe, D. J. *J. Org. Chem.* **1979**, *44*, 1771–1774.
- (191) Sforazzini, G.; Orentas, E.; Bolag, A.; Sakai, N.; Matile, S. *J. Am. Chem. Soc.* **2013**, *135*, 12082–12090.
- (192) Frost, J. R.; Jacob, N. T.; Papa, L. J.; Owens, A. E.; Fasan, R. *ACS Chem. Biol.* **2015**, *10*, 1805–1816.
- (193) Wu, Z.; Glaser, R. *J. Am. Chem. Soc.* **2004**, 10632–10639.
- (194) Spletstoser, J. T.; Flaherty, P. T.; Himes, R. H.; Georg, G. I. *J. Med. Chem.* **2004**, *47*, 6459–6465.
- (195) Stoermer, D.; Vitharana, D.; Hin, N.; Delahanty, G.; Duvall, B.; Ferraris, D. V.; Grella, B. S.; Hoover, R.; Rojas, C.; Shanholtz, M. K.; Smith, K. P.; Stathis, M.; Wu, Y.; Wozniak, K. M.; Slusher, B. S.; Tsukamoto, T. *J. Med. Chem.* **2012**, *55*, 5922–5932.
- (196) Sander, F.; Peterle, T.; Ballav, N.; von Wrochem, F.; Zharnikov, M.; Mayor, M. *J. Phys. Chem. C* **2010**, *114*, 4118–4125.
- (197) Oae, S.; Doi, J. *Organic Sulfur Chemistry; Organic Sulfur Chemistry (Florida)*; Taylor & Francis, **1991**, Chapter 1.
- (198) Yakovenko, A. V.; Boyko, V. I.; Kalchenko, V. I.; Baldini, L.; Casnati, A.; Sansone, F.; Ungaro, R.;

-
- Usberti, V. G. P. A.; Giusti, V.; V, V. *J. Org. Chem.* **2007**, *72*, 3223–3231.
- (199) Durmaz, M.; Bozkurt, S.; Nevin, H.; Yilmaz, M.; Sirit, A. *Tetrahedron: Asymmetry*, **2011**, *22*, 791–796.
- (200) Armstrong, D. W.; Ward, T. J.; Armstrong, R. D.; Beesley, T. E. *Science*, **1985**, *232*, 1132–1135.
- (201) Lingenfelter, D. S.; Helgeson, R. C.; Cram, D. J. *J. Org. Chem.* **1981**, *46*, 393–406.
- (202) Yamashita, T. *Tetrahedron Lett.* **1995**, *36*, 7669–7672.
- (203) Roy, D. H. Investigations into the Synthesis of Inherently Chiral Calix[4]arenes, MSc thesis, University of East Anglia, 2016.
- (204) Otsuka, H.; Shinkai, S.; Suzuki, Y. *Tetrahedron* **1998**, *54*, 423–446.
- (205) Dondoni, A.; Ghiglione, C.; Marra, A.; Scoconi, M.; Chimica, D.; Organica, C. *J. Org. Chem.* **1998**, *63*, 9535–9539.
- (206) Smith, G. B.; Dezeny, G. C.; Hughes, D. L.; King, A. O.; Verhoeven, T. R. *J. Org. Chem.* **1994**, *59*, 8151–8156.
- (207) Miyaura, N.; Suzuki, A. *Chem. Rev.* **1995**, *95*, 2457–2483.
- (208) Amatore, C.; Jutand, A.; Le Duc, G. *Chem. - A Eur. J.* **2011**, *17*, 2492–2503.
- (209) Juneja, R. K.; Robinson, K. D.; Johnson, C. P.; Atwood, J. L. *J. Am. Chem. Soc.* **1993**, *115*, 3818–3819.
- (210) Mastalerz, M.; Dyker, G.; Flörke, U.; Henkel, G.; Oppel, I. M.; Merz, K. *European J. Org. Chem.* **2006**, *3*, 4951–4962.
- (211) Mendez-Arroyo, J.; Barroso-Flores, J.; Lifschitz, A. M.; Sarjeant, A. A.; Stern, C. L.; Mirkin, C. A. *J. Am. Chem. Soc.* **2014**, *136*, 10340–10348.
- (212) Sameni, S.; Jeunesse, C.; Matt, D.; Toupet, L. *Chem. A Eur. J.* **2009**, *15*, 10446–10456.
- (213) Tidwell, T. T. *Org. React. (New York)* **1990**, *39*, 297–572.
- (214) Holsworth, D. D. In *Name React. Funct. Group Transform. (New Jersey)*; John Wiley & Sons, Inc., 2007; pp 218–236.
- (215) Ireland, R. E.; Liu, L. *J. Org. Chem.* **1993**, *58*, 2899.

-
- (216) Sharma, R.; Margani, R.; Mobin, S. M.; Misra, R. *RSC Adv.* **2013**, *3*, 5785–5788.
- (217) Dilmaghani, K. A.; Pur, N. *Turkish J. Chem.* **2011**, *35*, 455–462.
- (218) Taghvaei-Ganjali, S.; Zadmard, R. *Supramol. Chem.* **2008**, *20*, 527–530.
- (219) Galli, M.; Berrocal, J. A.; Di Stefano, S.; Cacciapaglia, R.; Mandolini, L.; Baldini, L.; Casnati, A.; Ugozzoli, F. *Org. Biomol. Chem.* **2012**, *10*, 5109–5112.
- (220) Böhmer, V.; Kraft, D.; Tabatabai, M. J. *Incl. Phenom. Mol. Recognit. Chem.* **1994**, *19*, 17–39.
- (221) Scheerder, J.; Vreekamp, R. H.; Engbersen, J. F. J.; Verboom, W.; Duynhoven, J. P. M. Van; Reinhoudt, D. N. J. *J. Org. Chem.* **1996**, *61*, 3476–3481.
- (222) Conner, M.; Janout, V.; Regen, S. L., *Phys. Org. Chem.* **1991**, *113*, 9670–9671.
- (223) Knoppe, S.; Vanbel, M.; van Cleuvenbergen, S.; Vanpraet, L.; Bürgi, T.; Verbiest, T. *J. Phys. Chem. C* **2015**, *119*, 6221–6226.
- (224) Gutsche, D. C.; Lin, L.-G. *Tetrahedron* **1985**, *42*, 1633–1640.
- (225) Wong, M. S.; Xia, P. F.; Lo, P. K.; Sun, X. H.; Wong, W. Y.; Shuang, S. *J. Org. Chem.* **2006**, *71*, 940–946.
- (226) Csékei, M.; Novák, Z.; Kotschy, A. *Tetrahedron* **2008**, *64*, 975–982.
- (227) Graham, E. M.; Miskowski, V. M.; Perry, J. W.; Coulter, D. R.; Stiegman, A. E.; Schaefer, W. P.; Marsh, R. E. *J. Am. Chem. Soc.* **1989**, *111*, 8771–8779.
- (228) Casnati, A.; Sartori, A.; Pirondini, L.; Bonetti, F.; Pelizzi, N.; Sansone, F.; Ugozzoli, F.; Ungaro, R. *Supramol. Chem.* **2006**, *18*, 199–218.